G-000-107 .47

5617

# GROUNDWATER REPORT VOLUME 13 OF 13 DECEMBER 1990

12/17/90

FMPC-0004-2
DOE-FMPC
172
REPORT

# GROUNDWATER REPORT

FEED MATERIALS PRODUCTION CENTER
FERNALD, OHIO

REMEDIAL INVESTIGATION AND FEASIBILITY STUDY

VOLUME 13 OF 13

Appendix N - Groundwater Elevation and Uranium Concentration Versus Time Graphs
Appendix O - Historical Uranium Concentration Versus Time Graphs
Appendix P - Results of Issues 3 and 5 Geochemical Program
Appendix Q - Fence Diagrams

December 1990

U.S. DEPARTMENT OF ENERGY
OAK RIDGE OPERATIONS OFFICE

DRAFT

FMPC-0004-1
November 15, 1990

# GROUNDWATER ELEVATION AND URANIUM CONCENTRATION VERSUS TIME GRAPHS

Appendix N contains groundwater elevation and uranium concentration versus time graphs for selected well clusters where uranium values are above the background level. The graphs contain water level data for the 2000, 3000, and 4000 Series wells and total uranium concentrations from the water samples collected from those wells. The maps are presented in order of location number. Appendix C contains the tabulated groundwater elevation data. Appendix E contains the tabulated groundwater quality data, and Appendix L contains the groundwater uranium concentration maps.

DRAFT

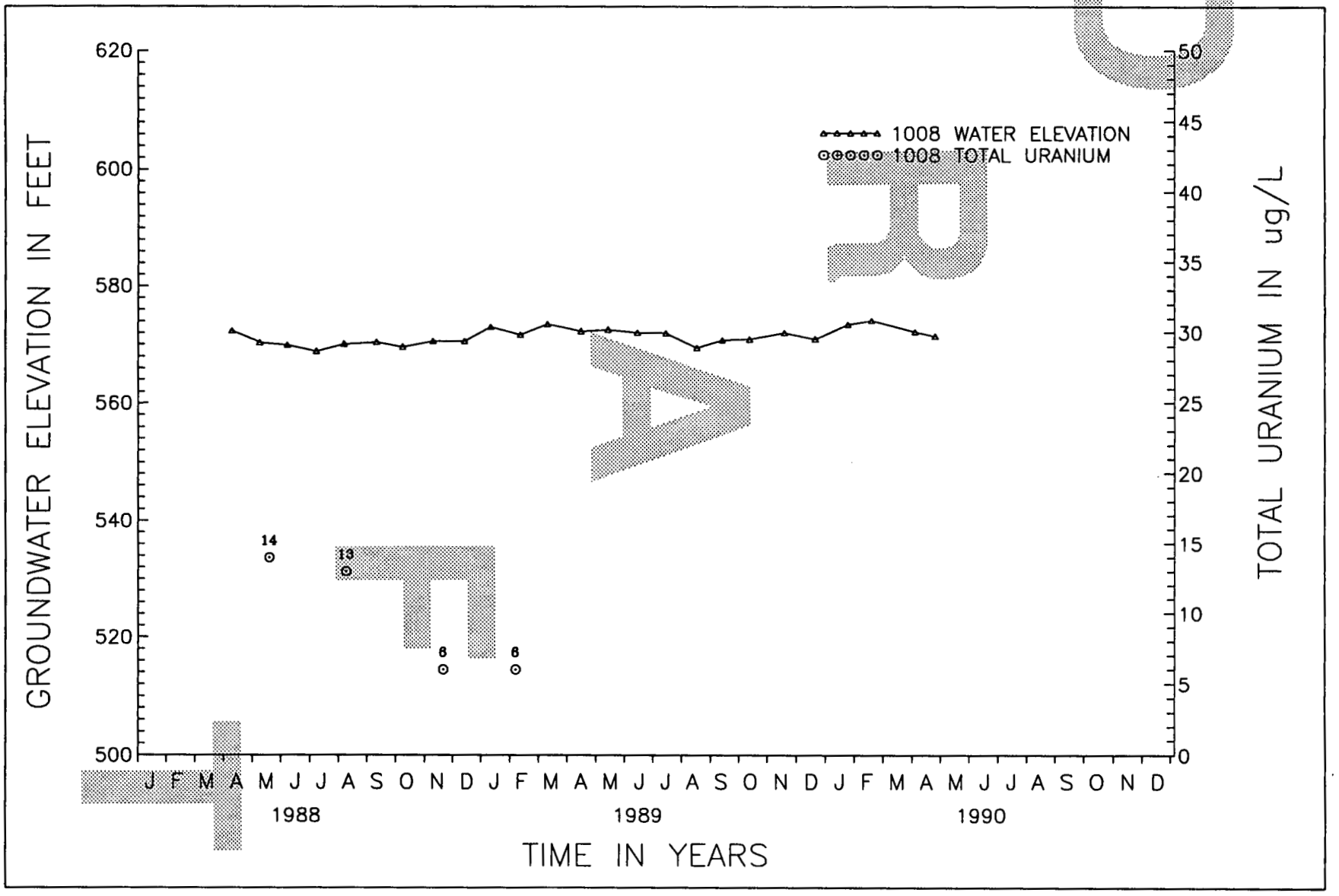


FIGURE N-1. HYDROGRAPH AND TOTAL URANIUM FOR WELL 1008

000003

5618

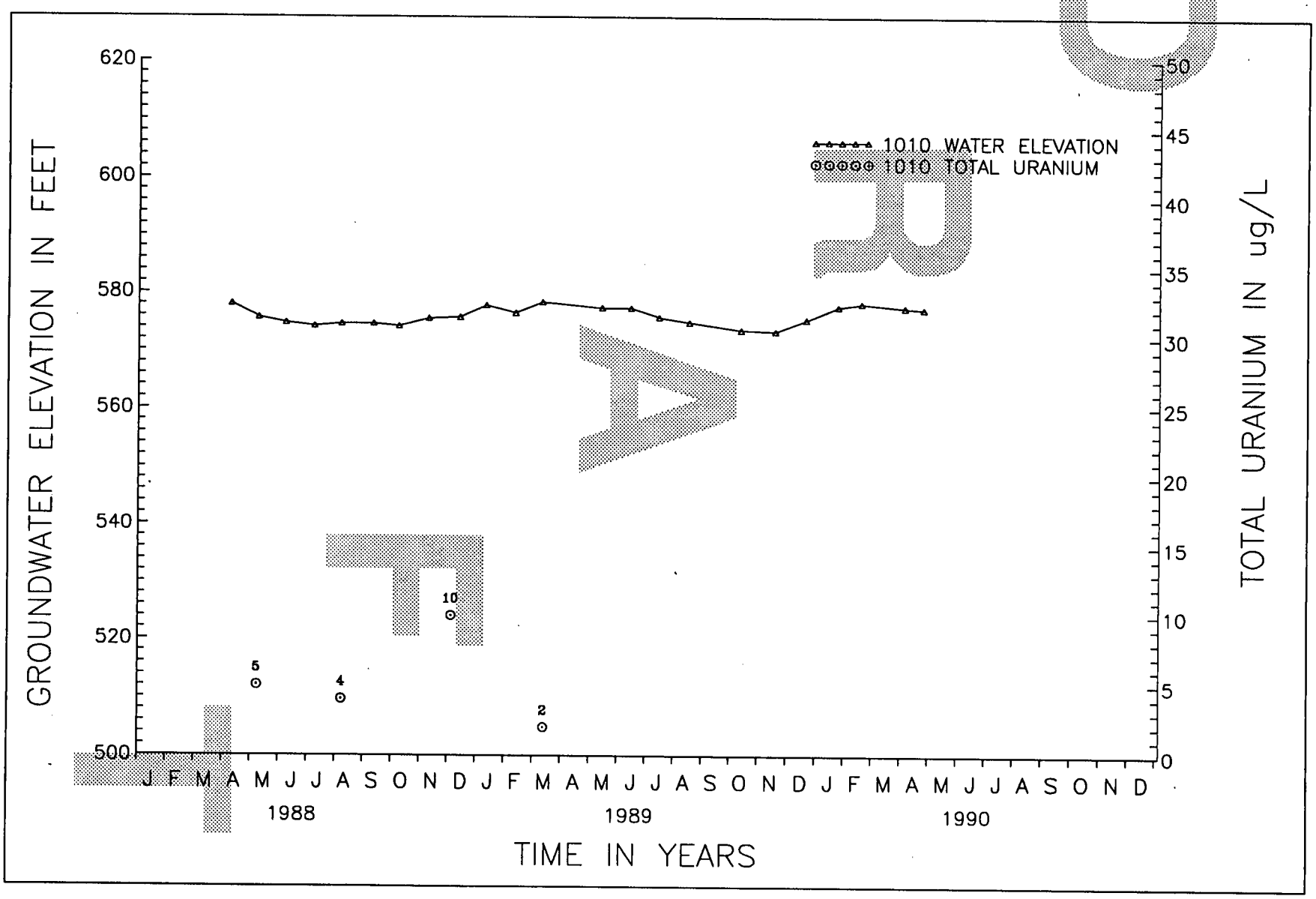


FIGURE N-2. HYDROGRAPH AND TOTAL URANIUM FOR WELL 1010

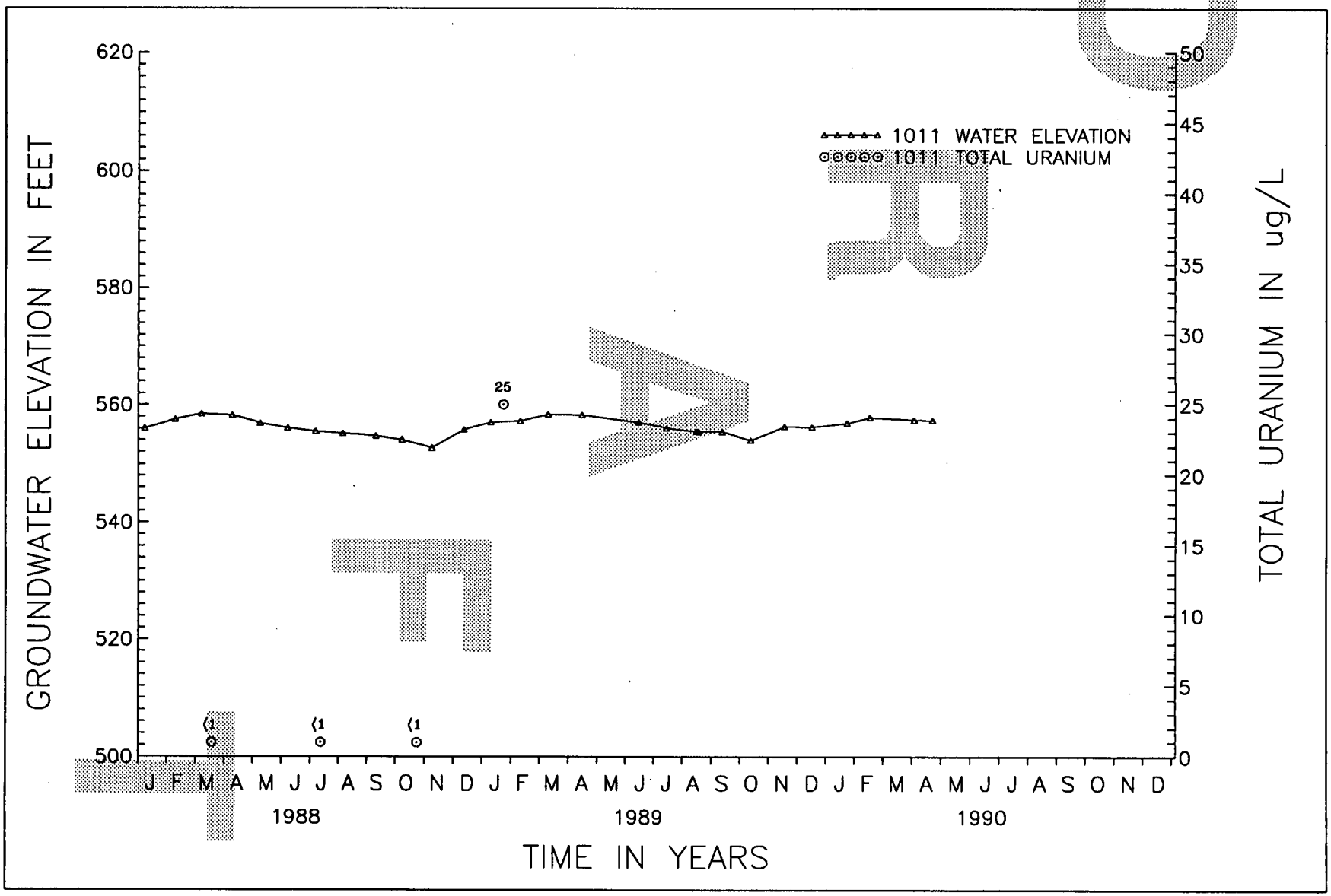


FIGURE N-3. HYDROGRAPH AND TOTAL URANIUM FOR WELL 1011

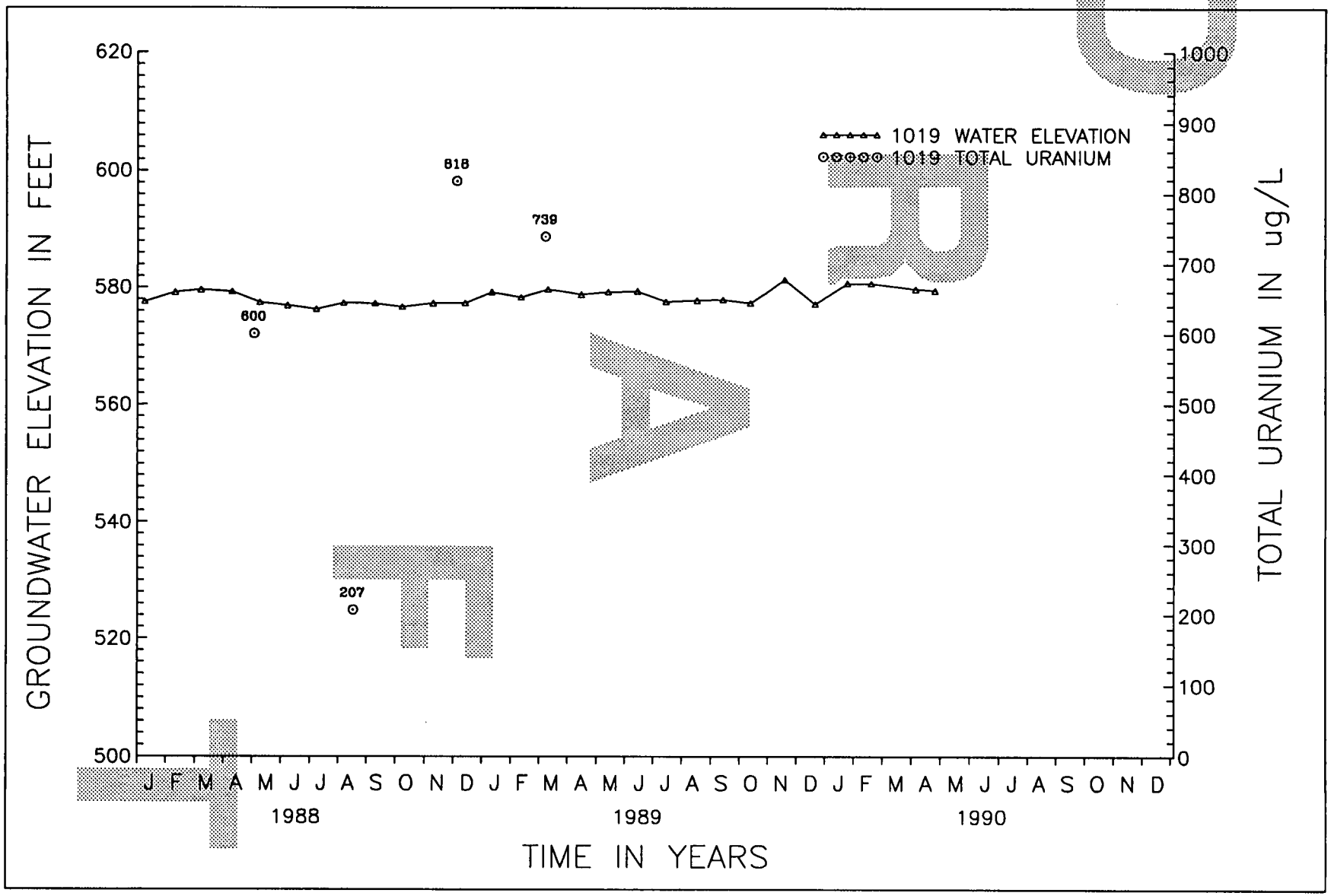


FIGURE N-4. HYDROGRAPH AND TOTAL URANIUM FOR WELL 1019

900000

6617

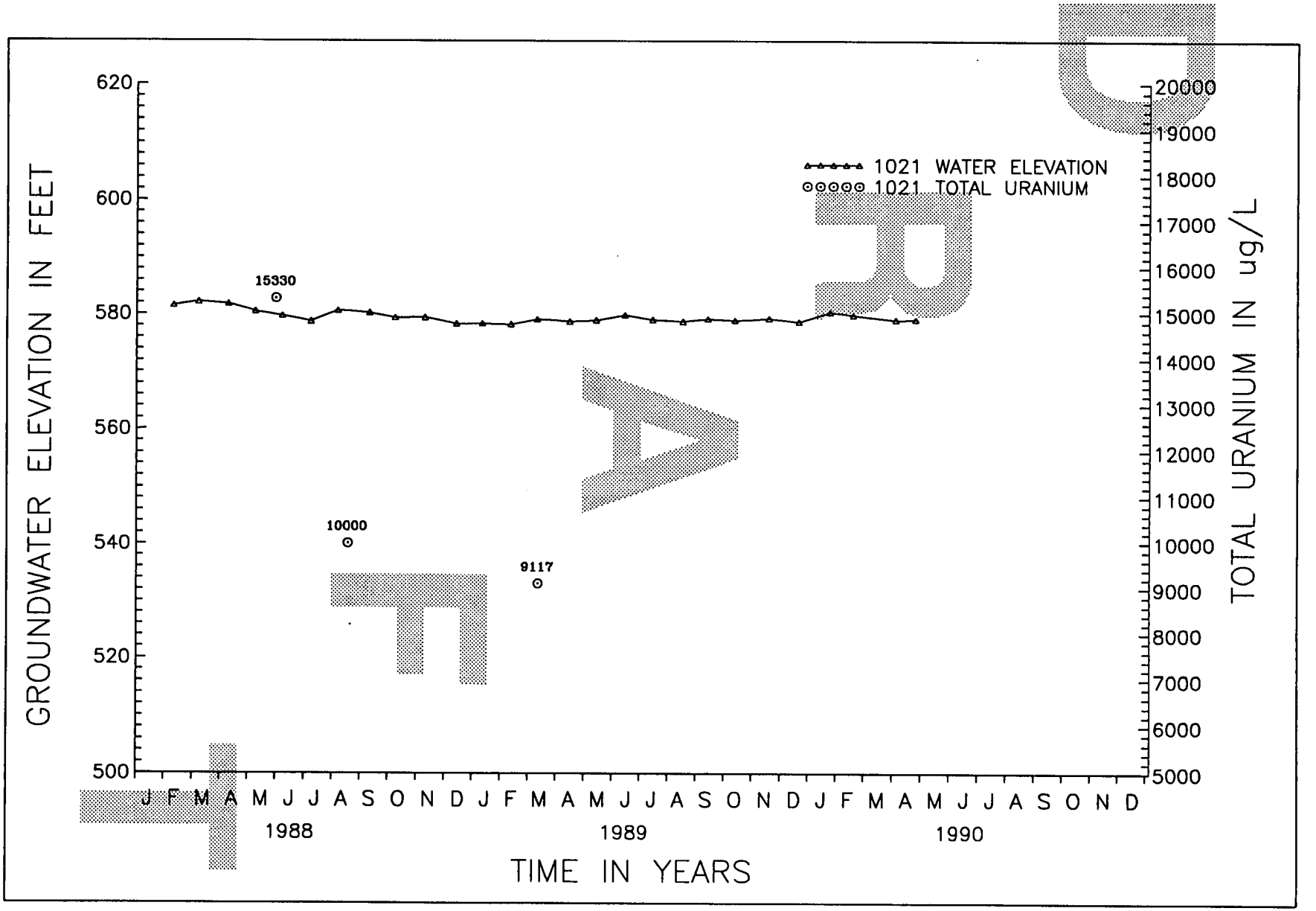


FIGURE N-5. HYDROGRAPH AND TOTAL URANIUM FOR WELL 1021

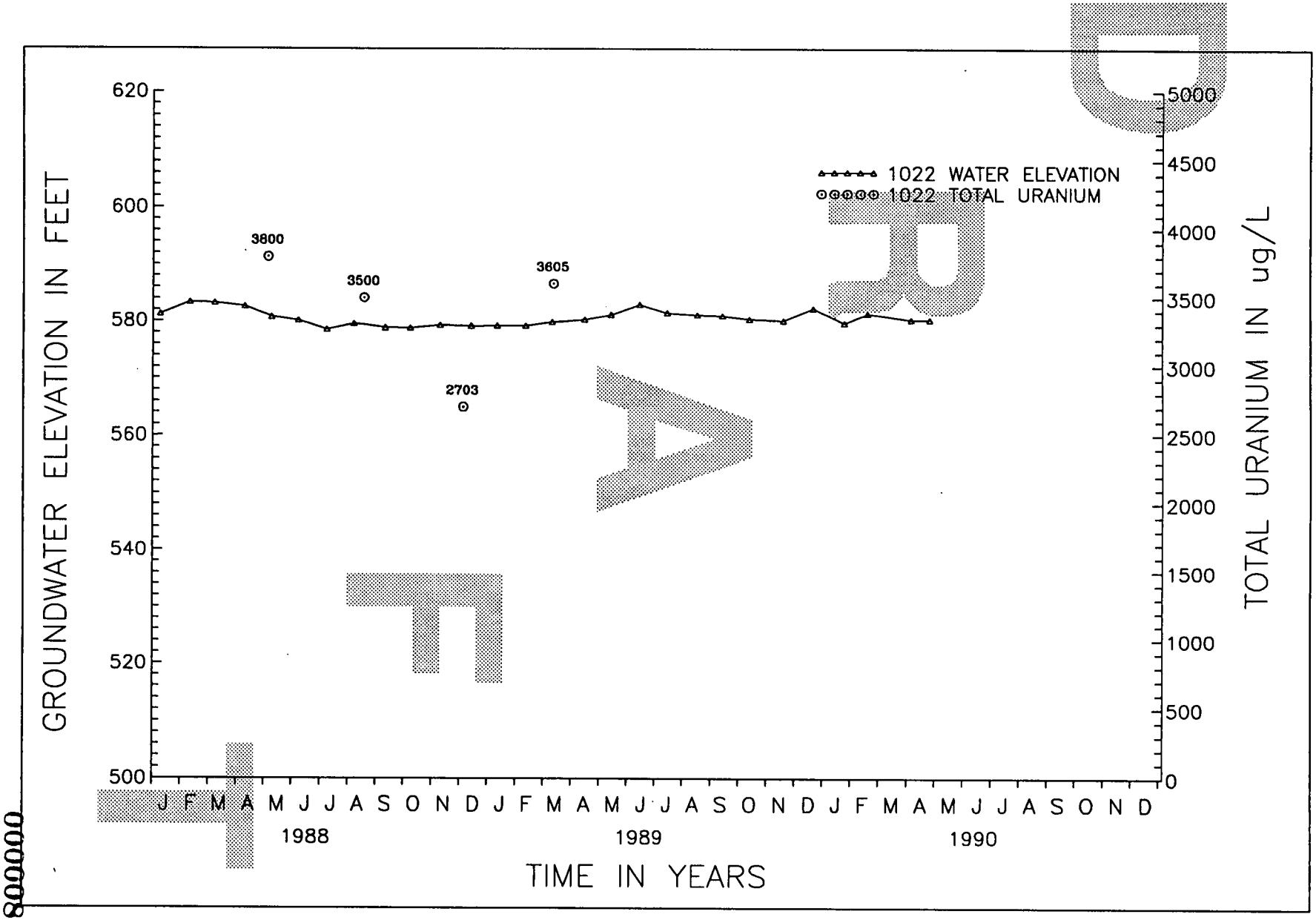


FIGURE N-6. HYDROGRAPH AND TOTAL URANIUM FOR WELL 1022

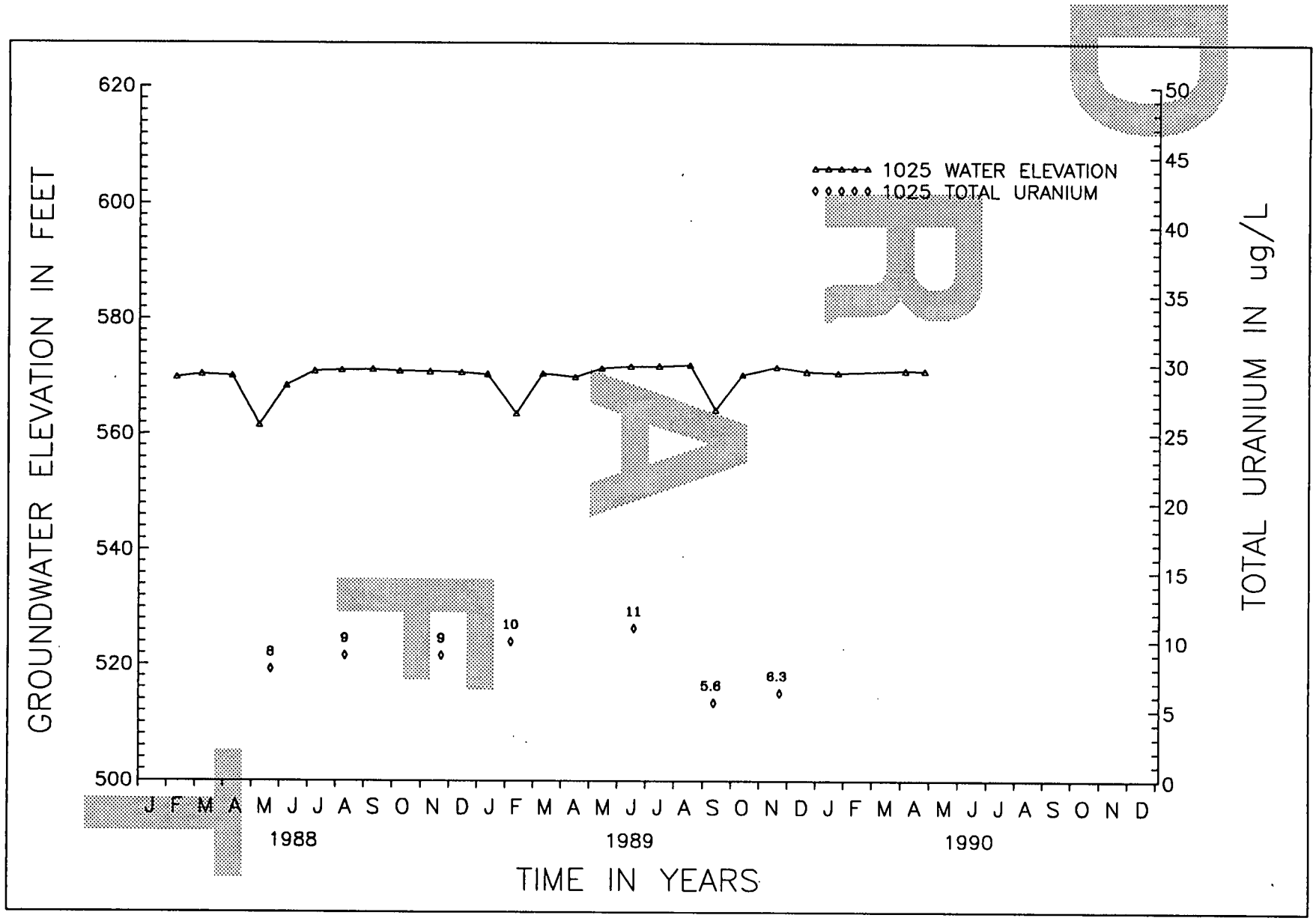


FIGURE N-7. HYDROGRAPH AND TOTAL URANIUM FOR WELL 1025

600000

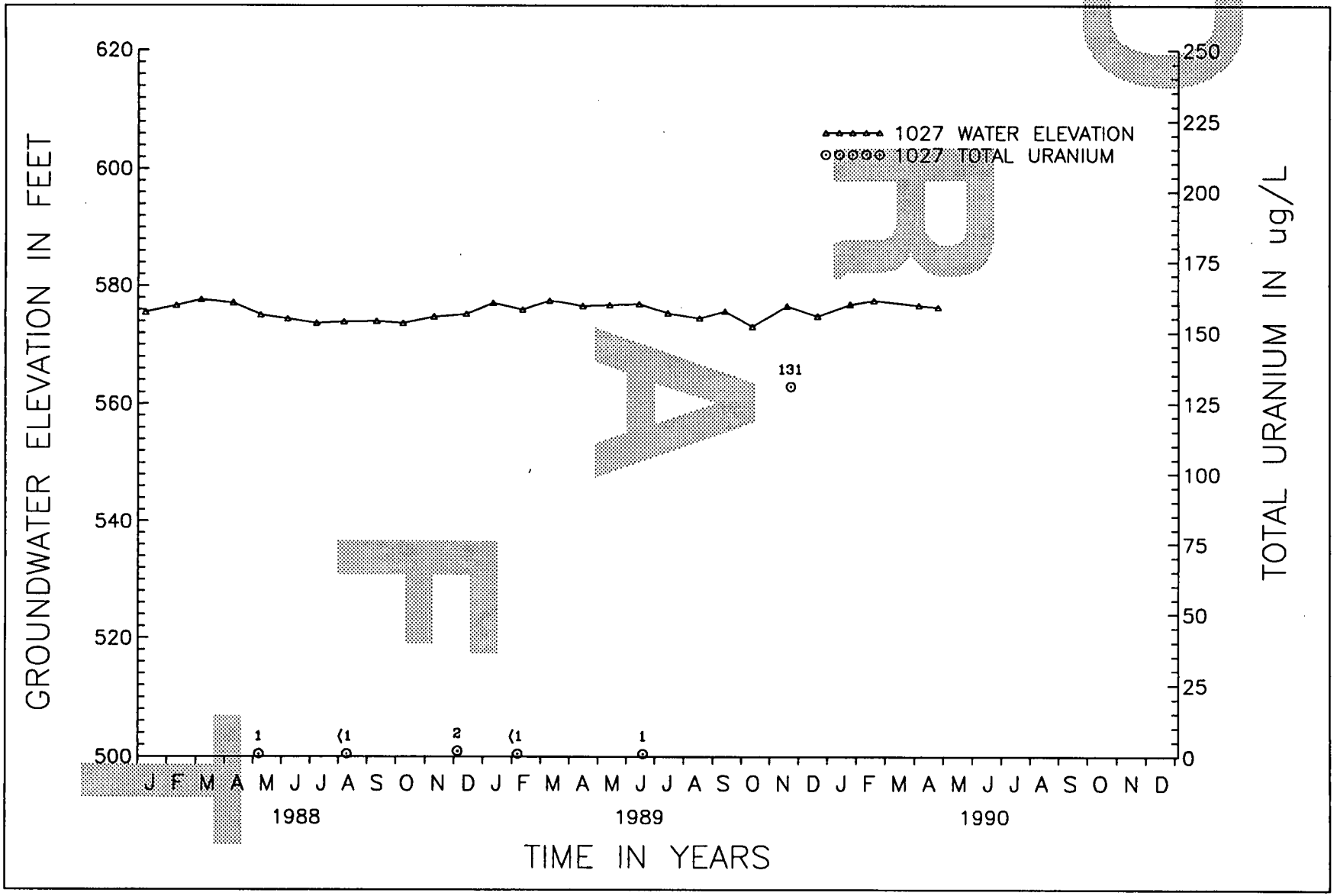


FIGURE N-8. HYDROGRAPH AND TOTAL URANIUM FOR WELL 1027

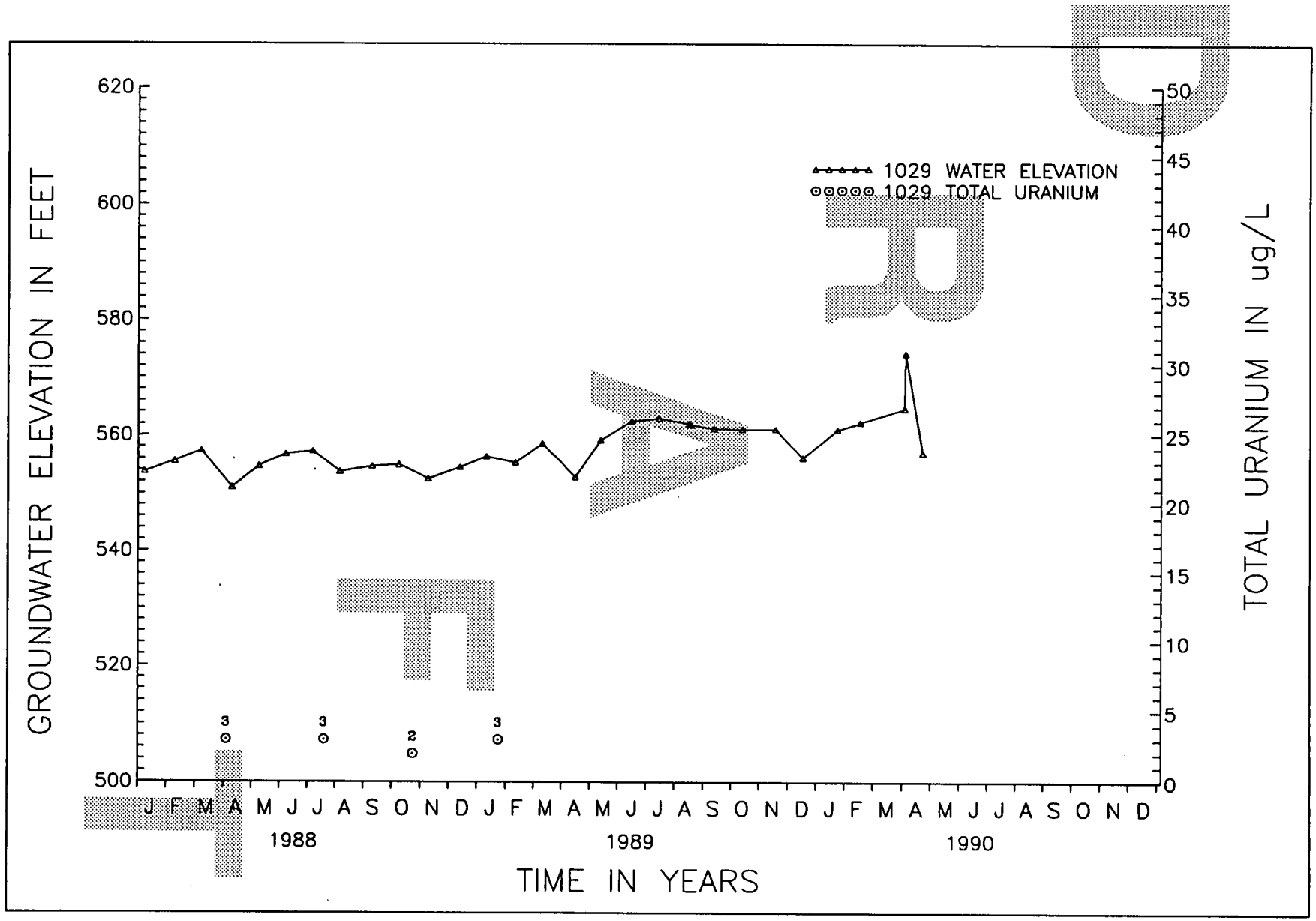


FIGURE N-9. HYDROGRAPH AND TOTAL URANIUM FOR WELL 1029

000011

5617

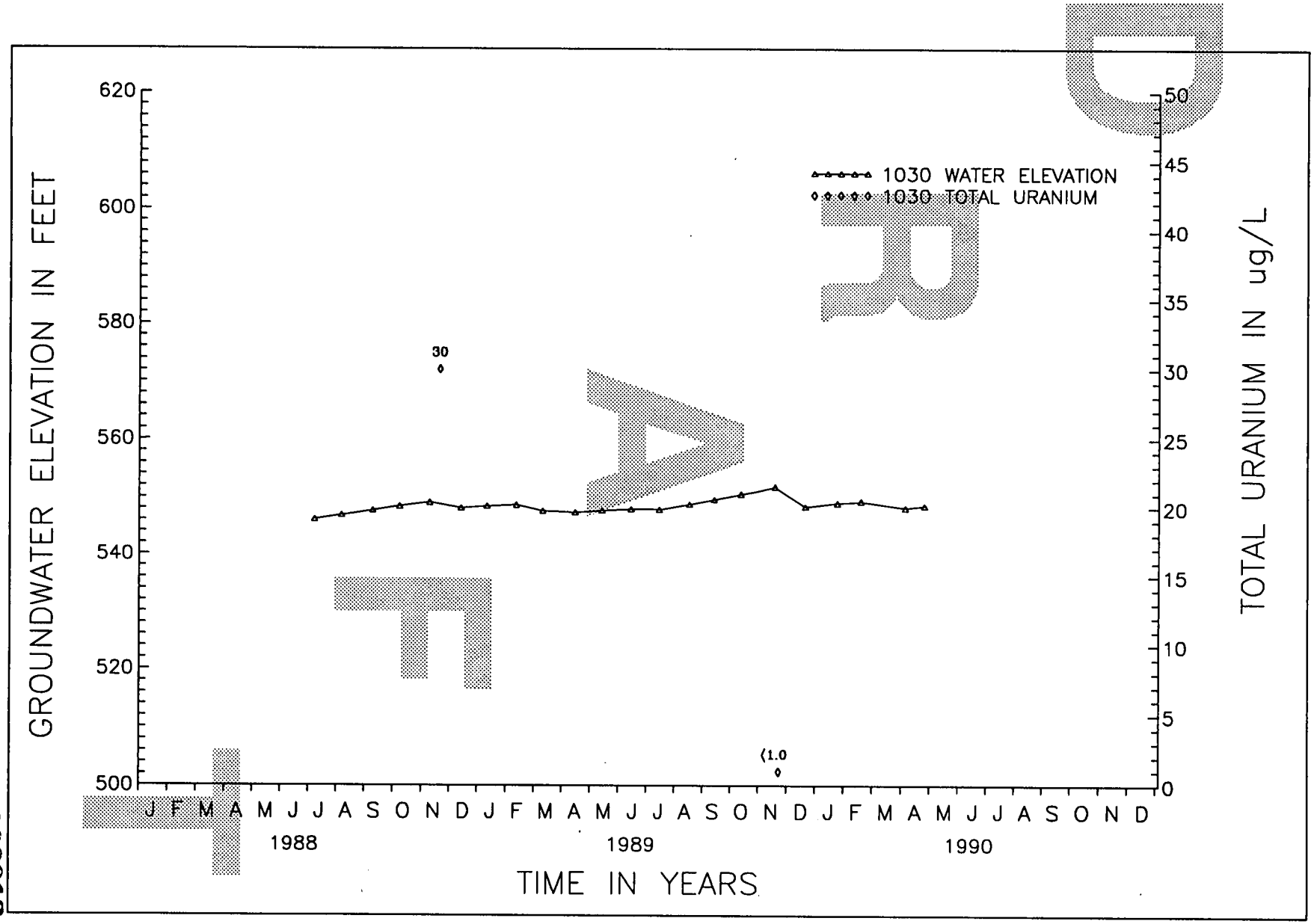


FIGURE N-10. HYDROGRAPH AND TOTAL URANIUM FOR WELL 1030

000012

5617

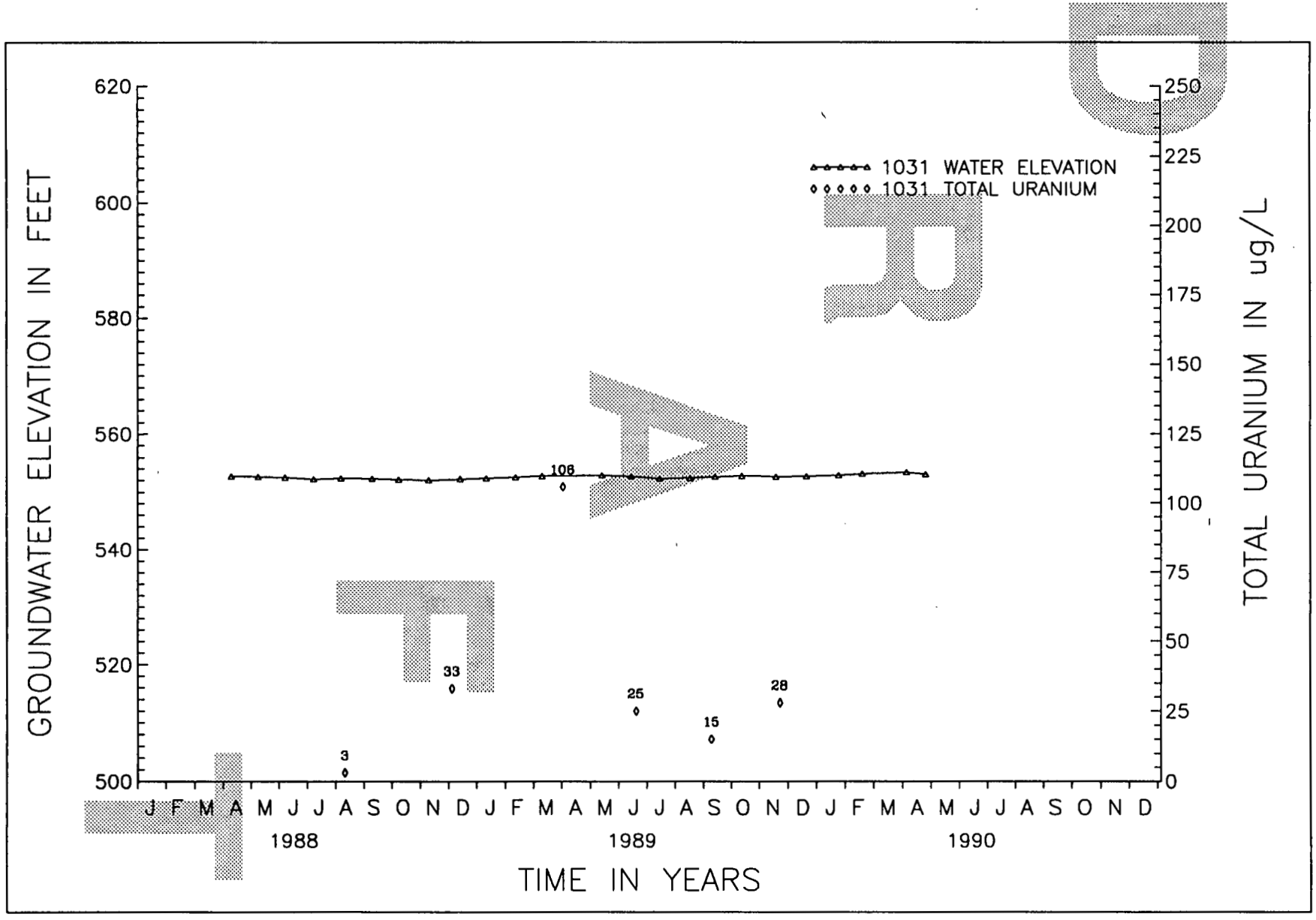


FIGURE N-11. HYDROGRAPH AND TOTAL URANIUM FOR WELL 1031

000013

5617

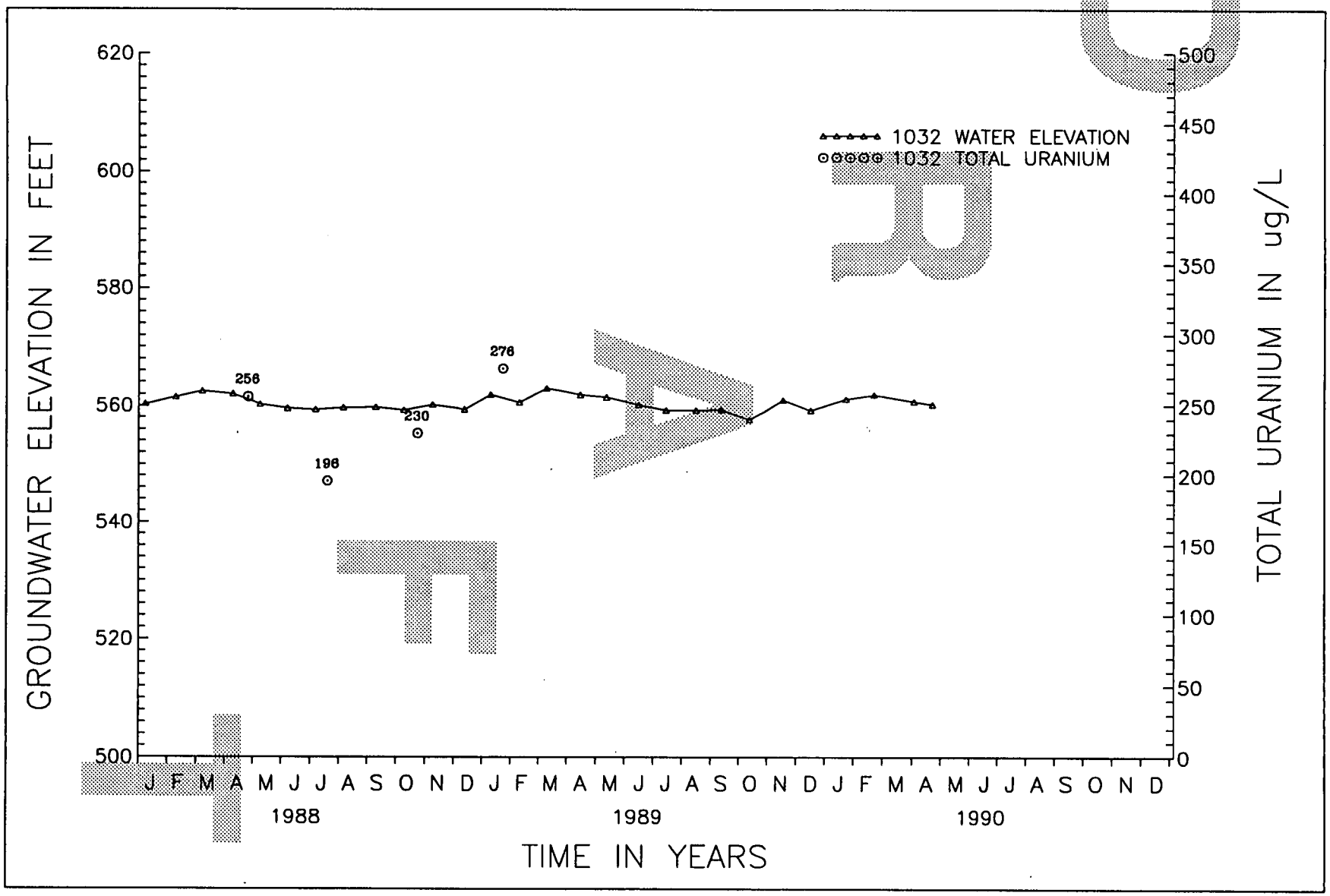


FIGURE N-12. HYDROGRAPH AND TOTAL URANIUM FOR WELL 1032

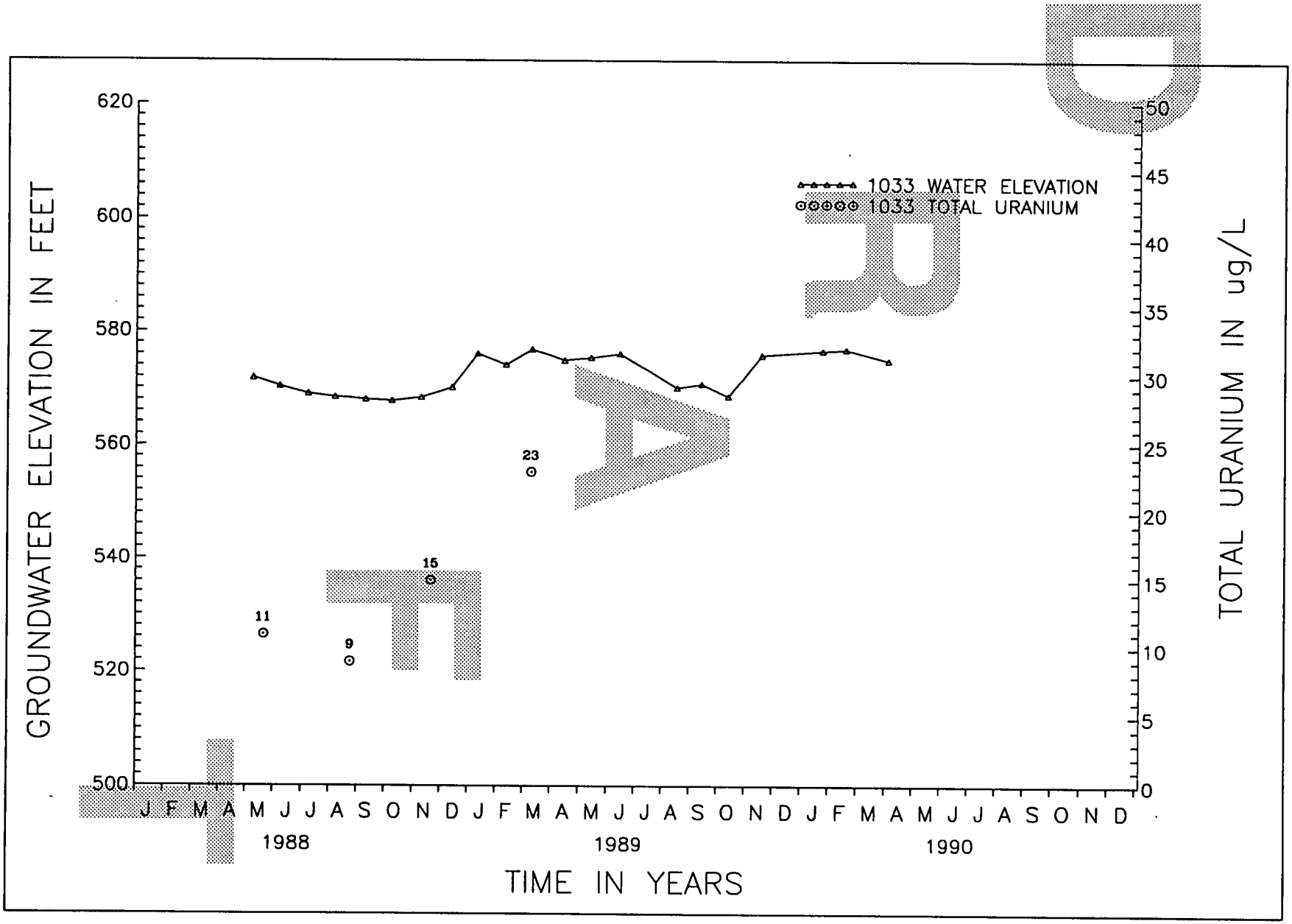


FIGURE N-13. HYDROGRAPH AND TOTAL URANIUM FOR WELL 1033

000015

6617

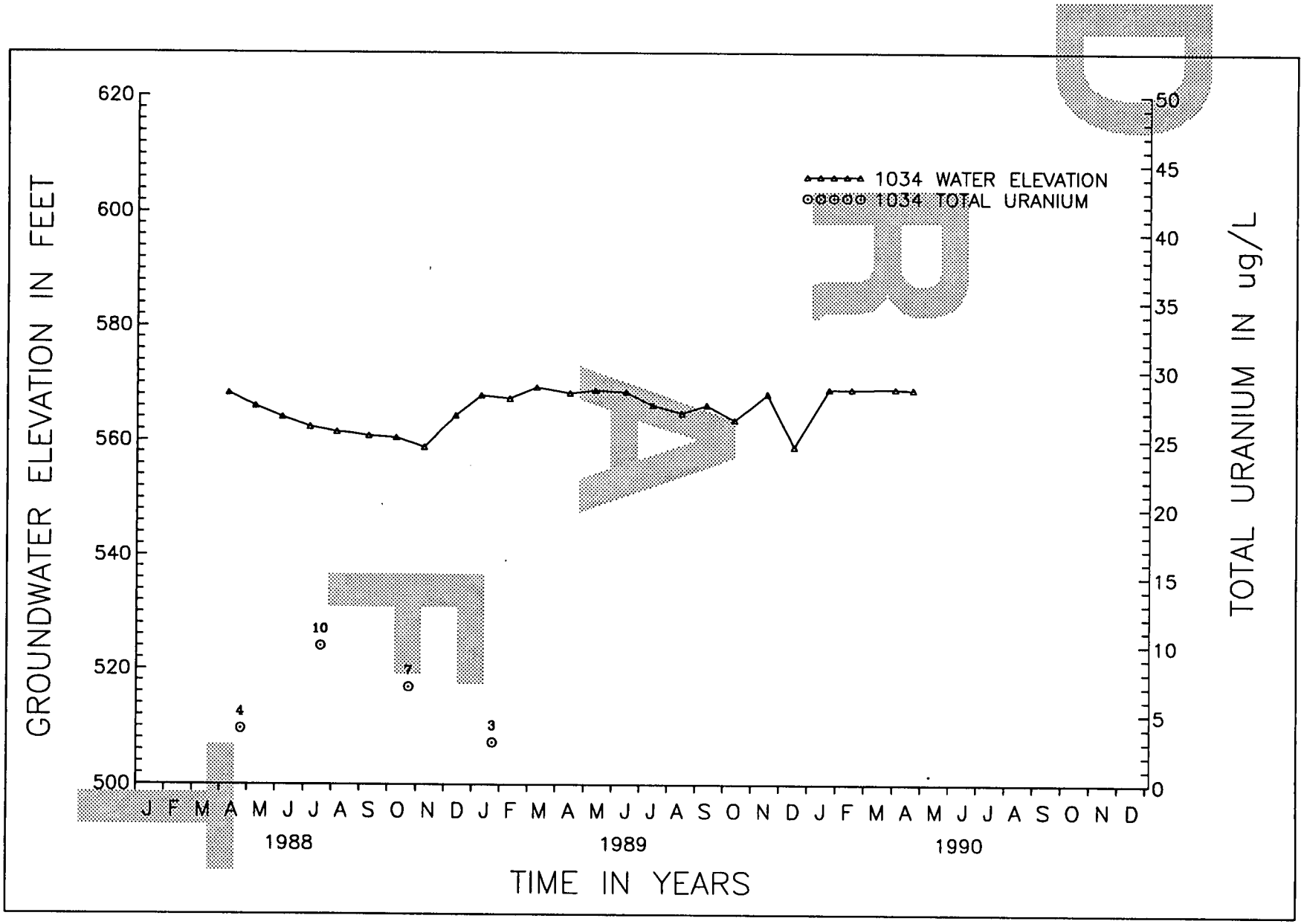


FIGURE N-14. HYDROGRAPH AND TOTAL URANIUM FOR WELL 1034

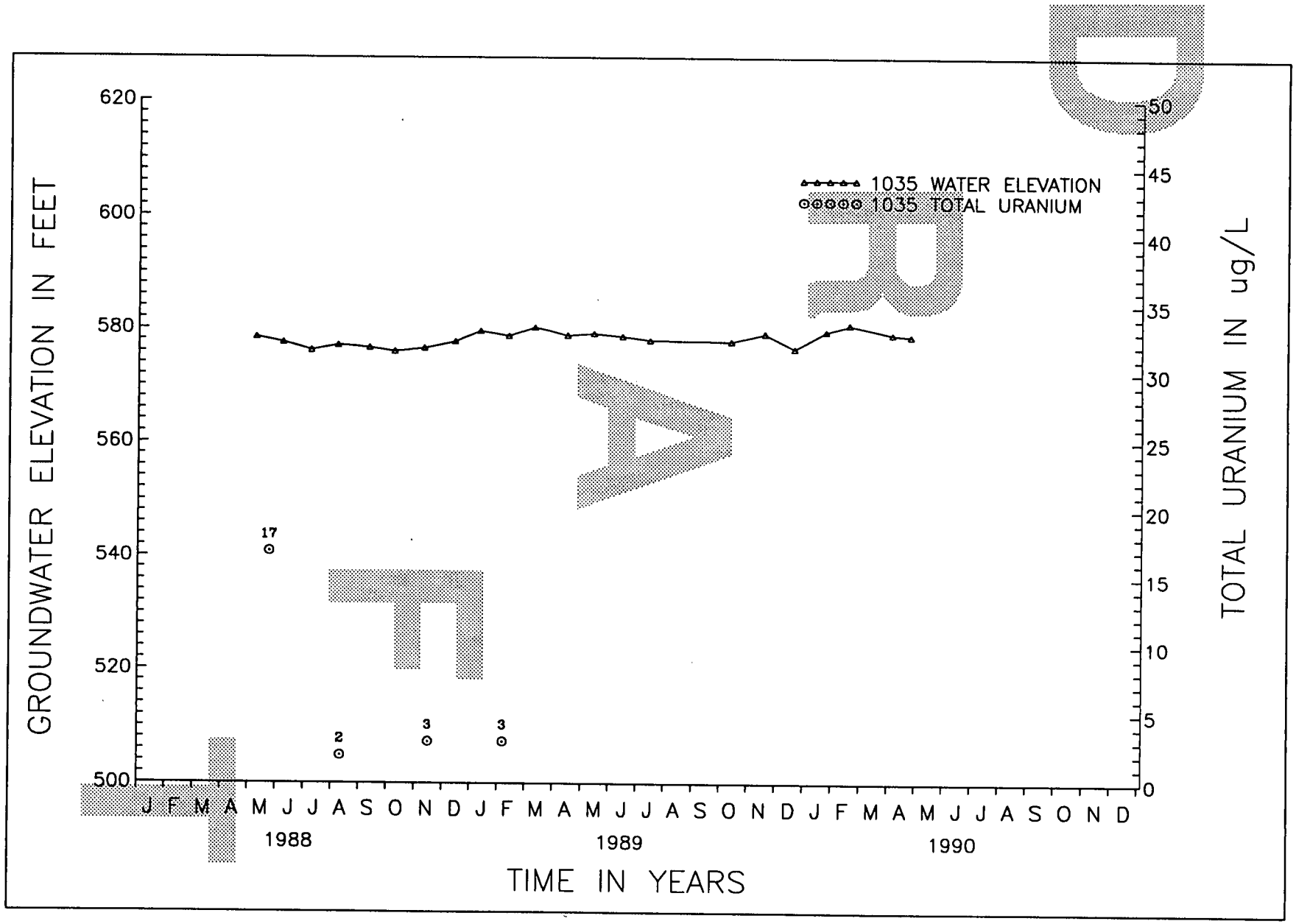


FIGURE N-15. HYDROGRAPH AND TOTAL URANIUM FOR WELL 1035

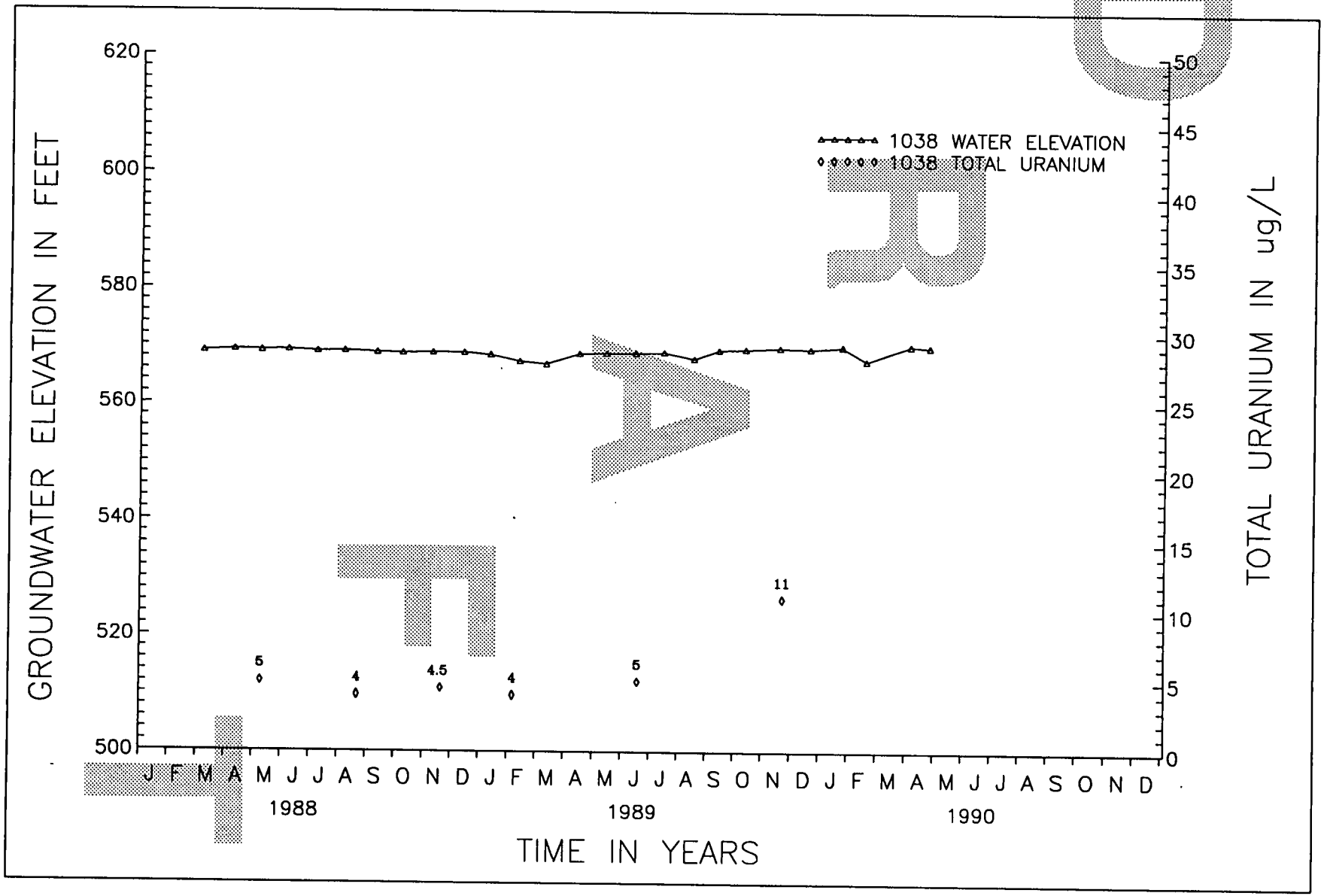


FIGURE N-16. HYDROGRAPH AND TOTAL URANIUM FOR WELL 1038

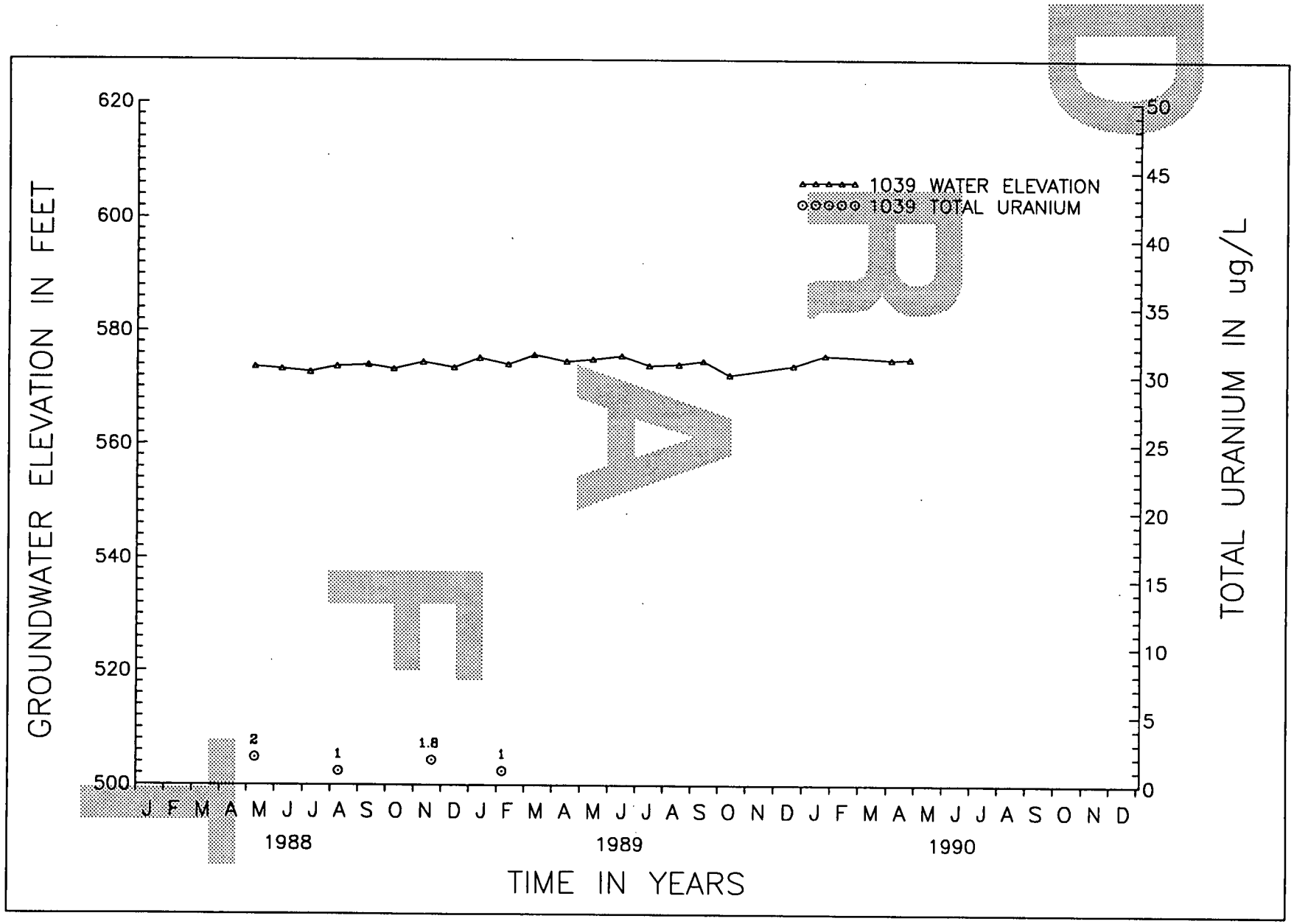


FIGURE N-17. HYDROGRAPH AND TOTAL URANIUM FOR WELL 1039

000019

5617

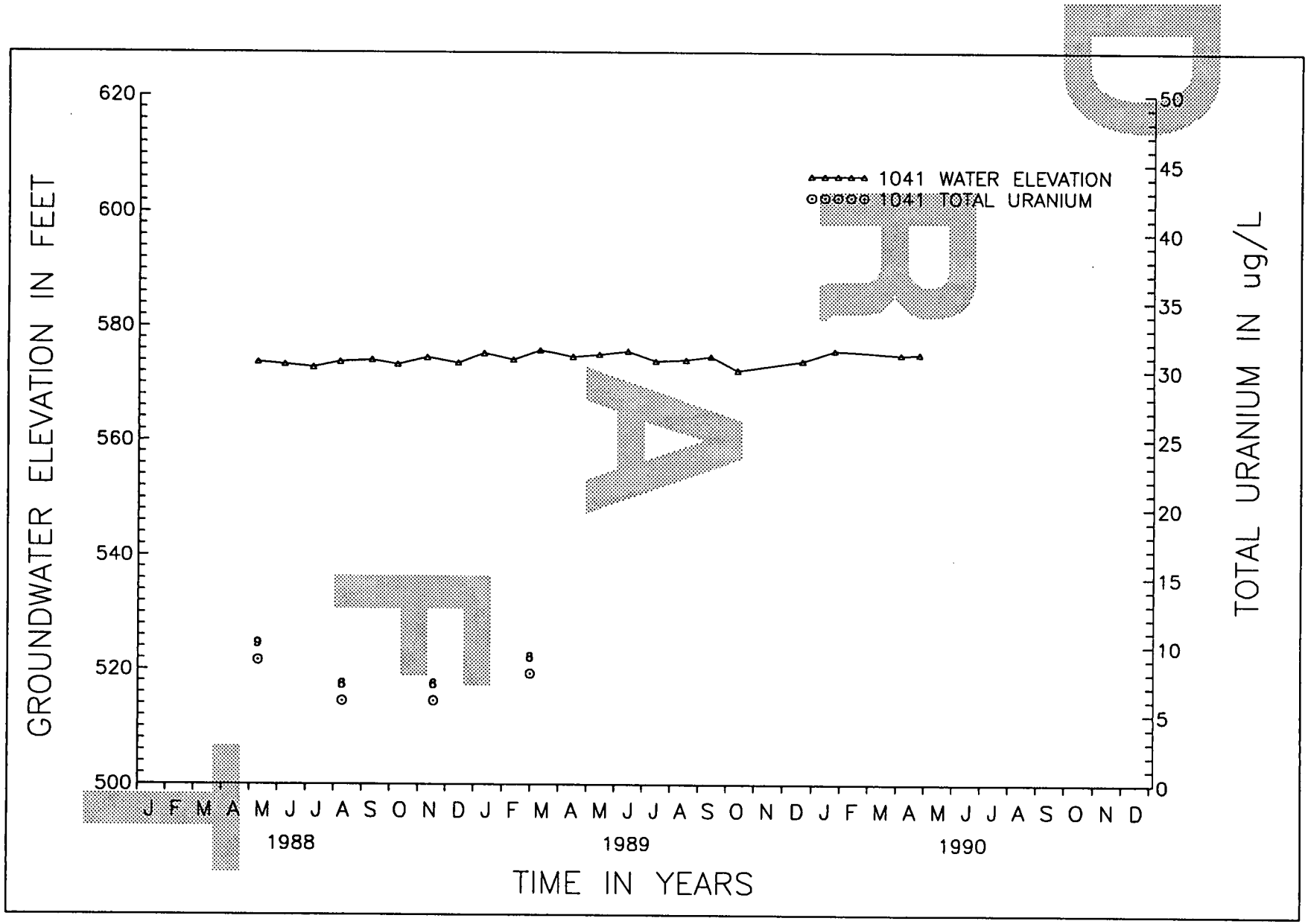


FIGURE N-18. HYDROGRAPH AND TOTAL URANIUM FOR WELL 1041

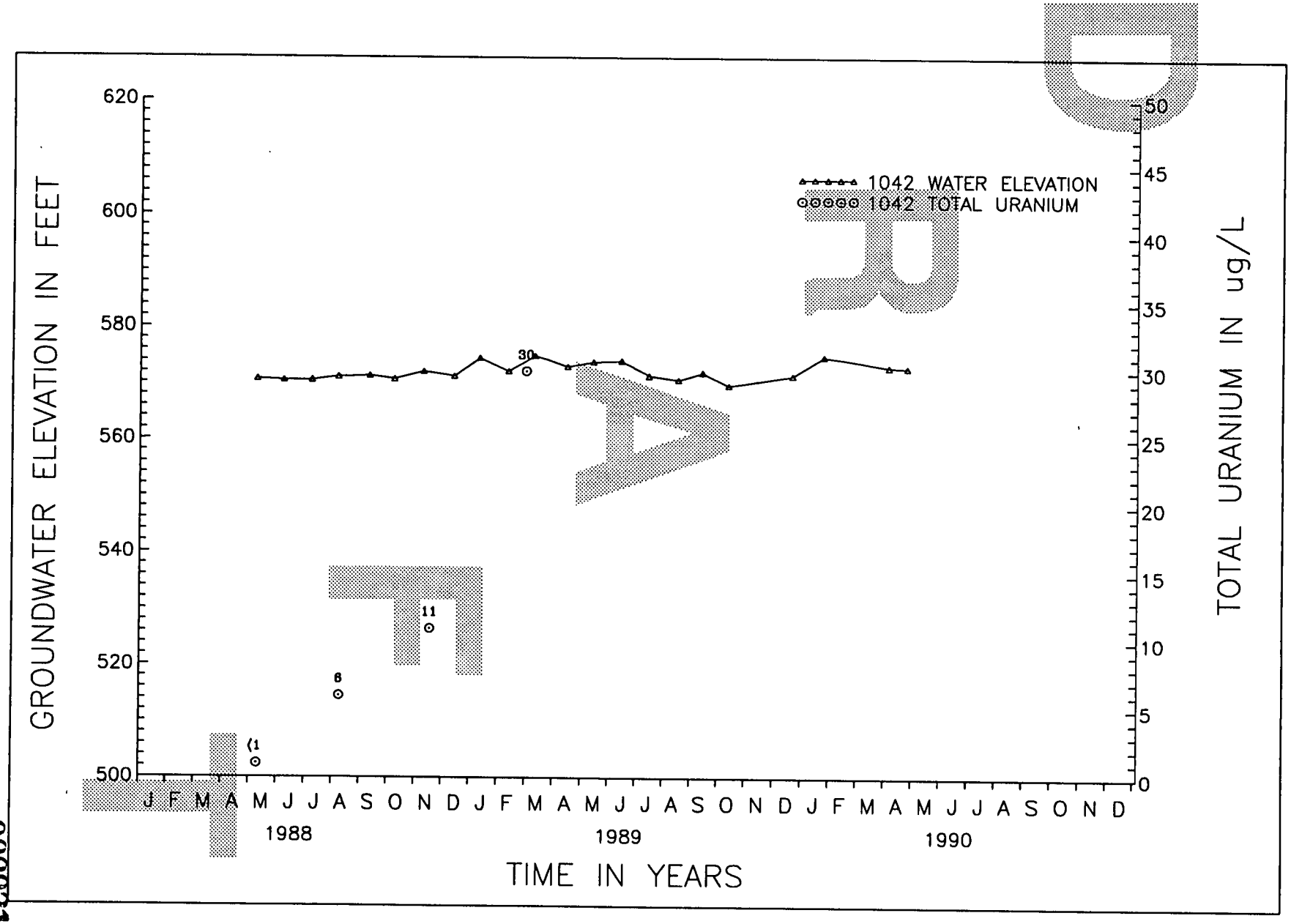


FIGURE N-19. HYDROGRAPH AND TOTAL URANIUM FOR WELL 1042

000021

5617

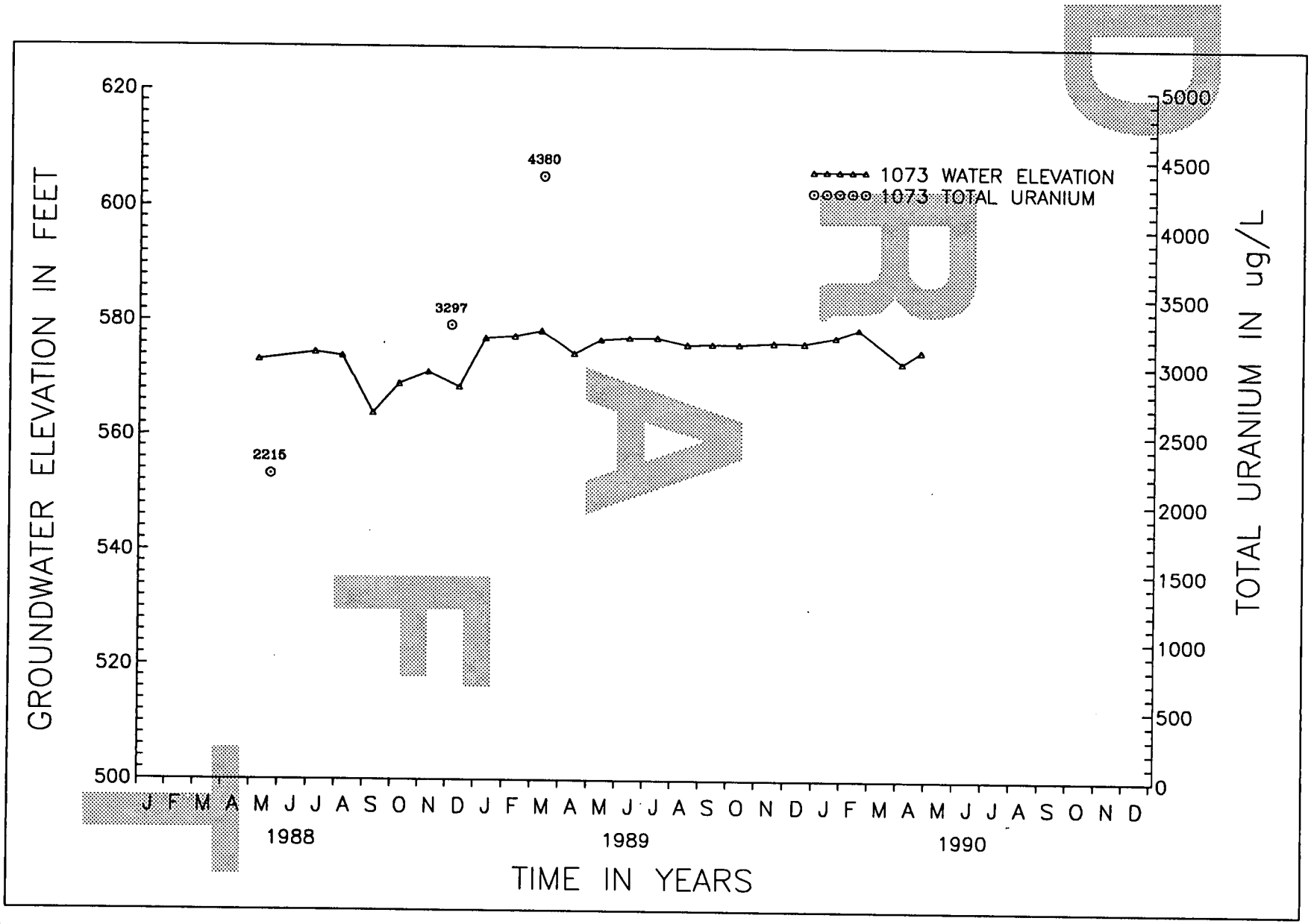


FIGURE N-20. HYDROGRAPH AND TOTAL URANIUM FOR WELL 1073

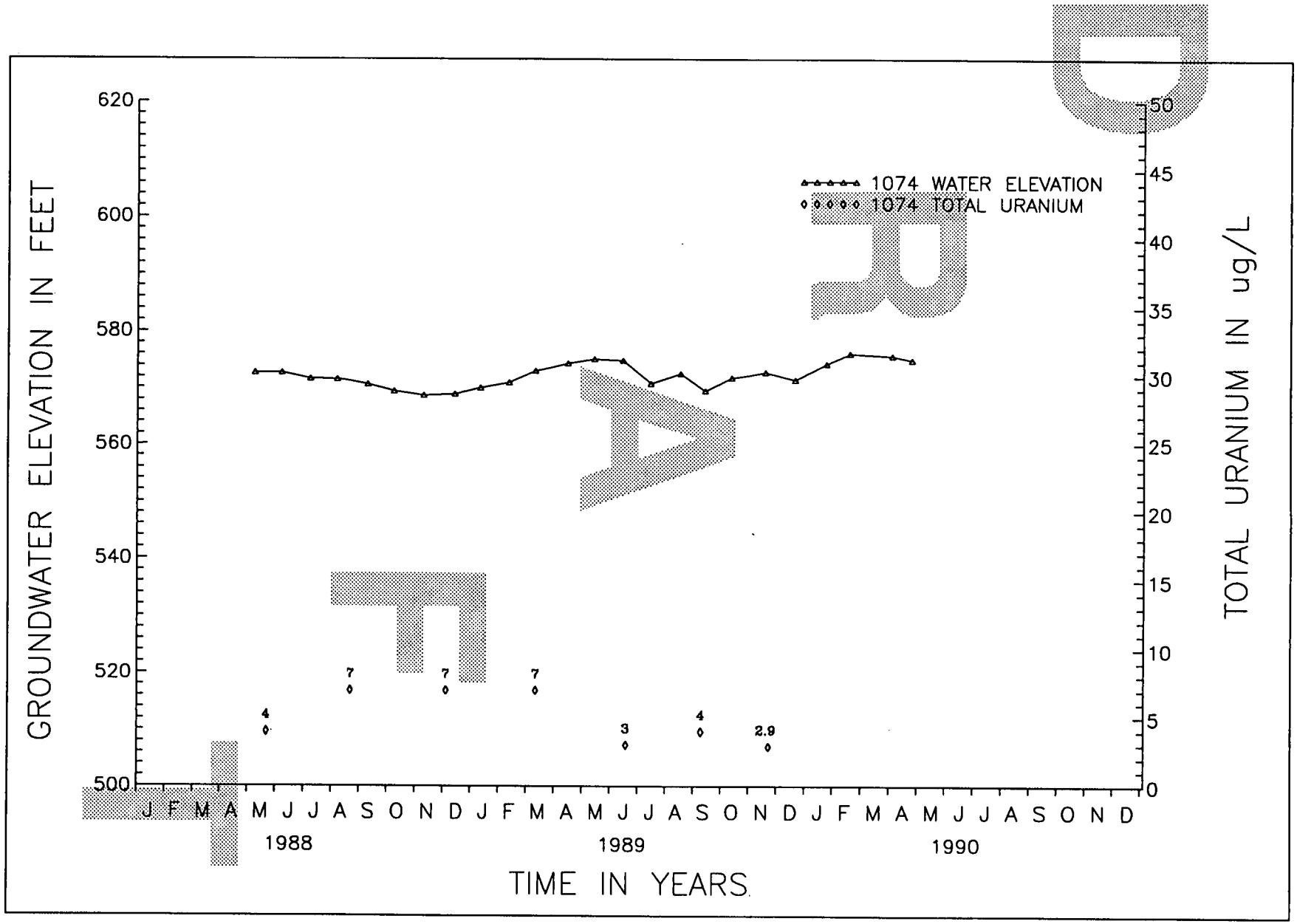


FIGURE N-21. HYDROGRAPH AND TOTAL URANIUM FOR WELL 1074

000023

5 of 7

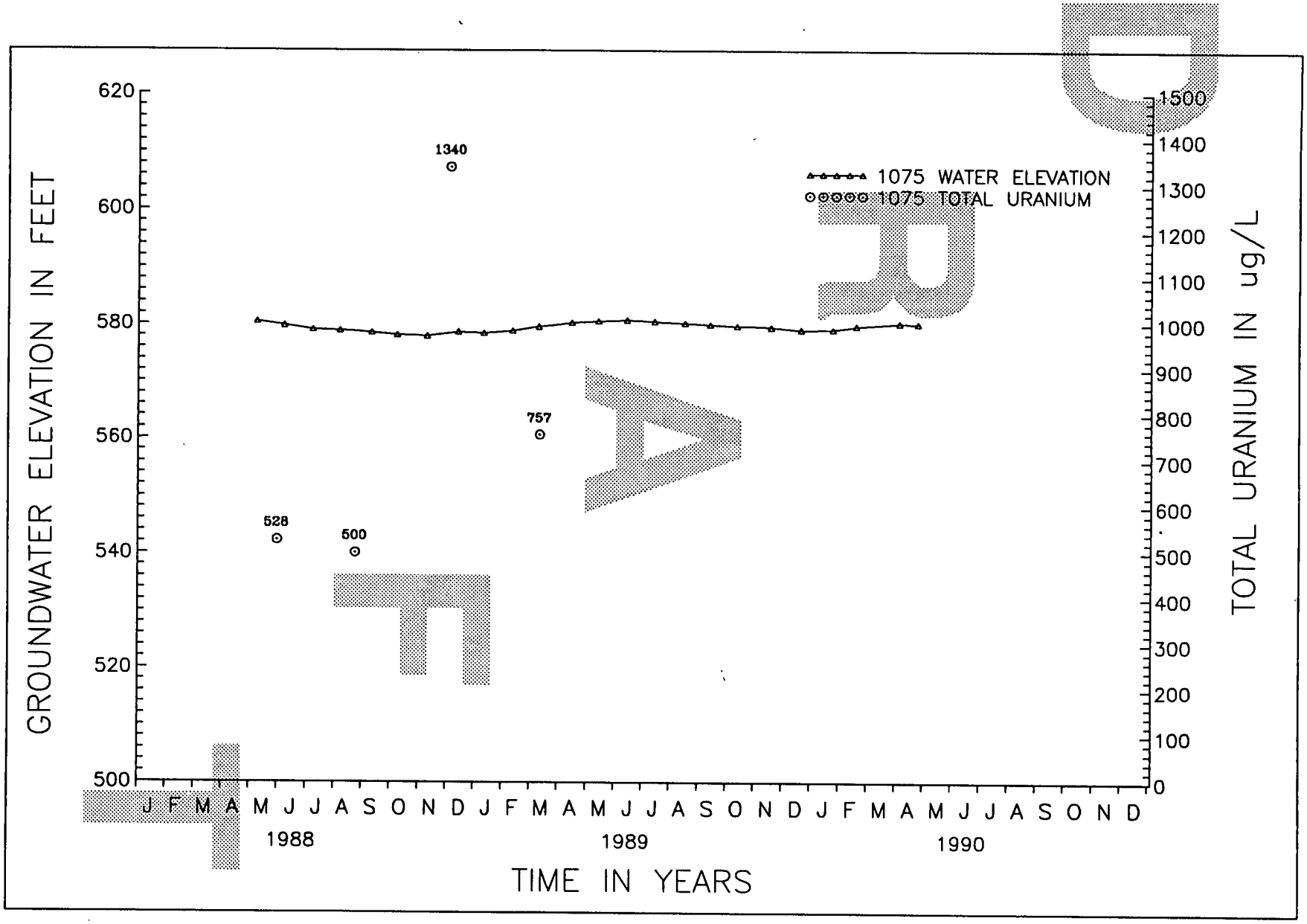


FIGURE N-22. HYDROGRAPH AND TOTAL URANIUM FOR WELL 1075

000024

5617

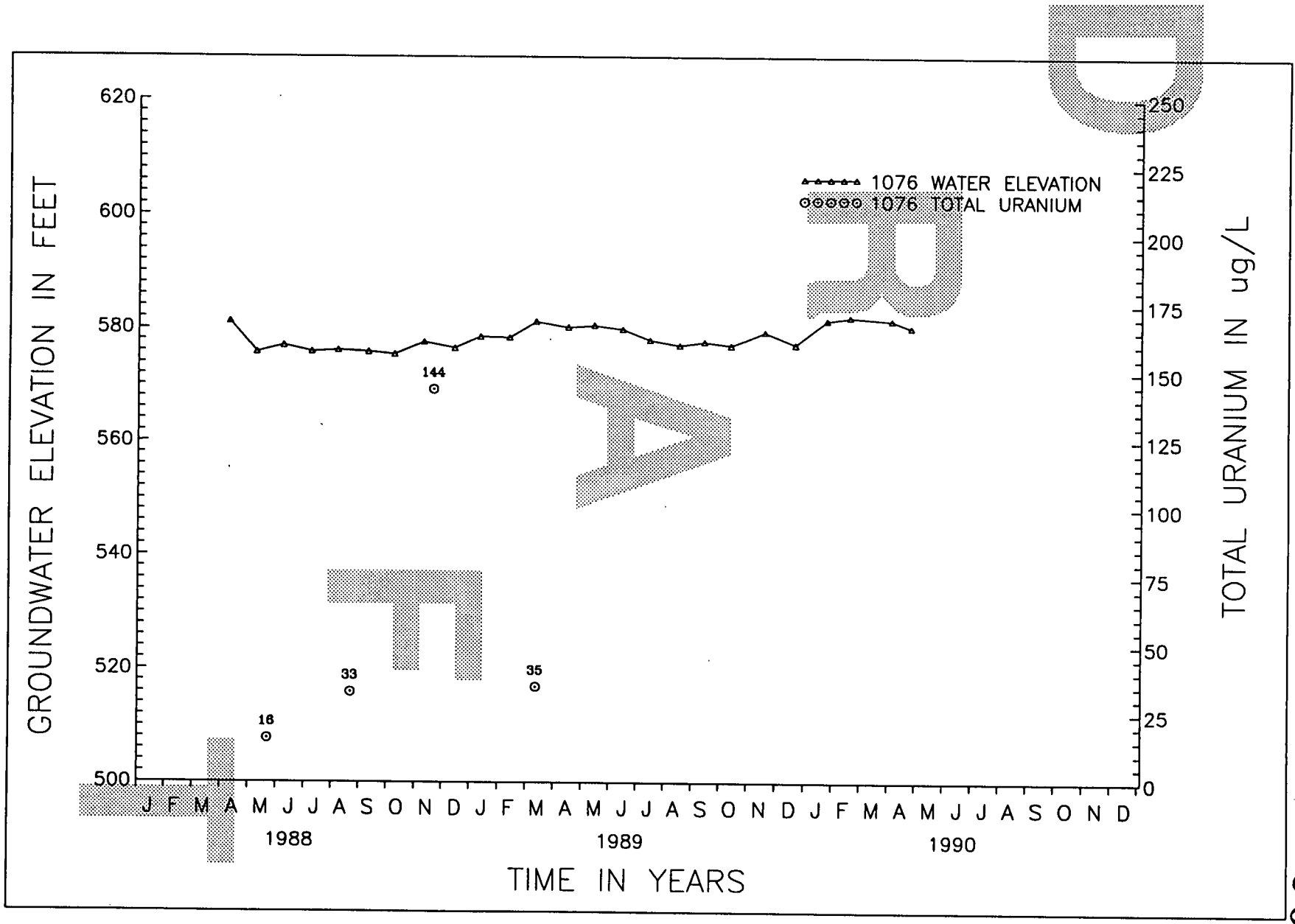


FIGURE N-23. HYDROGRAPH AND TOTAL URANIUM FOR WELL 1076

000025

5617

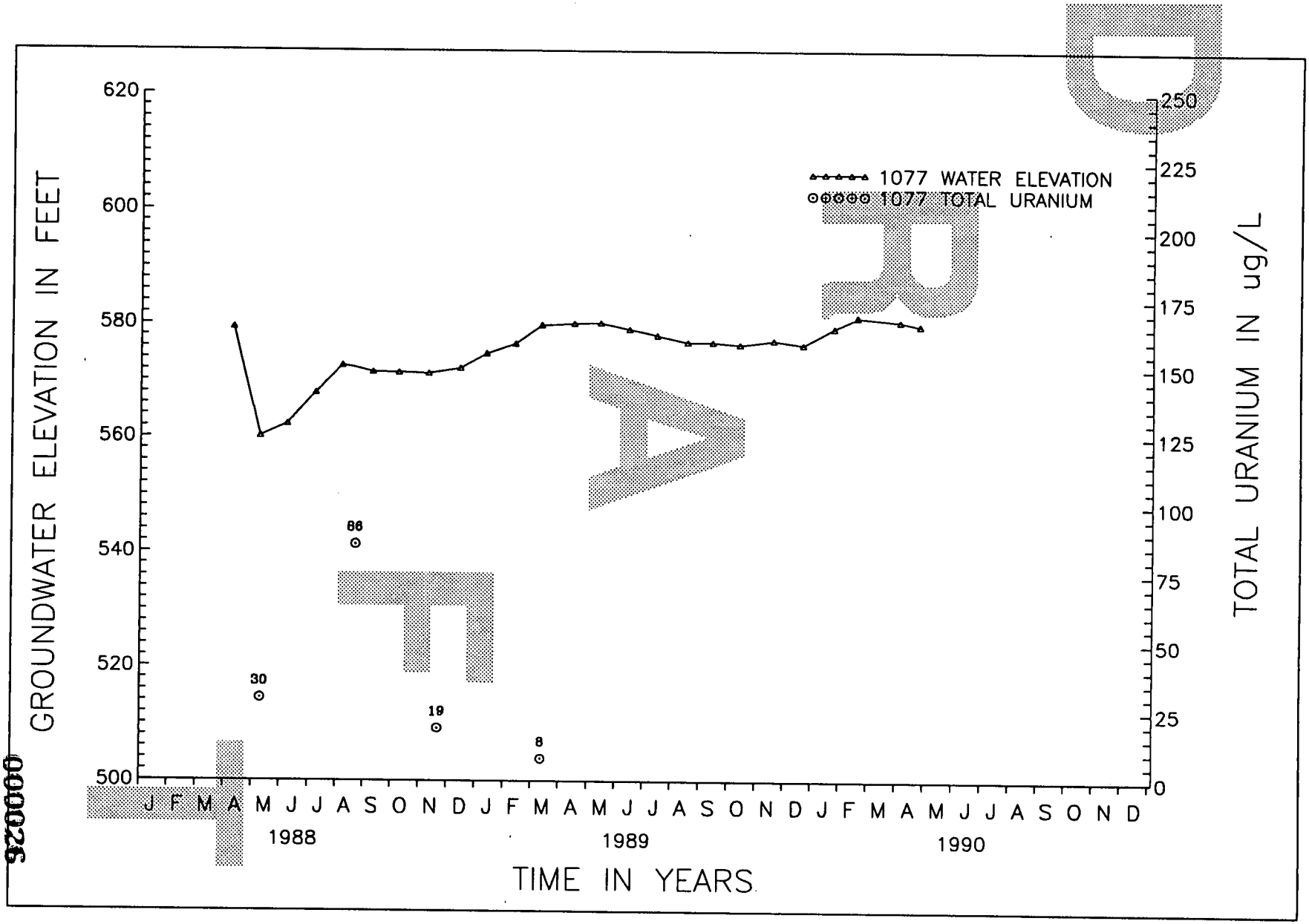


FIGURE N-24. HYDROGRAPH AND TOTAL URANIUM FOR WELL 1077

000026

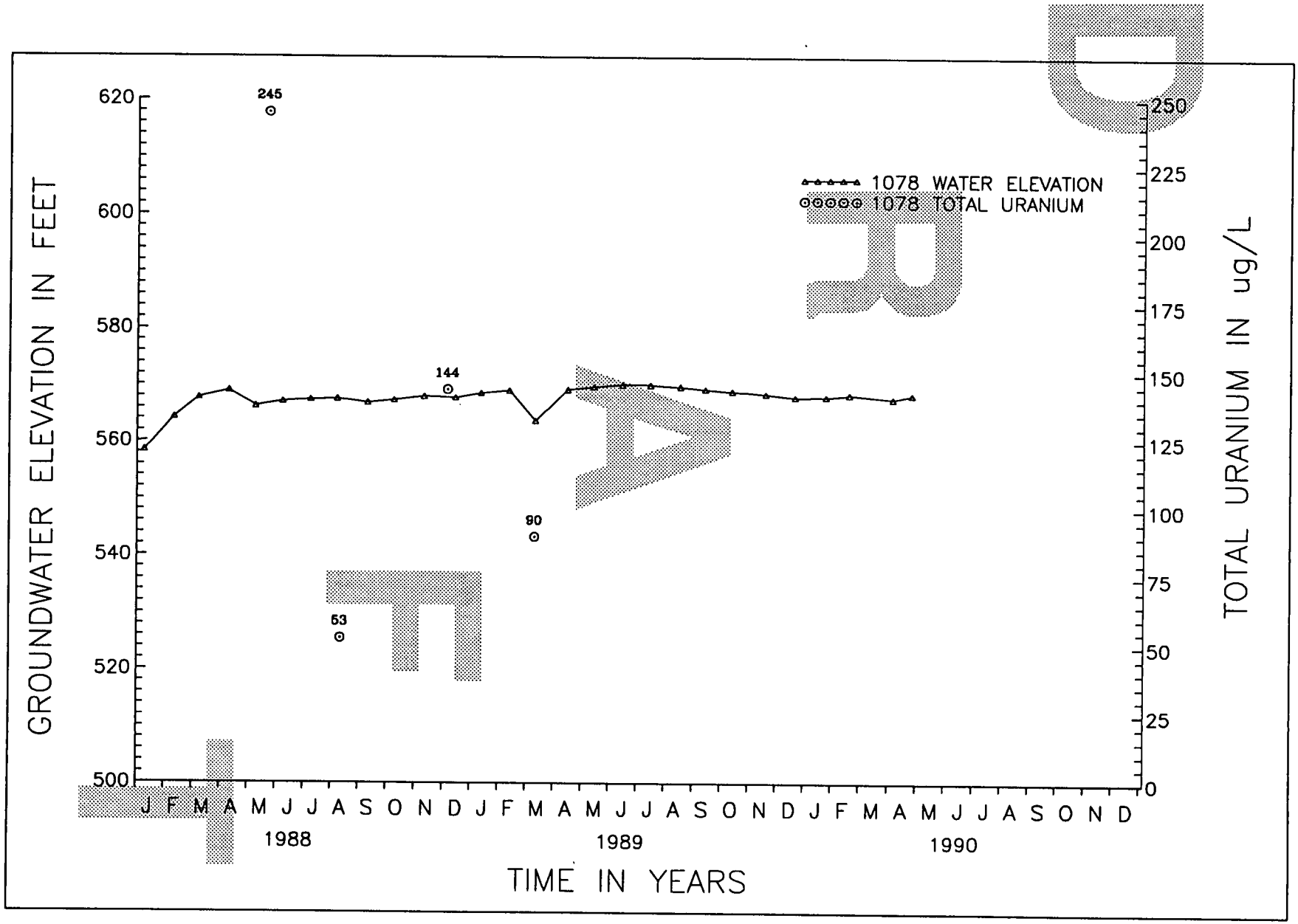


FIGURE N-25. HYDROGRAPH AND TOTAL URANIUM FOR WELL 1078

000027

6617

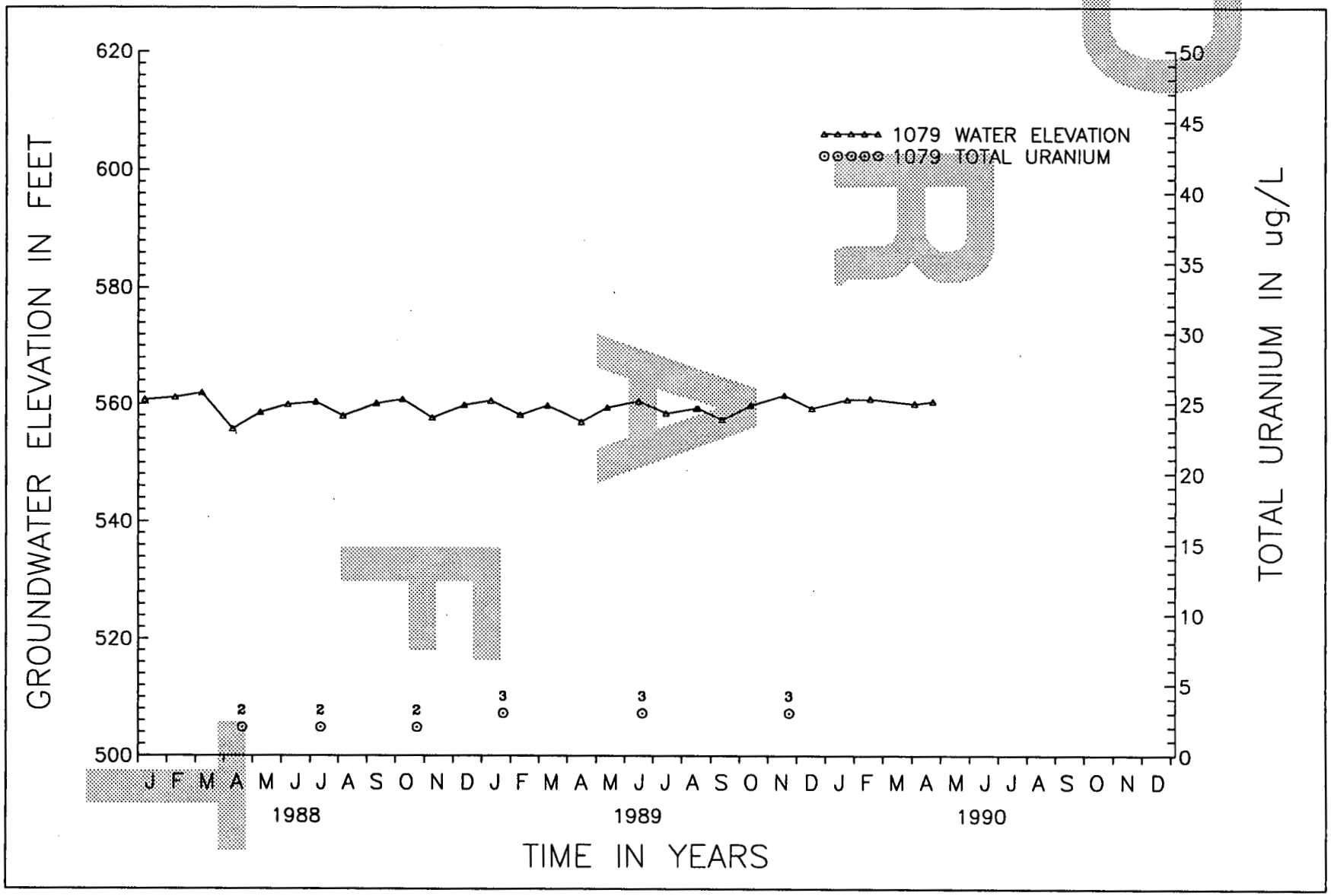


FIGURE N-26. HYDROGRAPH AND TOTAL URANIUM FOR WELL 1079

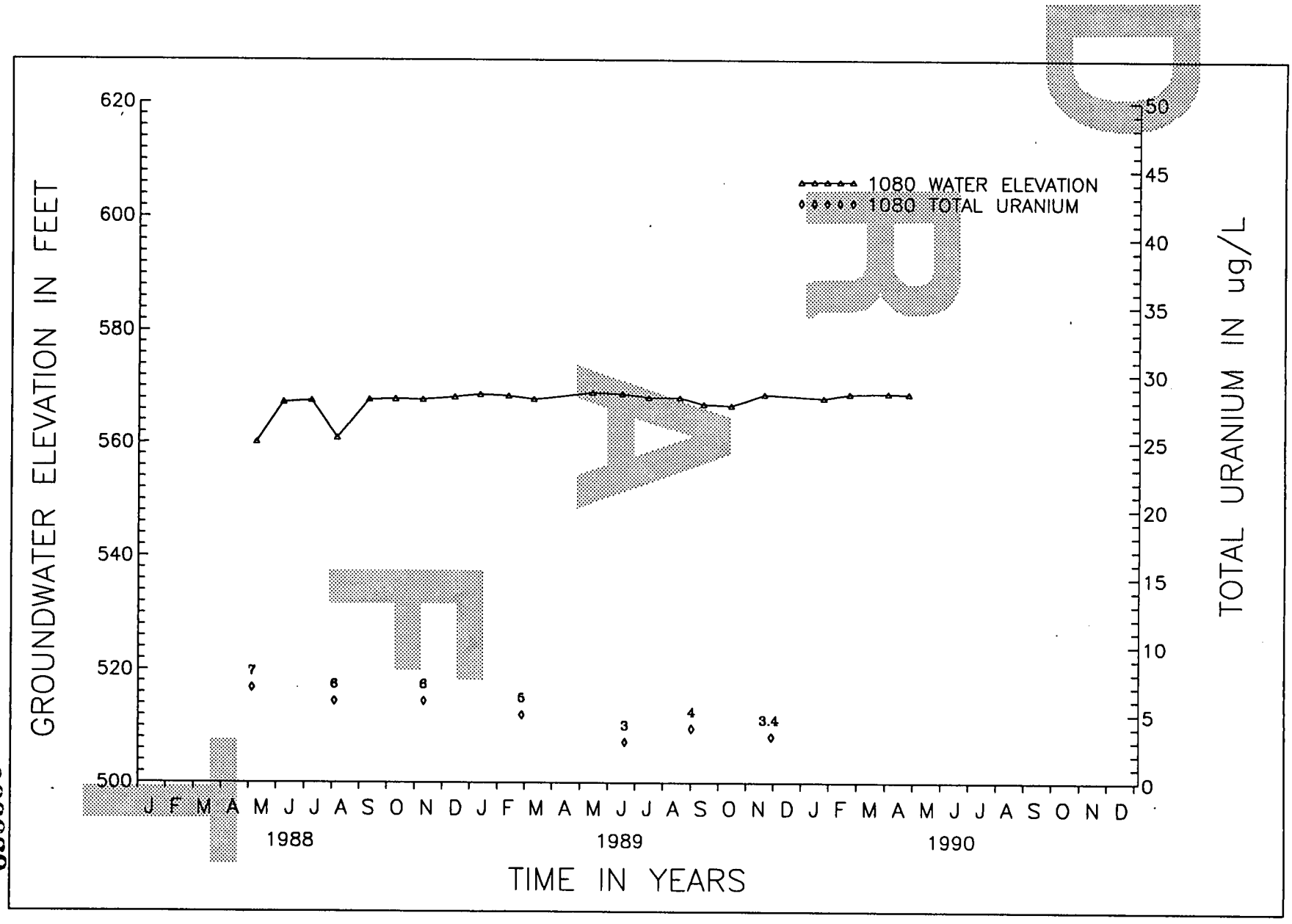


FIGURE N-27. HYDROGRAPH AND TOTAL URANIUM FOR WELL 1080

000029

6617

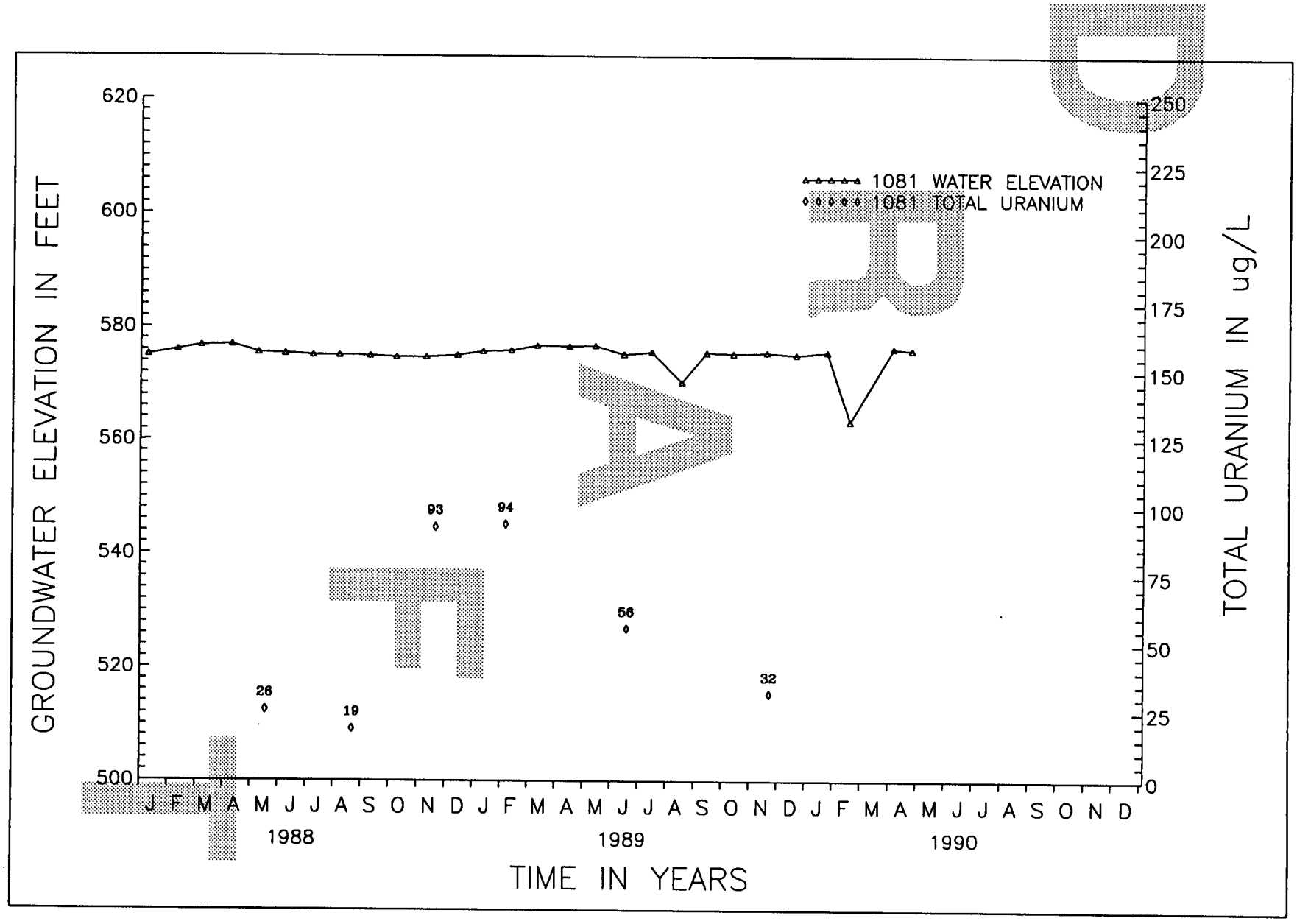


FIGURE N-28. HYDROGRAPH AND TOTAL URANIUM FOR WELL 1081

000030

561 2

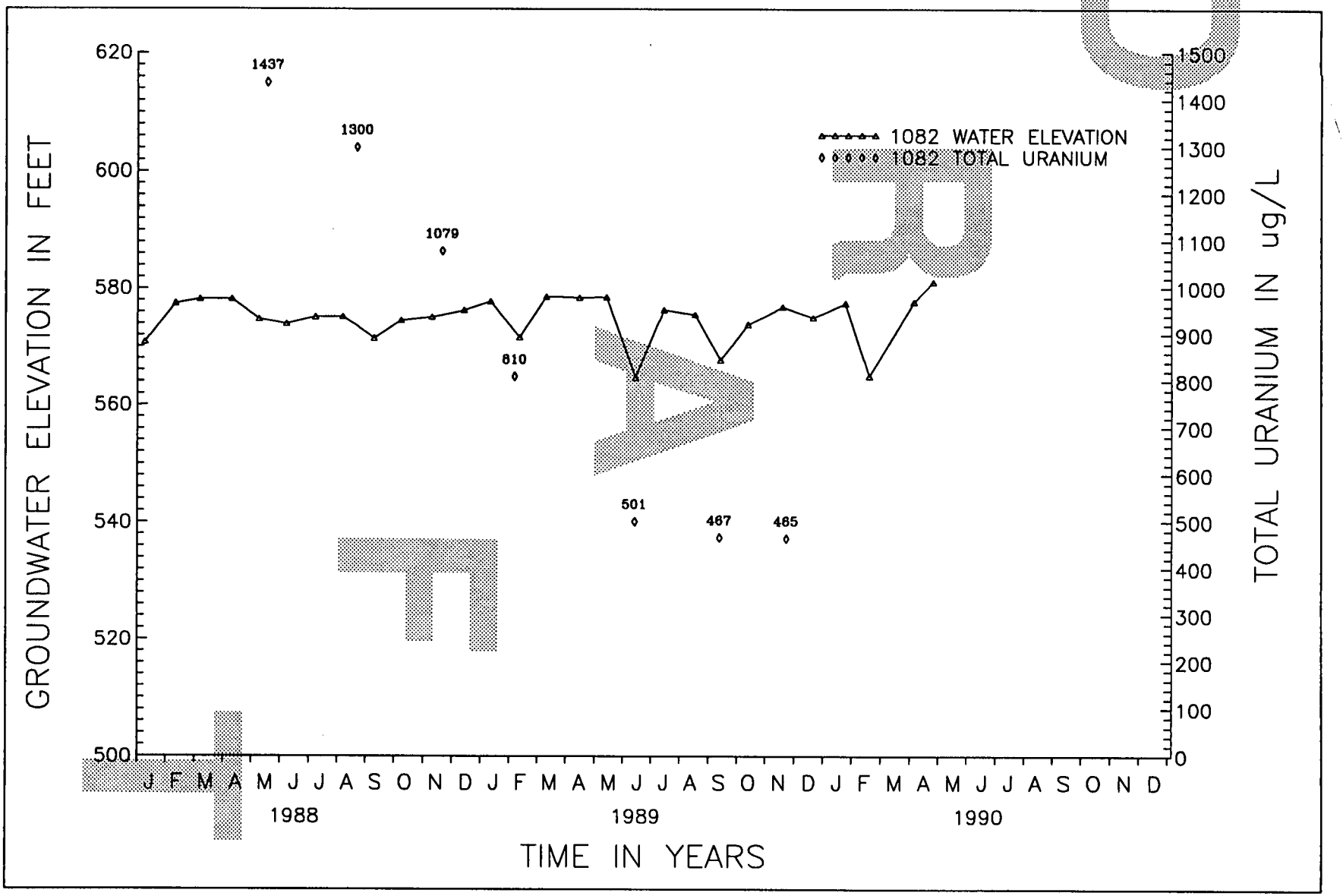


FIGURE N-29. HYDROGRAPH AND TOTAL URANIUM FOR WELL 1082

000031

5 of 7

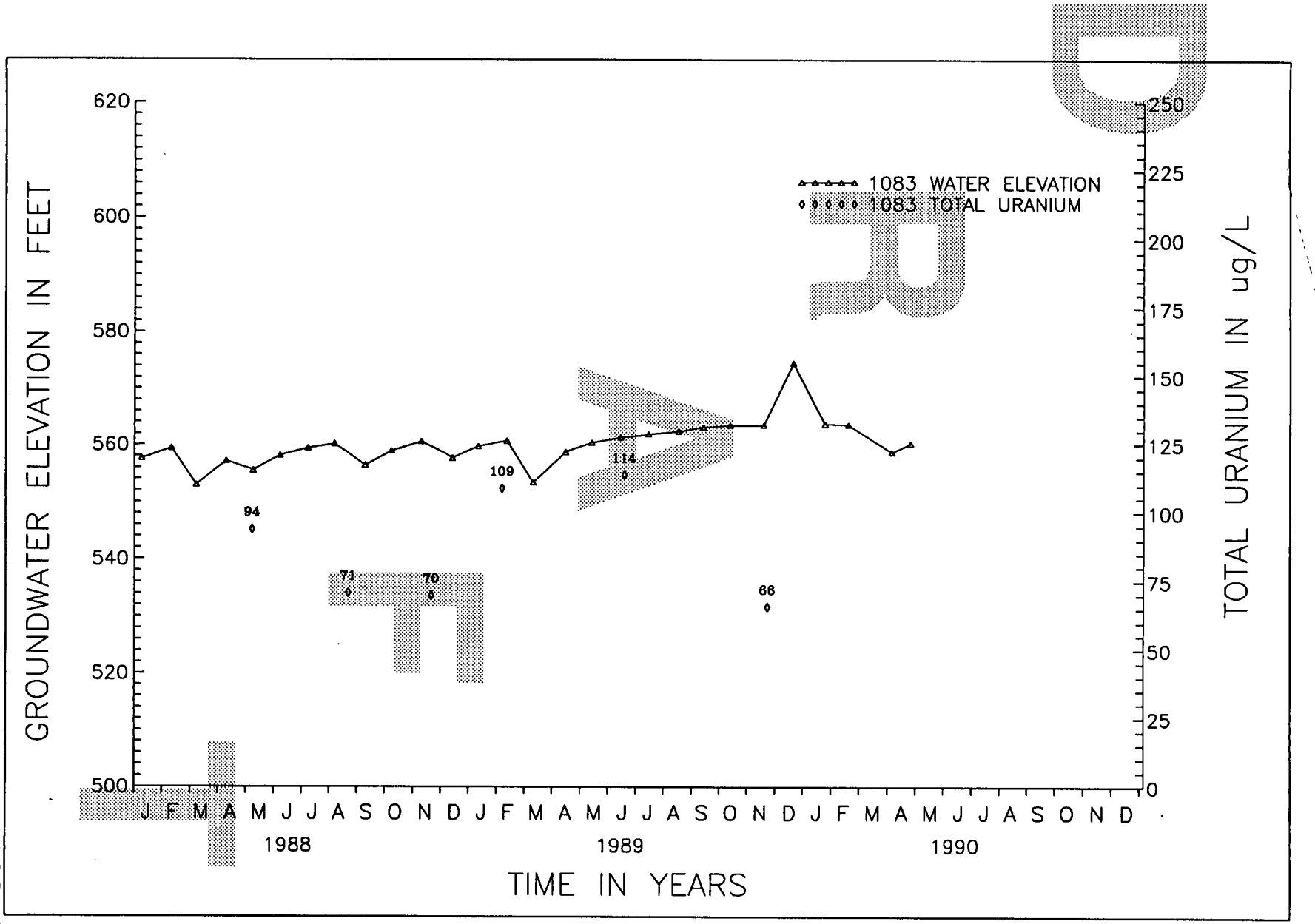


FIGURE N-30. HYDROGRAPH AND TOTAL URANIUM FOR WELL 1083

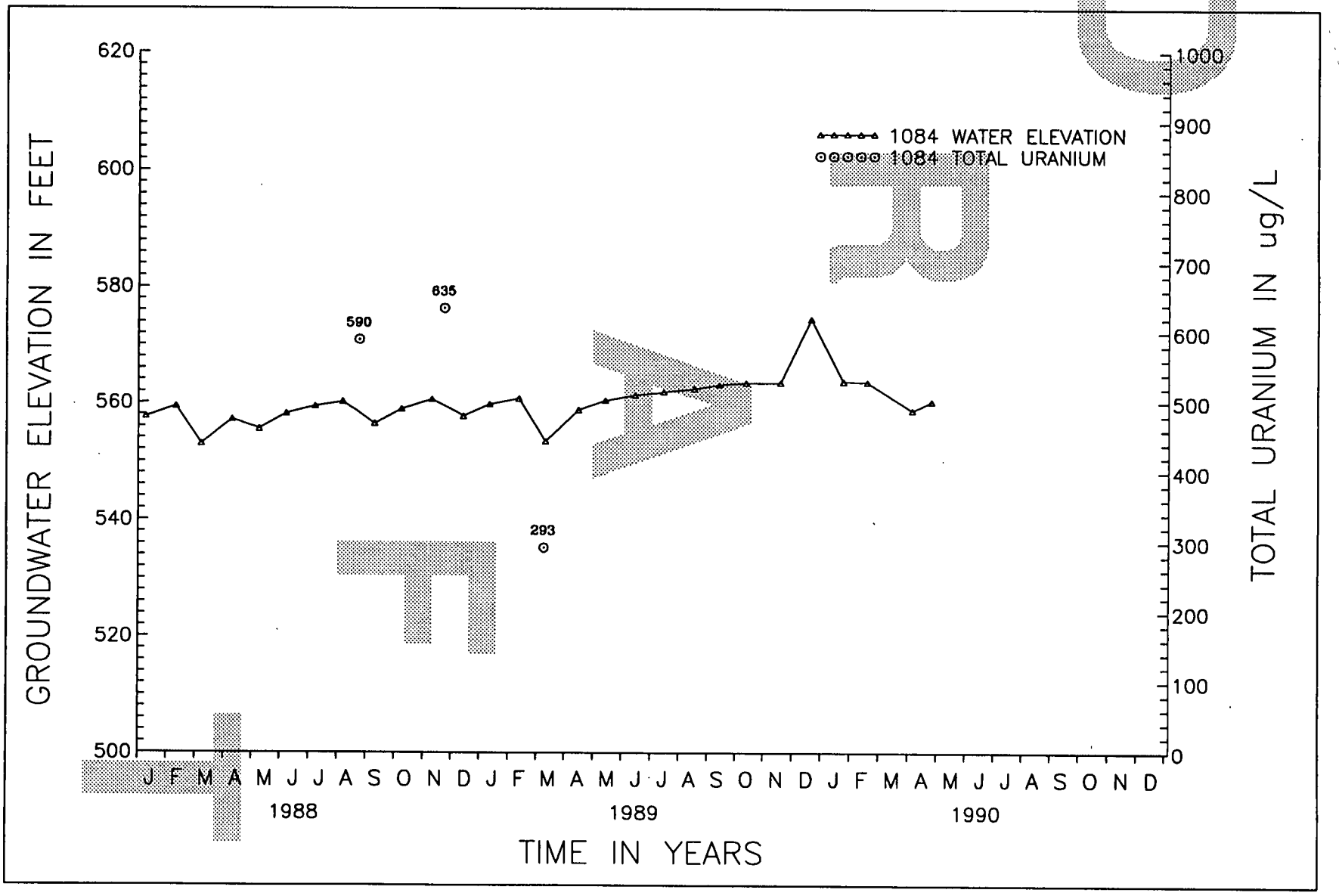


FIGURE N-31. HYDROGRAPH AND TOTAL URANIUM FOR WELL 1084

000033

2 of 2

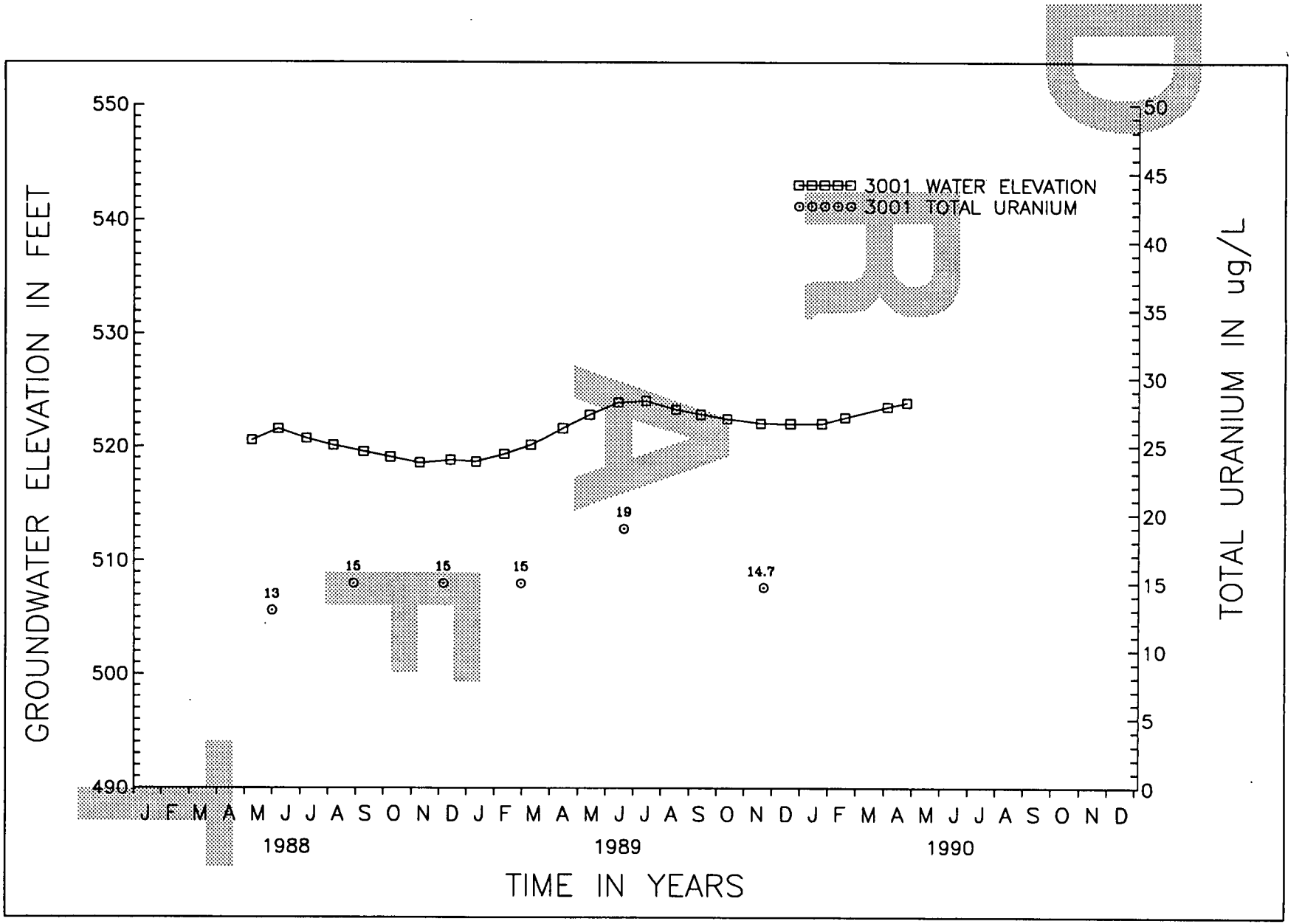


FIGURE N-32. HYDROGRAPH AND TOTAL URANIUM FOR WELL CLUSTER AT LOCATION 001

000034

6617

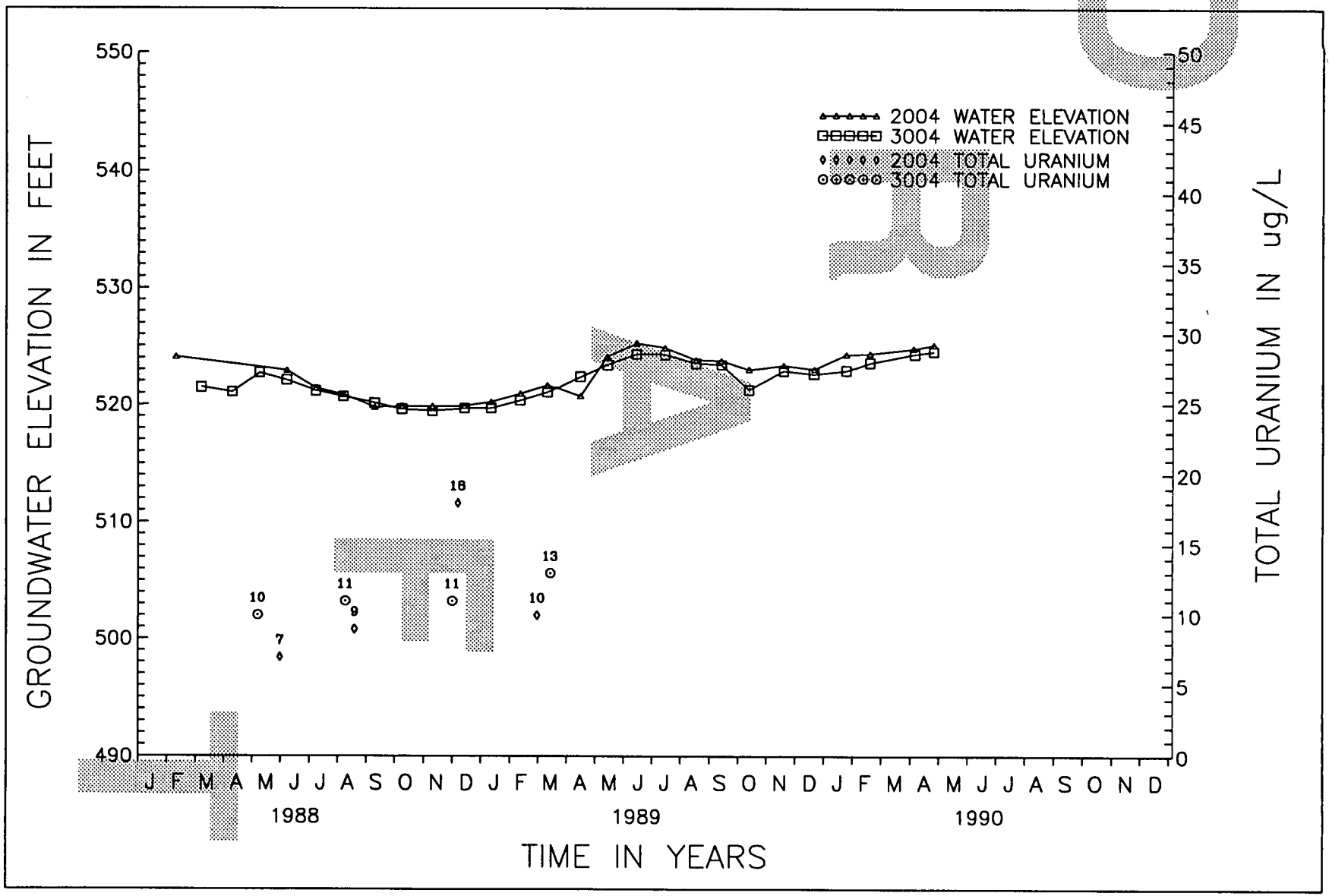


FIGURE N-33. HYDROGRAPH AND TOTAL URANIUM FOR WELL CLUSTER AT LOCATION 004

000035

5 of 7

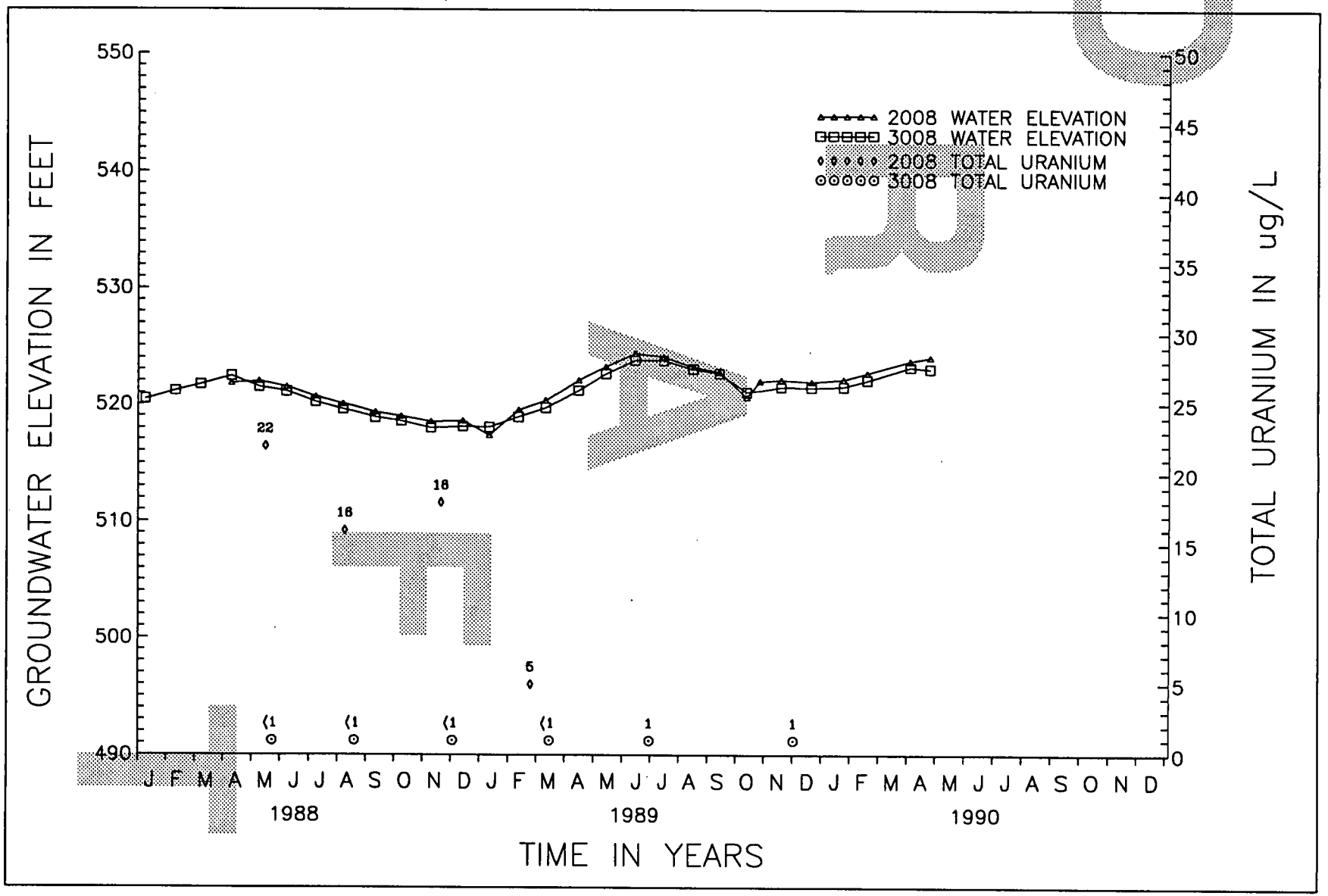


FIGURE N-34. HYDROGRAPH AND TOTAL URANIUM FOR WELL CLUSTER AT LOCATION 008

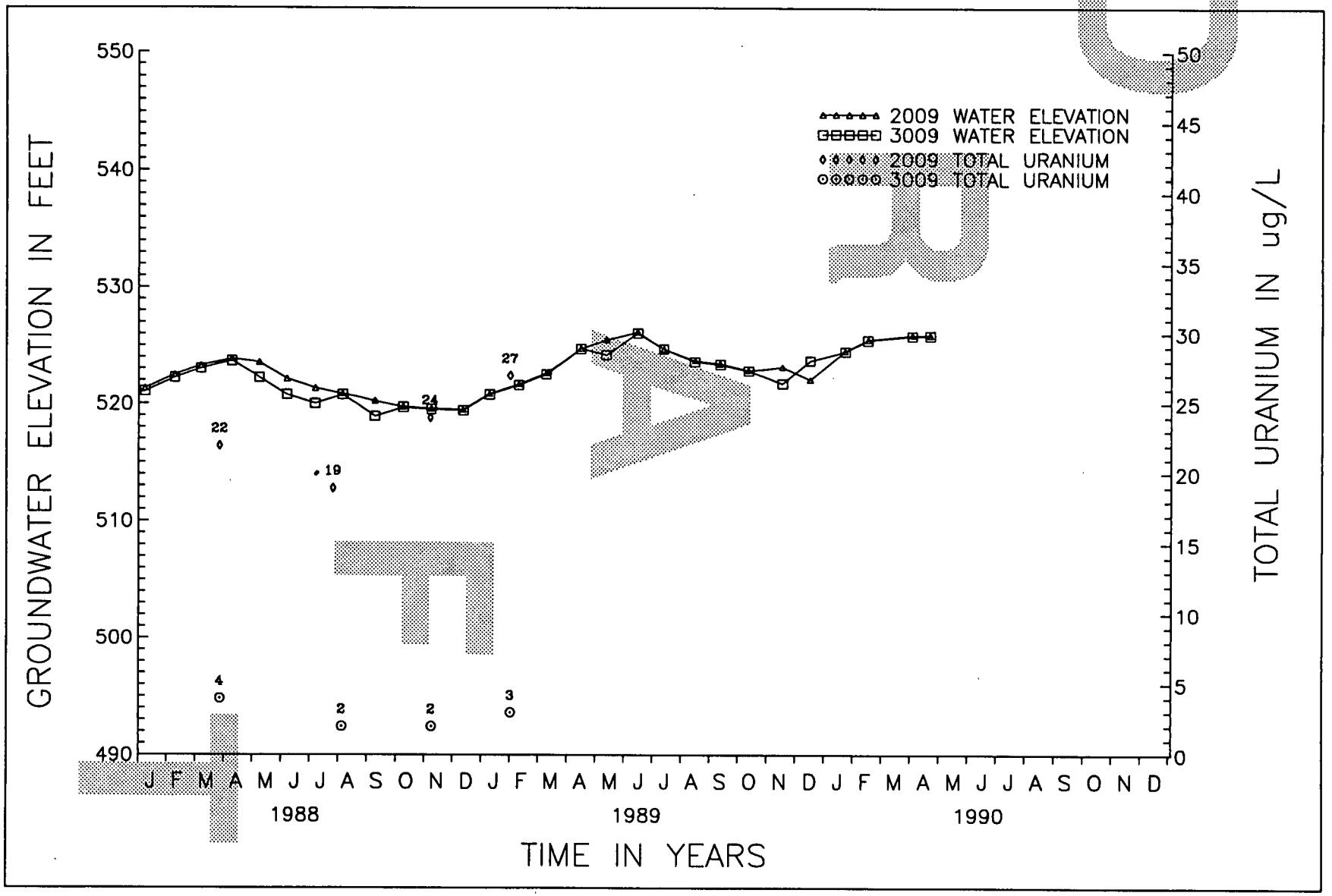


FIGURE N-35. HYDROGRAPH AND TOTAL URANIUM FOR WELL CLUSTER AT LOCATION 009

000037

6617

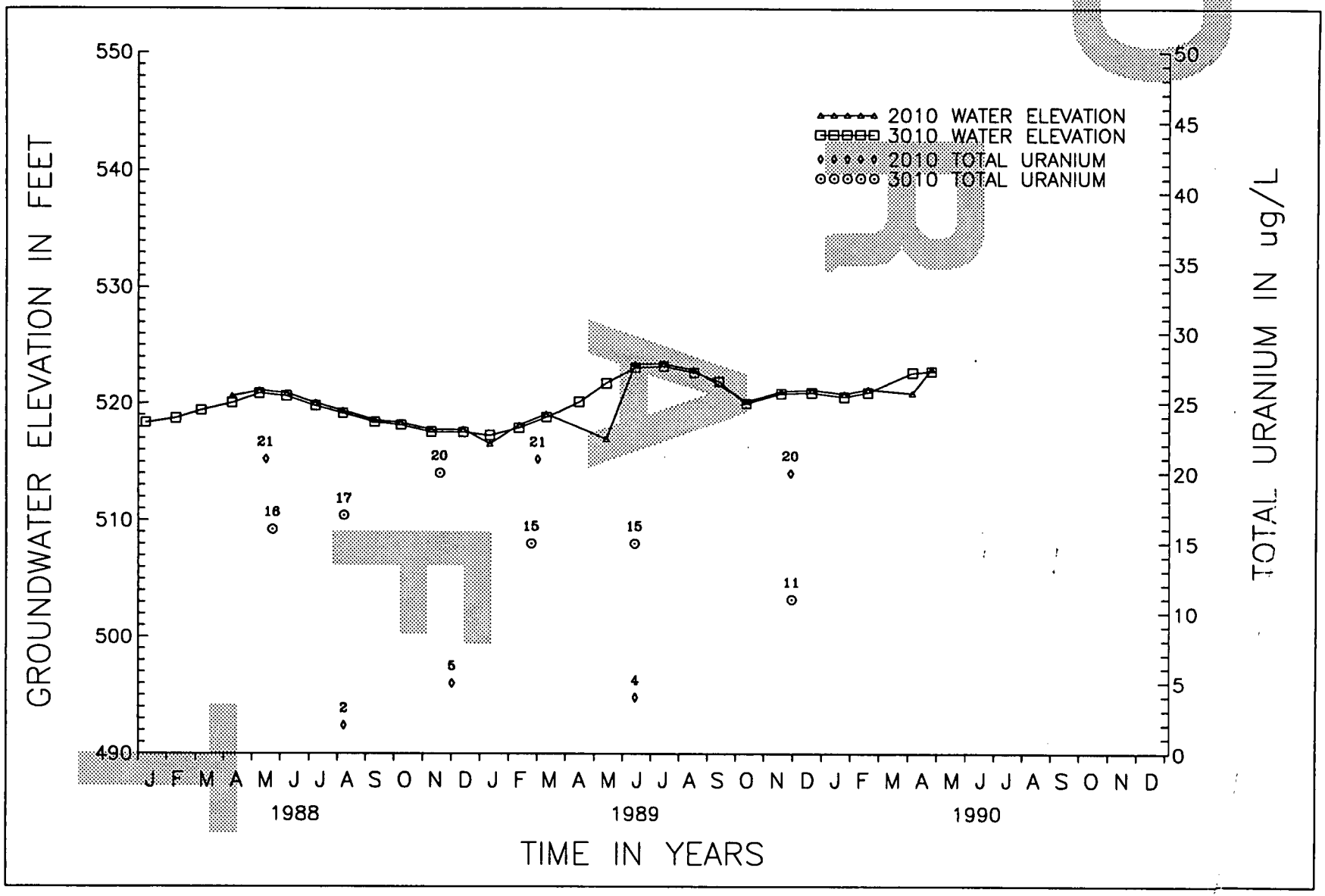


FIGURE N-36. HYDROGRAPH AND TOTAL URANIUM FOR WELL CLUSTER AT LOCATION 010

000038

5612

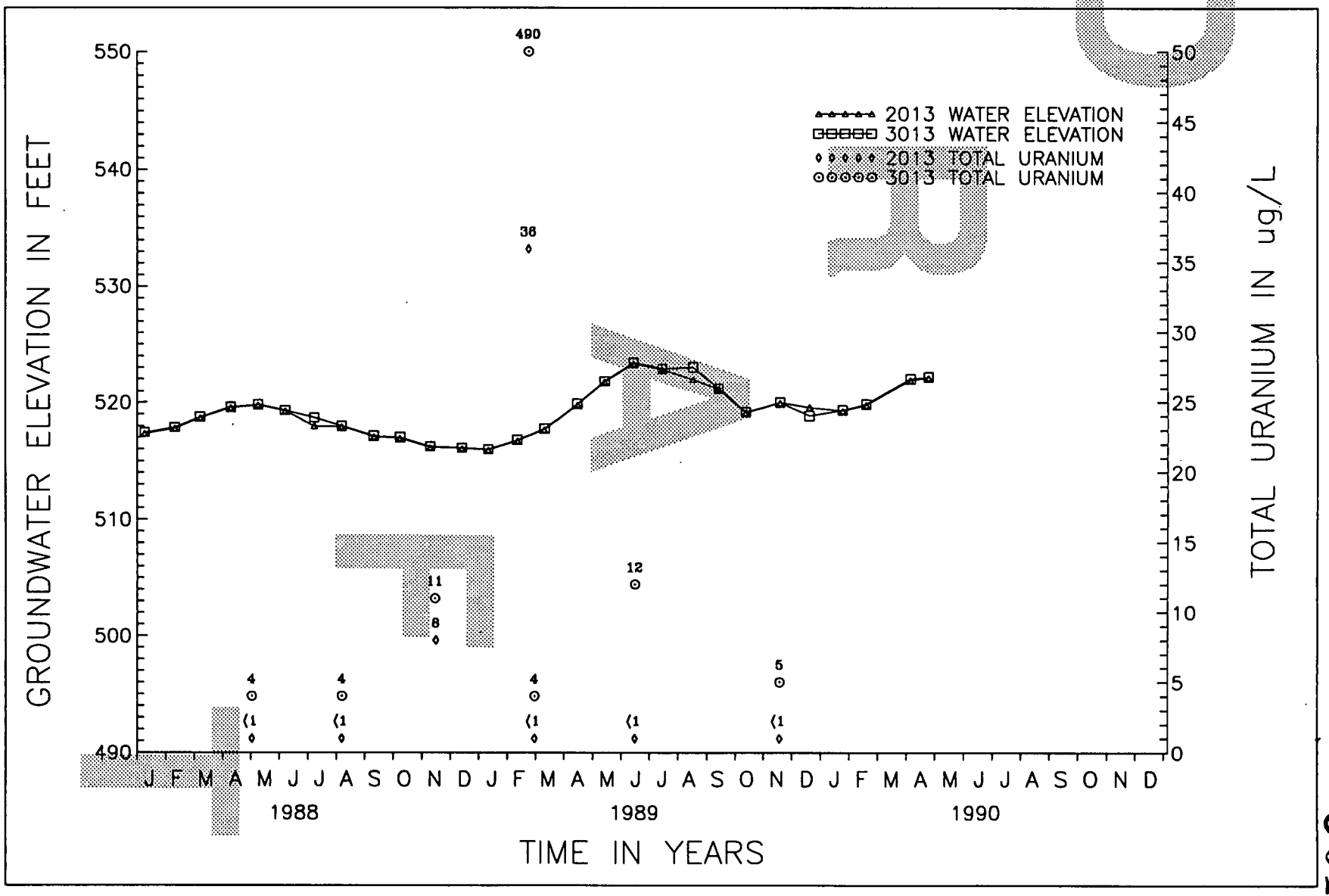


FIGURE N-37. HYDROGRAPH AND TOTAL URANIUM FOR WELL CLUSTER AT LOCATION 013

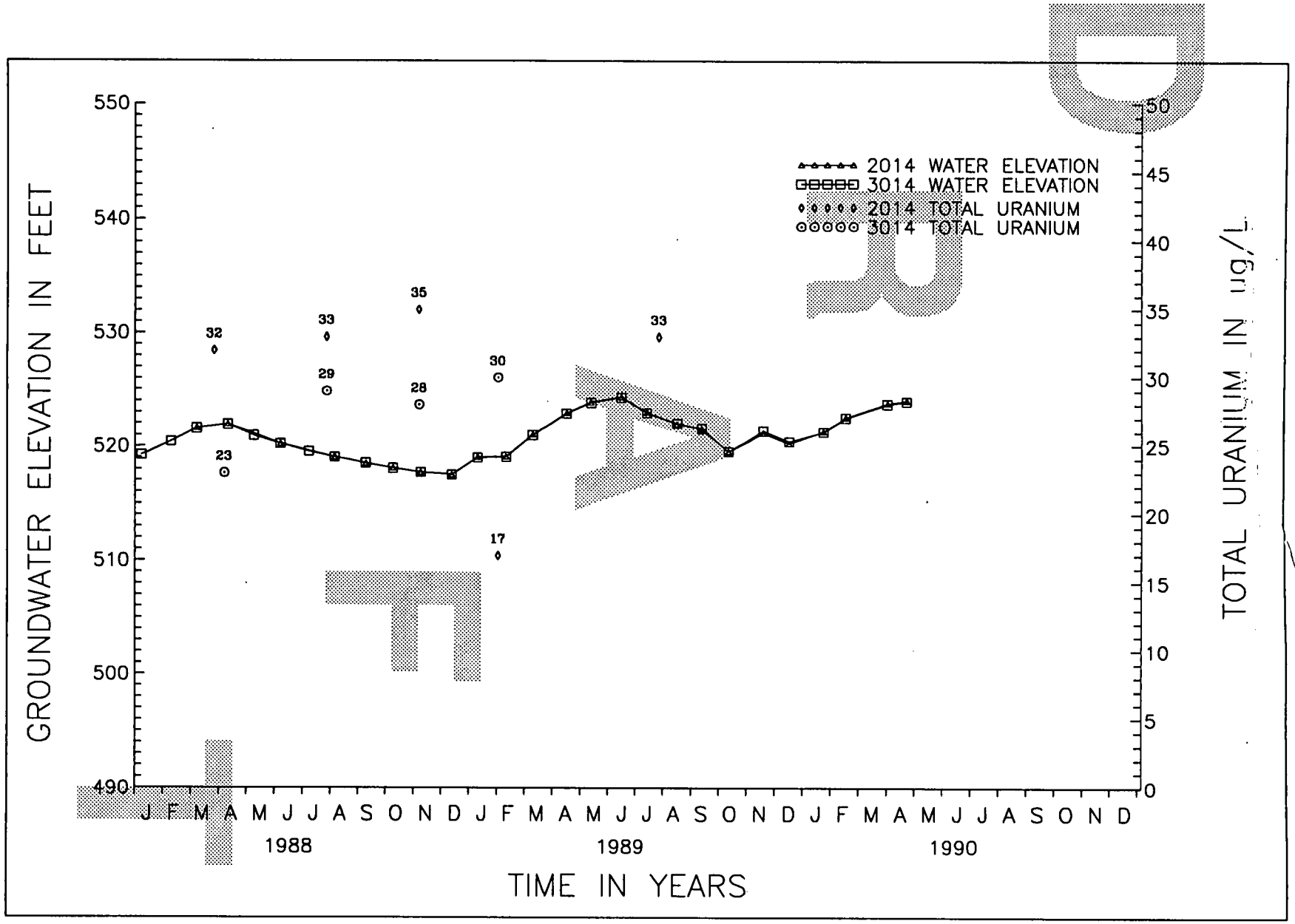


FIGURE N-38. HYDROGRAPH AND TOTAL URANIUM FOR WELL CLUSTER AT LOCATION 014

000040

5617

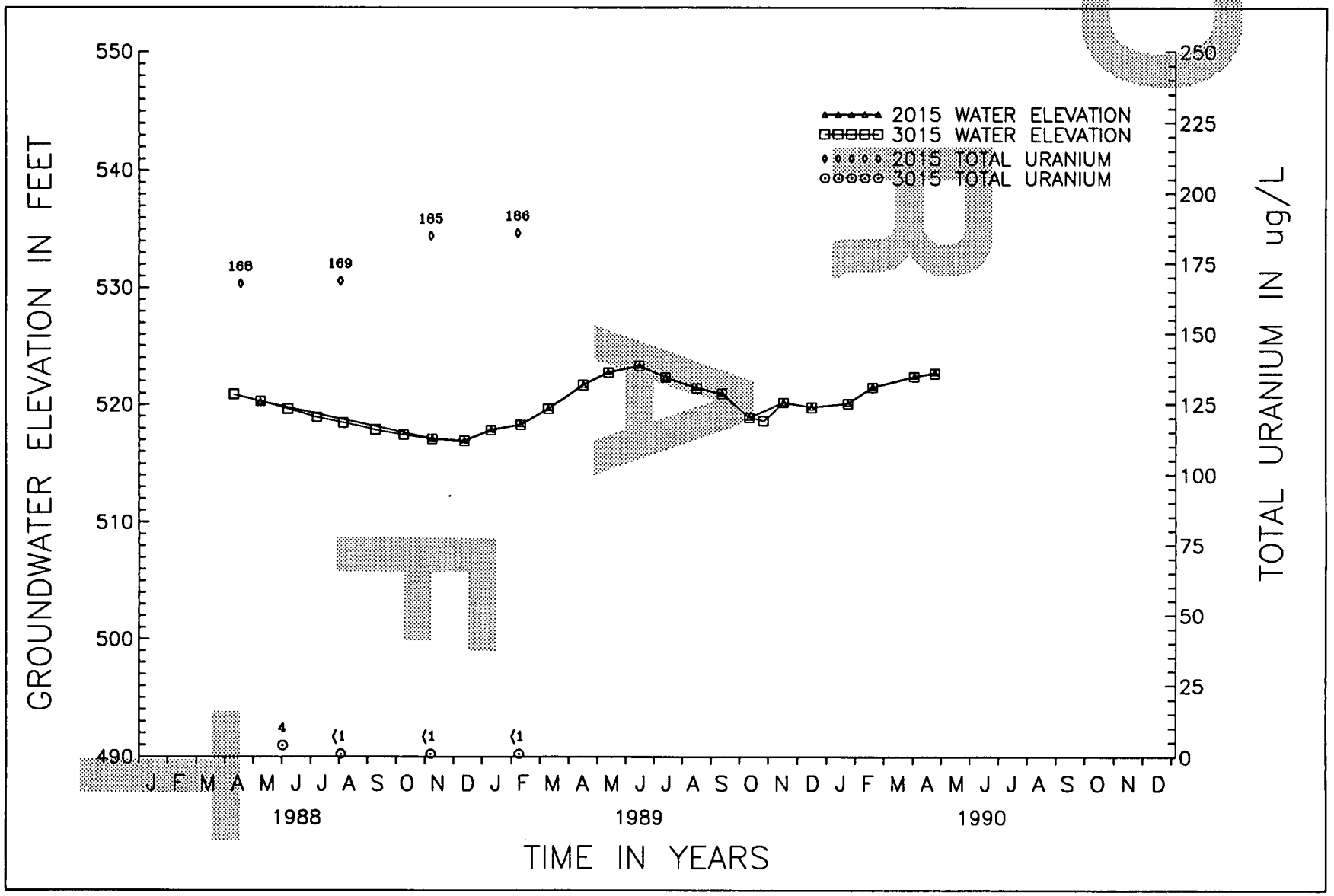


FIGURE N-39. HYDROGRAPH AND TOTAL URANIUM FOR WELL CLUSTER AT LOCATION 015

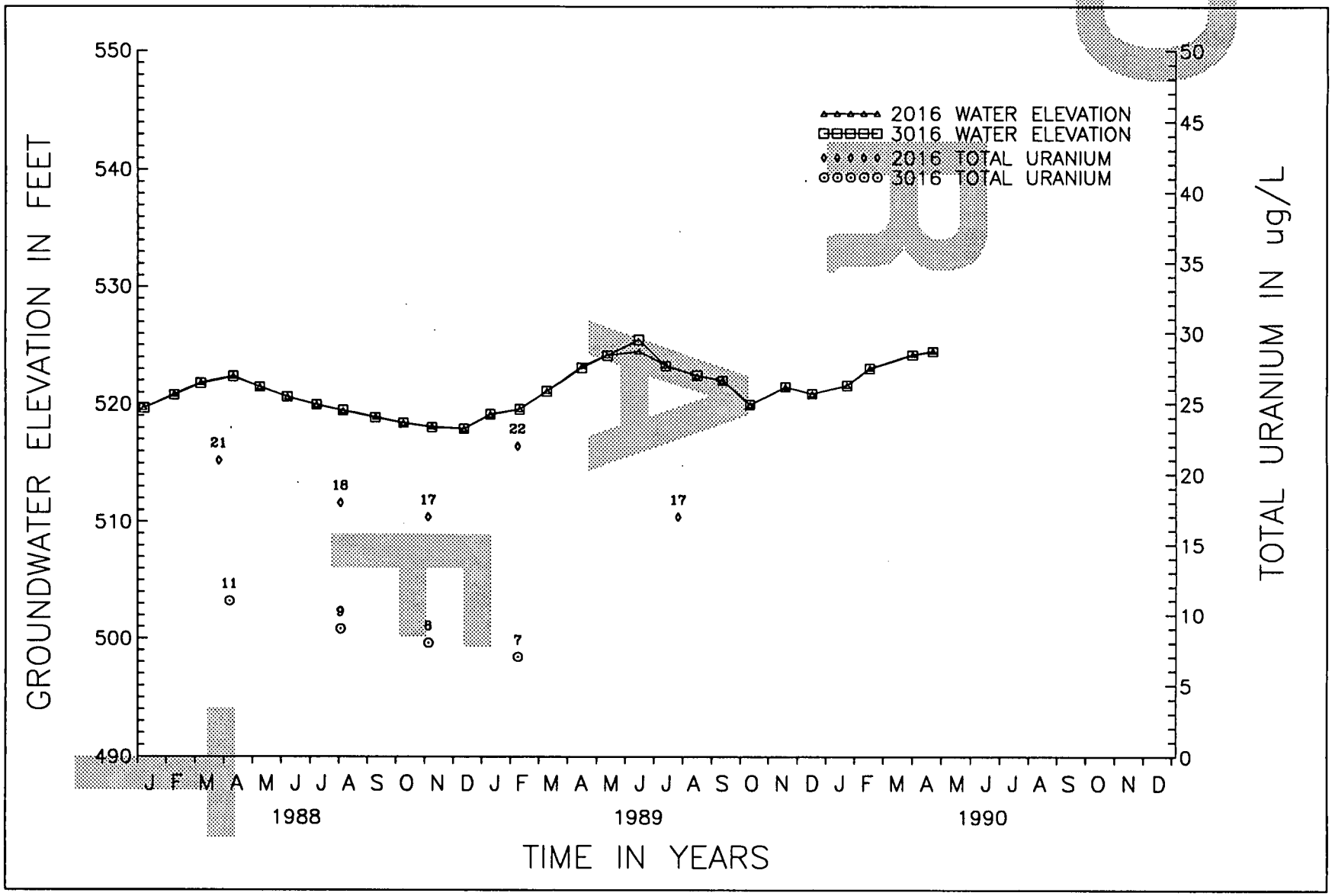


FIGURE N-40. HYDROGRAPH AND TOTAL URANIUM FOR WELL CLUSTER AT LOCATION 016

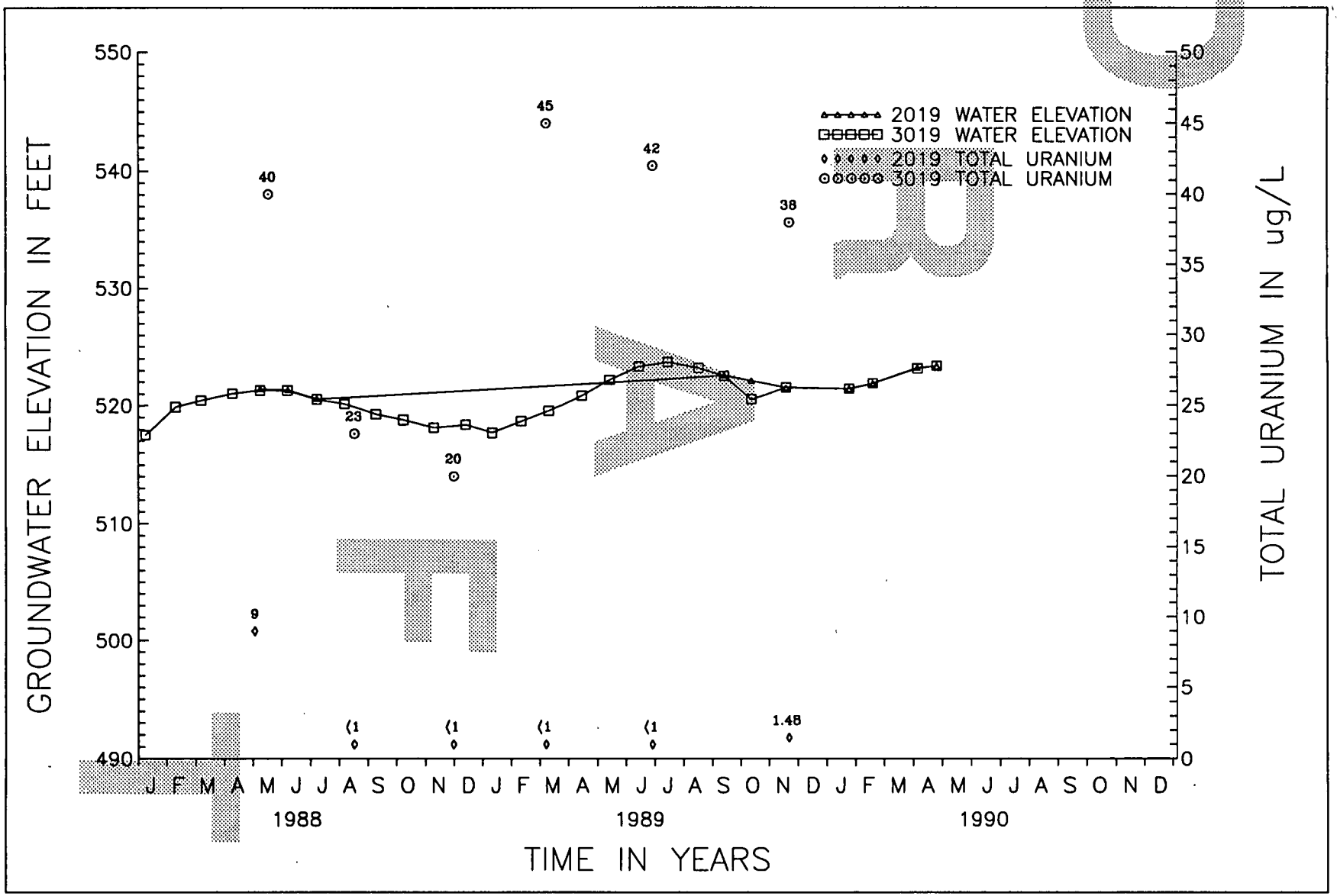


FIGURE N-41. HYDROGRAPH AND TOTAL URANIUM FOR WELL CLUSTER AT LOCATION 019

000043

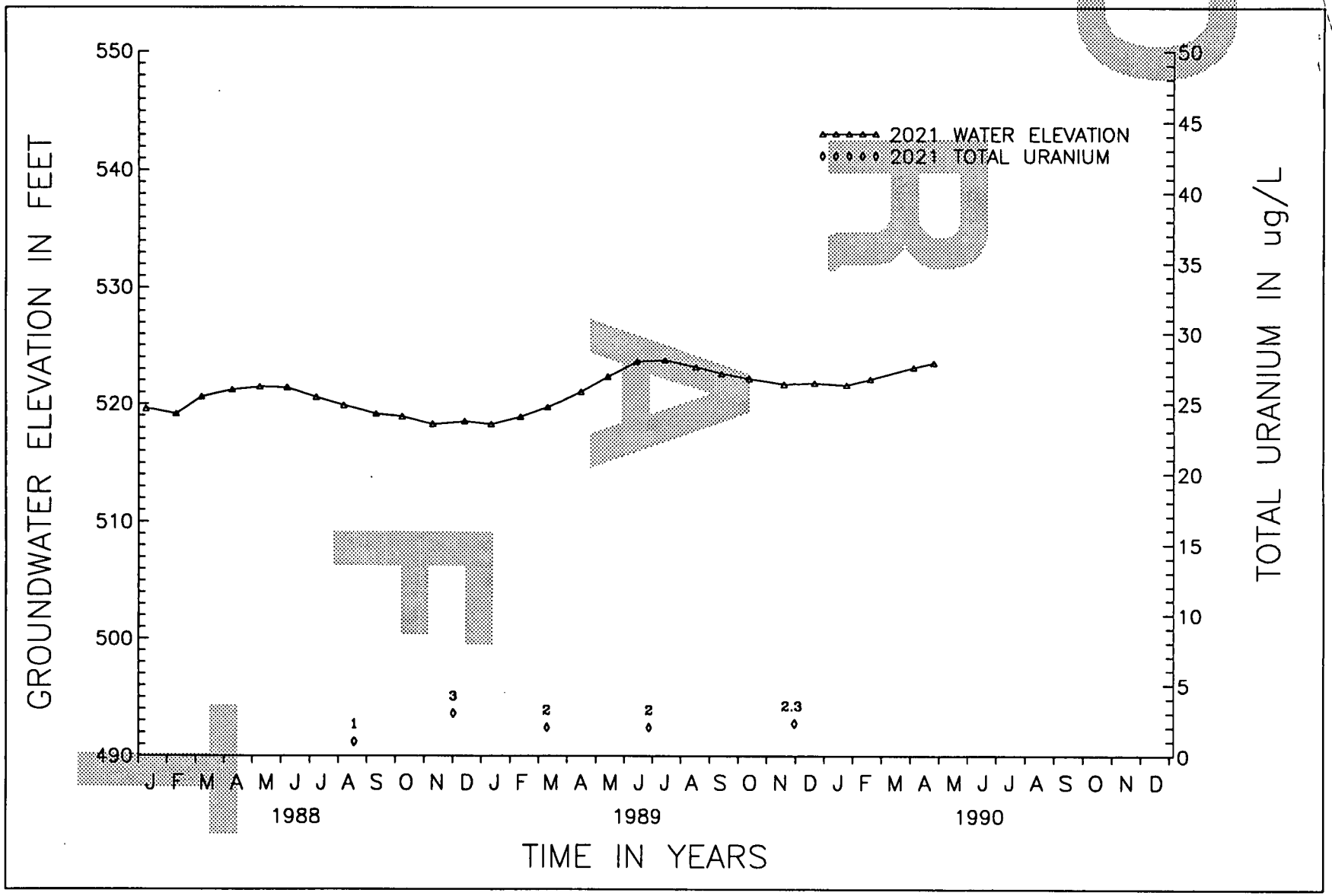


FIGURE N-42. HYDROGRAPH AND TOTAL URANIUM FOR WELL CLUSTER AT LOCATION 021

000044

5617

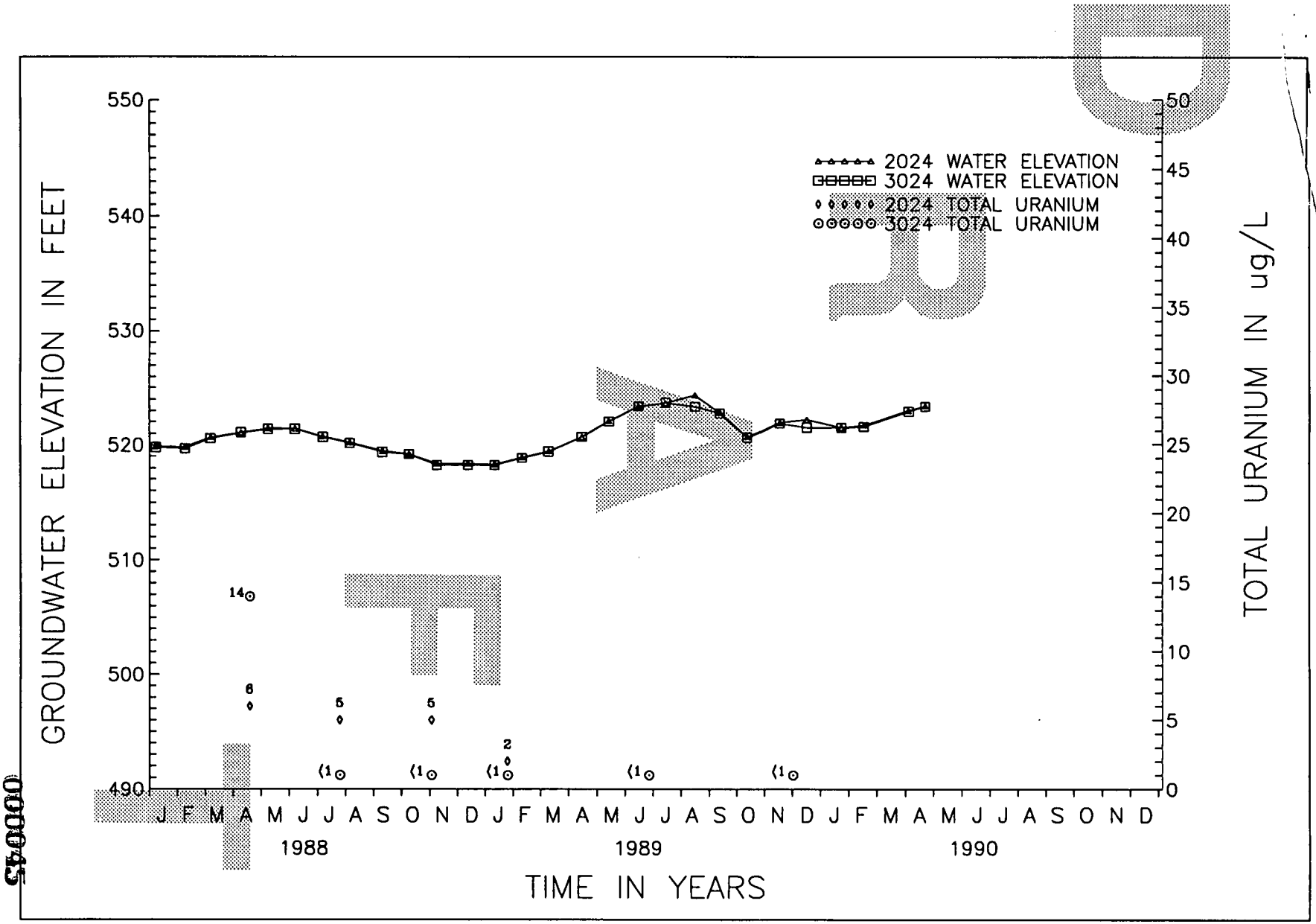


FIGURE N-43. HYDROGRAPH AND TOTAL URANIUM FOR WELL CLUSTER AT LOCATION 024

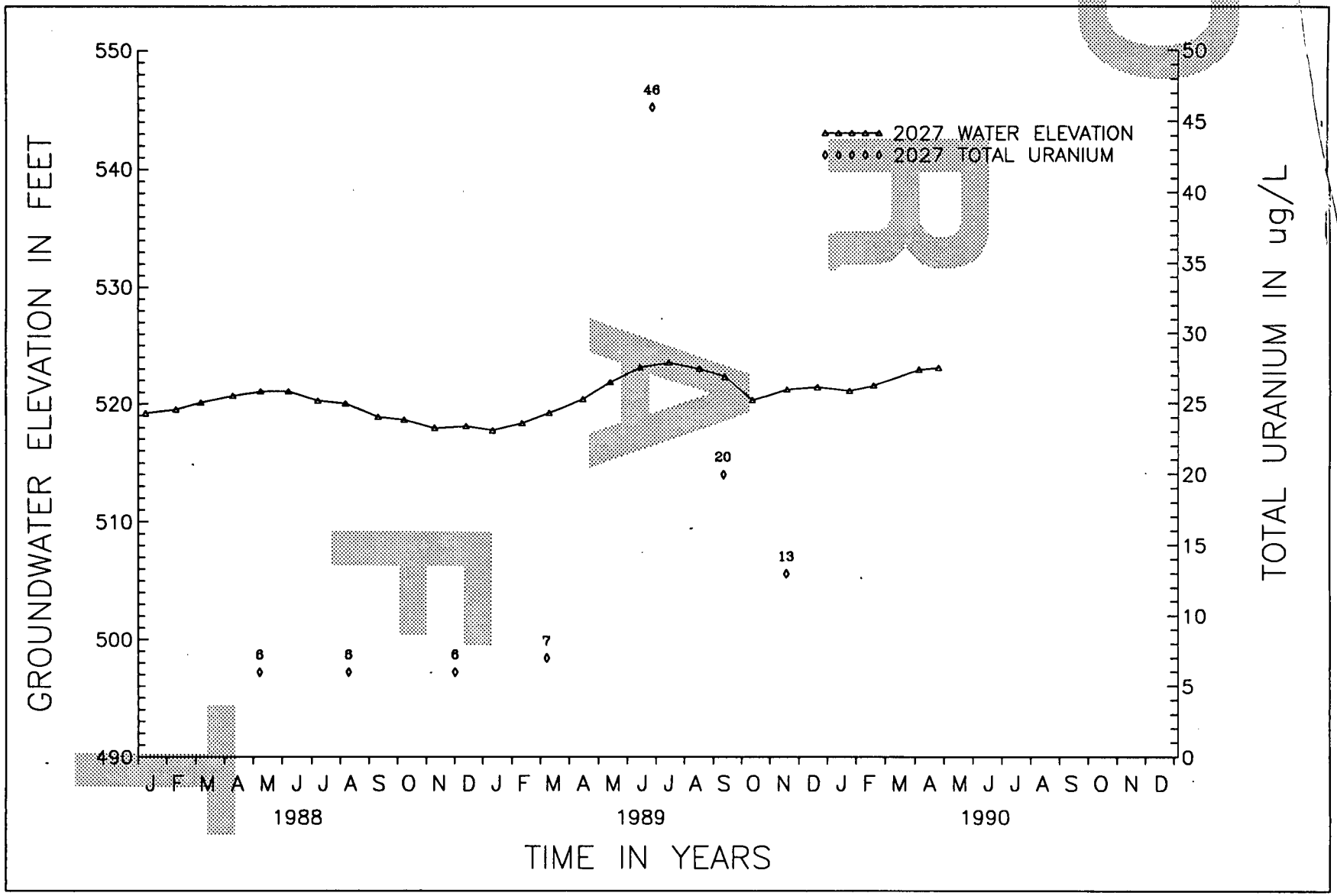


FIGURE N-44. HYDROGRAPH AND TOTAL URANIUM FOR WELL CLUSTER AT LOCATION 027

000046

6617

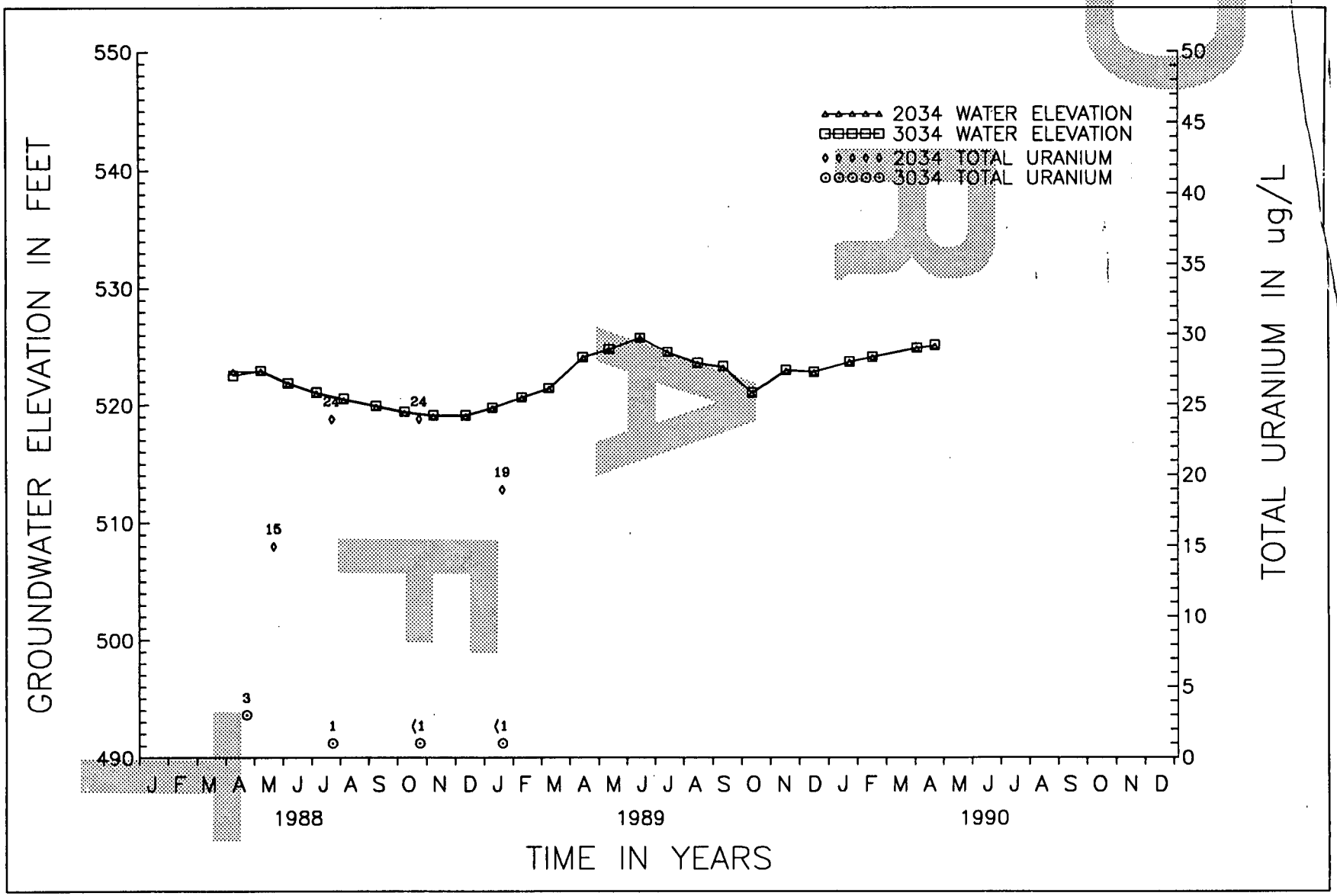


FIGURE N-45. HYDROGRAPH AND TOTAL URANIUM FOR WELL CLUSTER AT LOCATION 034

000047

5617

# HISTORICAL URANIUM CONCENTRATION VERSUS TIME GRAPHS

Appendix O contains historical uranium concentration versus time graphs for wells where records extend back before the RI/FS began.

DRAFT

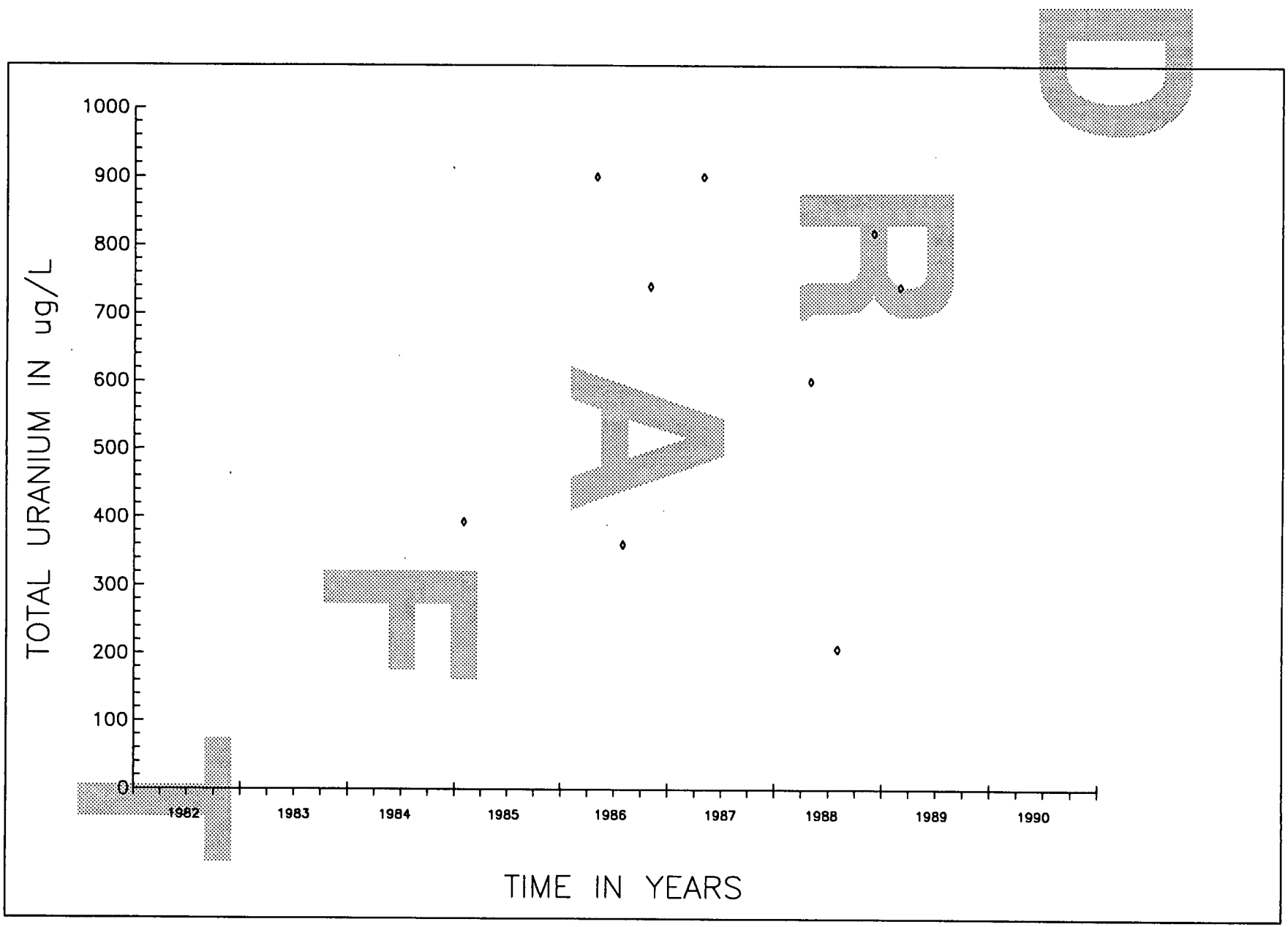


FIGURE O-1. TOTAL URANIUM CONCENTRATION VS. TIME FOR WELL 1019

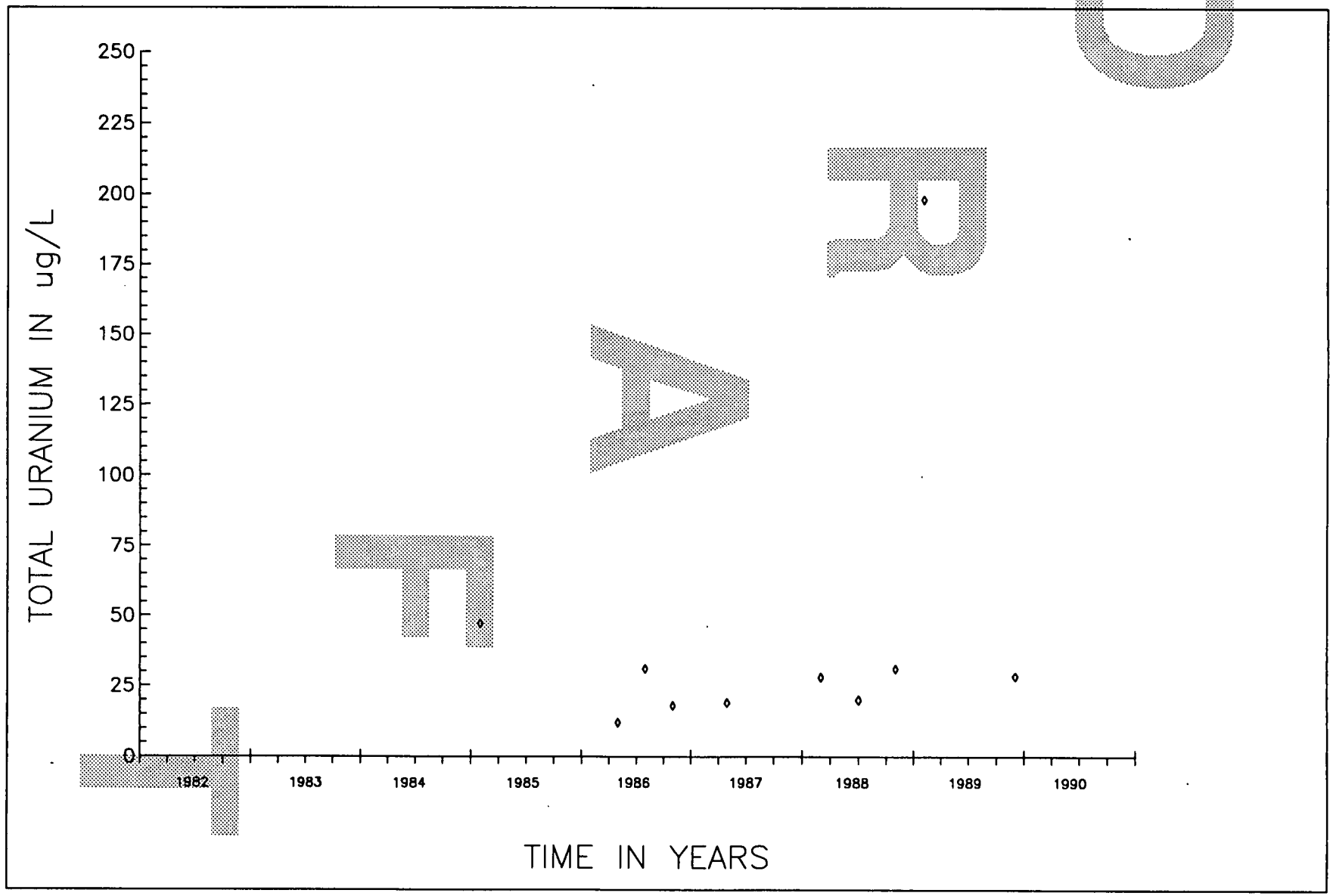


FIGURE O-2. TOTAL URANIUM CONCENTRATION VS. TIME FOR WELL 1020

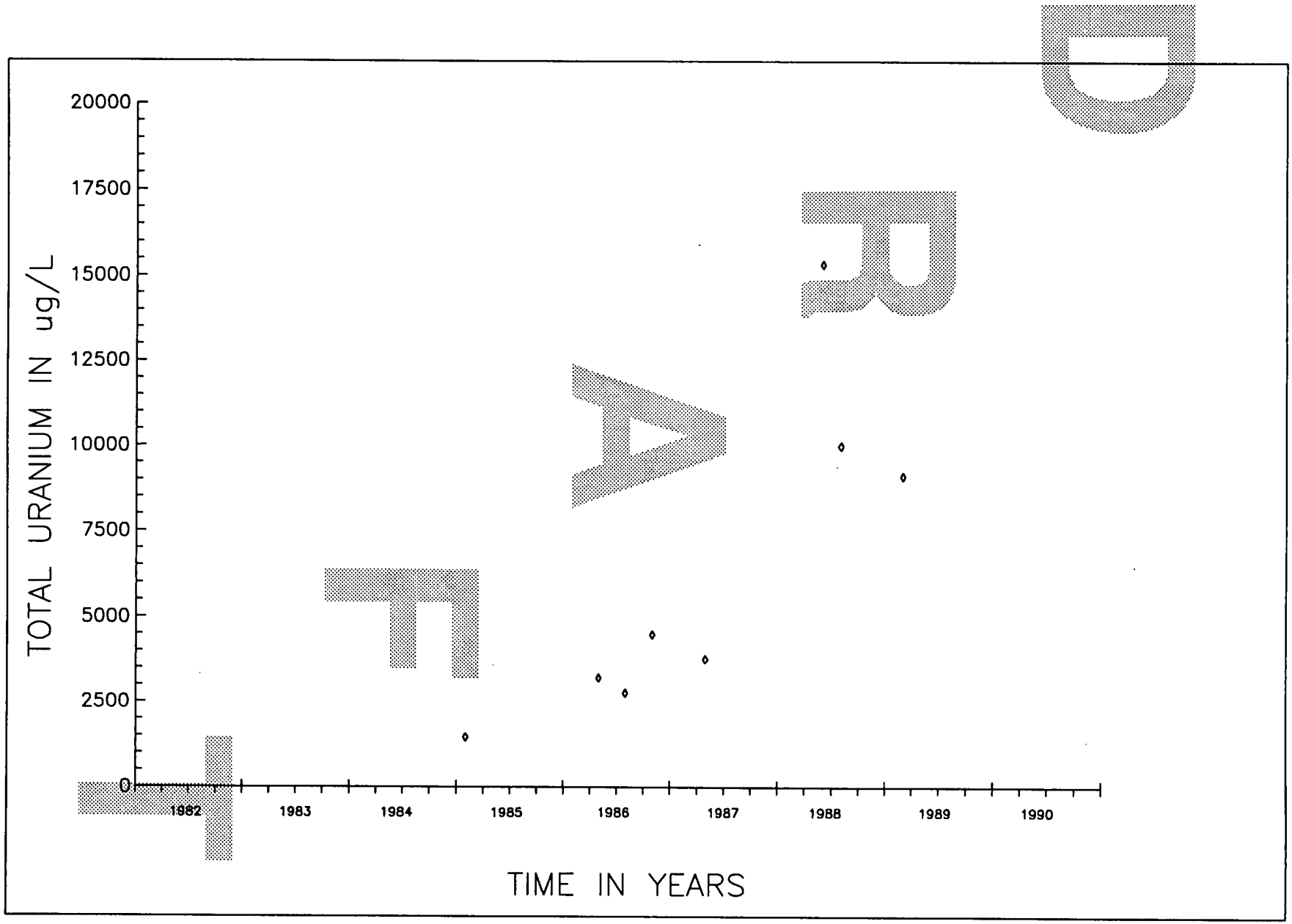


FIGURE O-3. TOTAL URANIUM CONCENTRATION VS. TIME FOR WELL 1021

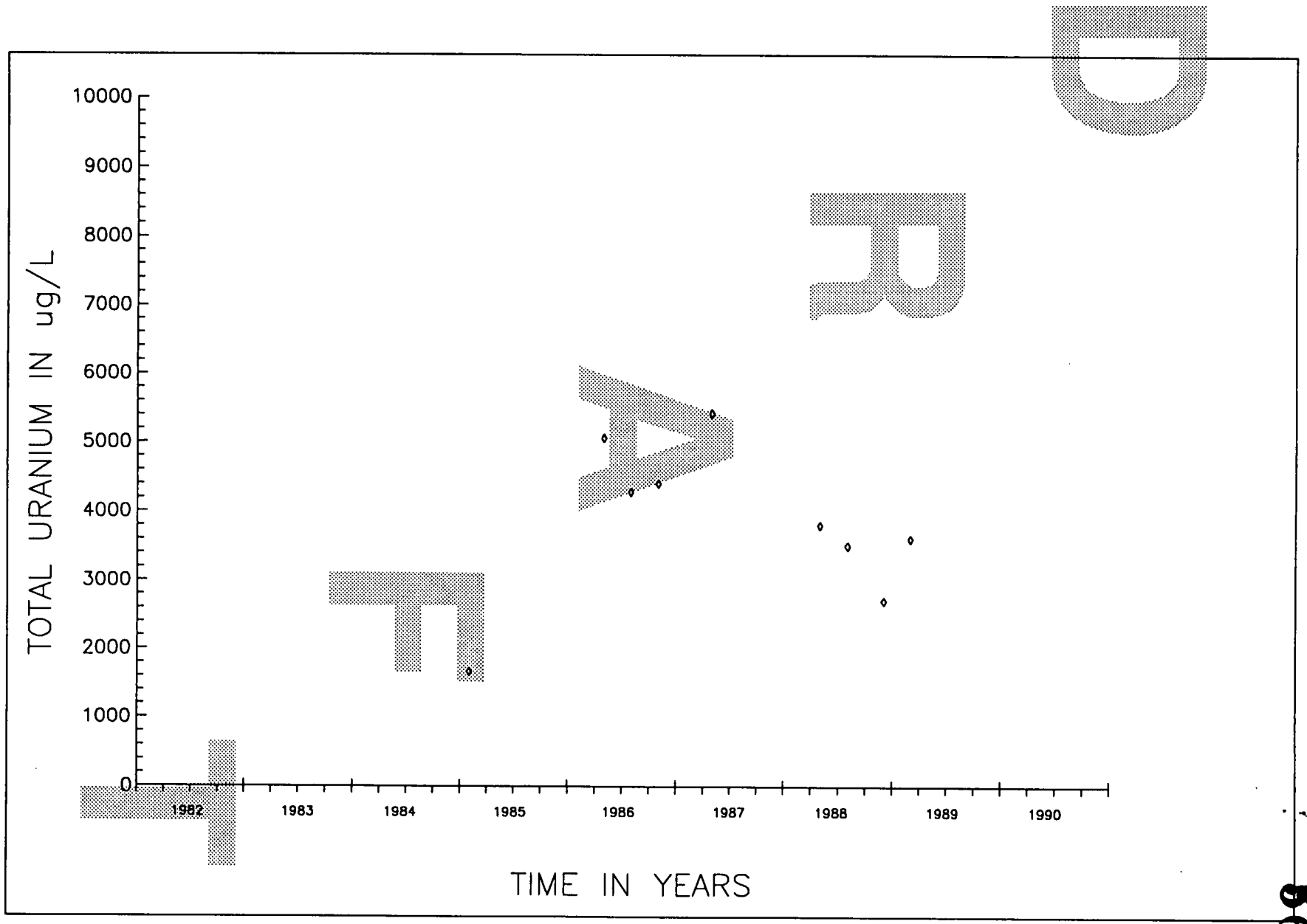


FIGURE O-4. TOTAL URANIUM CONCENTRATION VS. TIME FOR WELL 1022

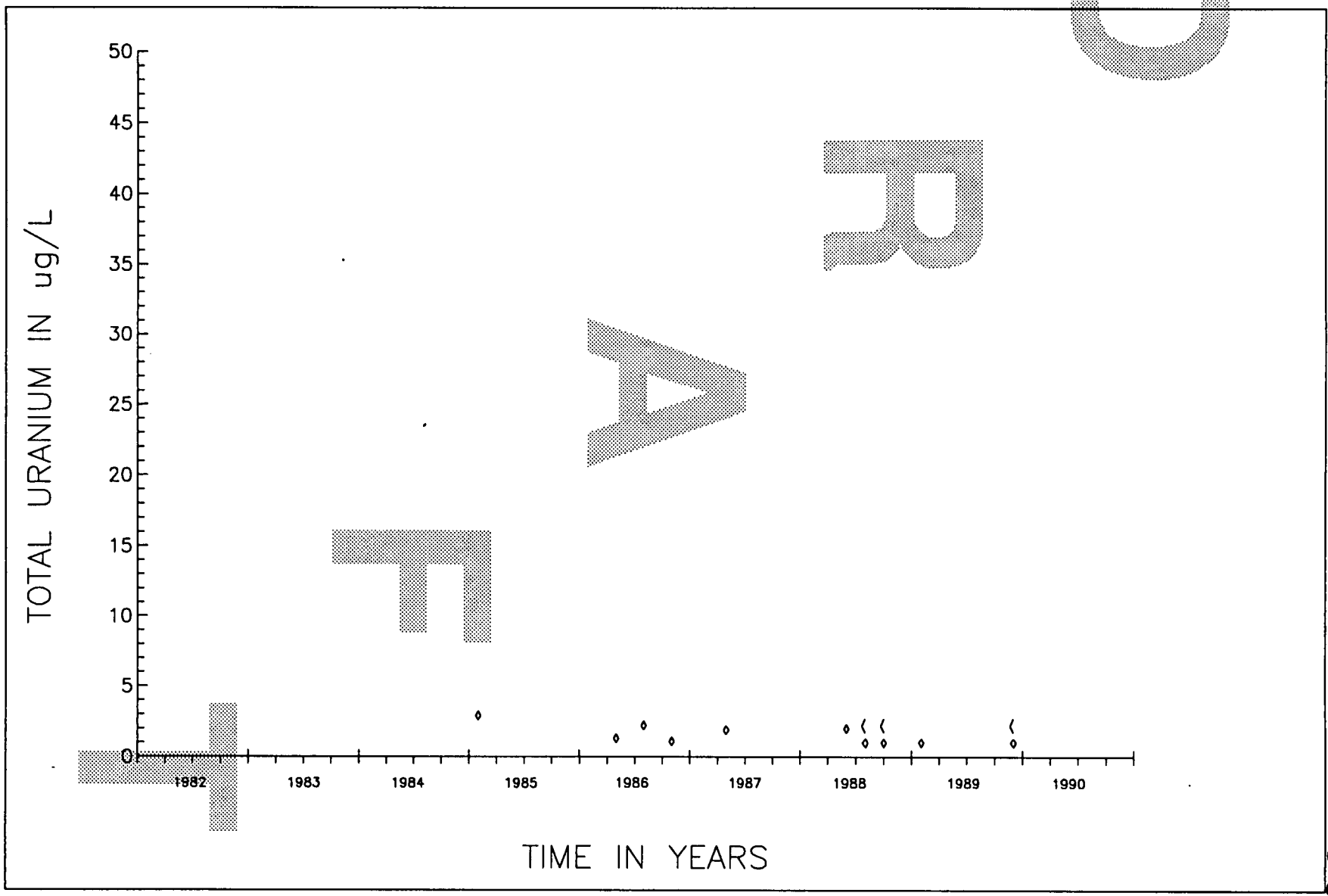


FIGURE O-5. TOTAL URANIUM CONCENTRATION VS. TIME FOR WELL 1060

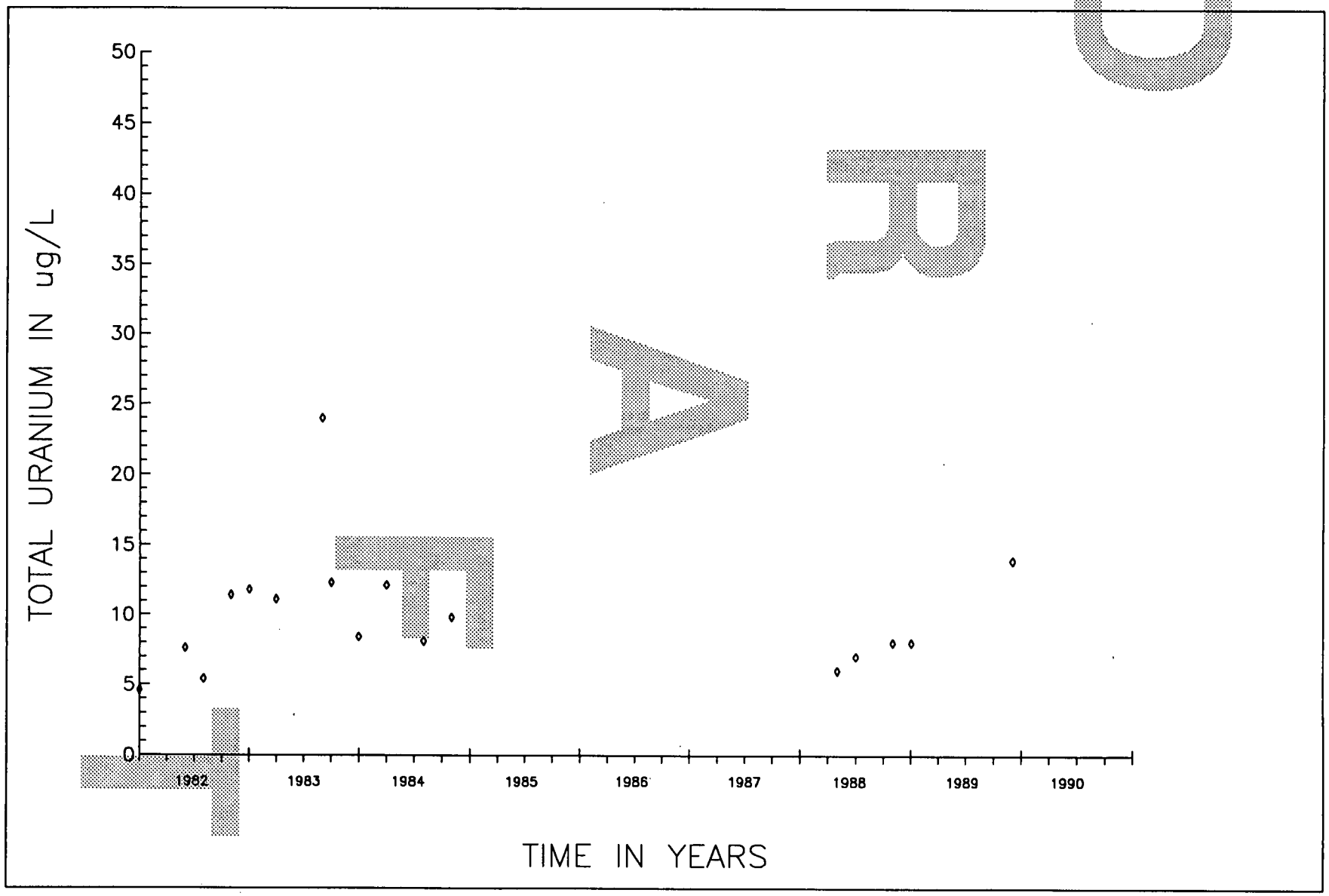


FIGURE O-6. TOTAL URANIUM CONCENTRATION VS. TIME FOR WELL 1124

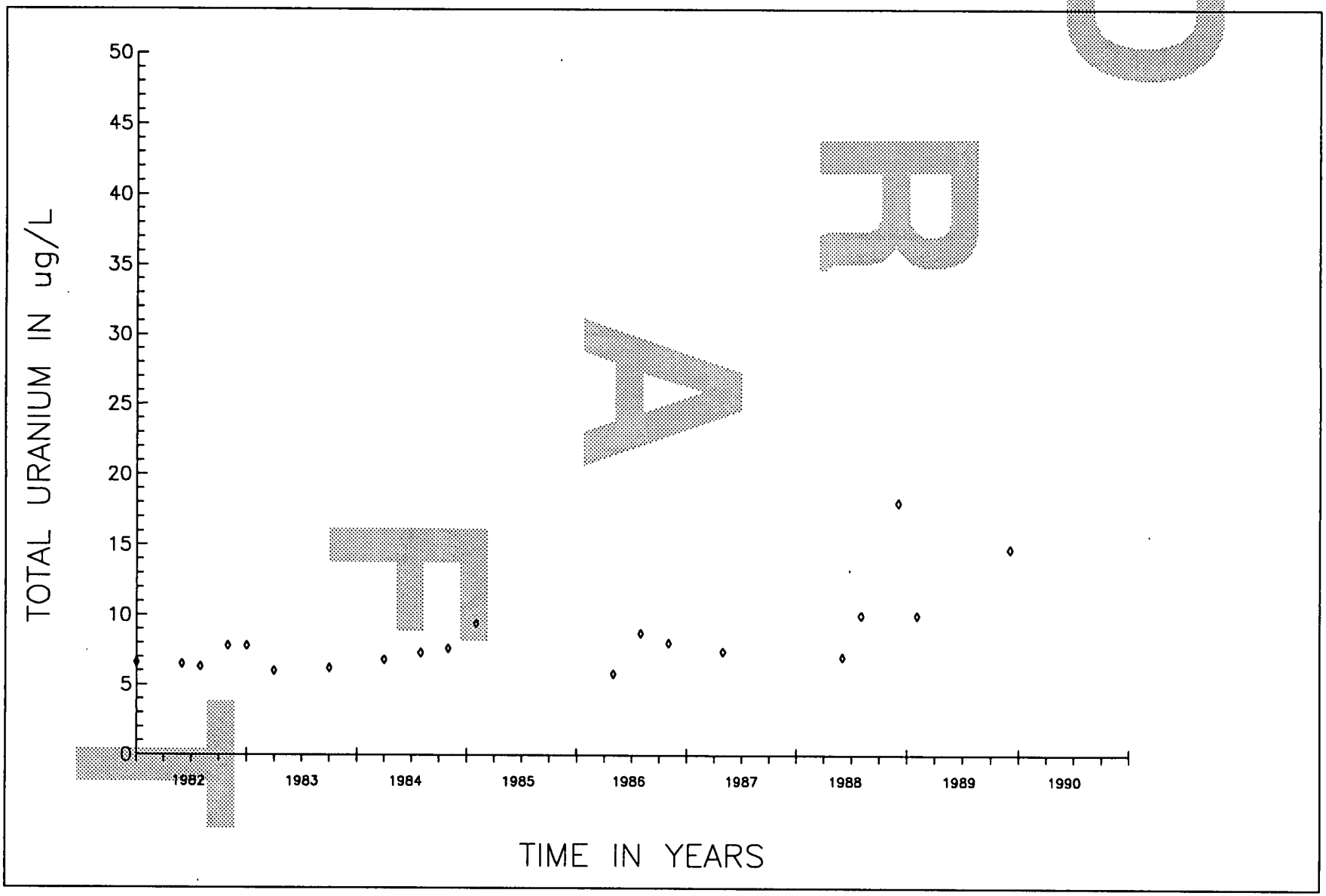


FIGURE O-7. TOTAL URANIUM CONCENTRATION VS. TIME FOR WELL 2004

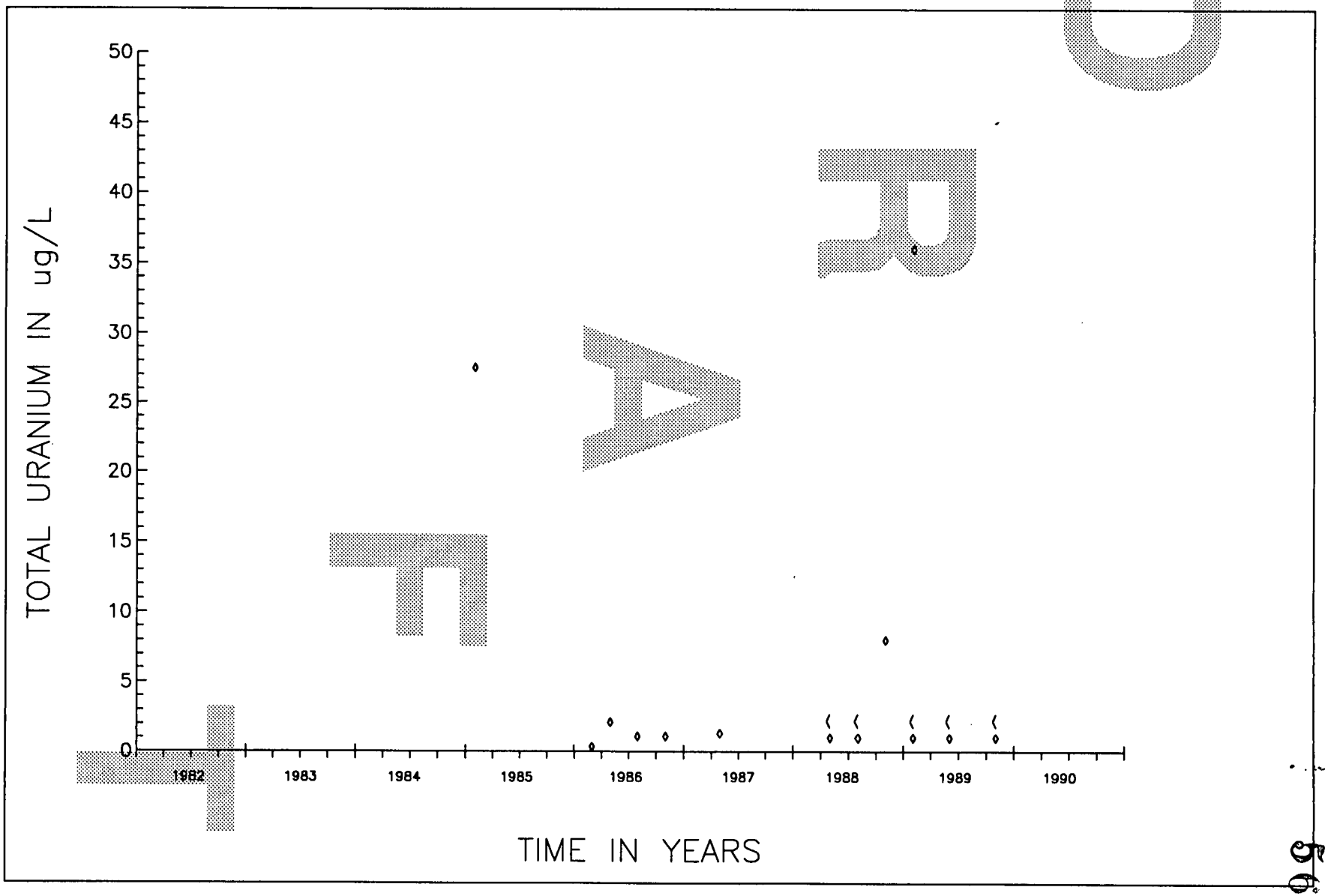


FIGURE O-8. TOTAL URANIUM CONCENTRATION VS. TIME FOR WELL 2013

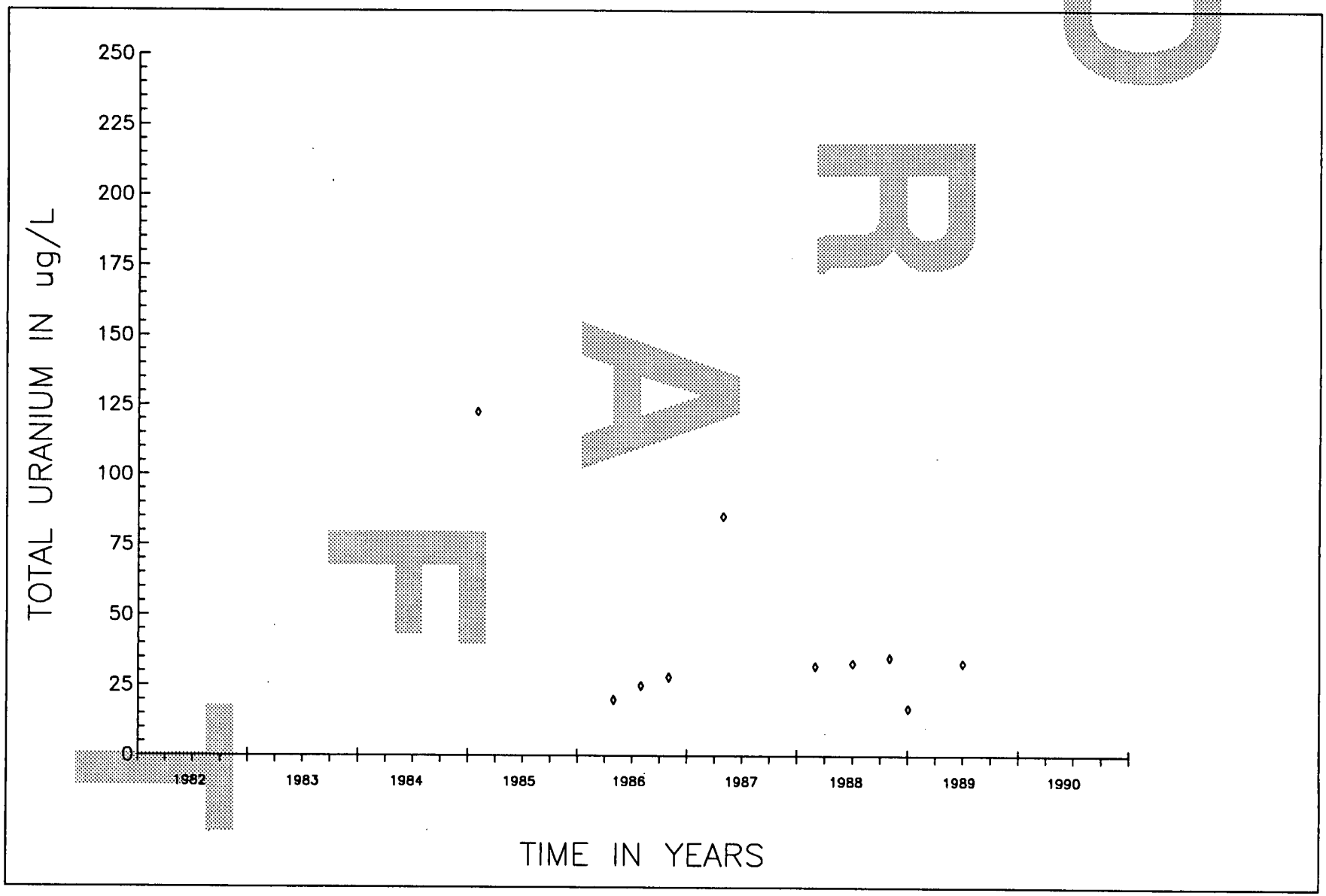


FIGURE O-9. TOTAL URANIUM CONCENTRATION VS. TIME FOR WELL 2014

DRAFT

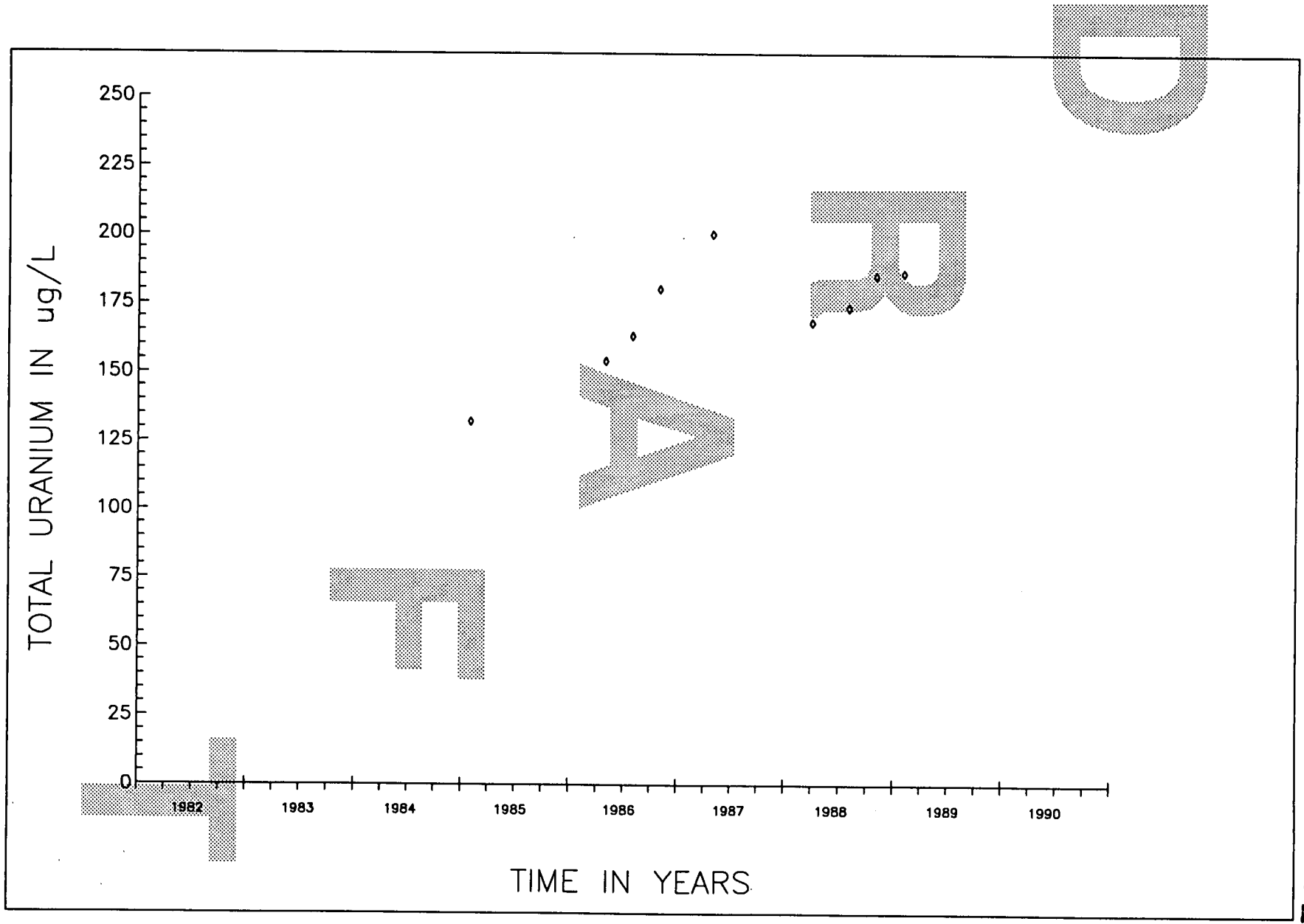


FIGURE O-10. TOTAL URANIUM CONCENTRATION VS. TIME FOR WELL 2015

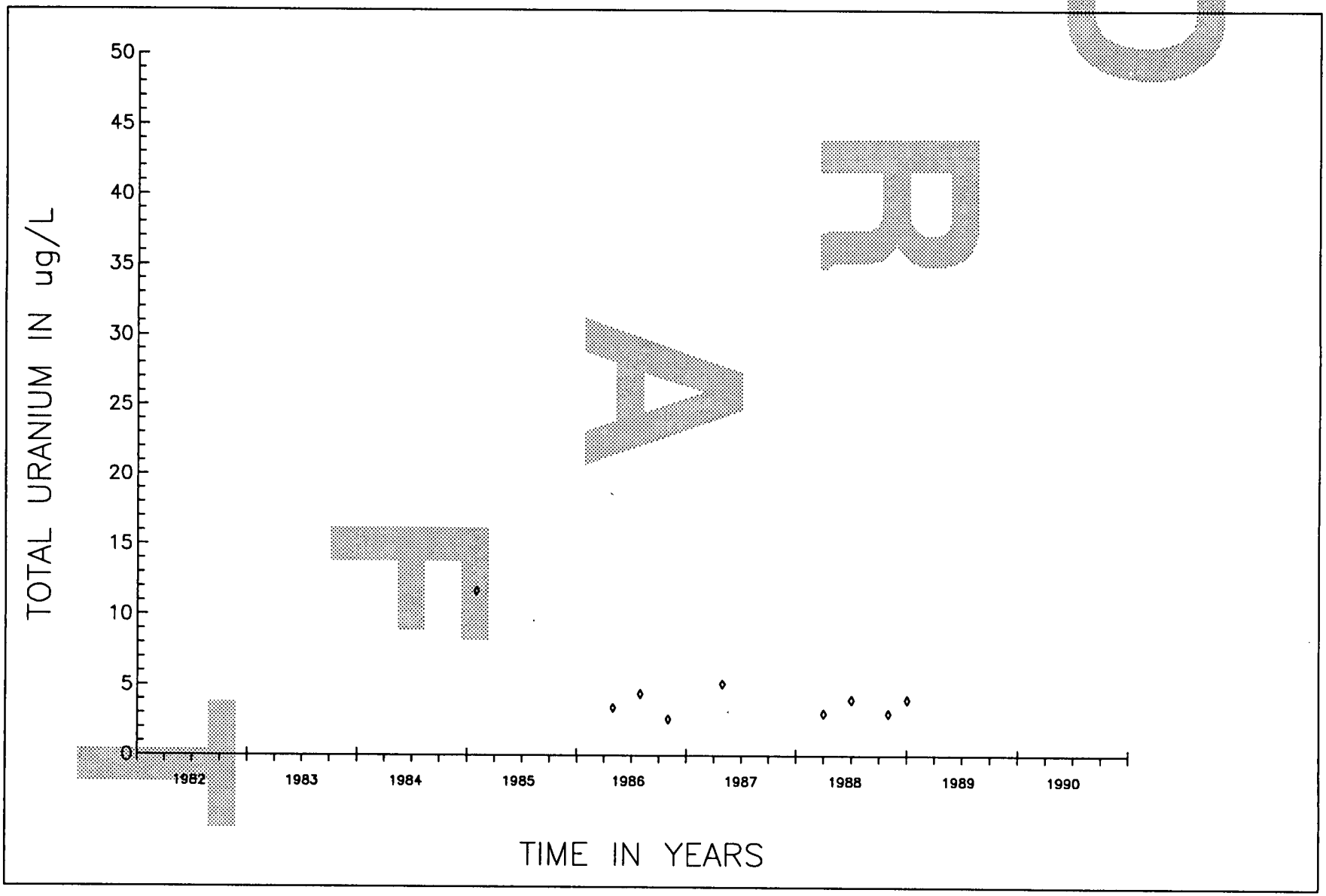


FIGURE O-11. TOTAL URANIUM CONCENTRATION VS. TIME FOR WELL 2017

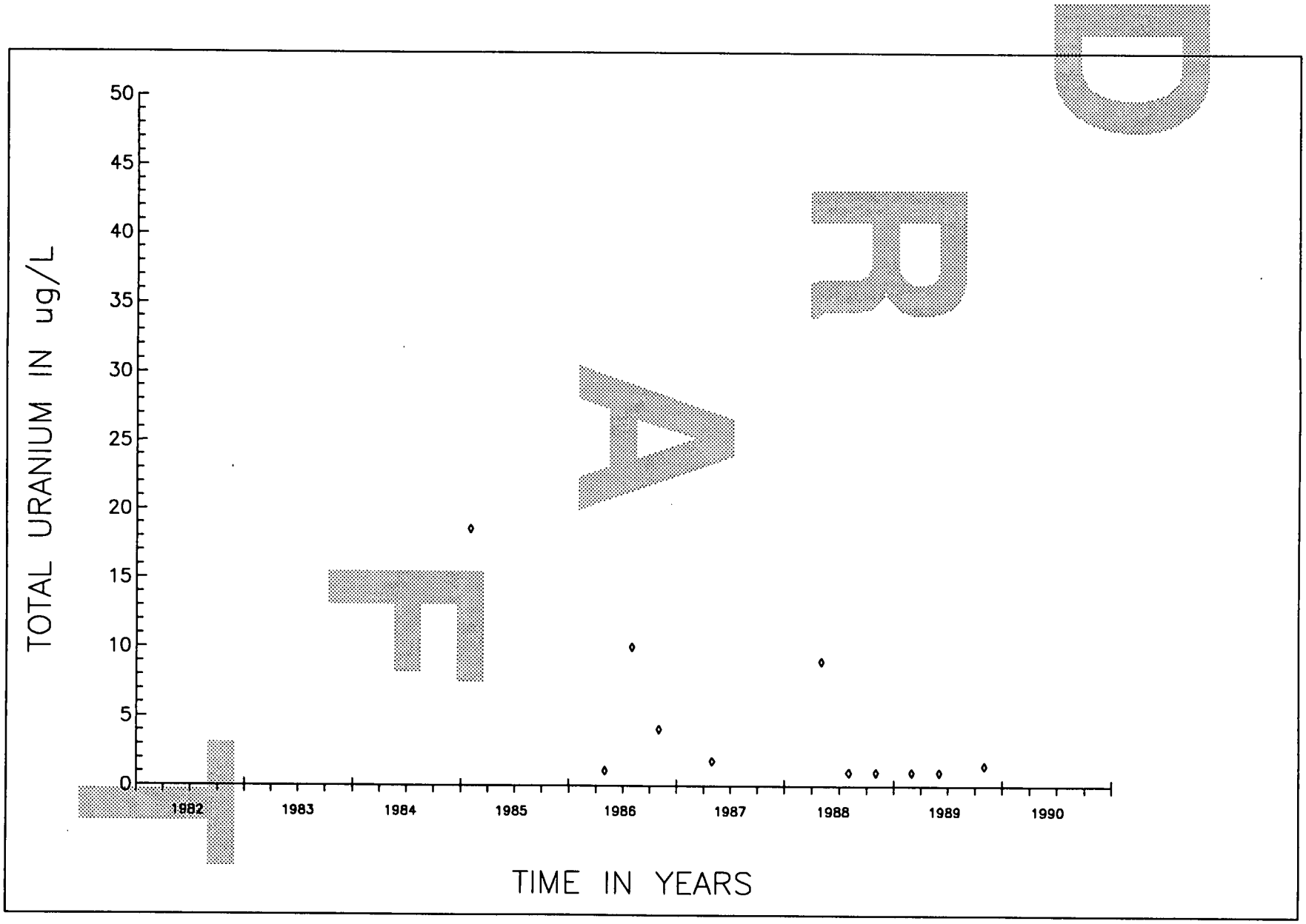


FIGURE O-12. TOTAL URANIUM CONCENTRATION VS. TIME FOR WELL 2019

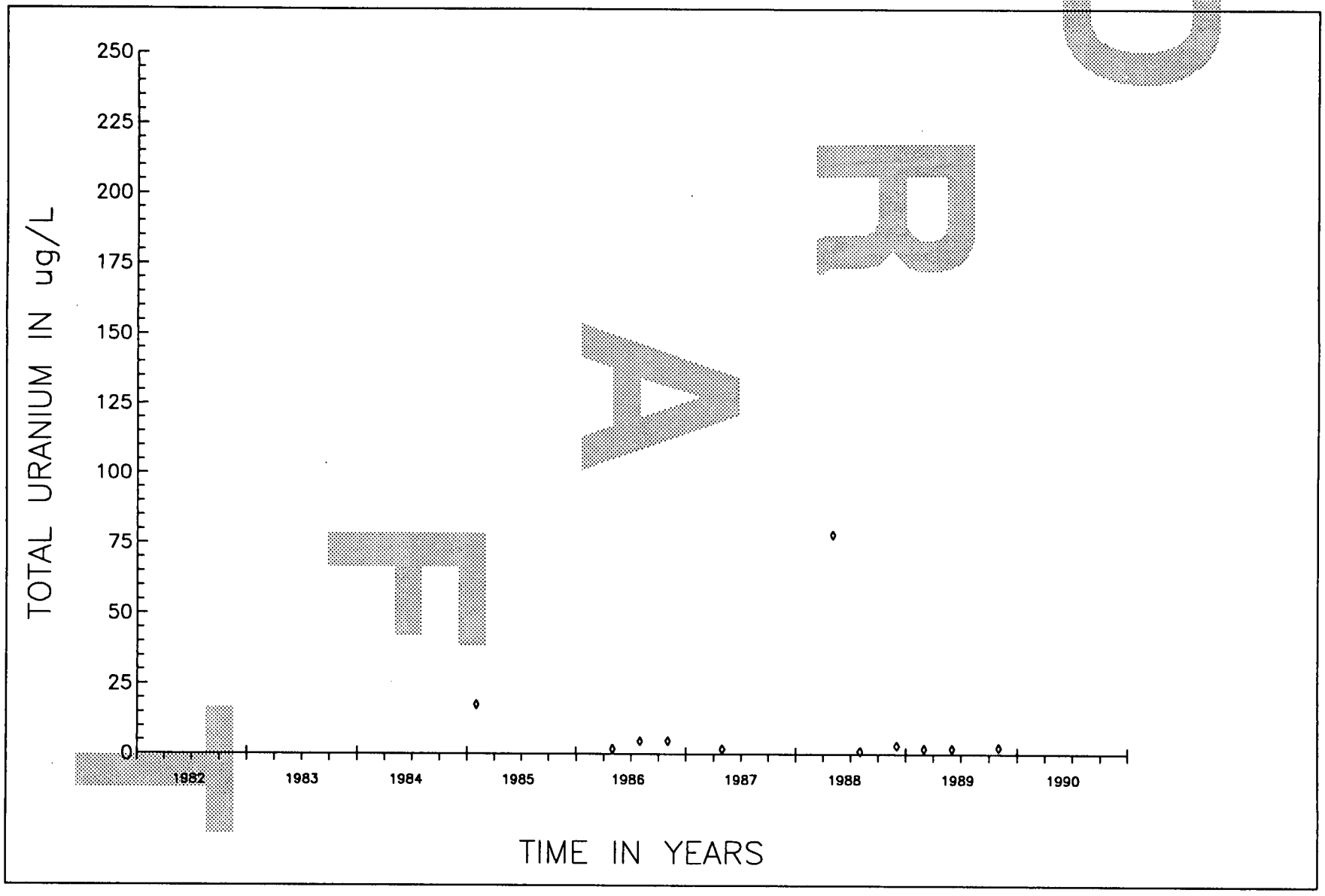


FIGURE O-13. TOTAL URANIUM CONCENTRATION VS. TIME FOR WELL 2021

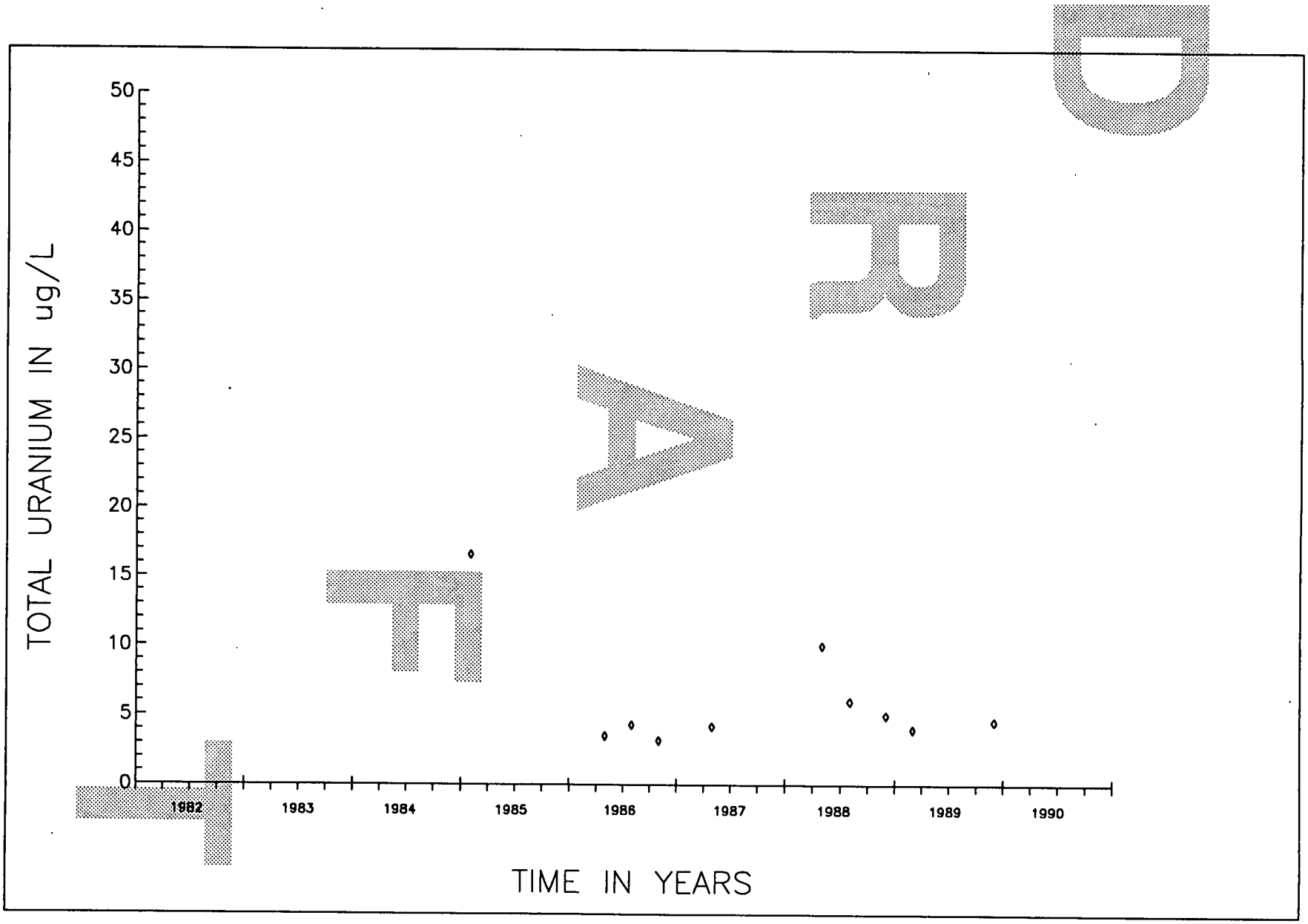


FIGURE O-14. TOTAL URANIUM CONCENTRATION VS. TIME FOR WELL 2022

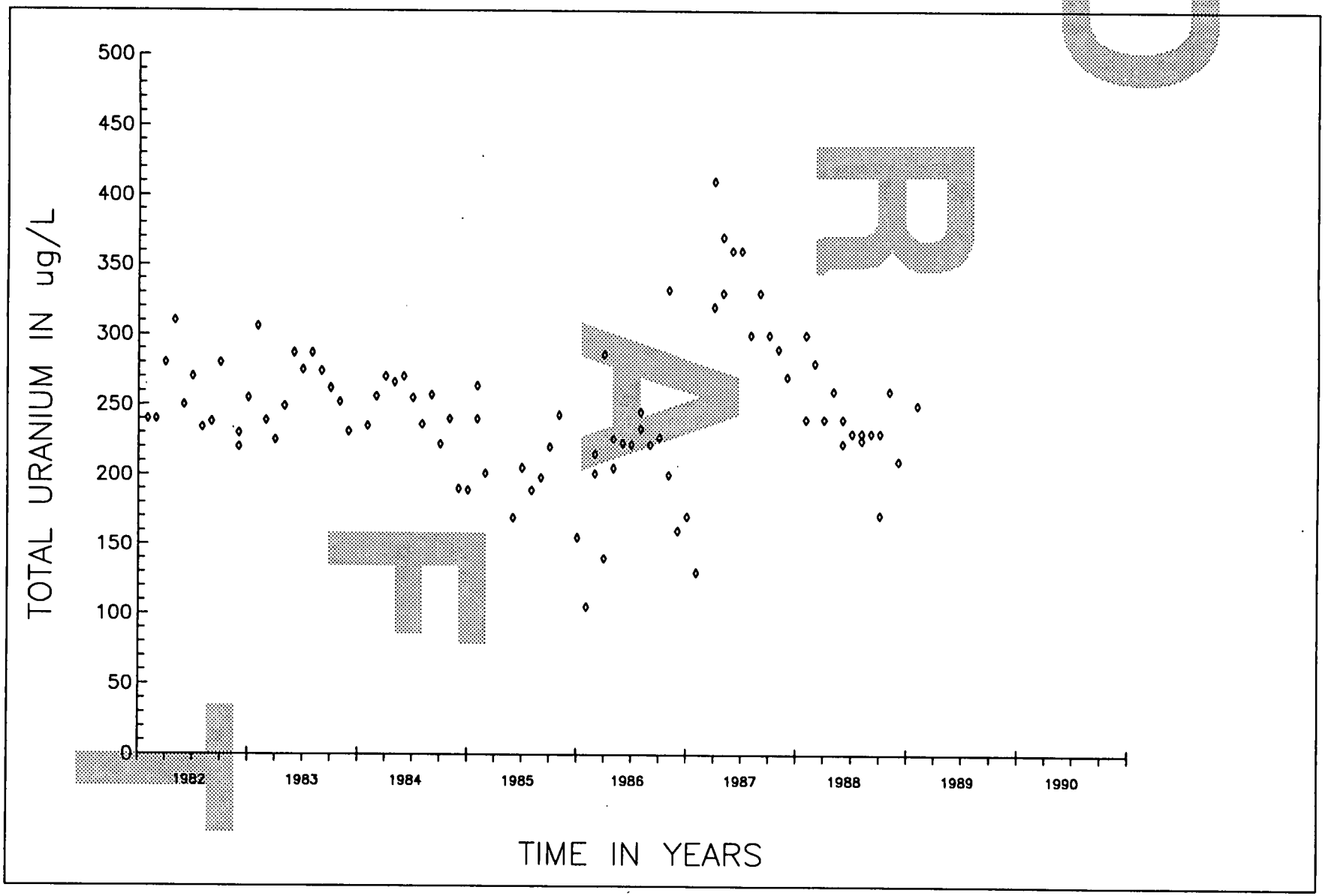


FIGURE O-15. TOTAL URANIUM CONCENTRATION VS. TIME FOR WELL 2060

000063

561 7

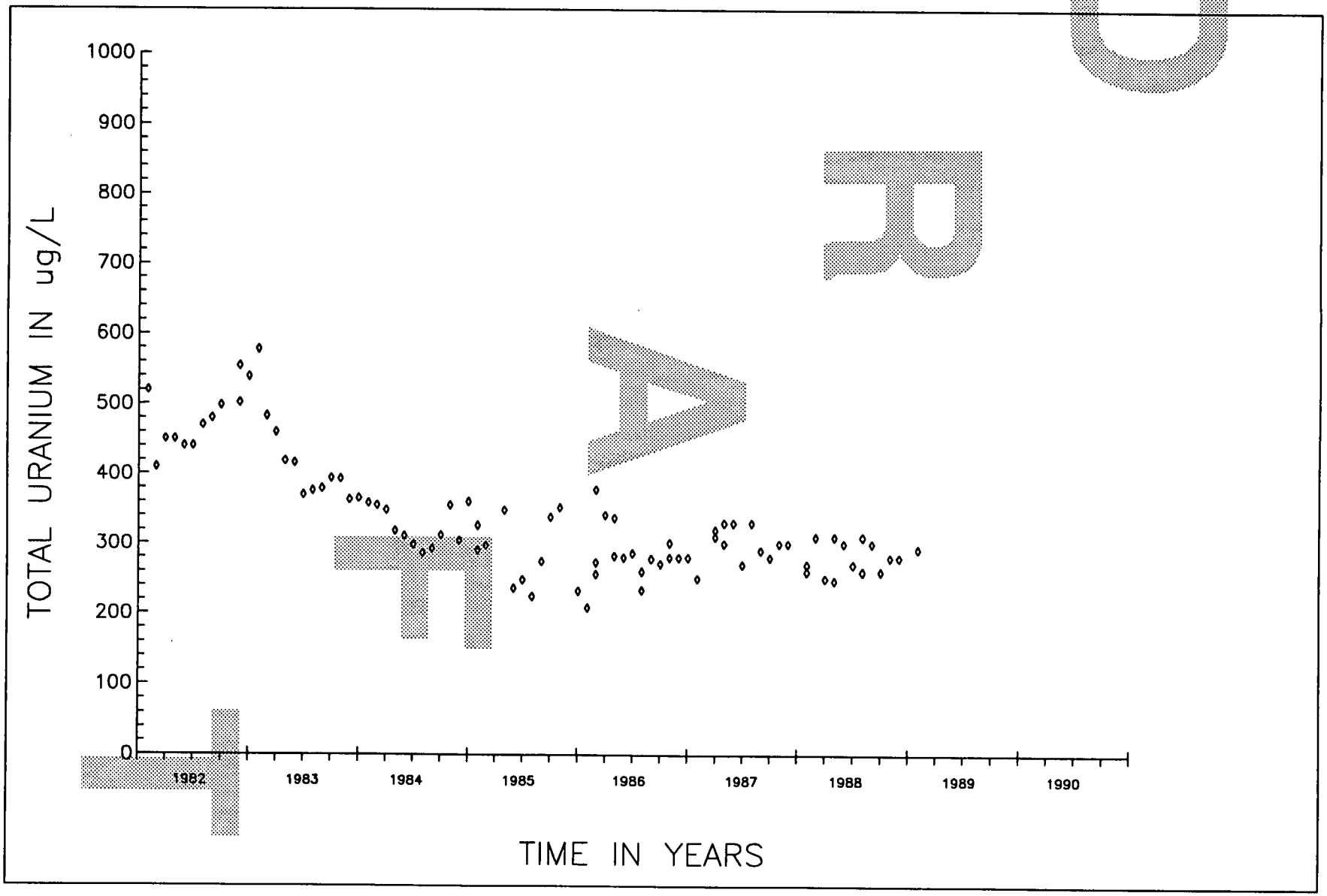


FIGURE O–16. TOTAL URANIUM CONCENTRATION VS. TIME FOR WELL 2061

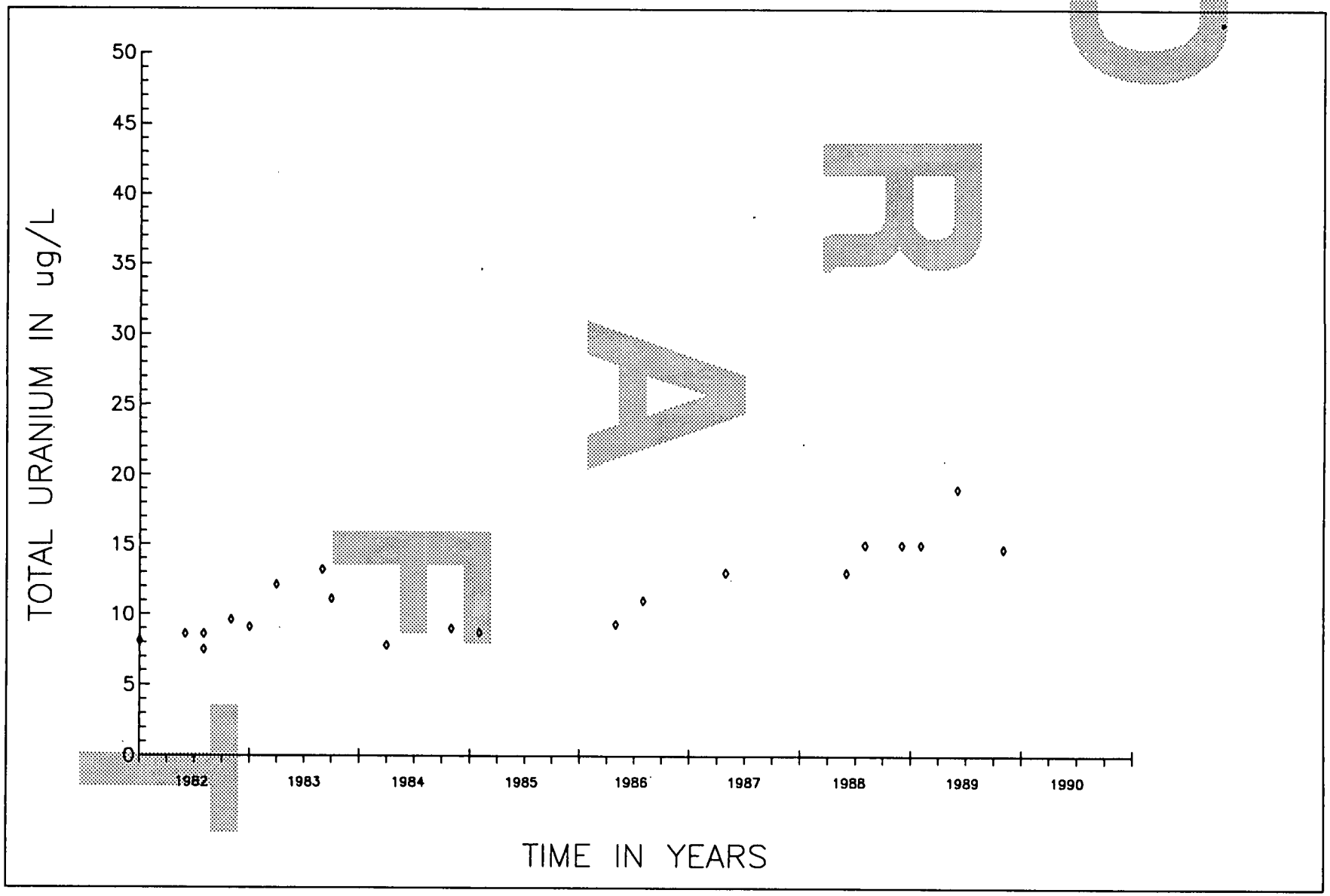


FIGURE O-17. TOTAL URANIUM CONCENTRATION VS. TIME FOR WELL 3001

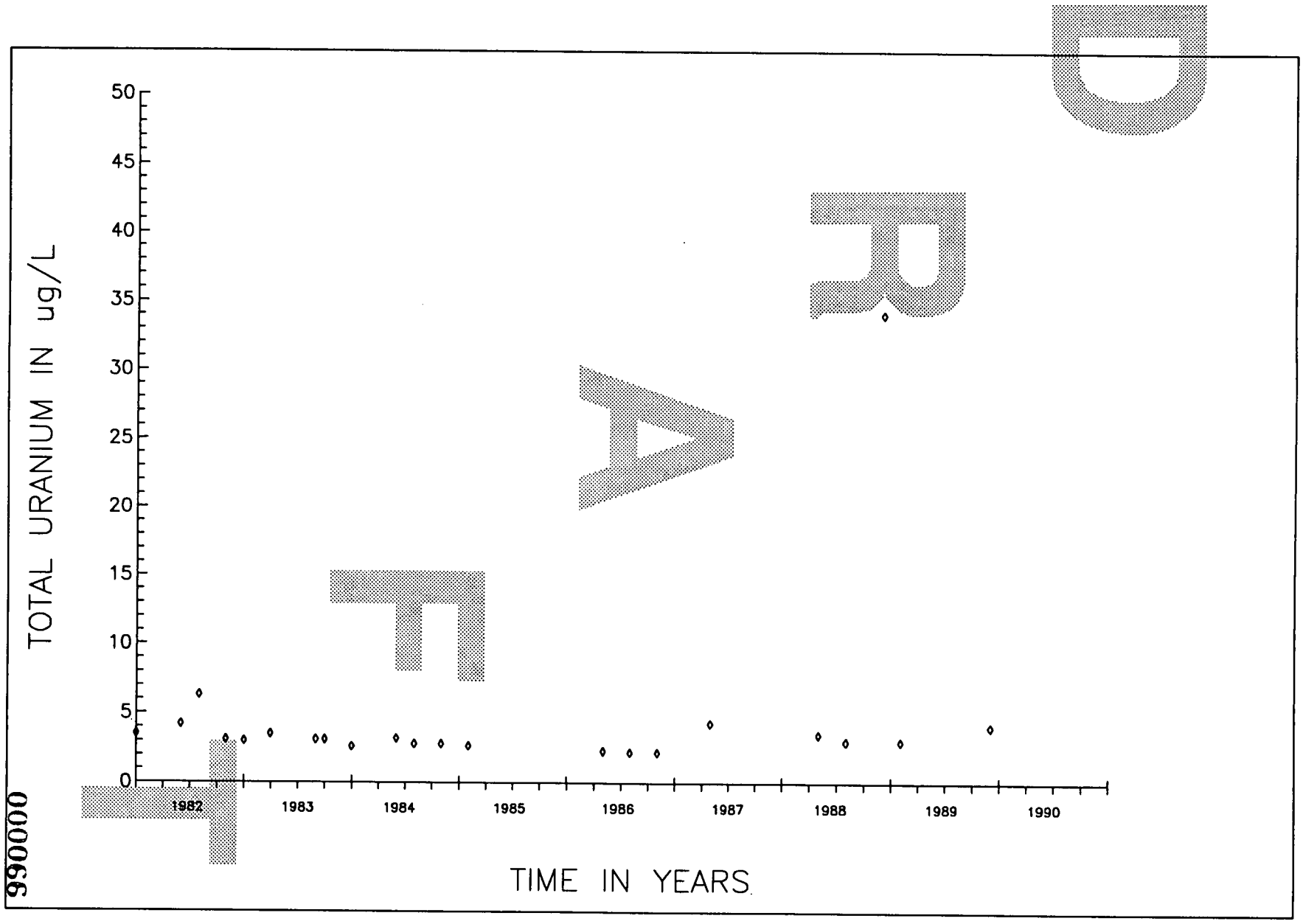


FIGURE O-18. TOTAL URANIUM CONCENTRATION VS. TIME FOR WELL 3003

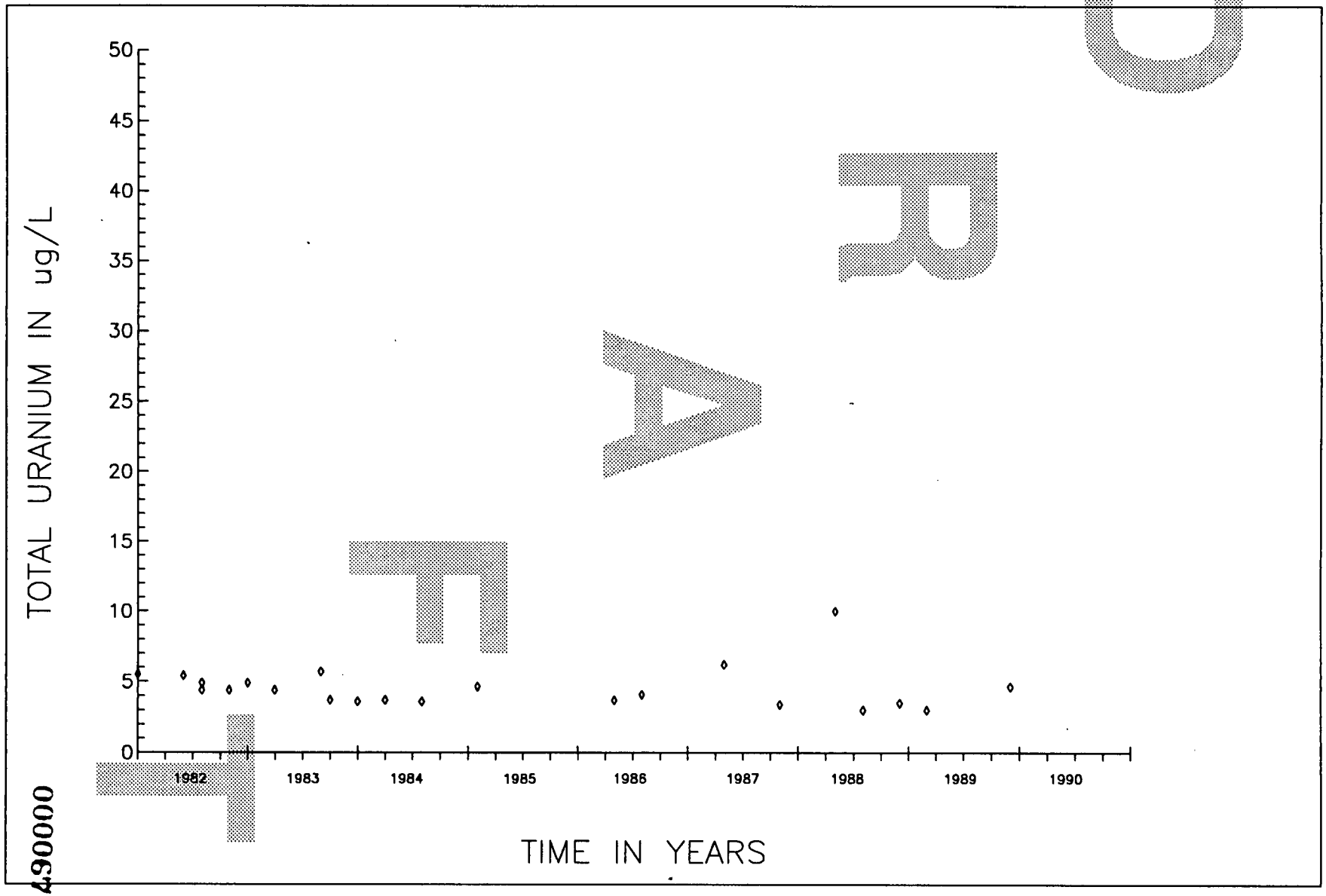


FIGURE O-19. TOTAL URANIUM CONCENTRATION VS. TIME FOR WELL 3005

490000

5617

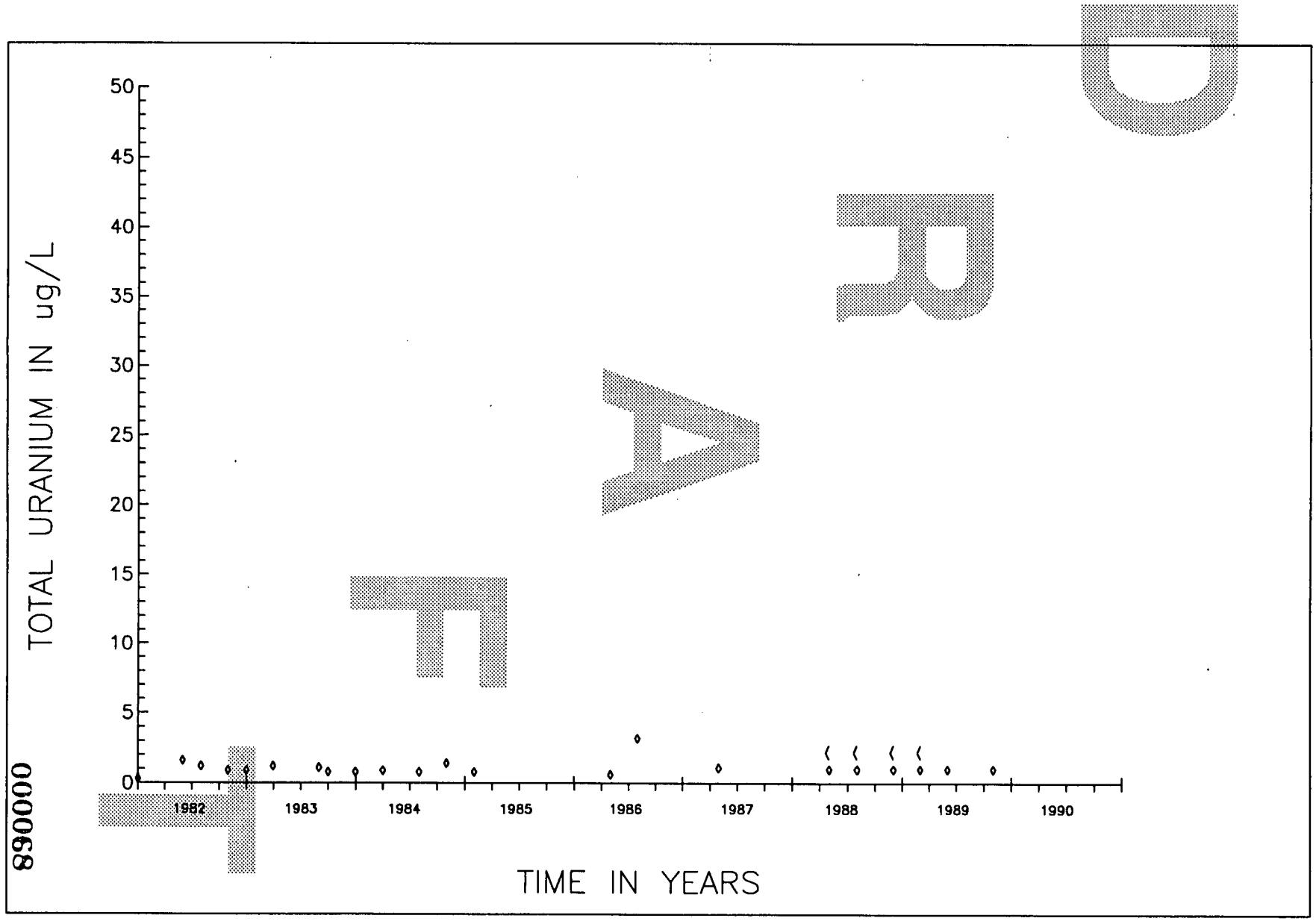


FIGURE O-20. TOTAL URANIUM CONCENTRATION VS. TIME FOR WELL 3008

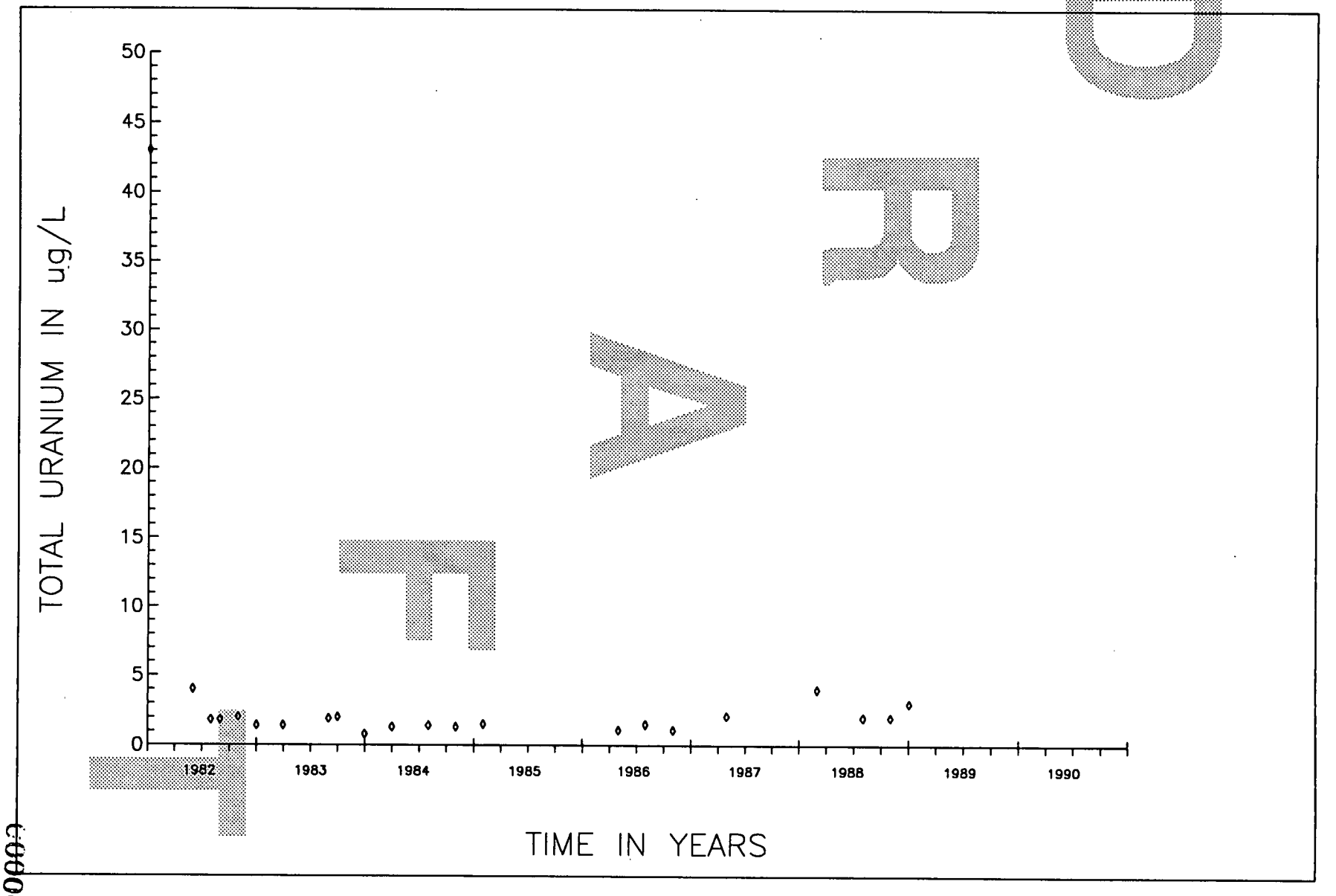


FIGURE O-21. TOTAL URANIUM CONCENTRATION VS. TIME FOR WELL 3009

000069

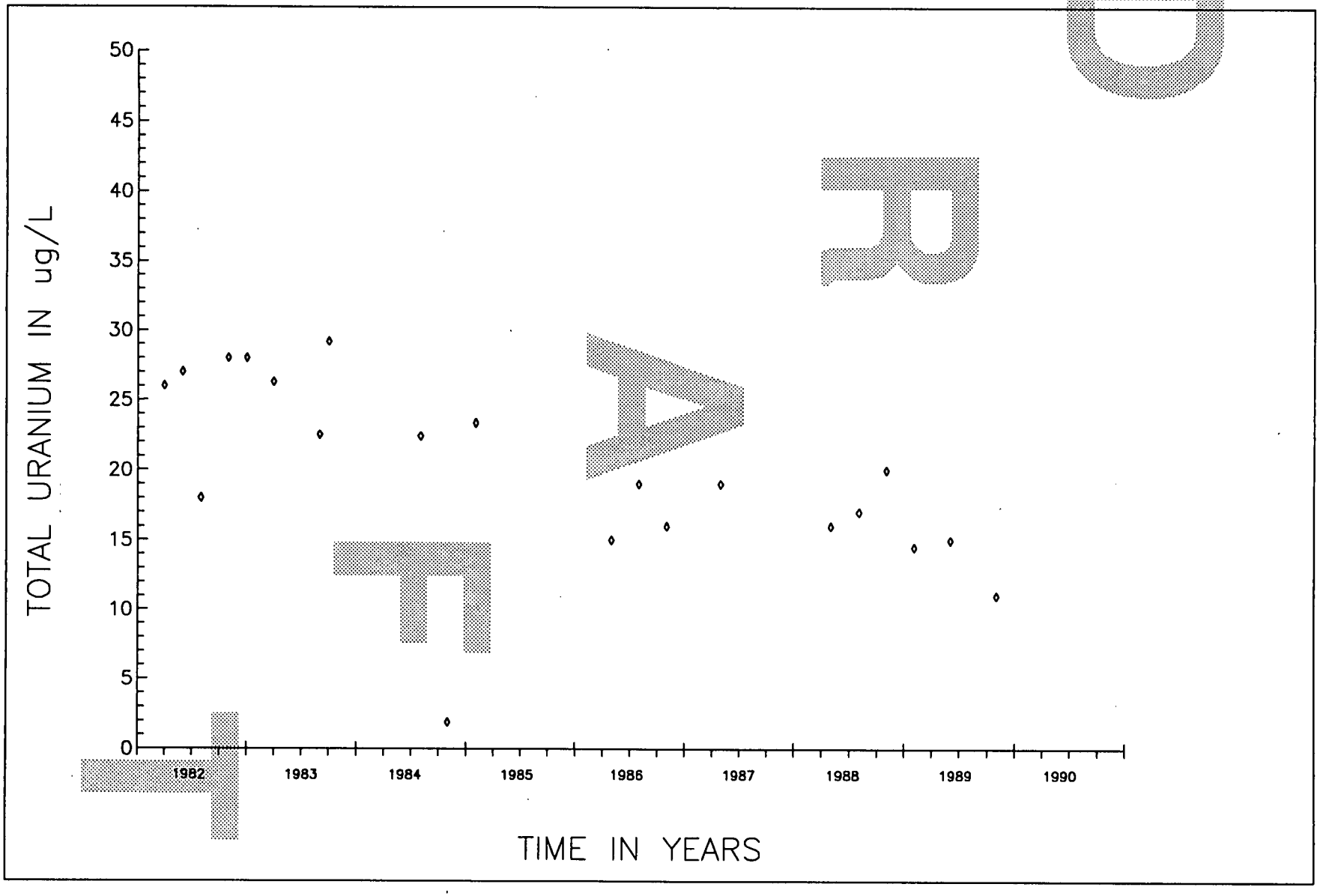


FIGURE O-22. TOTAL URANIUM CONCENTRATION VS. TIME FOR WELL 3010

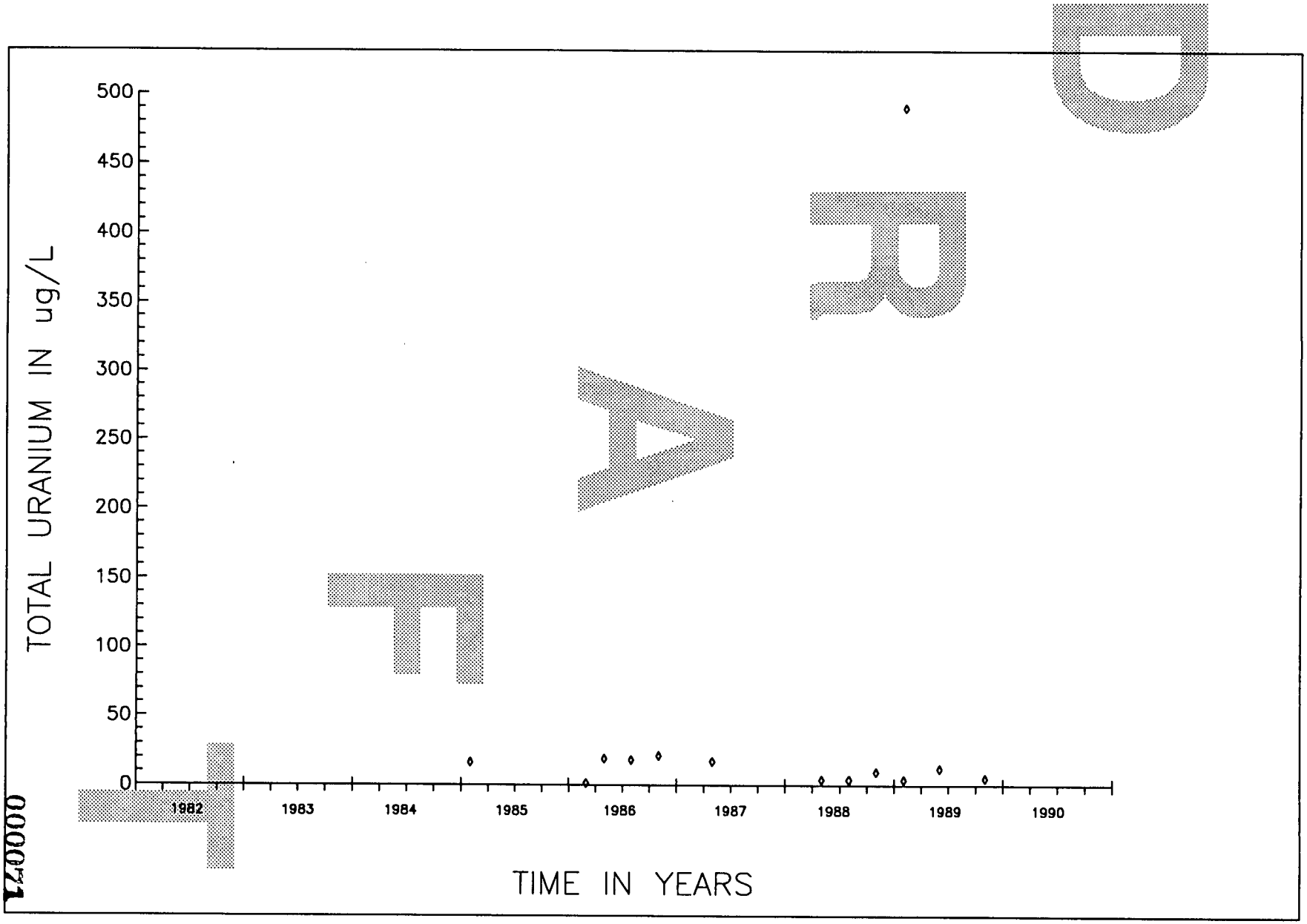


FIGURE O-23. TOTAL URANIUM CONCENTRATION VS. TIME FOR WELL 3013

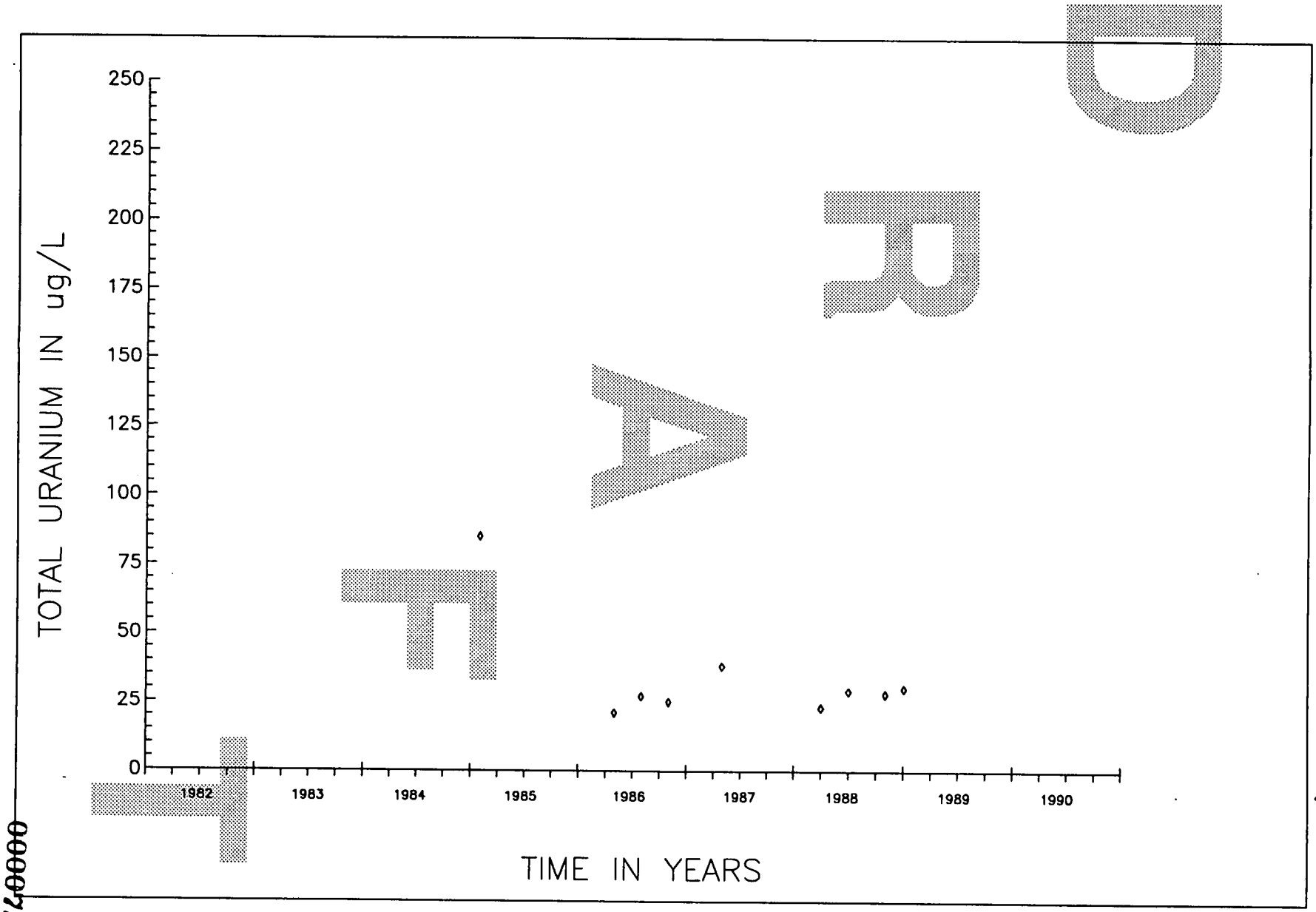


FIGURE O-24. TOTAL URANIUM CONCENTRATION VS. TIME FOR WELL 3014

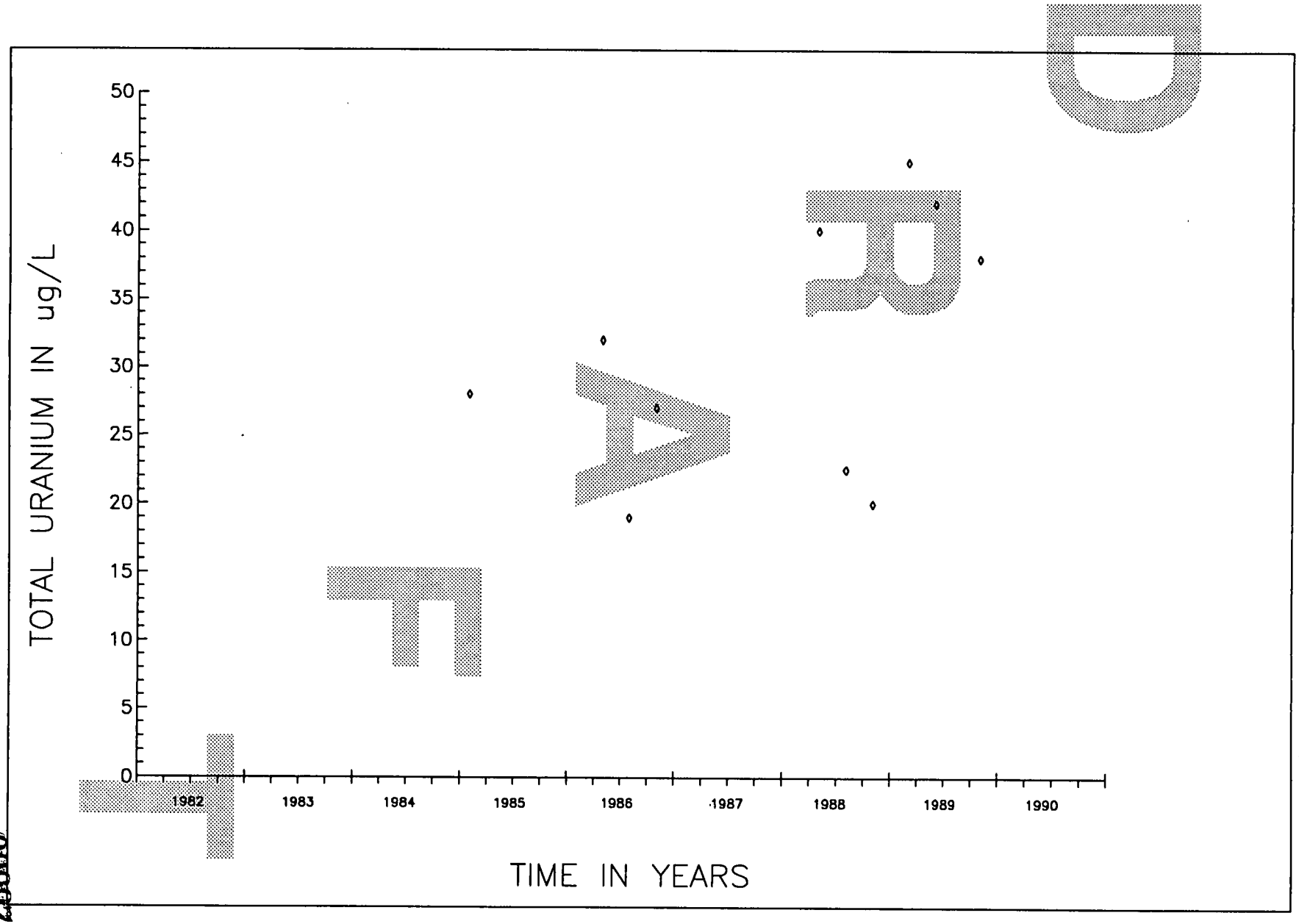


FIGURE O-25. TOTAL URANIUM CONCENTRATION VS. TIME FOR WELL 3019

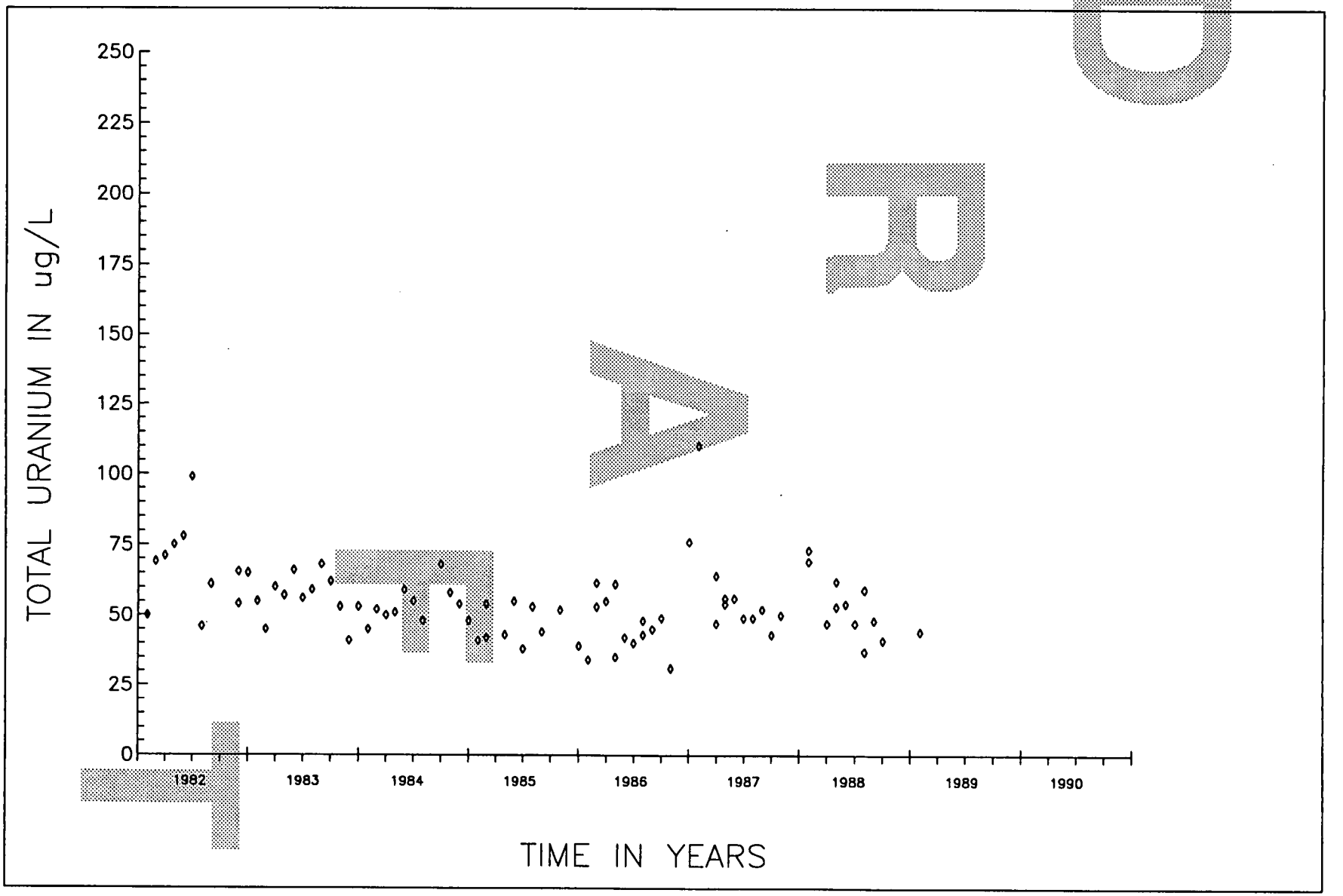


FIGURE O-26. TOTAL URANIUM CONCENTRATION VS. TIME FOR WELL 3062

000074

6172

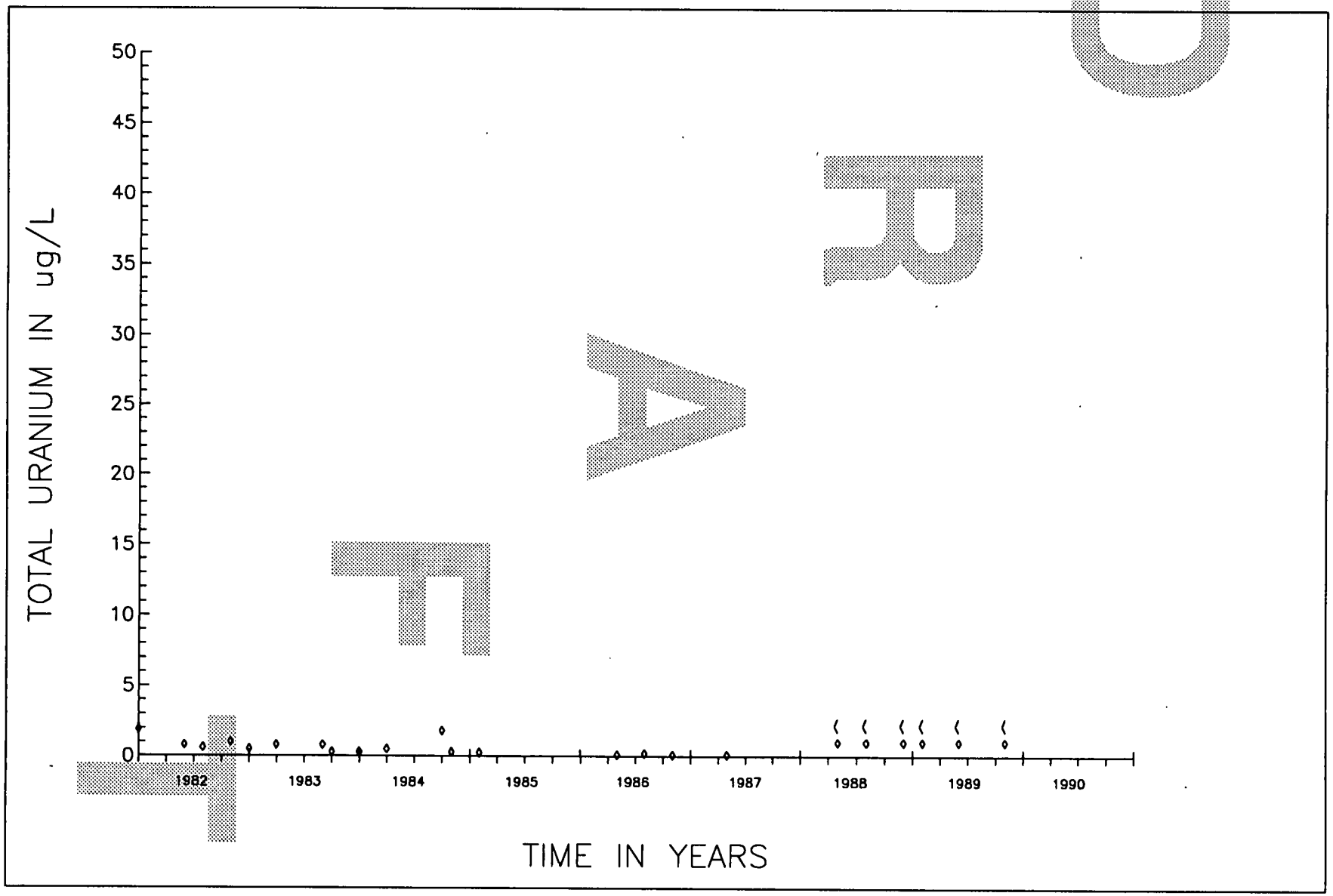


FIGURE O-27. TOTAL URANIUM CONCENTRATION VS. TIME FOR WELL 4001

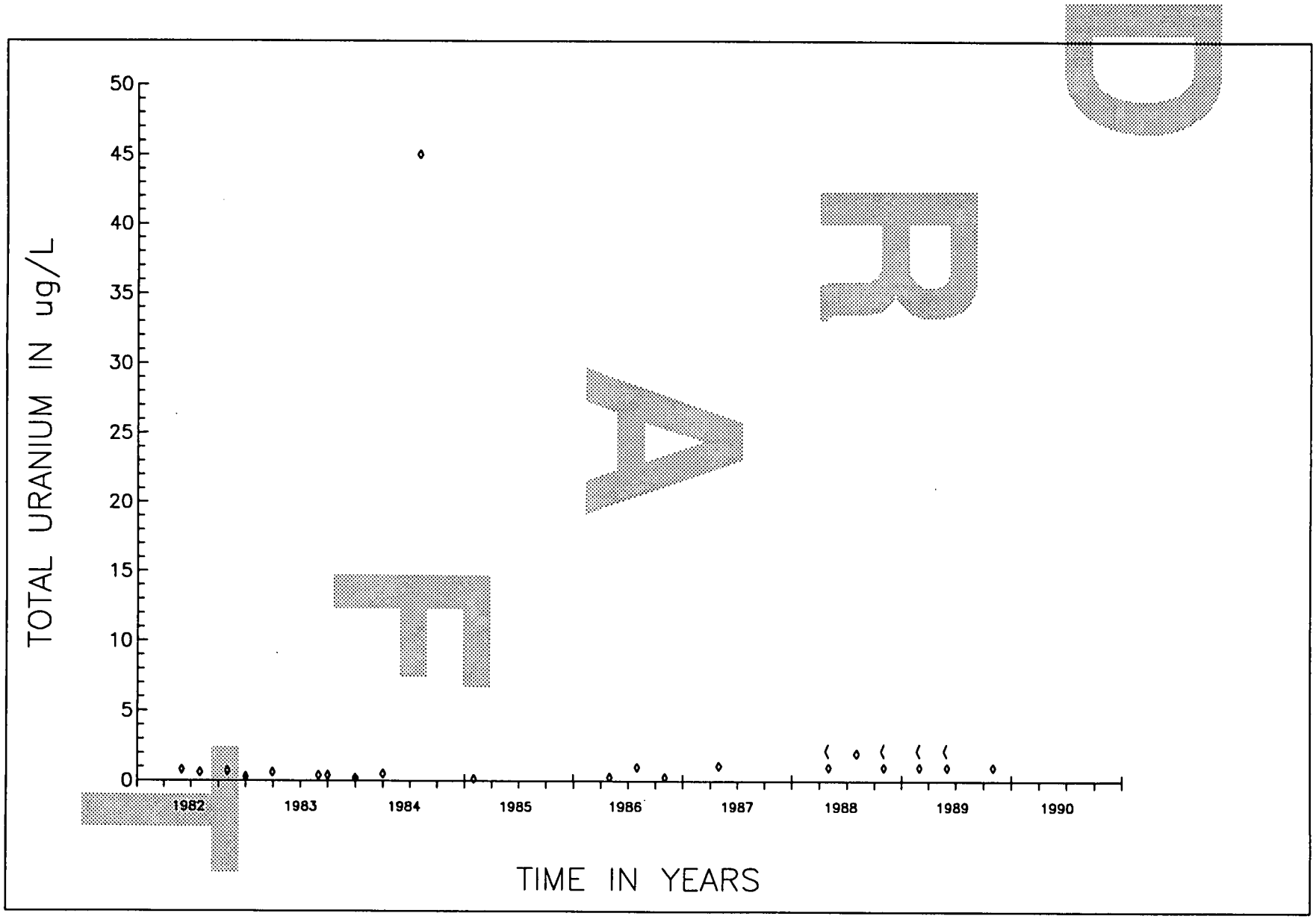


FIGURE O-28. TOTAL URANIUM CONCENTRATION VS. TIME FOR WELL 4008

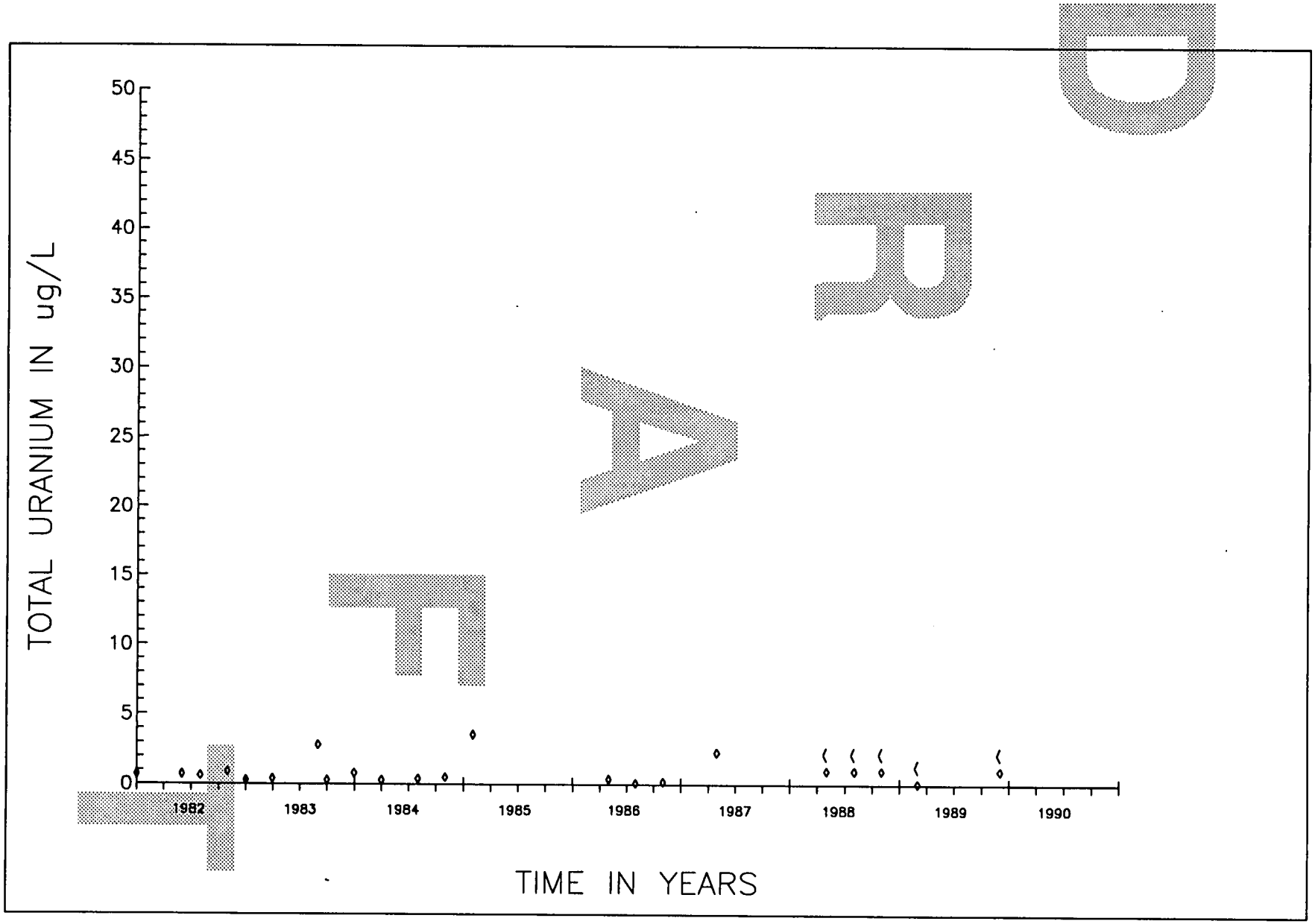


FIGURE O-29. TOTAL URANIUM CONCENTRATION VS. TIME FOR WELL 4101

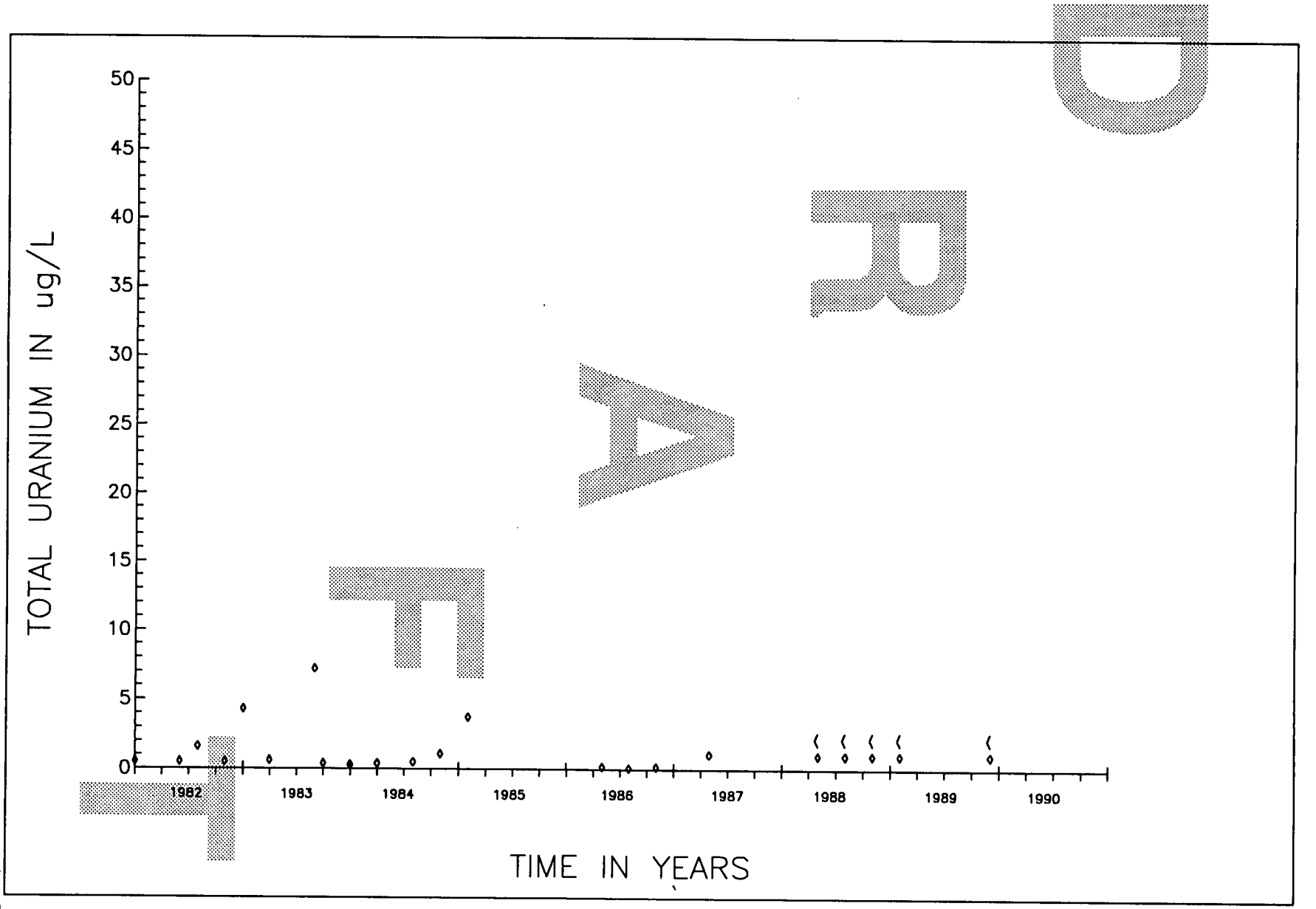


FIGURE O-30. TOTAL URANIUM CONCENTRATION VS. TIME FOR WELL 4102

000078

5612

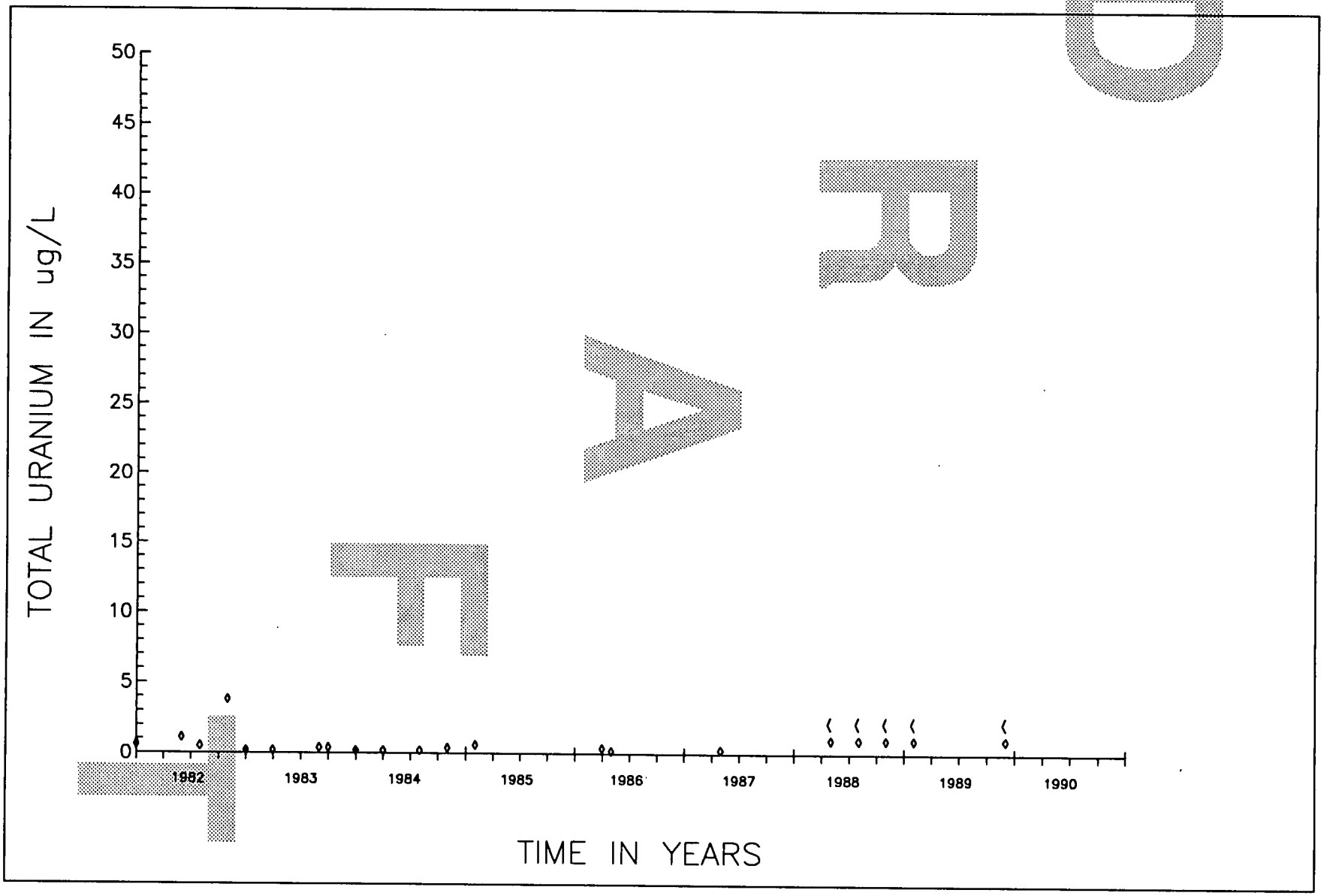


FIGURE O-31. TOTAL URANIUM CONCENTRATION VS. TIME FOR WELL 4103

FMPC-0004-2
December 17, 1990

# GEOTECHNICAL PROGRAM: ISSUES 3 AND 5

Appendix P contains the results of Issues 3 and 5 of the FMPC RI/FS Geochemical Program. Issue 3 was designed to establish whether sediment and subsurface soil beneath the Paddys Run and storm sewer outfall ditch represent a past, continuing, or future source of uranium to groundwater. The purpose of Issue 5 was to estimate a uranium distribution coefficient (Kd) for the Great Miami Aquifer.

DRAFT

# TABLE OF CONTENTS


| | Page |
|---|---|
| List of Tables/List of Figures | iii |
| P.1.0 Introduction | P-1 |
| P.1.1 Background | P-1 |
| P.1.2 Issues of the Geochemical Program | P-2 |
| P.1.3 Issue Three: Paddys Run and the Storm Sewer Outfall Ditch | P-2 |
| P.1.3.1 Purpose and Scope | P-2 |
| P.1.3.2 Analytical Methods and Field Sampling | P-4 |
| P.1.3.2.1 Field-Sampling Procedure for Subsurface Soils | P-4 |
| P.1.4 Issue Five: Parameters for Solute Transport Model | P-5 |
| P.1.4.1 Purpose and Scope | P-5 |
| P.1.4.2 Analytical Methods and Field Sampling | P-6 |
| P.1.4.2.1 Field-Sampling Procedure for $U^{+4}$ and Total U | P-6 |
| P.2.0 Analytical Methods and Results | P-7 |
| P.2.1 Analytical Methods | P-7 |
| P.2.1.1 Gamma Spectrometry | P-7 |
| P.2.1.2 Differential Leaching Tests for Uranium | P-8 |
| P.2.1.3 Leaching Technique for Iron and Manganese | P-9 |
| P.2.2 Analytical Results | P-9 |
| P.2.2.1 Issue Three | P-9 |
| P.2.2.1.1 Subsurface Soils | P-9 |
| P.2.2.1.2 Surface Waters | P-10 |
| P.2.2.2 Issue Five | P-11 |
| P.2.2.2.1 Aquifer Solids | P-11 |
| P.2.2.2.2 Anomalous Uranium Results | P-12 |
| P.2.2.2.3 Groundwaters | P-13 |
| P.2.3 Discussion | P-14 |
| P.2.3.1 Issue Three | P-14 |
| P.2.3.2 Issue Five | P-15 |
| P.3.0 Geochemical Modeling | P-16 |
| P.3.1 Selection Criteria for Groundwater Samples | P-17 |
| P.3.2 Modeling Assumptions and Constraints | P-18 |
| P.3.2.1 Electrical Charge Imbalances | P-18 |
| P.3.2.2 Eh Calculations | P-18 |


DRAFT

## TABLE OF CONTENTS
(continued)


| | Page |
|---|---|
| P.3.3 Uranium Speciation | P-19 |
| P.3.3.1 Discussion | P-20 |
| P.3.3.1.1 Data Base Integrity | P-20 |
| P.4.0 Uranium Adsorption | P-21 |
| P.4.1 Speciation and Experimental Studies | P-21 |
| P.4.1.1 Adsorption of Uranyl-Carbonate Species by Montmorillonite | P-22 |
| P.4.1.2 Adsorption of Uranyl-Carbonate Species by Amorphous Ferric Oxyhydroxide | P-23 |
| P.4.1.3 Empirical Determination of a Uranium Distribution Coefficient | P-23 |
| P.4.2 Aquifer Solids, Leachates, and Groundwaters | P-26 |
| P.4.3 Comparison of Empirical and Calculated $K_d$ Values | P-27 |
| P.4.4 Estimation of the Uranium $K_d$ for the Fernald Site Aquifer | P-28 |
| P.5.0 Conclusions | P-29 |
| P.5.1 Issue Three | P-29 |
| P.5.2 Issue Five | P-30 |
| P.5.2.1 Best Estimate of the Uranium $K_d$ for the Aquifer | P-31 |
| References | |
| Tables | |
| Figures | |
| Attachment P.I - Analytical Results for Soil Samples | |
| Attachment P.II - Analytical Results for Surface Waters | |
| Attachment P.III - Analytical Results for Aquifer Solids | |
| Attachment P.IV - Analytical Results for Modeled Groundwaters | |


DRAFT

## LIST OF TABLES


| Table | Title |
|---|---|
| P-1 | Results for Uranium Speciation in Waters Recovered from Fernald Monitoring Wells |
| P-2 | Results for Uranium Speciation in Surface Waters Recovered from Paddys Run, Fernald Site |
| P-3 | Empirical Uranium Distribution Coefficients for Selected Monitoring Wells |
| P-4 | Calculated Uranium Distribution Coefficients for Selected Monitoring Wells |


## LIST OF FIGURES


| Figure | Title |
|---|---|
| P-1 | Geochemical Program, Issue 3, Surface Water and Subsurface Soil Sampling Locations |
| P-2 | Uranium Concentrations in Subsurface Soils of Paddys Run |
| P-3 | Uranium Concentrations in Subsurface Soils of the Storm Sewer Outfall Ditch |
| P-4 | Weight Percent of Silt + Clay versus Leachable Iron, Manganese, and Uranium |
| P-5 | Weight Percent of Silt + Clay versus Total Organic Carbon |
| P-6 | Weight Percent of Silt + Clay versus Cation Exchange Capacity |
| P-7 | Uranium Concentrations in Aquifer Solids |
| P-8 | Results of the Uranium Differential-Leach Test |
| P-9 | Geochemical Program, Issue 5, Location of Groundwater Monitoring Wells and Subsurface Borings |
| P-10 | Uranium Redox Ratio versus Total Iron |
| P-11 | Uranium Speciation as a Function of the Groundwater Eh |
| P-12 | Calculated $K_d$ versus Predicted $K_d$ |


DRAFT

# P.1.0 INTRODUCTION

## P.1.1 BACKGROUND

A Work Plan for the site-wide Remedial Investigation and Feasibility Study (RI/FS) at the U.S. Department of Energy's (DOE's) Feed Materials Production Center (FMPC) in Fernald, Ohio was developed to evaluate potential uranium sources to the underlying aquifers and provide geochemical parameters for a three-dimensional model of groundwater flow and radionuclide transport. Recognizing the need for site-specific modeling data on the physiochemical processes that could affect radionuclide migration and attenuation, a geochemical testing program was included in the RI/FS Work Plan as part of the Subsurface Soils Sampling Plan. The geochemical program included analytical testing for total uranium, differential leaching of uranium, total cation exchange capacity, total organic carbon, leachable iron and manganese, and grain size on about 40 subsurface solid samples from three stratigraphic horizons below the FMPC. The purpose of the geochemical testing program was to quantify chemical parameters on aquifer solids which would enhance the evaluation of radionuclide migration and attenuation.

Subsequent to the submission of the original RI/FS Work Plan, a reconsideration of the geochemical data needs indicated a deficiency in some of the proposed analytical work. For groundwater samples, a field determination of dissolved oxygen and alkalinity, and laboratory analysis of calcium, potassium and phosphate, were considered critical additions to the program to satisfy the data needs for the geochemical modeling effort. For aquifer-solid samples, the leachates produced from the leachable iron and manganese test were split, and one split of each sample was retained for total fluorimetric uranium analysis. Each of these additional analytical procedures were eventually integrated into the geochemical testing program.

Because the groundwater-flow and solute-transport model will simulate only the sand and gravel aquifer underlying the FMPC and surrounding region, contamination reaching the aquifer as a result of vertical migration through the overlying till is dealt with as a source term to the model. That is, any past, present, or future uranium release from the till will be input to the model as a known quantity from each principal source. The role of the geochemical program was expanded to account for this model design and served as the focal point to evaluate the source terms for the model.

## P.1.2 ISSUES OF THE GEOCHEMICAL PROGRAM

The geochemical program conducted in support of the RI/FS is designed to:

- Evaluate past, current and future releases of uranium from several primary sources to the underlying aquifer
- Develop representative values for geochemical parameters that will be used to model solute transport in the groundwater

In order to provide the most substantive results in a cost-effective manner, the technical approach to satisfy these objectives was developed around five key, site-specific issues. These five issues are:

- Does soil contamination from air deposition represent a source of uranium to groundwater?
- Do soluble uranium spills represent a past, continuing or future source of uranium to groundwater?
- Does Paddys Run and/or the Storm Sewer Outfall Ditch represent a past, continuing, or future source of uranium to groundwater?
- Do the waste pits represent a past, continuing or future source of uranium to the underlying aquifers?
- Should geochemical parameters for radionuclide transport and attenuation in the sand and gravel aquifer be estimated for use in the solute transport model?

The first four issues focus on field and laboratory data to estimate the amount of uranium available from potential sources, while the fifth issue additionally utilizes geochemical modeling and published literature to quantify a uranium distribution coefficient ($K_d$) for the aquifer. The uranium distribution coefficient is defined as the concentration of sorbed uranium per kg of aquifer solid divided by the concentration of uranium per liter of ground water [$K_d$ = (mg/kg)/(mg/ ) = /kg]. This interim report will address Issues Three and Five of the RI/FS Geochemical Program.

## P.1.3 ISSUE THREE: PADDYS RUN AND THE STORM SEWER OUTFALL DITCH

### P.1.3.1 Purpose and Scope

The purpose of Issue Three is to establish whether uranium-bearing surface water has infiltrated and/or continues to infiltrate vertically downward through the bottom of Paddys Run and the Storm Sewer Outfall Ditch. Additionally, the disposition of this uranium prior to reaching the underlying sand and gravel aquifer needs to be established. To address this issue, subsurface soils and surface waters from Paddys Run and the Storm Sewer Outfall Ditch (Figure P-1) have been sampled and

analyzed to evaluate the retention capability of the soils and the degree of infiltration of uranium-bearing surface water to the underlying aquifer. Surface water samples were analyzed for chemical parameters and the analytical data used to construct an equilibrium geochemical model that predicts the dominant uranium specie in the surface water. This information, along with analytical results on leachable iron, manganese and uranium produced from the subsurface soil samples, was used to evaluate the degree of uranium retardation (if any) by the sediment and soil beneath Paddys Run and the Storm Sewer Outfall Ditch. The analytical results for subsurface soil samples were used to investigate three cases:

- No attenuation of uranium as it passes through the sediment and soil into the underlying aquifer (i.e., the vertical distribution of uranium in the subsurface soil samples is similar to background levels)
- Uranium is historically bound up in the subsurface soil samples (i.e., uranium is retarded by the sediment and subsurface soil, but has not broken through to the underlying aquifer)
- Uranium is present in the underlying aquifer solids (i.e., uranium has partially or completely broken through to the underlying aquifer)

These cases were evaluated by analyzing stream bed borings obtained from Paddys Run and the Storm Sewer Outfall Ditch for total uranium. Boring locations are shown in Figure P-1. In Paddys Run, one boring (P1; 1408) was placed upstream just below the Waste Pit Area and K-65 silos. A second boring (P2; 1409) was located in an area considered to be a significant zone of recharge to the underlying aquifer. The third boring (P3; 1410) is downstream from the confluence with the Storm Sewer Outfall Ditch. These locations were chosen to allow a comparison of segments of Paddys Run impacted by the flow from the Storm Sewer Outfall Ditch and those segments upstream from the confluence.

In the Storm Sewer Outfall Ditch, the upstream location (S1; 1405) was placed above the spillover of the storm water retention basin to evaluate the level of uranium retained by an inactive reach of the Storm Sewer Outfall Ditch. The second location (S2; 1406) is on an existing depression in the channel bottom, thought to be the remnants of a small, abandoned settling basin. This area is proximal to the easternmost fly ash pile and could serve to account for any associated impacts of fly ash on the Storm Sewer Outfall Ditch and underlying aquifer. A third boring (S3; 1407) is located near the confluence with Paddys Run,which accounts for cumulative effects of fly ash piles and/or whether most uranium is lost prior to reaching this point.

P.1.3.2 Analytical Methods and Field Sampling

IT Analytical Services (ITAS-Oak Ridge) analyzed surface waters for chemical and radiological parameters and subsurface soils for total uranium. In addition, the parameters Eh, pH, dissolved oxygen, conductivity, temperature, and alkalinity were measured during the collection of samples. The collection, handling and analysis of subsurface soils and surface waters conformed to the procedures and conventions established in Revision 3 of the FMPC RI/FS Work Plan and Quality Assurance Project Plan (QAPP). Modifications to the collection and analysis of subsurface soil samples were addressed in the Field Sampling and Laboratory Procedure Plan for the Geochemical Program. A summary of the field sampling procedure appears below, and analytical methods are discussed in Chapter P.2.0.

P.1.3.2.1 Field-Sampling Procedure for Subsurface Soils

Details on the procedures and conventions used for the collection, handling, and analysis of subsurface soil samples can be found in Revision 3 of the FMPC RI/FS Work Plan and QAPP, and the Field Sampling and Laboratory Procedure Plan for the Geochemical Program. The field sampling procedure is summarized as follows:

- Split-spoon samples were collected continuously in six-inch intervals from the stream bed surface to the sand and gravel aquifer water table.
- Samples were two- to six-inch sections of the split-spoon core.
- If the water table was not detected because of wet subsurface material throughout, borings were advanced to the following depths:

  - P1 (1408) to 24 feet
  - P2 (1409) to 20 feet
  - P3 (1410) to 20 feet
  - S1 (1405) to 34 feet
  - S2 (1406) to 17 feet
  - S3 (1407) to 9 feet

- Changes in lithology and/or geochemistry took precedence over the depth-interval sampling criterion (e.g., if iron staining begins at a depth of 12 feet, a new sample begins at 12 feet).
- The sample log recorded the percent recovery for a given 1.5-foot interval and any interval where soil was not recovered.
- If the first or second split-spoon interval was refused, the boring was restarted from the ground surface.
- Samples were bottled immediately after screening, and no samples were collected for volatile organic analysis (VOA), regardless of HNu or organic vapor analysis (OVA) reading.

DRAFT

- Boring logs emphasized lithology, stratigraphy and geochemical descriptions.
- A maximum of eight soil samples from each boring were sent to the laboratory for total uranium analysis.
- Samples not analyzed were archived for future use, if necessary.

## P.1.4 ISSUE FIVE: PARAMETERS FOR SOLUTE TRANSPORT MODEL

### P.1.4.1 Purpose and Scope

The purpose of Issue Five is to estimate a uranium distribution coefficient ($K_d$) for the sand and gravel aquifer. In developing a technical approach to satisfy this objective, the following assumptions were made:

- The application of the solute transport model is limited to the sand and gravel aquifer.
- The relatively uniform characteristics of the sand and gravel aquifer imply related published information could provide $K_d$ values without site-specific, laboratory-attenuation studies.
- Only uranium is currently proposed for detailed consideration in the solute transport model, and the $K_d$ value for uranium is the focus of this issue.

Two methods were proposed to determine a uranium $K_d$ value for the aquifer. The first method relied on analytical data from groundwaters as input to a geochemical equilibrium model (EQ3NR; Wolery 1983) to predict the dominant uranium species in solution. This information was to be combined with mineralogic data on the sand and gravel aquifer and the two sets of site-specific data compared to results of published $K_d$ studies. A second method was proposed to evaluate independently the uranium $K_d$ by conducting laboratory sorption studies with the sand and gravel solids.

The first method was modified to exclude mineralogic identification of aquifer solids after initial geochemical modeling and aquifer-solid analyses indicated that the dominant uranium specie was $UO_2(CO_3)_3^{-4}$, a negatively-charged specie that would not exhibit significant sorption on clay minerals with high cation-exchange capacity. To resolve this problem, the analytical results on leachable iron were used to estimate the amount of amorphous iron (which has a strong affinity for negatively-charged complexes) that could be present as coatings on clay minerals and along fractures in the aquifer. Using these estimates, and a published study on uranium sorption by

amorphous iron oxyhydroxide, empirical calculations were carried out to derive an apparent uranium $K_d$ value.

The second method cited above has not been carried out at this time. However, an alternative method was substituted to maintain two independent calculations of the uranium $K_d$ value. Using the total uranium values obtained on leachates derived from the leachable iron and manganese test, and uranium analyses of groundwater, a $K_d$ was calculated directly from the uranium concentration in the solid (after a correction for background levels) and groundwater $K_d$ = (mg U/kg solid)/ (mg U/L groundwater).

P.1.4.2 Analytical Methods and Field Sampling

ITAS-Oak Ridge performed the differential leaching/total uranium analysis of aquifer solids and the chemical and radiological analyses of groundwaters. Field parameters were measured on all groundwaters. To assist in determining the redox potential (Eh) of groundwater, 16 wells were sampled and analyzed for $U^{+4}$ and total U ($U^{+6}$ = total U - $U^{+4}$). $U^{+4}$ and $U^{+6}$ are defined as the sum of all uranium species for each oxidation state. The $U^{+4}$ and total U analyses were done by United Nuclear Corporation Geotech Laboratories (UNC Geotech), Grand Junction, Colorado. In support of the partitioning studies, IT-Export carried out analyses on the aquifer solids for total cation-exchange capacity, total organic carbon, grain size, and leachable iron and manganese. A leachate split was sent to ITAS-Oak Ridge for total U analysis.

The collection, handling, and analysis of aquifer solids and groundwaters conformed to the procedures and conventions established in Revision 3 of the FMPC RI/FS Work Plan and Quality Assurance Project Plan (QAPP). Detailed procedures for the differential leaching analysis of aquifer solids, and $U^{+4}$ and total U field sampling and analytical methods are given in the appendix of the Field Sampling and Laboratory Procedure Plan for the Geochemical Program. A summary of the $U^{+4}$ and total U field sampling procedure appears below, and analytical methods are discussed in Chapter P.2.0.

P.1.4.2.1 Field-Sampling Procedure for $U^{+4}$ and Total U

Groundwater samples were collected for total U and $U^{+4}$ analysis to estimate independently the Eh of the groundwater. The $U^{+4}$ in solution is complexed with cerium and precipitated with hydrofluoric acid. $U^{+6}$ is determined by the difference of total U and $U^{+4}$. The procedure is summarized as follows:

- Approximately 250 milliliter (ml) of sample is collected after filtering the groundwater through a 0.45 micron filter.

- The sample is split and half is acidified with $HNO_3$ to pH < 2 and shipped to the laboratory for total U analysis.
- 25 ml of the remaining filtered sample is placed into a 125-ml plastic bottle, and 0.125 ml of cerium solution is added to the sample and mixed well.
- 1.25 ml of reagent grade HF is added to the solution, and the solution is mixed thoroughly and cooled for 15 minutes in a cooler.
- The sample is removed from the cooler, shaken, and filtered through a 0.1 micron filter.
- The sample bottle is rinsed three times with distilled water and the rinse solution is passed through the 0.1 micron filter.
- The filter funnel and filter paper are rinsed with distilled water prior to placing the filter paper in a container for shipment to the laboratory, where it is analyzed for $U^{+4}$.

## P.2.0 ANALYTICAL METHODS AND RESULTS

### P.2.1 ANALYTICAL METHODS

Standard analytical methods (e.g., Methods for Chemical Analysis of Waste and Water; EPA-600 4-79-020) were used for the analysis of surface waters and groundwaters and will not be discussed here. Subsurface soils and aquifer solids were analyzed by gamma spectrometry for total uranium. Aquifer solids were also subjected to leaching tests to determine the amount of leachable iron, manganese, and uranium. Leachates recovered from these tests were analyzed for iron, manganese, and uranium by standard procedures (e.g, atomic absorption, inductively coupled plasma or laser fluorimetry). Some of the analytical methods employed for subsurface soils and aquifer solids are site-specific applications and are summarized below. Detailed laboratory procedures for the leaching tests can be found in Revision 3 of the FMPC RI/FS Work Plan, the Work Plan for the Geochemical Program, and the Field Sampling and Laboratory Procedure Plan for the Geochemical Program.

#### P.2.1.1 Gamma Spectrometry

Solid samples analyzed by the gamma spectrometry method are generally 500 gram splits of crushed and homogenized material. After sample preparation is completed, the samples are placed in containers that will yield an analytical geometry identical to that of standards used to calibrate the instrument. The standards have known concentrations of each uranium isotope that emits gamma by radiation and are used to construct a calibration curve prior to sample analysis. Most instruments used for this procedure employ sophisticated software that contains a complex algorithm

5617

to account for sample instrument geometry, sample weight, the coefficient of absorbence for gamma radiation in the sample material, and interfering gamma radiation from other radionuclides present in the sample. The sample geometry and weight are given as input parameters prior to analysis, and the algorithm calculates the total uranium concentration in the sample based on the contribution of each uranium isotope. Output from the algorithm is the total uranium concentration in ug/g (ppm).

P.2.1.2 Differential Leaching Tests for Uranium

The differential leaching tests distinguish between easily mobilized and available uranium (i.e., sorbed or amorphous uranium phases) from insoluble uranium (i.e., U in mineral lattices such as zircon) that is not available to the groundwater environment. The four leaching tests are designed to provide the following information:

- Uranium present in fine-grained carbonate minerals (i.e., pore cement)
- Uranium present as sorbed species on clay minerals and amorphous iron and aluminum oxyhydroxides
- Uranium present as sorbed species or within organics in the soils or wastes
- Uranium present in amorphous solids or oxide phases such as $UO_2$ or $U_3O_8$

The uranium of most concern is probably bound on amorphous iron and aluminum oxyhydroxides that coat clay minerals, or is present with the organics and amorphous oxide phases. This uranium (if present) could be available for transport through the aquifer. Uranium which is present in the lattices of clay minerals, apatite, monazite and zircon is naturally occurring and generally immobile, and can be considered representative of the background concentration level.

The four-step extraction technique can be summarized as follows:

- Sodium acetate is used to digest the fine-grained carbonate minerals
- Disodium ethylenediaminetetracetic acid (EDTA) is used to strip sorbed uranium from clay minerals, and amorphous iron and aluminum oxyhydroxides
- Hydrogen peroxide is used to digest organic material
- Nitric acid (1:1 with distilled $H_2O$) is used to dissolve amorphous solids and oxides of uranium

At each step, the reagent is agitated with the sample and the solution fraction (leachate) was recovered by centrifuging. The leachates were analyzed for total uranium by laser fluorimetry.

P.2.1.3 Leaching Technique for Iron and Manganese

This leaching technique recovers iron and manganese from amorphous-oxyhydroxide coatings on grains or fractures and crystalline oxide minerals using a solution of acetic acid and hydroxylamine hydrochloride. The solid is mixed with the leaching solution, agitated, and the leachate recovered by centrifuging. Unlike the differential leaching procedure which recovers "historical" uranium (i.e., recently bound uranium), this procedure will also recover ancient uranium locked in the mineral lattices of detrital grains or fracture coatings. Therefore, uranium sorbed to iron- and manganese-oxyhydroxide coatings on grain surfaces or fractures is removed and mixed with uranium recovered from the lattice sites in iron- and manganese-oxide minerals (i.e., detrital grains or fracture coatings of hematite or pyrolusite). The two uranium components cannot be distinguished in the analysis, and the background component (i.e., uranium in mineral lattices) must be estimated from aquifer solids which are known to be uncontaminated.

P.2.2 ANALYTICAL RESULTS

Analytical results for samples of subsurface soils, surface waters, aquifer solids, and groundwaters are given in Attachment P.I. Groundwater analyses reported in Attachment P.I are limited to the samples chosen for geochemical modeling. The analytical results for uranium on subsurface soil and surface water samples obtained from Paddys Run and the Storm Sewer Outfall Ditch were used to evaluate a source term for these drainages (Issue Three). Analytical results on groundwaters and aquifer solids were used to calculate apparent uranium distribution coefficients for the sand and gravel aquifer (Issue Five).

P.2.2.1 Issue Three

Analytical results for total uranium were obtained on subsurface soils and surface waters in Paddys Run and the Storm Sewer Outfall Ditch to evaluate a source term for these drainages.

P.2.2.1.1 Subsurface Soils

Samples of subsurface soils obtained from Paddys Run and the Storm Sewer Outfall Ditch (Figure P-1) were analyzed for total uranium by gamma spectrometry. The samples consist primarily of well-graded sand and gravel with horizons of poorly-graded sand and silty clay. Borehole depth ranged from 20 to 24 feet and 9 to 34 feet, respectively, in Paddys Run and the Storm Sewer Outfall Ditch. The deepest borehole in the Storm Sewer Outfall Ditch (S1; 1405) penetrated an iron- and manganese-stained horizon between 25 and 30 feet below the surface, which

was interpreted as a possible redox zone. Uranium results for six of the sampling sites are illustrated in Figures P-2 and P-3.

Soil samples recovered from Paddys Run (Figure P-2) had total uranium concentrations of less than 1 to 4 ug/g (ppm). However, significant 2-sigma counting errors (generally > 50 percent and up to 100 percent of the reported value) precludes any discussion of significant variation in the uranium concentration with depth (i.e., no variation observed within the range of 2-sigma counting errors; Figure P-2). Additionally, for uranium concentrations in these soil samples, it is not possible to separate components of contamination (if present) from regional background levels, which in common rocks are: carbonates, 2.2 ppm; shales, 3.7 ppm; and granites, 5 ppm (Faure 1977; Krauskopf 1979). Site environmental monitoring data have established uranium background levels of 1 to 3 ppm in the aquifer solids.

Total uranium values for soil samples recovered from the Storm Sewer Outfall Ditch ranged from 1 to 10 ppm (Figure P-3). Large 2-sigma counting errors make discussion of uranium variation with depth equivocal for Site S3 (1407). However, the soil profiles from Sites S1 (1405) and S2 (1406) show uranium variation that is significant (i.e., greater than 3 ppm). Site S1 (1405) is most proximal to the Fernald compound (Figure P-1) and is located above the spillover for the storm water retention basin. Soil samples recovered from this boring indicate a decrease in the uranium concentration from 10 to 4 ppm within the top 4 feet of soil (Figure P-3). The high uranium concentrations in the upper 3 feet of this boring coincide with a clay-rich horizon between 0.5 and 2 feet, suggesting uranium may have sorbed onto the clay (see Section P.2.5.1).

Site S2 (1406) is located near a fly ash pile and in a depression which may be an abandoned settling basin. Very little (if any) soil is present at Site S2 (1406), and the boring penetrates the top of the sand and gravel aquifer. The uranium profile from this site indicates uranium concentrations of 6 to 8 ppm over the interval of 5 to 15 feet (background uranium is less than 3 ppm). Because the soil present at this site is negligible, the profile indicates "historical" uranium is present in the aquifer.

P.2.2.1.2 Surface Waters

Analytical results for three surface water samples (W-7, W-11, and ASIT003 sampled May 14, 1989 are given in Attachment P.I. Samples were collected in each flowage above the confluence of Paddys Run and the Storm Sewer Outfall Ditch (W-11 and ASIT003, respectively) and below the confluence (W-7; Figure P-1). The surface samples are oxygenated waters (Eh approximately 450 mV) with a pH of about 8.5 and their solution chemistry is dominated by

$HCO_3^-$ (> 200 mg/L) and Ca (> 70 mg/L), reflecting the interaction of these waters with carbonate rock in the subsurface. Uranium concentrations in the surface water samples ranged from 0.002 (ASIT003) to 0.015 (W-07) mg/L. The sample obtained from the Storm Sewer Outfall Ditch (ASIT003) has a uranium concentration similar to background levels established for Paddys Run (0.001 to 0.004 mg/L), using site-specific environmental monitoring data. Samples recovered from Paddys Run, above and below the confluence with the Storm Sewer Outfall Ditch, have uranium concentrations above the background level maximum, indicating these surface waters might contribute uranium to the underlying aquifer by vertical infiltration. Modeling results for uranium speciation are presented in Section P.3.3.

P.2.2.2 Issue Five

Analytical results for total uranium were obtained on aquifer solids and groundwaters to calculate an apparent distribution coefficient [$K_d$ = (mg U/kg solid)/(mg U/L groundwater)] for the sand and gravel aquifer. Additionally, geochemical modeling on the speciation of uranium in groundwater was combined with analytical results on leachable iron to derive empirically a distribution coefficient.

P.2.2.2.1 Aquifer Solids

Thirty-one subsurface samples consisting of gravel, sand, silt and clay were analyzed for leachable iron, manganese and uranium, total organic carbon, total cation exchange capacity, and grain-size variation. Thirteen of these samples were also utilized for total uranium analysis (6) and differential-leaching uranium analysis (7). Analytical results are given in Attachment P.I and illustrated in Figures P-4 to P-6.

Figure P-4 is a plot of leachable iron, manganese, and uranium against the particle size of the sample. Based on the sieve analysis, two sample populations exist: (1) silt plus clay greater than 50 weight percent and (2) silt plus clay less than 25 weight percent. The leachable fraction of iron, manganese, and uranium in the majority of aquifer solid samples is not a function of the particle size, because the range of values for the metals is similar for the two sample populations. This observation suggests that the majority of iron and manganese solids accessed by the groundwater are present as amorphous- or crystalline-oxyhydroxide coatings along fractures in the fluid-flow path, rather than as detrital grains or surface coatings on the aquifer particles. This hypothesis is consistent with sample preparation procedures which avoided crushing the sample below its natural aggregated size (i.e., clay minerals were not mechanically disaggregated prior to the leaching test).

Three clay samples in the first population have leachable iron values greater than 2 mg/g, suggesting surface coatings on clay minerals and/or complexation 001500 with organic-carbon (see below) controls the leachable fraction of iron in these samples. A lack of correlation between the sum of leachable iron and manganese versus total uranium (inset Figure P-4) indicates that:

- Sorption of uranium on amorphous iron- and manganese-oxyhydroxide coatings may not be occurring in the aquifer.
- The leachable iron and manganese in the solids is primarily from the digestion of crystalline oxyhydroxide phases.

Results for total organic carbon versus grain size are illustrated in Figure P-5. As in Figure P-4, there is no correlation between the total organic carbon content of the aquifer solids and the weight percent of silt and clay in the sample. The majority of samples, irrespective of silt and clay content, have total organic carbon values below 8 mg/g. Two samples obtained from a major clay interbed in the sand and gravel aquifer contain 15 to 16 mg/g of total organic carbon. These two samples are coincident with the highest leachable iron values in Figure P-4. The correlation of high organic carbon content to high leachable iron values implies iron is associated with or adsorbed on organic materials in the clay interbed.

In contrast to results presented in Figures P-4 and P-5, the cation exchange capacity of the aquifer solids is a strong function of the silt and clay content (Figure P-6). Samples containing less than 25 weight percent of silt and clay have a total cation exchange capacity (CEC) of less than 0.04 meq/g, whereas those samples with greater than 50 weight percent silt and clay have CEC up to 0.28 meq/g.

P.2.2.2.2 Anomalous Uranium Results

Thirteen aquifer-solid samples were chosen for total-uranium analysis by gamma spectrometry. Seven of the 13 samples were selected for a differential leaching procedure designed to strip uranium sequentially from the solids using a series of four progressively stronger leaching reagents (see analytical methods in the appendix of the Field Sampling and Laboratory Procedure Plan for the Geochemical Program). Results for the total uranium and differential leaching analysis are reported in Attachment P.I and illustrated in Figures P-7 and P-8. It is emphasized that these results are anomalous with respect to those obtained previously for total uranium of aquifer solids.

Figure P-7 is a plot of total uranium (ug/g or ppm) versus sample depth for 6 of the 13 samples. Mean uranium concentrations in these aquifer solids range from about 11 to 16 ppm, but show no variation within their 2-sigma counting errors. The mean uranium values are about 3 to 5 times

higher than the maximum uranium background level of 3 ppm (based on uranium analyses of subsurface solids from uncontaminated wells). Possible causes of the elevated uranium values are:

- Uranium sorption on particles along the flow path
- Precipitation of uranium solids along the flow path
- The presence of naturally-occurring uranium-bearing minerals (i.e., zircon, apatite or monazite) in the aquifer sands
- Problems with the procedures and analytical methods used to determine the uranium concentration (see Section P.2.5.2)

Uranium results from the differential leaching procedure are shown in Figure P-8. The seven samples analyzed had mean uranium concentrations of 95 to 150 ppm prior to leaching and, within their 2-sigma counting error, were unchanged after leaching. Additionally, sample-to-sample variation in uranium concentration is not observed within the 2-sigma counting error. These solids have uranium concentrations 1 to 2 orders of magnitude higher than background uranium concentrations (see above), and an order of magnitude higher than the results shown in Figure P-7. Sorption and precipitation of uranium along the flow path cannot be responsible for the high concentrations in these samples, because the leachates (analyzed by laser fluorimetry) from the solids had less than 2.5 ppb of uranium. Likewise, the uranium-bearing mineral apatite, and to a lesser degree monazite, cannot contribute significantly to the high uranium concentrations because they are soluble in nitric acid (used in final leaching step). The results presented in Figure P-8 can be explained by high concentrations of insoluble uranium-bearing minerals (i.e., zircon) in the aquifer sands or problems with the analytical procedures and methods (see Section P.2.5.2).

P.2.2.2.3 Groundwaters

Analytical results for groundwater samples used in the geochemical modeling appear in Attachment P.I. These groundwaters were collected from 20 monitoring wells (locations shown in Figure P-9) during Round 3 (Fourth Quarter, 1988) and Round 4 (First Quarter, 1989) sampling. The dominant chemical characteristics of the groundwaters include: near-neutral pH values (6 - 8), Eh values of 50 to 450 mV, $HCO_3^-$ concentrations of 200 to 400 mg/L, and Ca concentrations of 70 to 200 mg/L. These chemical characteristics suggest the groundwaters are in equilibrium with carbonate rocks in the aquifer. Uranium concentrations in these samples vary from 0.005 to 4.38 mg/L, with most modeling samples having concentrations greater than expected for natural waters (i.e., U > 0.0001 to 0.010 mg/L; Hem 1970). Modeling results for the uranium speciation are presented in Section P.3.3.

## P.2.3 DISCUSSION

### P.2.3.1 Issue Three

Uranium concentrations in most subsurface soil samples overlap with the range of values reported for common rock types (i.e., 2-5 ppm) and do not appear to reflect the sorption and/or precipitation of uranium from infiltrating groundwater. The lack of uranium contamination in the majority of the soil samples suggests any one or all of the following:

- The soils were not exposed to uranium-bearing water.
- Uranium that had sorbed onto the soils has been subsequently desorbed by uncontaminated water.
- Uranium was in the form of nonsorptive species.

Therefore, the soil profiles from Sites P1 (1408), P2 (1409), P3 (1410), and S3 (1407) may conform to the first case scenario (Section 1.3.1), which states that if surface waters with high uranium concentrations infiltrated these soils, no attenuation took place (i.e., the soil profile for uranium reveals background levels). This scenario supports the speciation results for surface waters (Section P.3.3, Table P-2), which indicate the neutral complex $UO_2(H_2PO_4)_2$ is present and little (if any) attenuation of uranium will occur as surface waters vertically infiltrate to the underlying aquifer. The scenario also supports modeling results which indicate the anionic uranyl-carbonate species are present if amorphous iron oxyhydroxide is absent (i.e., no sorption on the soil particles).

Exceptions are Sites S1 (1405) and S2 (1406). At Site S1 (1405), uranium values up to 10 ppm in the upper 2 to 3 feet of soil suggest uranium sorption and/or precipitation may have occurred. Site S1 (Figure P-3) is proximal to the discharge point for the Storm Sewer Outfall Ditch, and higher uranium concentrations in these subsurface soil samples are in agreement with known periodic discharges of uranium-bearing waters. The elevated uranium concentrations in the upper 3 feet of this boring are coincident with a clay rich horizon between 0.5 and 2 feet. This observation suggests that uranium is being retarded by sorption processes in this area. Therefore, this uranium is a potential source for future releases to the underlying aquifer.

Site S2 (1406) shows slightly elevated uranium concentrations (6 to 8 ppm) over a depth interval of 5 to 15 feet. However, this observation cannot be correlated with clay-rich horizons found in the soil profile at Site S1, because little (if any) soil is present at this site. This site is proximal to a fly ash pile and may also be situated on the remnants of an abandoned settling basin. Either of these observations could account for the presence of "historical" uranium in the S2 profile.

Uranium may be retarded along this profile by sorption onto iron- and manganese-oxyhdroxide coatings, which formed along the fluid-flow path, or by precipitation of amorphous uranium compounds. Because Site S2 (1406) is located in an area where the till is absent, this uranium is currently present in the aquifer and is a potential source for future release and transport through the aquifer.

The soil profile from Site S1 (1405) supports the second case scenario (Section P.1.3.1), which states that uranium present above the expected background level is "historical" uranium bound in the subsurface soil (i.e., no breakthrough has occurred to the underlying aquifer). However, the profile from Site S2 (1406) indicates partial breakthrough of uranium to the sand and gravel aquifer (case three, Section P.1.3.1). For both of these cases, modeling results which predict the dominant uranium specie as $UO_2(CO_3)_3^{-4}$ (Section P.3.3, Table P-2) support the hypothesis of uranium sorption on amorphous iron- and aluminum-oxyhydroxide films. Alternatively, uranium may be retarded by precipitation of amorphous uranium compounds.

P.2.3.2 Issue Five

Analytical results for uranium concentrations in aquifer solids are highly suspect because the differential leaching procedure did not lower uranium values in aquifer solids that are 1 to 2 orders of magnitude larger than background uranium concentrations. Those samples which did not undergo the differential leaching procedure had uranium concentrations 2 to 8 times higher than common rocks, but are also suspect because the differential leaching procedure indicates a lack of sorbed or amorphous uranium (i.e., all uranium present is within mineral lattice structures), which is in contrast to uranium results obtained on leachates derived from the iron and manganese experiments (see below). Petrographic data on the composition of aquifer sands are not available, although it is unlikely that high concentrations of an insoluble uranium-bearing phase such as zircon would be found to account for the elevated uranium concentrations. The most probable cause of the anomalously high uranium concentrations is a variation in the standard analytical procedure or method.

Gamma spectrometry is used to analyze for total uranium in the aquifer solids. This analytical method is sensitive to the mass of solid analyzed and the geometry of the sample with respect to the detector. Standards used to calibrate the instrument are 500-gram aliquots that are dried and ground to homogenize the solid prior to analysis. Aquifer-solid samples of 4 to 40 grams were analyzed without drying and homogenizing the material, and the small sample volumes resulted in poor geometry configurations with respect to the detector. These deviations from standard

procedures requires that the analytical results for total uranium in aquifer solids be treated as qualitative.

In contrast, the total uranium in the leachate fractions produced from the differential leaching procedure were analyzed by laser fluorimetry and results are considered to be quantitative. These results indicate that less than 2.5 ppb of uranium is sorbed onto the aquifer solids, which is in contrast to uranium values of 33 to 783 ppb obtained from the leachate produced by the iron- and manganese-oxyhydroxide stripping procedure. Reagents specific to each procedure can account for the difference in uranium results, as the analytical method was identical for all leachates. The differential leaching is a four-step procedure; initial leaching with sodium acetate followed by EDTA, hydrogen peroxide, and nitric acid solutions. This procedure removes:

- Uranium sorbed to inorganic and organic particles
- Uranium complexed within amorphous aluminum, iron, or manganese oxyhydroxides
- Amorphous uranium solids present in the sample

In contrast, the iron- and manganese-oxyhydroxide procedure utilizes acetic acid and hydroxylamine hydrochloride to attack amorphous and crystalline iron- and manganese- oxyhydroxide minerals (Chester and Hughes 1967). Therefore, the latter procedure will contain a uranium component derived from crystallized iron and manganese minerals (i.e., detrital minerals older than the Holocene), while the former will not. The uranium in the detrital minerals is not of recent origin, and the concentrations of less than 1 ppm are well below the average of 3.7 ppm reported for shales (Krauskopf 1979).

Because of the suspect nature of the uranium analytical results for aquifer solids and leachates, calculated distribution coefficients ($K_d$) should be interpreted cautiously. However, the calculations are useful as an independent check on partitioning estimates based on speciation modeling (Section P.3.3) and experimental studies (Section P.4.1.7).

## P.3.0 GEOCHEMICAL MODELING

Geochemical modeling of the uranium speciation in surface waters was carried out to assist in the evaluation of the potential source term in Paddys Run and the Storm Sewer Outfall Ditch (Issue Three), and in groundwaters to support the calculation of the uranium distribution coefficient for the aquifer (Issue Five). Modeling was conducted with the EQ3NR geochemical code (Ver. 3245;

Wolery 1983), which is an industry standard, speciation/solubility code developed by Lawrence Livermore National Laboratory for use in predicting the behavior of metals, radionuclides, and other contaminants in the natural environment. The code accesses a data base containing the thermodynamic properties of 47 elements, 686 aqueous species, 713 minerals, and 11 gases. This data base includes 49 uranium-bearing aqueous species and 53 uranium-bearing minerals, constituting the most complete data base available for modeling the behavior of uranium in natural waters.

Modeling results must be interpreted cautiously. Values for thermodynamic parameters utilized by the EQ3NR code for speciation and solubility calculations are experimentally determined by many investigators, and the quality of their results is variable. Personnel at Lawrence Livermore National Laboratory have qualified the thermodynamic data utilized by the code by indicating whether the data are poor, fair, good, or uncertain. Uncertain generally indicates that independent workers have reached conflicting results for the indicated value and the problem is currently unresolved. All aqueous-uranium species and uranium minerals considered in this investigation have thermodynamic values which have been judged to be good.

Additionally, it must be emphasized that results obtained from geochemical modeling of natural systems are not unique. At best, modeling can present a snapshot of a point in time for the dynamic natural system. However, modeling studies are useful to establish boundary conditions for a system, which may enhance the development of remediation techniques and/or the solution to contaminant problems.

P.3.1 SELECTION CRITERIA FOR GROUNDWATER SAMPLES

Over 100 groundwater analyses from Round 3 (Fourth Quarter, 1988) and Round 4 (First Quarter, 1989) were available for modeling. Because of the large number of analyses received, selection criteria were developed to choose samples from the entire spectrum of analyses, thus reducing the number of analyses to model. All groundwaters with reported uranium concentrations greater than 0.3 mg/L (7 analyses) were modeled. Analyses deemed to be representative of "typical" local groundwaters were screened for uranium content, and 14 samples were chosen that had uranium concentrations of 0.005 to 0.3 mg/L (greater than 50 percent of the samples received had reported uranium concentrations of less than 0.005 mg/L). Additional criteria focused on anomalous concentrations of calcium, phosphorous, potassium and sulfate, and Eh values (based on platinum electrode measurements) that were below 100 mV (6 analyses). It is important to reiterate that the selection criteria for groundwater samples used in the geochemical modeling is biased toward those analyses with high uranium concentrations.

## P.3.2 MODELING ASSUMPTIONS AND CONSTRAINTS

Analytical results received for surface and groundwaters did not contain values for total dissolved solids (TDS) and specific gravity (SG). Many results also lacked a reported value for the redox potential (Eh) of the water. Values for these parameters must be included on the input file for the EQ3NR code and were estimated as follows:

- TDS was calculated by summing the concentrations (in mg/L) of analytes that were above the detection limit
- SG was assumed to be 1 g/cc, based on the low TDS values (400 - 600 mg/L)
- Eh was calculated by the EQ3NR code using the $NH_4^+/NO_3^-$ and $O_2/H_2O$ redox couples, and with solubility constraints based on pyrolusite ($MnO_2$) and uraninite ($UO_2$) saturation (Eh calculations are discussed in detail in Section P.3.2.2)

### P.3.2.1 Electrical Charge Imbalances

The 26 water analyses utilized for modeling had electrical charge balances ranging from -27 to +64 percent of the total charge (Table P-1). About half of the analyses have reasonable charge balances that lie between -5 and +5 percent of the total charge. Electrical imbalances greater than +5 or less than -5 percent suggest either errors in the analysis of a major constituent or the omission of a major constituent in the analysis. The omission of a major constituent will usually cause a consistent bias (positive or negative) in the electrical imbalance, thus the range of imbalances observed here suggests random errors in the analyses. A reduced level of confidence should be placed on those analyses with large electrical imbalances (i.e., those that lie outside of the range -5 to +5 percent) and the corresponding uranium speciation calculated from the analytical data. However, uranium speciation will probably not be affected by large electrical imbalances resulting from analytical errors in the determination of calcium, potassium, magnesium, sodium, or sulfate, but can be affected if the phosphorous concentration, alkalinity, or pH is in error (see discussion of uranium speciation in Section P.3.3).

### P.3.2.2 Eh Calculations

Platinum-electrode measurements were not provided with all groundwater analyses and a variety of redox couples and mineral-solubility limits were utilized to constrain the system Eh. Eh values were calculated with the $O_2/H_2O$ (770 to 800 mV), $NH_4^+/NO_3^-$ (324 to 350 mV), and $U^{+4}/UO_2^{+2}$ (-120 to -160 mV) redox couples, and by lowering the $O_2/H_2O$ redox value in increments until the solution reached saturation with respect to, first, pyrolusite (MnO2; 575 to 605 mV) and then uraninite (UO2; 35 to 50 mV). Eh values bounded by the pyrolusite and uraninite solubility limits overlap with the range obtained by platinum-electrode measurements in the field (454 to 75 mV).

The O2/H2O and $U^{+4}/U^{+6}$ redox couples overestimated and underestimated, respectively, the redox state of the groundwaters. For the O2/H2O couple, the high Eh value may be due to addition of atmospheric O2 during sample collection or the inability of the geochemical code to evaluate the kinetic rate of the O2-H2O half-cell reaction. Calculation of the groundwater Eh with the U+4/U+6 couple produced values inconsistent with mineral solubilities and platinum-electrode measurements. Low uranium redox values (-120 to -160 mV) indicate concentrations of $U^{+4}$ are too high. The high $U^{+4}/U^{+6}$ ratios measured in these groundwaters are attributed to the sorption of uranyl species on iron-bearing colloids (Figure P-10), which comprised a portion of the filtered residue analyzed for $U^{+4}$ (see field sampling technique for $U^{+4}$ and total U in the Field Sampling and Laboratory Procedure Plan for the Geochemical Program).

Because a wide range of Eh values were used to model uranium speciation, several groundwater compositions were modeled over an Eh range of 50 to 650 mV to determine the effect (if any) of Eh variation. Results for this test are shown in Figure P-11, and indicate that variation in the Eh estimate of groundwaters does not affect the speciation results for uranium.

### P.3.3 URANIUM SPECIATION

Uranium speciation was investigated in 26 groundwater samples (20 unique wells) and 3 surface water samples. Results for the speciation modeling are presented in Tables P-1 and P-2. Speciation results for the groundwaters support calculations to estimate a uranium distribution coefficient for the aquifer (Issue Five). Table P-1 reveals that 11 samples had greater than 99 percent of the uranium partitioned into the aqueous specie $UO_2(H_2PO_4)_2$. 9 samples (phosphorous not reported or below the detection limit) had greater than 99 percent of the uranium partitioned into the aqueous species $UO_2(CO_3)_3^{-4}$, $UO_2(CO_3)_2^{-2}$, and $UO_2(CO_3)$, and 6 samples (five with uranium greater than 0.3 mg/L) partitioned the uranium into a combination of the above three species. These results indicate that uranyl ion ($UO_2^{+2}$) will form negatively charged complexes with carbonate ion (CO3-2) in this environment, only if the molar concentration (moles per liter) of uranium is greater than one-half the molar concentration of phosphorous (i.e., [U] > 0.5[P]). When uranyl-carbonate complexes form, $UO_2(CO_3)_3^{-4}$ is the dominant specie in these groundwaters at neutral and slightly alkaline pH. Three surface waters were chosen for uranium-speciation modeling to evaluate the potential of introducing uranium to the underlying aquifer by vertically infiltrating surface waters (Issue Three). Analyses for these three samples reported uranium concentrations of 0.002 to 0.015 mg/L, with phosphorous ranging from below the detection limit < 0.02 mg/L to 0.16 mg/L (Attachment P.I). Because of the relatively low uranium concentrations in these surface waters, all uranium was partitioned into the neutral phosphate complex in waters which contained detectable amounts of phosphorous (Table P-2). Surface waters without reportable

phosphorous concentrations (i.e., W-11; Table P-2) partitioned uranium into the anionic carbonate complexes.

P.3.3.1 Discussion

Preliminary results on the feasibility of recovering uranium from groundwaters by anion-exchange processes show 90 percent of the uranium is recovered by this method (personal communication, Khan 1989). The experimental results are in good agreement with the majority of modeling results (i.e., negatively-charged uranyl-carbonate species). However, modeling results also indicate that uranium is complexed as the neutral $UO_2(H_2PO_4)_2$ specie in 11 of 26 groundwaters.

Several factors could account for the observed sorptive behavior of uranium. First, phosphorous (measured as total P and converted to phosphate) may form organic complexes in the groundwaters, which would reduce the activity of the phosphate complex and decrease the amount of $UO_2(PO_4)_2$ formed. Organic-phosphate speciation was not modeled because thermodynamic data are limited to inorganic-phosphate complexes, which results in $UO_2(PO_4)_2$ concentrations that may be overestimated. Second, the association constant for $UO_2(HPO_4)_2$ may not be correct (see 3.3.1.1 below); therefore, significant partitioning of uranium into this specie cannot be ruled out. The presence of $UO_2(HPO_4)_2$ in the groundwaters would be consistent with removal of uranium by anion exchange. Finally, the $UO_2(H_2PO_4)_2$ specie may exhibit weak dipole properties (similar to $H_2O$) that, despite the neutral charge, result in retardation along the flow path in an anion-exchange column.

P.3.3.1.1 Data Base Integrity

The speciation results for surface and groundwaters indicate that the uranyl ion has a strong affinity to form an unchanged complex with phosphate. A 002500-phosphorous concentration of 0.02 mg/L (the limit of detection) would allow up to 0.071 mg/L uranium to be complexed as $UO_2(H_2PO_4)_2$. Since the majority of analyses received (not modeled) have uranium concentrations less than 0.071 mg/L and phosphate values greater than 0.02 mg/L, the modeling results suggest carbonate complexation may not occur in these groundwaters. However, the speciation results for groundwaters containing phosphorous appear to be in conflict with published studies (Scanlan 1977; Tripathi 1984; Koss 1988), which indicate $UO_2^{+2}$ will form carbonatge complexes in bicarbonate waters at neutral pH. In addition, studies by Moskvin et al. (1967), and Dongarra and Langmuir (1980) concluded that the dominant uranyl-phosphate complex in natural waters of neutral pH is the single-protonated, negatively-charged $UO_2(HPO_4)_2^{-2}$ complex, which is in contrast to the neutral, double-protonated $UO_2(H_2PO_4)_2$ specie predicted by the EQ3NR code.

To resolve this apparent discrepancy, the thermodynamic values for the aqueous uranium species active in this study were checked to ensure data base integrity. Association constants for $UO_2(H_2PO_4)_2$ (log K = 45.24; Baes, 1956; Tripathi, 1984), $UO_2(CO_3)_2^{-2}$ and $UO_2(CO_3)_3^{-4}$ (log K = 17.08 and 21.70, respectively; Scanlan, 1977; Tripathi, 1984) were verified to be correctly entered in the thermodynamic data base. However, single-protonated uranyl-phosphate complexes (e.g., $UO_2(HPO_4)$ and $UO_2(HPO_4)_2^{-2}$ were not present in the thermodynamic data base. Lawrence Livermore National Laboratory removed single-protonated uranyl-phosphate complexes from the EQ3NR data base as a result of the conclusions reached by Tripathi (1984). Tripathi argued that the studies of Moskvin et al. (1967) and Dongarra and Langmuir (1980) who concluded that $UO_2(HPO_4)_2^{-2}$ (association log K = 18.3) is the dominant specie in oxygenated waters with pH between 4 and 8 are not valid because their experiments were carried out with acidic solutions pH = 0 to 4) and uranyl complexation with $H_2PO_4^-$ and $H_3PO_4$ was not considered. The omission of the single-protonated uranyl-phosphate complex from the data base was hypothesized to be insignificant because of the much larger association constant for $UO_2(H_2PO_4)_2$ relative to $UO_2(HPO_4)_2^{-2}$ (log K = 45.24 versus 18.3, respectively). This hypothesis was verified by reinserting the thermodynamic data of Dongarra and Langmuir (1980) into the data base and finding no change in the speciation after rerunning several groundwaters.

## P.4.0 URANIUM ADSORPTION

Partitioning of uranium between aquifer solids and groundwater was evaluated to calculate an apparent distribution coefficient [$K_d$ = (mg U/kg solid)/(mg U/L groundwater)] for uranium in the sand and gravel aquifer. This task was carried out to meet the objectives of Issue Five. Uranium adsorption was evaluated by:

- Modeling the uranium speciation of groundwater using the EQ3NR geochemical code and comparing the speciation output to published $K_d$ studies
- Calculating distribution coefficients based on uranium concentrations reported for archived aquifer solids, leachates, and groundwaters.

### P.4.1 SPECIATION AND EXPERIMENTAL STUDIES

Speciation results presented in Section P.3.3 indicate the expected uranium complexes in groundwaters recovered from Fernald monitoring wells are dominantly $UO_2(CO_3)_3^{-4}$ and $UO_2(CO_3)_2^{-2}$, and $UO_2(H_2PO_4)_2$ when phosphorous is present. The modeling results are in good agreement with studies by Ferri et al. (1981), which show uranium is present as the $UO_2(CO_3)_3^{-4}$ complex in carbonate solutions between pH 7 and 12. Neutral aqueous species (e.g.,

$UO_2(H_2PO_4)_2$ ) are not expected to sorb appreciably (perhaps slightly if the molecule has a strong dipole) and, consequently, are not considered in experimental studies. Therefore, this discussion focuses on studies which have addressed the adsorption of uranium from carbonate solutions.

P.4.1.1 Adsorption of Uranyl-Carbonate Species by Montmorillonite

Canterford and Sparrow (1983) studied the adsorption of uranium using a montmorillonite and carbonate solution mixture. A simple solution was prepared by adding 4 g of $Na_2CO_3$ and 8.4 g of $UO_2(NO_3)_2.6H_2O$ to one liter of distilled water, yielding $CO_3^{-2}$ and U concentrations of, respectively, 2.26 g/L (0.038 mole/L) and 3.97 g/L (0.017 mole/L) at a final pH of 7.7. The montmorillonite suspension was 0.48 weight percent solids at a pH of 7.6. Five ml of the uranium solution was added to 195 ml of the montmorillonite suspension and samples were stirred and agitated for 96 hours. Results for this experiment indicate an apparent $K_d$ for uranium of 65.78 L/kg at a final pH of 8.

However, the large $K_d$ value for uranium in this simple system is suspect with respect to sorption of anionic uranyl-carbonate species by montmorillonite. Note that the experiments of Canterford and Sparrow (1983) had about 0.004 mole/L of excess uranium that could not be complexed as the specie $UO_2(CO_3)_3^{-4}$ (the dominant specie at pH = 8; Ferri and Salvatore 1981). That is, the amount of carbonate ion in the system, 0.038 mole/L, requires only 0.0127 mole/L of the available 0.017 mole/L of uranium to form $UO_2(CO_3)_3^{-4}$. Therefore, the excess 0.004 mole/L of uranium could be present as the $UO_2^{+2}$ specie, which would readily sorb to montmorillonite in these neutral and slightly alkaline pH waters because of its low zero point of charge (montmorillonite $pH_{zpc}$ = 2.5; Stumm and Morgan 1981).

The pH at which a clay mineral surface has a zero point of charge ($pH_{zpc}$) is very important with respect to sorption of charged aqueous species. At a solution pH value below the $pH_{zpc}$, the surface of the clay mineral contains only free positively-charged sites, which would attract negatively-charged ions [e.g., $UO_2(CO_3)_3^{-4}$]. Similarly, for solution pH values above the $pH_{zpc}$, a clay mineral surface will have only free negatively-charged sites and sorb positively-charged ions (e.g., $UO_2^{+2}$).

An alternate hypothesis for the large $K_d$ value reported by Canterford and Sparrow (1983) is that uranium partitioning is balanced to allow for $UO_2(CO_3)_3^{-4}$ (U = 0.004 moles/L) and $UO_2(CO_3)_2^{-2}$ (U = 0.013 moles/L) complexation without $UO_2^{+2}$. If this latter hypothesis holds, then the large $K_d$ value for this system suggests amorphous AlOOH and FeOOH ($pH_{zpc}$ = 8.2 and 7.8, respectively; Stumm and Morgan 1981) films on the montmorillonite surface are sorbing the anionic complexes.

This latter scenario is less credible because the dominant uranium specie in the solutions of pH = 8 (Canterford and Sparrow 1983) would have to be $UO_2(CO_3)_2^{-2}$, which is in contrast to the $UO_2(CO_3)_3^{-4}$ specie predicted by experimental studies (Ferri et al. 1981) and modeling results.

P.4.1.2 Adsorption of Uranyl-Carbonate Species by Amorphous Ferric Oxyhdroxide

Ames et al. (1983), investigated sorption of uranium on amorphous ferric oxyhydroxide ($pH_{zpc}$ = 7.8 to 8.5; Stumm and Morgan 1981) at 25 and 60 C from 0.01 molar (moles/L) $NaHCO_3$ solutions over an initial uranium concentration range of 0.0001 to 0.00000055 molar (23.8 to 0.13 mg/L). Their amorphous ferric oxyhydroxide was prepared by mixing 1 ml of 0.1 molar $FeCl_3$ with 30 ml of 0.01 molar NaOH. Uranyl-carbonate solutions were added to the ferric oxyhdroxide precipitate to yield an iron mass to solution volume ratio of 0.279 g/L. Solutions and ferric oxyhydroxide were sealed in polypropylene tubes and agitated for seven days. Blanks containing uranyl-carbonate solutions but no ferric oxyhydroxide indicated less than 2 percent tube-wall sorption. A count on the initial and final solutions determined the sorbed uranium by difference. Apparent $K_d$ values at 25 C and average final pH of 8.6 to 8.7 ranged from about 4,000 L/kg at U = 23.8 mg/L to about 26,000 L/kg at U = 0.13 mg/L. The apparent $K_d$ values increased to 5,000 and 34,000 L/kg, respectively, at 60 C.

The results of Ames et al. (1983) indicate a strong potential for sorption of anionic uranyl-carbonate species onto amorphous ferric-oxyhydroxide surfaces in slightly alkaline solutions (maximum loading = 3.116 moles U per kg ferric oxyhydroxide). However, these apparent $K_d$ values were calculated for a simple system and do not take into account the presence of other ligands (e.g., $SO_4^{-2}$, $PO_4^{-3}$, etc.) in natural waters. Sulfate and phosphate complexes would compete for the available anion sorption sites on ferric oxyhydroxide and lower uranium $K_d$ values considerably, primarily due to the much greater concentrations of sulfate and phosphate, relative to uranium, in solution.

P.4.1.3 Empirical Determination of a Uranium Distribution Coefficient

Using the maximum uranium loading on ferric oxyhydroxide (3.116 moles/kg; Ames et al. 1983), an apparent $K_d$ between aquifer solids and groundwater was calculated. The calculation is based on the following assumptions:

- Groundwater and aquifer solids are in equilibrium at 25 C
- The composition of the groundwater is the same prior to and at equilibrium
- All uranium is speciated into $UO_2(CO_3)_3^{-4}$

- The experimentally determined maximum uranium loading on ferric oxyhydroxide (3.116 moles/kg) is taken as the total moles of anionic species that can be sorbed
- All Fe leached from the aquifer solids was in the form FeOOH
- Each sorption site on FeOOH is occupied by either HCO-3, $NO^{3-}$, $HPO_4^{-2}$, $SO_4^{-2}$, or $UO_2(CO_3)_3^{-4}$
- The affinity of a molecule to sorb on FeOOH is proportional to its charge and concentration

Assumptions three and five may introduce the greatest uncertainty in the $K_d$ calculation. For instance, modeling results for uranium speciation in groundwaters (Table P-1) indicates and $UO_2(H_2PO_4)_2$ $UO_2(CO_3)_2^{-2}$ are important species in addition to $UO_2(CO_3)_3^{-4}$. This uncertainty can be estimated by comparing the calculated $K_d$ value based on the assumptions above with that calculated for speciation based on modeling results (Table P-3). Partitioning of all iron into amorphous ferric oxyhydroxide is the most tenuous assumption, as the analytical leaching technique is known to recover iron from both amorphous- and crystalline-oxyhydroxide phases, and it is not possible to distinguish between these two iron components. However, even if the partitioning of iron among these components was known, the $K_d$ value would probably not decrease by more than a factor of two, and this uncertainty is probably no greater than uncertainties associated with the remaining assumptions.

Noting the limitations of the above assumptions, empirical $K_d$ values were calculated for all wells (17) with groundwater and aquifer-solid analyses (Table P-3). The 1000 Series wells (2) are in a discontinuous glacial-till horizon which overlies the sand and gravel aquifer (i.e., the till is not part of the regional aquifer). Groundwater from Well 3016 has been paired with a clay interbed sample that is probably impermeable and, therefore, not interacting with groundwater in the aquifer. These three well numbers have been excluded from discussions which refer to the range and average $K_d$ value. The remaining groundwater-solid pairs (14) have $K_d$ values that range from 0 to 3.89 L/kg, and individual wells had variation in their $K_d$ values from round to round (Table P-3). For example, the $K_d$ value calculated for the Round 3 (Fourth Quarter, 1988) groundwater analysis of Well 2010 is less than that of the Round 4 (First Quarter, 1989) $K_d$ value because of the larger sulfate value reported for the Round 3 analysis (i.e., less FeOOH sites available for uranium species in Round 3 groundwater).

Empirical $K_d$ values are dependent on the amount of leachable iron (i.e., FeOOH) present in the aquifer solids, the concentration and speciation of uranium in the groundwater, and the aqueous

concentrations of remaining ligands. In general, all anionic complexes except uranium being fixed, the uranium $K_d$ value will:

- Double if the leachable iron in the aquifer solids is doubled, while holding the uranium concentration constant
- Double if the uranium concentration in solution is doubled, while holding leachable iron constant
- Decrease by half if the leachable iron in the aquifer solids is decreased by half, with uranium concentration held constant
- Decrease by half if the uranium concentration in solution decreases by half, with leachable iron held constant
- Decrease by half to zero if all uranium is partitioned into $UO_2(CO_3)_2^{-2}$ or $UO_2(H_2PO_4)_2$, respectively, while leachable iron is held constant

Points three and five merit special emphasis because of their sensitivity to the assumptions used in calculating the $K_d$ values. As noted above, iron leached from the aquifer solids can be derived from amorphous- and crystalline-oxyhydroxide grains, and organic complexes. Unfortunately, there is no quantitative way to separate these components and refine the amount of Fe that is partitioned solely into amorphous ferric oxyhydroxide. Therefore, the empirically calculated $K_d$ values overestimate the "true" $K_d$ value.

Point five is important because speciation modeling predicts most wells to have phosphate concentrations in excess of that required to complex uranium as UO2(H2PO4)20 (see Section P.3.3). Table P-3 reports the $K_d$ value for the empirical model based on the available speciation results for a limited number of groundwaters. Note that $K_d$ values approach zero for those wells which partition greater than 99 percent of the uranium into the neutral phosphate complex (e.g., 1082, 2046, 2095). Based on the present modeling results for uranium speciation, the groundwater-aquifer-solid pairs in Table P-3 that were not modeled for speciation would probably have $K_d$ values close to zero, because the phosphate and uranium concentrations suggest most uranium will be partitioned into the neutral phosphate complex. However, for reasons discussed in Section P.3.3.1, it is unlikely that the neutral phosphate complex plays as significant a role as predicted by the EQ3NR geochemical code and, if present, this complex would still exhibit some sorptive capacity due to dipole attractions. Therefore, empirical $K_d$ values based on the partitioning of greater than 99 percent of the uranium into $UO_2(H_2PO_4)_2$ will probably underestimate the "true" $K_d$ of the aquifer.

## P.4.2 AQUIFER SOLIDS, LEACHATES, AND GROUNDWATERS

Analytical results for uranium concentrations in groundwaters, leachates and aquifer solids were used to calculate apparent distribution coefficients for 17 monitoring sites. The following assumptions were used in calculating the apparent $K_d$s:

- The analyzed groundwater samples were in equilibrium with their respective aquifer solids (i.e., kinetic rates for uranium sorption were faster than solution flow rates through a given volume element)
- All uranium species sorb at the same rate
- The background concentration of uranium in the aquifer solids is 3 mg/kg and in the leachates 0.142 mg/kg
- The adsorbed uranium concentration is equal to the concentration of uranium obtained for the aquifer solid or leachate minus the background concentration of uranium
- The apparent $K_d$ is equal to the sorbed uranium concentration (mg/kg) divided by the groundwater uranium concentration (mg/L)

Apparent distribution coefficients were calculated from reported uranium concentrations for aquifer solids from Wells 2046 (U = 16 mg/kg) and 4010 (U = 13.8 mg/kg), and Round 4 groundwater analyses from Wells 2046 (U = 0.309 mg/L) and 4010 (U = 13.8 mg/kg), and Round 4 groundwater analyses from Wells 2046 (U = 0.309 mg/L) and 4010 (< 0.001 mg/L). These samples were chosen because they bound the range of aqueous uranium concentrations available for groundwater analyses that can be matched to the aquifer solids. Using the uranium values cited above, $K_d$s for Wells 2046 and 4010 are 42 and 10,800 L/kg, respectively. The $K_d$ for Well 4010 was calculated with the uranium detection-limit value of 0.001 mg/L. Utilizing the 2-sigma error range for uranium concentrations in the aquifer solids (12.3 to 19.7 mg/kg and 9.7 to 17.9 mg/kg, respectively), the corresponding range in $K_d$ for the respective wells is 30 to 54 L/kg and 6,700 to 14,900 L/kg. Because of the similar uranium concentrations reported for the unleached aquifer solids, the $K_d$ is primarily a function of the uranium concentration in the groundwater. It is important to reemphasize that the uranium concentrations reported for aquifer solids analyzed by gamma spectrometry are suspect, and $K_d$ calculations using these anomalous results yield partition coefficients that are too great for the aquifer.

Results for total uranium concentrations in the leachate fractions derived from the differential leaching procedure indicate less than 2.5 ppb of uranium is sorbed on aquifer solids (i.e., $K_d$ = 0). In contrast, a range of 33 to 783 ppb of uranium was reported for leachates derived from aquifer solids which underwent the iron- and manganese-leaching procedure (see Section P.2.5.2). Utilizing

the above assumptions, and a background uranium concentration in the leachates of 0.142 mg/kg (obtained by averaging the leachate uranium values obtained from samples 7790, 10407, 10460, 10607 and 10696, which have reported uranium concentrations in groundwater of less than 1 ppb), $K_d$ values calculated for 14 aquifer wells (1000 Series wells and clay interbed sample are not included) ranged from 0 to 68.2 L/kg (Table P-4). About a third of the samples have a $K_d$ value of zero, but most of these are from wells considered to be representative of uranium background levels and do not reflect "true" $K_d$ values. Three samples have distribution coefficients greater than 10. The samples which produced high $K_d$ values were obtained from the waste pit region bounding the northwest corner of the Fernald compound, and may indicate that precipitated uranium solids are contributing to the sorption $K_d$ value.

### P.4.3 COMPARISON OF EMPIRICAL AND CALCULATED $K_d$ VALUES

Figure P-12 is a plot of the calculated $K_d$ from groundwater and leachate analyses versus the predicted $K_d$ based on the empirical sorption model. Wells in the regional aquifer were broken down into areas adjacent to and within the FMPC compound. The areas are identified as the South Plume (south of the FMPC), waste pit (northwest of the FMPC), and within the FMPC compound. The 1000 Series wells in the glacial till are in the Waste Pit Area, but have been plotted separately because they are not part of the regional aquifer. The plot was constructed with the data in Tables P-3 and P-4 after averaging multiple $K_d$ values for individual wells and omitting Well 3016, which had groundwater matched to an anomalous clay-interbed sample.

Monitoring wells in the regional aquifer, representing the South Plume and Waste Pit areas, were identified and plotted separately to construct regression lines for these areas. A slope of one on this plot, and a correlation coefficient (r) near one, would indicate a perfect fit between the calculated and predicted $K_d$. The regression line for the South Plume data has a slope of 0.87, but a less than ideal "r" value of 0.65. Data points representing the Waste Pit Area define a regression line with a slope of 6.44 and an "r" value of 0.29, indicating a poor fit between the predicted and calculated $K_d$ values. Wells within the FMPC compound and glacial till lie near the South Plume regression line (but have not been used in the calculation of the regression line). The poor fit between predicted and calculated $K_d$ values for aquifer samples from the waste pit may indicate that precipitation of amorphous uranium solids has occurred in those samples with calculated $K_d$ values greater than 30 (e.g., 2007, 2010, 2027). If precipitation and sorption are mechanisms responsible for retardation of uranium in the Waste Pit Area, the empirical model would not be expected to predict accurately the $K_d$ because it is based only on the sorption of uranium.

The precipitation hypothesis is supported by uranium concentrations in groundwater recovered from Waste Pit Area Wells 1073 and 1082 (0.8 to 4.4 mg/L), and 3010 (0.015 to 0.020 mg/L). These samples were obtained from the glacial till above the aquifer (1073 and 1082) and, within the aquifer, from below (3010) the 2000 Series samples with high $K_d$ values. If uranium-rich waters in the glacial till vertically infiltrated to the underlying aquifer, mixing at the till/aquifer interface could have resulted in precipitation of amorphous uranium solids in the 2000 Series horizon, thus limiting breakthrough to the 3000 Series horizon.

P.4.4 ESTIMATION OF THE URANIUM $K_d$ FOR THE FERNALD SITE AQUIFER

Results presented in Tables P-3 and P-4 and Figure 12 indicate that the most reliable indicators of uranium $K_d$ values in the Fernald site aquifer come from well locations in the South Plume area. This conclusion is based on the similarity of $K_d$ estimates derived from two independent methods. Wells in the Waste Pit Area are not considered in the estimation of the aquifer $K_d$, because large calculated values for 2000 Series wells (Table P-4) suggest uranium is also present as amorphous oxide solids. Additionally, calculated $K_d$ values (Table P-4), rather than empirical $K_d$ values (Table P-3), were used to estimate the site $K_d$ because assumptions based on the former are more valid and defensible.

To derive the estimate of the aquifer $K_d$, 2000 and 3000 Series wells from the south plume area (Table P-4) were averaged (if Round 3 and Round 4 values were reported) to produce a single $K_d$ value for each well. Wells with reported $K_d$ values of zero were not considered because of the inability to estimate a reasonable $K_d$ (i.e., a distribution coefficient is a finite number). A simple average of the $K_d$ value for each well was considered to be the best approach, because there is no basis on which to weigh individual wells at this time. After satisfying the preceding criteria, four wells (2016, 2046, 2095 and 3095) were used to estimate the aquifer $K_d$. The mean $K_d$ value for the four wells is 2.38, with a standard deviation of 1.42.

The mean uranium $K_d$ value can be converted to a retardation factor with the relationship:

$$R_f = 1 + (rho/n) * K_d$$

where:

$R_f$ = retardation factor
rho = density
n = porosity
$K_d$ = distribution coefficient

Using the mean $K_d$ value of 2.38 L/kg (note: a L/kg = ml/g), and typical values for rho (2.6 g/cc; cc = ml) and n (0.25) in the sand and gravel aquifer, the $R_f$ value is 25.8. This retardation factor implies that uranium species present in the groundwater will move one meter for every 25.8 meters traversed by the groundwater front. Unfortunately, this retardation value is based on the uranium recovered from the iron and manganese leachates, and the uranium present as "historical" uranium (if any) is estimated from subtracting an "estimated" background level from the total. Additionally, recall that the differential leaching of aquifer solids (6 samples) for uranium recovered less than 2.5 ppb uranium, which suggests the above retardation factor is far too great. Resolving these problems will require additional data on the mineral composition of aquifer solids (i.e., petrographic and X-ray diffraction studies to estimate detrital iron-oxide minerals) and a larger sample-size population for the differential-leaching analysis.

Noting the limitations of the present estimate of the aquifer $K_d$, it is recommended that the solute transport model be evaluated using the limits defined by the standard deviation of the mean $K_d$ value. This approach requires two runs of the model at bounding conditions of 0.96 L/kg (estimated lower limit) and 3.80 L/kg (estimated upper limit), and would bracket the majority of $K_d$ values calculated for the site (excluding 2000 Series wells in the Waste Pit Area). The bounding conditions can be cautiously applied to the Waste Pit Area, noting that additional analytical data are required to evaluate the retardation process occurring in these 2000 Series wells. Given the current data base available to work with, this is the recommended application of the estimated $K_d$ value to the solute transport model.

## P.5.0 CONCLUSIONS

### P.5.1 ISSUE THREE

Subsurface soils and surface waters from Paddys Run and the Storm Sewer Outfall Ditch (Figure P-1) have been sampled and analyzed to evaluate the degree of infiltration of uranium-bearing surface water to the underlying aquifer. Presently, there is no indication of contamination at four of the six soil sample sites. If uranium-rich waters had infiltrated these soil horizons, the present observation suggests uranium was not attenuated (e.g., the dominant specie in the infiltrating waters may have been $UO_2(H_2PO_4)_2$) and/or uranium that had sorbed (e.g., $UO_2(CO_3)_3^{-4}$) or precipitated was desorbed or dissolved prior to sampling and analysis of the soils. Both of these scenarios are compatible with the modeling results, which predict the presence of neutral uranyl-phosphate and anionic uranyl-carbonate species in the surface waters (Table P-2).

The top ten feet of material at Sites S1 (1405) and S2 (1406) have concentrations of uranium that are about twice the level of background values. This observation indicates uranium has been retarded at these sites by sorption or precipitation processes occurring in the soil (site S1) and regional aquifer (Site S2). The uranium profiles for these sites (Figure 3) are compatible with scenarios of no breakthrough to the underlying aquifer (i.e., all uranium is retarded by the soil, Site S1) and partial breakthrough to the aquifer (i.e., "historical" uranium is present in the aquifer, Site S2). If the retardation of soluble uranium by the soil and aquifer solids is taking place via a sorption process in the unsaturated zone, modeling results indicate the uranium is in the form of anionic uranyl-carbonate species (Table P-2).

The presence of sorbed or precipitated uranium at these sites presents the potential for future releases to the underlying aquifer.

P.5.2 ISSUE FIVE

Partitioning of uranium between aquifer solids and groundwater (see Figure P-9 for well locations) was evaluated to calculate an apparent distribution coefficient ($K_d$) for uranium in the sand and gravel aquifer. The $K_d$ was evaluated by:

- Modeling the uranium speciation of groundwater using the EQ3NR geochemical code and comparing the speciation output to published $K_d$ studies (i.e., the empirical method)
- Obtaining analyses for total uranium on archived aquifer solids, leachates and groundwaters to calculate a $K_d$ directly

Empirically derived $K_d$ values for well sites in the regional aquifer ranged from 0 to 3.89 L/kg (Table P-3). Distribution coefficients near zero for wells that have greater than 99 percent of their uranium partitioned into $UO_2(H_2PO_4)_2$ (e.g., 2046 and 2095, Table P-3) are probably too low, and reflect the inability to model organic phosphate complexation and sorption processes that take credit for molecular dipole attraction. Speciation results were not available for all groundwaters evaluated with the $K_d$ model, and $UO_2(CO_3)_3^{-4}$ was assumed to be the specie present. This assumption is supported by:

- Speciation results which indicate $UO_2(CO_3)_3^{-4}$ is the dominant specie if phosphate concentrations are below the detection limit of 0.02 mg/L (Table P-1)
- Experimental anion-exchange tests that recovered greater than 90 percent of the uranium from site groundwater samples (Khan 1989; personal communication)

- Documented experimental studies that indicate the dominant uranyl ion in bicarbonate solutions at neutral and slightly alkaline pH is $UO_2(CO_3)_3^{-4}$ (Ferri et al. 1981)

Additionally, the empirical $K_d$ values are strongly dependent on the amount of iron that is partitioned into amorphous ferric oxyhydroxide. Because it is not possible to separate the leachable iron into amorphous and crystalline components, all iron was assumed to be partitioned into the amorphous phase. This assumption yields $K_d$ values that overestimate the "true" $K_d$ of the aquifer.

Distribution coefficients calculated directly from analyses of uranium in aquifer solids, leachates, and groundwaters range from 0 to greater than 10,000. Calculations of distribution coefficients based on gamma spectrometry analysis of uranium in aquifer solids (30 to 14,900 L/kg) are not reliable and are excluded from interpretations based on the leaching results. The differential-leaching procedure revealed that less than 2.5 ppb of uranium is present as sorbed or amorphous uranium products, which suggests the uranium $K_d$ is zero for these samples. However, the iron- and manganese-leaching technique recovered 33 to 783 ppb of uranium from the aquifer solids, resulting in a range of 0 to 68 L/kg for calculated $K_d$ values (Table 4). A background level was subtracted from the uranium values obtained from the iron and manganese leachate prior to the calculation (adsorbed U = total U - background U), and about a third of the samples had a calculated concentration of adsorbed uranium equal to zero, which resulted in a $K_d$ of zero for that sample. It is important to note that those wells with calculated $K_d$ values of zero are mainly from 3000 and 4000 Series horizons, which in general show no indication of uranium contamination.

P.5.2.1 Best Estimate of the Uranium $K_d$ for the Aquifer

The best estimate of the uranium $K_d$ value for the aquifer was derived from calculated $K_d$ values for south plume wells. Empirical $K_d$ values were not used because the assumptions supporting the derivation are not as valid and defensible as the calculated $K_d$ assumptions. Calculated $K_d$ values for Waste Pit Area wells were also excluded from the estimate of the site $K_d$, because 2000 Series wells in this area have apparent $K_d$ values that are anomalously high with respect to values calculated for the majority of wells (Figure P-12). These anomalous values may indicate uranium is being retarded by sorption and precipitation processes in the Waste Pit Area.

Using the calculated $K_d$ values from four South Plume wells (2016, 2046, 2095 and 3095; Table P-4), the aquifer $K_d$ was estimated as 2.38 L/kg. This $K_d$ indicates the retardation factor for uranium in the aquifer will be close to 26, which appears to be too great as evidenced by the differential-leaching tests. However, it is recommended that the solute transport model be evaluated at the lower (0.96 L/kg) and upper (3.80 L/kg) standard-deviation limits. These two bounding cases

would bracket the majority of $K_d$ values calculated for the south plume and Waste Pit Area wells (excluding the 2000 Series waste pit wells). The bounding cases may be cautiously applied to the Waste Pit Area, but additional analytical work on aquifer solids is required to evaluate critically how the mechanisms of sorption and precipitation retard uranium in 2000 Series wells from this area.

DRAFT

## REFERENCES

Ames, L. L., J. E. McGarrah, B. A. Walker, and P. F. Salter, 1983, "Uranium and Radium Sorption on Amorphous Ferric Oxyhydroxide," Chemical Geology, Vol. 40, pp. 135-148.

Baes, C. F., 1956, "A Spectrophotometric Investigation of Uranyl Phosphate Complex Formation in Perchloric Acid Solution," Journal of Physical Chemistry, Vol. 60, pp. 878-883.

Canterford, J. H. and G. J. Sparrow, 1983, "Adsorption of Uranium from Carbonate Media," Society of Mining Engineers of AIME, Vol. 83-305, 10 pp.

Chester, R. and M. J. Hughes, 1967, "A Chemical Technique for the Separation of Ferro-Manganese Minerals, Carbonate Minerals and Adsorbed Trace Elements from Pelagic Sediments," Chemical Geology, Vol. 2, pp. 249-262.

Dongarra, G. and D. Langmuir, 1980, "The Stability of $UO_2OH^-$ and $UO_2(HPO_4)_2^{-2}$ Complexes at 25 C," Geochimica et Cosmochimica Acta, Vol. 44, pp. 1747-1751.

Faure, G., 1977, Principles of Isotope Geology, John Wiley & Sons, New York, 464 pp.

Ferri, D., I. Grenthe, and F. Salvatore, 1981, "Dioxouranium (IV) Carbonate Complexes in Neutral and Alkaline Solutions," Acta Chemica Scandinavia, Vol. A35, pp. 165-168.

Hem, J. D., 1970, "Study and Interpretation of the Chemical Characteristics of Natural Water," U.S. Geological Survey, Water-Supply Paper 1473, 363 pp.

IT Corporation, 1989, "Field Sampling and Laboratory Procedure Plan for the Geochemical Program: In Support of the Remedial Investigation Feasibility Study, Feed Materials Production Center, Fernald, Ohio."

IT Corporation, 1988, "Remedial Investigation and Feasibility Study at the U.S. Department of Energy's Feed Materials Production Center, Fernald, Ohio."

Kahn, M, 1989, Personal communication to Jon Myers.

Koss, V., 1988, "Modeling of Uranium (IV) Sorption and Speciation in a Natural Sediment-Groundwater System," Radiochimica Acta, Vol. 44/45, pp. 403-406.

Krauskopf, K. B., 1979, Introduction to Geochemistry, McGraw-Hill, San Francisco, 533 pp.

Moskvin, A. I., A. M. Shelyakina, and P. S. Perminov, 1967, "Solubility Product of Uranyl Phosphate and the Composition and Dissociation Constants of Uranyl Phosphato Complexes," Russian Journal of Inorganic Chemistry, Vol. 12, pp. 1756-1760.

Scanlan, J. P., 1977, "Equilibria in Uranyl Carbonate Systems, II: The Overall Stability Constant of $UO_2(CO_3)_2^{-2}$ and the Third Formation Constant of $UO_2(CO_3)_3^{-4}$," Journal of Inorganic Nuclear Chemistry, Vol. 39, pp. 635-639.

Stumm, W. and J. J. Morgan, 1981, Aquatic Chemistry, John Wiley & Sons, New York, 780 pp.

Tripathi, V. S., 1984, "Uranium (VI) Transport Modeling: Geochemical Data and Submodels," Ph.D. Dissertation, Stanford University, Stanford, California.

U.S. Environmental Protection Agency, Methods for Chemical Analysis of Waste, EPA-600, 4-79-020.

Wolery, T. J., 1983, EQ3NR, A Computer Program for Geochemical Aqueous Speciation-Solubility Calculations: User's Guide and Documentation, UCRL-53414, Lawrence Livermore National Laboratory, Livermore, California.

DRAFT

## TABLE P-1

## RESULTS FOR URANIUM SPECIATION IN WATERS RECOVERED FROM FERNALD MONITORING WELLS

DRAFT

| Well No. | Round | pH | Eh mV | U mg/L | P mg/L | Species | % | CB[a] |
|---|---|---|---|---|---|---|---|---|
| 1019 | 3 | 7 | 386[b] | 0.818 | 0.061 | $UO_2(CO_3)_3^{-4}$ | 52 | +14.84[c] |
| | | | | | | $UO_2(H_2PO_4)_2^{o}$ | 29 | |
| | | | | | | $UO_2(CO_3)_2^{-2}$ | 19 | |
| 1019 | 4 | 7 | 371[b] | 0.739 | 0.12 | $UO_2(H_2PO_4)_2^{o}$ | 62 | + 7.99 |
| | | | | | | $UO_2(CO_3)_3^{-4}$ | 26 | |
| | | | | | | $UO_2(CO_3)_2^{-2}$ | 12 | |
| 1073 | 3 | 7.6 | 321[b] | 3.297 | 0.493 | $UO_2(H_2PO_4)_2^{o}$ | 57 | + 2.60 |
| | | | | | | $UO_2(CO_3)_3^{-4}$ | 39 | |
| | | | | | | $UO_2(CO_3)_2^{-2}$ | 3 | |
| 1073 | 4 | 7.1 | 366[b] | 4.38 | NR | $UO_2(CO_3)_3^{-4}$ | 92 | +64.16[d] |
| | | | | | | $UO_2(CO_3)_2^{-2}$ | 8 | |
| 1082 | 3 | 7 | 350[e] | 1.079 | 3.79 | $UO_2(H_2PO_4)_2^{o}$ | > 99 | -26.85[f] |
| 1082 | 4 | 7.35 | 350[e] | 0.81 | 0.65 | $UO_2(H_2PO_4)_2^{o}$ | > 99 | +19.61[g] |
| 2013 | 3 | 6.85 | 137[h] | 0.008 | < 0.02 | $UO_2(CO_3)_2^{-2}$ | 67 | + 4.55 |
| | | | | | | $UO_2(CO_3)_3^{-4}$ | 31 | |
| | | | | | | $UO_2(CO_3)^{o}$ | 2 | |
| 2024 | 3 | 7.30 | 152[h] | 0.005 | 0.342 | $UO_2(H_2PO_4)_2^{o}$ | > 99 | - 9.46 |
| 2044 | 3 | 7.47 | 331[i] | 0.033 | 0.024 | $UO_2(H_2PO_4)_2^{o}$ | > 99 | - 9.82 |
| 2045 | 4 | 7.3 | 324[j] | 0.283 | NR | $UO_2(CO_3)_3^{-4}$ | 59 | + 5.79 |
| | | | | | | $UO_2(CO_3)_2^{-2}$ | 41 | |

See footnotes at end of table.

**TABLE P-1**
**(continued)**

DRAFT

| Well No. | Round | pH | Eh mV | U mg/L | P mg/L | Species | % | CB[a] |
|---|---|---|---|---|---|---|---|---|
| 2046 | 4 | 7.0 | 324[j] | 0.309 | 0.39 | $UO_2(H_2PO_4)_2^{\circ}$ | > 99 | +8.68 |
| 2060 | 3 | 7.50 | 605[k] | 0.171 | < 0.02 | $UO_2(CO_3)_3^{-4}$ | 61 | +4.07 |
| | | | | | | $UO_2(CO_3)_2^{-2}$ | 39 | |
| 2060 | 4 | 7.4 | 324[j] | 0.250 | 0.03 | $UO_2(H_2PO_4)_2^{\circ}$ | 45 | +3.74 |
| | | | | | | $UO_2(CO_3)_3^{-4}$ | 32 | |
| | | | | | | $UO_2(CO_3)_2^{-2}$ | 23 | |
| 2061 | 4 | 7.6 | 324[b] | 0.292 | 0.02 | $UO_2(CO_3)_3^{-4}$ | 50 | +4.87 |
| | | | | | | $UO_2(H_2PO_4)_2^{\circ}$ | 25 | |
| | | | | | | $UO_2(CO_3)_2^{-2}$ | 24 | |
| 2094 | 4 | 7.1 | 75[h] | 0.0045 | 1.92 | $UO_2(H_2PO_4)_2^{\circ}$ | > 99 | +54.91[l] |
| 2095 | 3 | 7.33 | 331[i] | 0.177 | 0.063 | $UO_2(H_2PO_4)_2^{\circ}$ | > 99 | +14.65[m] |
| 3001 | 3 | 8 | 81[n] | 0.015 | < 0.02 | $UO_2(CO_3)_3^{-4}$ | 89 | 20.52[o] |
| | | | | | | $UO_2(CO_3)_2^{-2}$ | 11 | |
| 3001 | 4 | 7.1 | 81[h] | 0.015 | 0.12 | $UO_2(H_2PO_4)_2^{\circ}$ | > 99 | +6.00 |
| 3013 | 3 | 6.30 | 139[n] | 0.011 | < 0.02 | $UO_2(CO_3)_2^{-2}$ | 77 | +4.83 |
| | | | | | | $UO_2(CO_3)_3^{-4}$ | 19 | |
| | | | | | | $UO_2(CO_3)^{\circ}$ | 4 | |

See footnotes at end of table.

**TABLE P-1**
**(continued)**

| Well No. | Round | pH | Eh mV | U mg/L | P mg/L | Species | % | CB[a] |
|---|---|---|---|---|---|---|---|---|
| 3013 | 4 | 8.4 | 139[h] | 0.49 | 0.02 | $UO_2(CO_3)_3^{-4}$ | 79 | +1.22 |
| | | | | | | $UO_2(H_2PO_4)_2°$ | 15 | |
| | | | | | | $UO_2(CO_3)_2^{-2}$ | 6 | |
| 3014 | 3 | 7.75 | 575[k] | 0.028 | < 0.02 | $UO_2(CO_3)_3^{-4}$ | 70 | +1.56 |
| | | | | | | $UO_2(CO_3)_2^{-2}$ | 30 | |
| 3016 | 3 | 7.60 | 331[i] | 0.008 | < 0.05 | $UO_2(CO_3)_3^{-4}$ | 64 | -15.24[p] |
| | | | | | | $UO_2(CO_3)_2^{-2}$ | 35 | |
| 3062 | 3 | 7.90 | 331[b] | 0.041 | < 0.02 | $UO_2(CO_3)_3^{-4}$ | 83 | +6.59 |
| | | | | | | $UO_2(CO_3)_2^{-2}$ | 17 | |
| 3069 | 3 | 7.60 | 331[i] | 0.005 | 0.662 | $UO_2(H_2PO_4)_2°$ | > 99 | -5.92 |
| 3094 | 4 | 7.1 | 99[h] | 0.0006 | 0.88 | $UO_2(H_2PO_4)_2°$ | > 99 | +58.57[l] |
| 4097 | 4 | 7.1 | 221[h] | 0.0019 | 0.11 | $UO_2(H_2PO_4)_2°$ | > 99 | +1.77 |

NR = No analysis reported.

[a]Charge balance expressed as percent of total charge.

[b]Eh estimated from the $NH_4^+/NO_3^-$ redox couple.

[c]Excessive charge balance probably due to high Mg or Na concentrations (159 and 437 mg/L, respectively).

[d]Excessive charge balance probably results from high Ca concentration (4000 mg/L).

[e]Eh estimated from results of $NH_4^+/NO_3^-$ redox couple in wells 1019 and 1073.

[f]Excessive charge balance probably due to high $SO_4^{-2}$ concentration (510 mg/L).

**Table P-1**
**(continued)**

[g]Excessive charge balance probably due to low $SO_4^{-2}$ concentration (19.6 mg/L).

[h]Platinum-electrode measurement.

[i]Eh value estimated from $NH_4^+/NO_3^-$ redox couple for Well 3062.

[j]Eh value estimated from $NH_4^+/NO_3^-$ redox couple for Well 2061.

[k]Eh based on pyrolusite saturation. [l]Excessive charge balance probably results from high K concentration (1800-1830 mg/L).

[m]Excessive charge balance probably due to low Cl concentration (4 mg/L).

[n]Eh value obtained from Round 4 analysis of same well number.

[o]Excessive charge balance probably due to high Ca and Na concentrations (173 and 24.4 mg/L, respectively), relative to Round 4 analysis of same well.

[p]Excessive charge balance probably due to high $SO_4^{-2}$ concentration (174 mg/L).

DRAFT

## TABLE P-2

## RESULTS FOR URANIUM SPECIATION IN SURFACE WATERS RECOVERED FROM PADDYS RUN, FERNALD SITE

| Sample No. | pH | Eh mV | P mg/L | U mg/L | Species | % | CB[a] |
|---|---|---|---|---|---|---|---|
| W-07 | 8.38 | 451 | 0.032 | 0.015 | $UO_2(H_2PO_4)_2^{\circ}$ | > 99 | +2.99 |
| W-11 | 8.58 | 441 | BDL | 0.009 | $UO_2(CO_3)_3^{-4}$ | 90 | +3.36 |
| | | | | | $UO_2(CO_3)_2^{-2}$ | 10 | +3.36 |
| ASIT003 | 8.57 | 452 | 0.161 | 0.002 | $UO_2(H_2PO_4)_2^{\circ}$ | > 99 | +1.99 |

[a]Charge balance expressed as percent of total charge.

BDL = Below detection limit.

DRAFT

## TABLE P-3

## EMPIRICAL URANIUM DISTRIBUTION COEFFICIENTS FOR SELECTED MONITORING WELLS

| Well | GW[a] | $HCO_3^-$ mg/L | $NO_3^-$ mg/L | $HPO_4^{-2}$ mg/L | $SO_4^{-2}$ mg/L | U mg/L | AS[b] | Fe[c] mg/g | $K_d$[d] L/kg | $K_d$[e] L/kg |
|---|---|---|---|---|---|---|---|---|---|---|
| Regional Aquifer | | | | | | | | | | |
| South Plume Area | | | | | | | | | | |
| 2016 | rd1[f] | 292 | < 22 | 0.87 | 59 | 0.021 | 10437 | 0.69 | 2.27 | NA[g] |
| 2046 | 3997 | 355 | 5.98 | 1.21 | 74 | 0.309 | 8956 | 0.81 | 2.15 | 0.02 |
| 2095 | 3787 | 352 | 77.5 | 0.20 | 18 | 0.177 | 10038 | 0.66 | 1.77 | 0.02 |
| 2095 | 3976 | 349 | 13.1 | 2.7 | 137 | 0.146 | 10038 | 0.66 | 1.48 | NA[g] |
| 3095 | 3786 | 370 | < 0.4 | 0.409 | 18 | 0.005 | 10049 | 1.00 | 3.08 | NA[g] |
| 3095 | 3971 | 335 | < 0.4 | 2.98 | 90 | 0.006 | 10049 | 1.00 | 2.67 | NA[g] |
| 4014 | rd4[f] | 285 | < 0.4 | NR[h] | 58 | < 0.001 | 10407 | 1.08 | 0.00 | NA[g] |
| 4016 | rd4[f] | 313 | < 0.4 | NR[h] | 98 | < 0.001 | 10460 | 0.38 | 0.00 | NA[g] |
| Waste Pit Area | | | | | | | | | | |
| [illegible]007 | rd5[f] | 311 | < 0.4 | 4.25 | 123 | 0.005 | 10796 | 1.08 | 2.76 | NA[g] |
| 2010 | 3715 | 368 | < 0.4 | 0.17 | 271 | 0.005 | 8426 | 1.50 | 2.55 | NA[g] |
| 2010 | 3902 | 382 | < 0.08 | 8.1 | 140 | 0.021 | 8426 | 1.50 | 3.18 | NA[g] |
| 2027 | 3941 | 406 | < 0.08 | 0.06 | 245 | 0.007 | 7874 | 1.58 | 2.67 | 2.45 |
| 2034 | 3646 | 287 | 9.74 | 0.136 | 39 | 0.024 | 8286 | 0.78 | 2.73 | 2.51 |
| 3010 | 3714 | 428 | 12.3 | < 0.06 | 712 | 0.020 | 10611 | 3.50 | 3.15 | NA[g] |
| 3010 | 3901 | 426 | 0.84 | 0.06 | 520 | 0.015 | 10611 | 3.50 | 3.89 | NA[g] |
| 4010 | rd4[f] | 399 | < 0.08 | 0.25 | 36 | < 0.001 | 10607 | 1.08 | 0.00 | NA[g] |
| FMPC Compound | | | | | | | | | | |
| 2013 | 3709 | 328 | < 0.4 | < 0.06 | 97 | 0.008 | 10670 | 0.65 | 1.74 | 1.12 |
| 2013 | 3900 | 311 | 0.13 | 0.37 | 110 | 0.036 | 10670 | 0.65 | 1.74 | NA[g] |
| 2054 | rd5[f] | 402 | < 0.4 | 0.82 | 666 | 0.026 | 8645 | 1.17 | 1.13 | NA[g] |
| Clay Interbed | | | | | | | | | | |
| 3016 | rd1[f] | 270.2 | 0.4 | < 0.15 | 56 | 0.011 | 10449 | 4.83 | 17.1 | 13.9 |
| 3016 | rd4[f] | 242.8 | 11.6 | 0.22 | 60 | 0.007 | 10449 | 4.83 | 17.7 | NA[g] |

See footnotes at end of table.

DRAFT

**TABLE P-3**
**(continued)**

| Well | GW[a] | $HCO_3^-$ mg/L | $NO_3^-$ mg/L | $HPO_4^{-2}$ mg/L | $SO_4^{-2}$ mg/L | U mg/L | AS[b] | Fe[c] mg/g | $K_d$[d] L/kg | $K_d$[e] L/kg |
|---|---|---|---|---|---|---|---|---|---|---|
| Glacial Till | | | | | | | | | | |
| Waste Pit Area | | | | | | | | | | |
| 1073 | 3775 | 481 | 420 | 1.53 | 612 | 3.297 | 8561 | 1.00 | 0.72 | 0.29 |
| 1073 | 3951 | 455 | 872 | NR[h] | 428 | 4.380 | 8561 | 1.00 | 0.65 | 0.62 |
| 1082 | 3765 | 531 | < 0.4 | 11.75 | 510 | 1.079 | 7667 | 0.81 | 0.82 | 0.01 |
| 1082 | 3949 | 518 | < 0.4 | 2.01 | 20 | 0.810 | 7667 | 0.81 | 1.80 | 0.02 |

[a]Groundwater sample ID.

[b]Aquifer-solid sample ID.

[c]Leachable iron obtained from aquifer solid.

[d]Distribution coefficient based on all U partioned into $UO_2(CO_3)_3^{-4}$.

[e]Distribution coefficient based on speciation in Table 1.

[f]Round number indicated because sample ID not available.

[g]Speciation results not available.

[h]Analysis not reported.

DRAFT

## TABLE P-4

## CALCULATED URANIUM DISTRIBUTION COEFFICIENTS FOR SELECTED MONITORING WELLS

| Well | GW[a] | U mg/L | AQ[b] | U mg/kg | $U_{ads}$[c] mg/kg | $K_d$[d] L/kg |
|---|---|---|---|---|---|---|
| Regional Aquifer South Plume Area | | | | | | |
| 2016 | rd1[e] | 0.021 | 10437 | 0.158 | 0.016 | 0.76 |
| 2046 | 3997 | 0.309 | 8956 | 0.675 | 0.533 | 1.72 |
| 2095 | 3787 | 0.177 | 10038 | 0.783 | 0.641 | 3.62 |
| 2095 | 3976 | 0.146 | 10038 | 0.783 | 0.641 | 4.39 |
| 3095 | 3786 | 0.005 | 10049 | 0.158 | 0.016 | 3.20 |
| 3095 | 3971 | 0.006 | 10049 | 0.158 | 0.016 | 2.67 |
| 4014 | rd4[e] | < 0.001 | 10407 | 0.117 | 0 | 0 |
| 4016 | rd4[e] | < 0.001 | 10460 | 0.033 | 0 | 0 |
| Waste Pit Area | | | | | | |
| 2007 | rd5[e] | 0.005 | 10796 | 0.483 | 0.341 | 68.2 |
| 2010 | 3715 | 0.005 | 8426 | 0.408 | 0.266 | 53.2 |
| 2010 | 3902 | 0.021 | 8426 | 0.408 | 0.266 | 12.7 |
| 2027 | 3941 | 0.007 | 7874 | 0.383 | 0.241 | 34.4 |
| 2034 | 3646 | 0.024 | 8286 | 0.117 | 0 | 0 |
| 3010 | 3714 | 0.020 | 10611 | 0.183 | 0.041 | 2.05 |
| 3010 | 3901 | 0.015 | 10611 | 0.183 | 0.041 | 2.73 |
| 4010 | rd4[e] | < 0.001 | 10607 | 0.217 | 0.075 | 0 |
| FMPC Compound | | | | | | |
| 2013 | 3709 | 0.008 | 10670 | 0.092 | 0 | 0 |
| 2013 | 3900 | 0.036 | 10670 | 0.092 | 0 | 0 |
| 2054 | rd5[e] | 0.023 | 8645 | 0.333 | 0.191 | 8.3 |
| Clay Interbed | | | | | | |
| 3016 | rd1[e] | 0.011 | 10449 | 0.133 | 0 | 0 |
| 3016 | rd4[e] | 0.007 | 10449 | 0.133 | 0 | 0 |

See footnotes at end of table.

DRAFT

DRAFT

**TABLE P-4**
**(Continued)**

| Well | GW[a] | U mg/L | AQ[b] | U mg/kg | $U_{ads}$[c] mg/kg | $K_d$[d] L/kg |
|---|---|---|---|---|---|---|
| Glacial Till Waste Pit Area | | | | | | |
| 1073 | 3775 | 3.297 | 8561 | 0.675 | 0.533 | 0.16 |
| 1073 | 3951 | 4.38 | 8561 | 0.675 | 0.533 | 0.12 |
| 1082 | 3765 | 1.079 | 7667 | 0.367 | 0.225 | 0.21 |
| 1082 | 3949 | 0.81 | 7667 | 0.367 | 0.225 | 0.28 |

[a]Groundwater sample number

[b]Aquifer-solid sample number

[c]Adsorbed uranium (total uranium - background of 0.142)

[d]Distribution coefficient calculated from adsorbed uranium and groundwater uranium values

[e]Round number indicated because sample ID not available

# ATTACHMENT P.I

## ANALYTICAL RESULTS FOR SOIL SAMPLES

DRAFT

| | | | | | |
|---|---|---|---|---|---|
| Boring No. | P1 | P1 | P1 | P1 | P1 |
| Sample ID | 98152 | 98153 | 98155 | 98162 | 98168 |
| Sample Date | 06/02/89 | 06/02/89 | 06/02/89 | 06/02/89 | 06/02/89 |
| Sample Depth (ft) | 0.0-0.5 | 1.5-2.0 | 3.5-4.0 | 8.0-8.5 | 12.0-12.5 |
| U-total (ug/g) | 4 | 2 | 2 | 2 | 1 |
| 2-sigma error | 3 | 2 | 2 | 1 | 1 |

| | | | | | |
|---|---|---|---|---|---|
| Boring No. | P1 | P1 | P1 | P2 | P2 |
| Sample ID | 98174 | 98180 | 98189 | 98116 | 98117 |
| Sample Date | 06/02/89 | 06/02/89 | 06/02/89 | 05/31/89 | 05/31/89 |
| Sample Depth (ft) | 15.5-16.0 | 19.0-19.5 | 23.5-24.0 | 0.0-0.5 | 1.5-2.0 |
| U-total (ug/g) | 2 | 2 | < 2 | < 2 | < 3 |
| 2-sigma error | 1 | 2 | | | |

| | | | | | |
|---|---|---|---|---|---|
| Boring No. | P2 | P2 | P2 | P2 | P2 |
| Sample ID | 98118 | 98119 | 98125 | 98132 | 98143 |
| Sample Date | 05/31/89 | 05/31/89 | 05/31/89 | 05/31/89 | 05/31/89 |
| Sample Depth (ft) | 2.0-2.5 | 3.0-3.5 | 6.5-7.0 | 10.0-10.5 | 15.5-16.0 |
| U-total (ug/g) | 2.1 | < 3.5 | < 3.0 | 2.0 | < 2.5 |
| 2-sigma error | 1.3 | | | 1.6 | |

| | | | | | |
|---|---|---|---|---|---|
| Boring No. | P2 | P3 | P3 | P3 | P3 |
| Sample ID | 98151 | 98029 | 98030 | 98032 | 98034 |
| Sample Date | 05/31/89 | 05/16/89 | 05/16/89 | 05/16/89 | 05/16/89 |
| Sample Depth (ft) | 19.5-20.0 | 0.0-0.5 | 1.5-2.0 | 3.0-3.5 | 4.5-5.0 |
| U-total (ug/g) | < 3.4 | 1.5 | 2.2 | 1.8 | 2.5 |
| 2-sigma error | | 1.4 | 1.1 | 1.5 | 1.5 |

## ATTACHMENT P.I
(continued)

DRAFT

| | | | | | |
|---|---|---|---|---|---|
| Boring No. | P3 | P3 | P3 | P3 | |
| Sample ID | 98040 | 98047 | 98054 | 98061 | |
| Sample Date | 05/22/89 | 05/22/89 | 05/22/89 | 05/22/89 | |
| Sample Depth (ft) | 8.5-9.0 | 12.5-13.0 | 16.0-16.5 | 19.5-20.0 | |
| U-total (ug/g) | 2.5 | 1.5 | < 2.9 | < 2.8 | |
| 2-sigma error | 1.8 | 1.3 | | | |
| Boring No. | S1 | S1 | S1 | S1 | S1 |
| Sample ID | 98062 | 98064 | 98066 | 98077 | 98089 |
| Sample Date | 05/24/89 | 05/24/89 | 05/24/89 | 05/24/89 | 05/24/89 |
| Sample Depth (ft) | 0.0-0.5 | 1.5-2.0 | 3.0-3.5 | 10.5-11.0 | 17.5-18.0 |
| U-total (ug/g) | 8.2 | 9.9 | 3.9 | 3.0 | 2.6 |
| 2-sigma error | 2.1 | 2.2 | 1.9 | 1.6 | 1.3 |
| Boring No. | S1 | S1 | S1 | S2 | S2 |
| Sample ID | 98100 | 98106 | 98115 | 98010 | 98011 |
| Sample Date | 05/24/89 | 05/24/89 | 05/24/89 | 05/16/89 | 05/16/89 |
| Sample Depth (ft) | 24.5-25.0 | 28.5-29.0 | 33.5-34.0 | 0.0-0.5 | 1.5-2.0 |
| U-total (ug/g) | 4.3 | < 3.0 | 2.7 | 7 | 4 |
| 2-sigma error | 1.8 | | 1.3 | 2 | 2 |
| Boring No. | S2 | S2 | S2 | S2 | S2 |
| Sample ID | 98012 | 98014 | 98017 | 98020 | 98024 |
| Sample Date | 05/16/89 | 05/16/89 | 05/16/89 | 05/16/89 | 05/16/89 |
| Sample Depth (ft) | 2.0-2.5 | 3.5-4.0 | 6.0-6.5 | 9.5-10.0 | 13.5-14.0 |
| U-total (ug/g) | 4 | 7 | 8 | 6 | 7 |
| 2-sigma error | 2 | 2 | 2 | 2 | 2 |

## ATTACHMENT P.I
(continued)

| | | | | | |
|---|---|---|---|---|---|
| Boring No. | S2 | S3 | S3 | S3 | S3 |
| Sample ID | 98028 | 98000 | 98001 | 98002 | 98003 |
| Sample Date | 05/16/89 | 05/16/89 | 05/16/89 | 05/16/89 | 05/16/89 |
| Sample Depth (ft) | 16.5-17.0 | 0.0-0.5 | 0.5-1.0 | 1.5-2.0 | 3.0-3.5 |
| U-total (ug/g) | 4 | 3 | 6 | 5 | 3 |
| 2-sigma error | 3 | 2 | 2 | 2 | 2 |

| | | | | |
|---|---|---|---|---|
| Boring No. | S3 | S3 | S3 | S3 |
| Sample ID | 98004 | 98006 | 98008 | 98009 |
| Sample Date | 05/16/89 | 05/16/89 | 05/16/89 | 05/16/89 |
| Sample Depth (ft) | 4.5-5.0 | 6.0-6.5 | 7.5-8.0 | 8.0-8.5 |
| U-total (ug/g) | 4 | 3 | 5 | 1 |
| 2-sigma error | 2 | 2 | 2 | 1 |

DRAFT

# ATTACHMENT P.II

## ANALYTICAL RESULTS FOR SURFACE WATERS

| Sample ID<br>Sample Date | ASIT003<br>05/14/89 | W-07<br>05/14/89 | W-11<br>05/14/89 |
|---|---|---|---|
| pH | 8.57 | 8.38 | 8.58 |
| Eh (mV) | 452 | 451 | 441 |
| $O_2$ (mg/L) | 8.6 | 10.2 | 11.8 |
| T ($^{o}$C) | 15.5 | 13 | 18 |
| Cl (mg/L) | 34 | 18.19 | 19.99 |
| F (mg/L) | 0.19 | 0.21 | 0.18 |
| $HCO_3^-$ (mg/L) | 200.5 | 256.5 | 212 |
| $NH_4^+$ (mg/L) | 0.162 | < 0.1[a] | < 0.1 |
| $NO_3^{-2}$ (mg/L) | 24.08 | 11.95 | 10.23 |
| P (mg/L) | 0.161 | 0.032 | < 0.02 |
| $SO_4^{-2}$ (mg/L) | 51.3 | 57.36 | 57.36 |
| Ag (mg/L) | < 0.01 | < 0.01 | < 0.01 |
| Al (mg/L) | 0.0866 | < 0.06 | 0.0764 |
| As (mg/L) | < 0.002 | < 0.002 | < 0.002 |
| Ba (mg/L) | 0.0399 | 0.0374 | 0.0313 |
| Ca (mg/L) | 72.3 | 84.7 | 71.8 |
| Cd (mg/L) | < 0.002 | < 0.002 | < 0.002 |
| Cr (mg/L) | < 0.01 | < 0.01 | < 0.01 |
| Cu (mg/L) | < 0.01 | < 0.01 | < 0.01 |
| Fe (mg/L) | 0.0659 | 0.0286 | 0.0415 |
| Hg (mg/L) | < 0.0002 | 0.0002 | 0.0003 |
| K (mg/L) | 1.84 | 1.55 | 1.68 |
| Mg (mg/L) | 19.9 | 21.4 | 20.9 |
| Mn (mg/L) | 0.0097 | 0.0152 | 0.0121 |
| Mo (mg/L) | < 0.01 | < 0.01 | < 0.01 |
| Na (mg/L) | 14.6 | 9.93 | 9.69 |

DRAFT

See footnote at end of table.

## ATTACHMENT P.II
(continued)

| Sample ID<br>Sample Date | ASIT003<br>05/14/89 | W-07<br>05/14/89 | W-11<br>05/14/89 |
|---|---|---|---|
| Ni (mg/L) | < 0.02 | < 0.02 | < 0.02 |
| Pb (mg/L) | 0.0026 | 0.0093 | 0.0074 |
| Se (mg/L) | < 0.002 | < 0.002 | < 0.002 |
| Si (mg/L) | 3.89 | 1.73 | 2.25 |
| Th (mg/L) | < 0.006 | < 0.002 | < 0.006 |
| U (mg/L) | 0.002 | 0.015 | 0.009 |
| V (mg/L) | < 0.01 | < 0.01 | < 0.01 |

[a]Less than sign indicates value is below detection limit.

DRAFT

# ATTACHMENT P.III
## ANALYTICAL RESULTS FOR AQUIFER SOLIDS

| Well No. | 1014 | 1046 | 1073 | 1075 | 1082 |
|---|---|---|---|---|---|
| Sample ID | 07363 | 08016 | 08561 | 08572 | 07667 |
| Sample Depth (ft) | 15.0-16.5 | 3.0-4.5 | 18.0-19.5 | 21.0-22.5 | 13.5-15.0 |
| Leached Metals[a] | | | | | |
| Fe (mg/g) | 1.33 | 0.68 | 1.00 | 0.92 | 0.81 |
| Mn (mg/g) | 0.28 | 0.69 | 0.47 | 0.33 | 0.28 |
| U-total (ug/g) | 0.150 | 0.442 | 0.675 | 0.750 | 0.367 |
| 2-sigma error | 0.017 | 0.050 | 0.067 | 0.083 | 0.042 |
| TOC[b] (mg/g) | 4.6 | 5.8 | 2.2 | 3.1 | 4.4 |
| CEC[c] (meq/g) | 0.026 | 0.190 | 0.190 | 0.150 | 0.140 |
| < 200 mesh[d] (wt %) | 5.03 | 82.50 | 66.63 | 70.90 | 58.24 |
| U-total (ug/g) | 11.6 | NA[e] | NA | NA | NA |
| 2-sigma error | 3.1 | | | | |

DRAFT

See footnotes at end of table.

## ATTACHMENT P.III
(continued)

| Well No. | 2007 | 2007 | 2009 | 2010 | 2027 |
|---|---|---|---|---|---|
| Sample ID | 10779 | 10796 | 07084 | 08426 | 07874 |
| Sample Depth (ft) | 13.5-15.0 | 65.0-66.5 | 38.5-40.0 | 70.0-71.5 | 65.0-66.5 |
| Leached Metals | | | | | |
| Fe (mg/g) | 2.33 | 1.08 | 0.52 | 1.50 | 1.58 |
| Mn (mg/g) | 0.42 | 0.28 | 0.15 | 0.29 | 0.23 |
| U-total (ug/g) | 0.292 | 0.483 | 0.108 | 0.408 | 0.383 |
| 2-sigma error | 0.033 | 0.058 | 0.017 | 0.042 | 0.042 |
| TOC (mg/g) | 4.7 | 5.2 | 3.9 | 4.7 | 3.2 |
| CEC (meq/g) | 0.110 | 0.018 | 0.028 | 0.018 | 0.027 |
| < 200 mesh (wt %) | 60.74 | 5.83 | 16.85 | 9.79 | 11.63 |
| U-initial[f] (ug/g) | NA | NA | 132 | NA | 105 |
| 2-sigma error | | | 31 | | 27 |
| U-final[g] (ug/g) | NA | NA | 124 | NA | 113 |
| 2-sigma error | | | 30 | | 29 |

DRAFT

See footnotes at end of table.

## ATTACHMENT P.III
(continued)

| Well No. | 2045 | 2046 | 2054 | 2054 | 2054 |
|---|---|---|---|---|---|
| Sample ID | 08947 | 08956 | 10414 | 10416 | 08645 |
| Sample Depth (ft) | 30.0-31.5 | 61.0-62.5 | 6.0-7.5 | 9.0-10.5 | 70.0-71.5 |
| Leaached Metals[a] | | | | | |
| Fe (mg/g) | 0.47 | 0.81 | 0.55 | 0.65 | 1.17 |
| Mn (mg/g) | 0.19 | 0.18 | 0.20 | 0.19 | 0.28 |
| U-total (ug/g) | 0.217 | 0.675 | 0.275 | 0.383 | 0.333 |
| 2-sigma error | 0.025 | 0.075 | 0.025 | 0.042 | 0.033 |
| TOC[b] (mg/g) | 3.0 | 6.3 | 8.2 | 3.9 | 3.7 |
| CEC[c] (meq/g) | 0.025 | 0.025 | 0.120 | 0.130 | 0.015 |
| < 200 mesh[d] (wt %) | 8.92 | 8.92 | 56.44 | 61.46 | 11.98 |
| U-total (ug/g) | NA[e] | 16 | NA | NA | NA |
| 2-sigma error | | 3.7 | | | |
| U-initial[f] (ug/g) | 150 | NA | NA | NA | NA |
| 2-sigma error | 38 | | | | |
| U-final[g] (ug/g) | 145 | NA | NA | NA | NA |
| 2-sigma error | 36 | | | | |

DRAFT

See footnotes at end of table.

## ATTACHMENT P.III
(continued)

| Well No. | 2055 | 2055 | 3034 | 3043 | 3043 |
|---|---|---|---|---|---|
| Sample ID | 10736 | 10766 | 08286 | 07619 | 07790 |
| Sample Depth (ft) | 1.5-3.0 | 70.0-71.5 | 50.0-51.5 | 7.5-9.0 | 108.0-109.5 |
| Leached Metals | | | | | |
| Fe (mg/g) | 0.79 | 1.17 | 0.78 | 0.60 | 1.00 |
| Mn (mg/g) | 1.00 | 0.26 | 0.23 | 0.32 | 0.09 |
| U-total (ug/g) | 0.108 | 0.142 | 0.117 | 0.258 | 0.100 |
| 2-sigma error | 0.008 | 0.017 | 0.017 | 0.033 | 0.008 |
| TOC (mg/g) | 3.1 | 4.1 | 5.0 | 3.9 | 3.2 |
| CEC (meq/g) | 0.150 | 0.022 | 0.029 | 0.120 | 0.022 |
| < 200 mesh (wt %) | 57.80 | 15.95 | 12.96 | 72.64 | 12.34 |
| U-total (ug/g) | NA | NA | 12.3 | NA | NA |
| 2-sigma error | | | 3.2 | | |
| U-initial (ug/g) | NA | NA | NA | NA | 106 |
| 2-sigma error | | | | | 26 |
| U-final (ug/g) | NA | NA | NA | NA | 116 |
| 2-sigma error | | | | | 27 |

DRAFT

See footnotes at end of table.

## ATTACHMENT P.III
(continued)

| Well No. | 3084 | 3095 | 3095 | 4010 | 4010 |
|---|---|---|---|---|---|
| Sample ID | 07558 | 10038 | 10049 | 10611 | 10607 |
| Sample Depth (ft) | 120.0-121.5 | 20.0-21.5 | 75.0-76.5 | 131.5-132 | 195.0-196.5 |
| Leached Metals[a] | | | | | |
| Fe (mg/g) | 7.67 | 0.66 | 1.00 | 3.50 | 1.08 |
| Mn (mg/g) | 0.16 | 0.28 | 0.29 | 0.12 | 0.16 |
| U-total (ug/g) | 0.300 | 0.783 | 0.158 | 0.183 | 0.216 |
| 2-sigma error | 0.033 | 0.083 | 0.017 | 0.017 | 0.025 |
| TOC[b] (mg/g) | 3.3 | 6.2 | 4.7 | 15.0 | 4.2 |
| CEC[c] (meq/g) | 0.250 | 0.028 | 0.018 | 0.260 | 0.022 |
| < 200 mesh[d] (wt %) | NA[e] | 12.52 | 6.52 | 67.38 | 11.26 |
| U-total (ug/g) | 11.5 | NA | NA | 13.8 | NA |
| 2-sigma error | 3.3 | | | 4.1 | |
| U-initial[f] (ug/g) | NA | 137 | 95 | NA | NA |
| 2-sigma error | | 33 | 24 | | |
| U-final[g] (u/g) | NA | 123 | 93 | NA | NA |
| 2-sigma error | | 32 | 25 | | |

DRAFT

See footnotes at end of table.

## ATTACHMENT P.III
(continued)

| Well No. | 4013 | 4013 | 4014 | 4016 | 4016 |
|---|---|---|---|---|---|
| Sample ID | 10670 | 10696 | 10407 | 10437 | 10449 |
| Sample Depth (ft) | 75.0-76.5 | 205.0-206.5 | 135.0-136.5 | 30.0-31.5 | 89.3-89.6 |
| Leached Metals | | | | | |
| Fe (mg/g) | 0.65 | 1.33 | 1.08 | 0.69 | 4.83 |
| Mn (mg/g) | 0.12 | 0.39 | 0.25 | 0.21 | 0.41 |
| U-total (ug/g) | 0.092 | 0.242 | 0.117 | 0.158 | 0.133 |
| 2-sigma error | 0.008 | 0.025 | 0.017 | 0.017 | 0.017 |
| TOC (mg/g) | 4.2 | 3.3 | 1.4 | 5.1 | 16.0 |
| CEC (meq/g) | 0.019 | 0.020 | 0.025 | 0.035 | 0.190 |
| < 200 mesh (wt %) | 6.54 | 3.50 | 20.88 | 7.24 | 78.50 |
| U-total (ug/g) | NA | NA | NA | NA | 14.0 |
| 2-sigma error | | | | | 4.2 |
| U-initial (ug/g) | NA | NA | NA | 107 | NA |
| 2-sigma error | | | | 28 | |
| U-final (ug/g) | NA | NA | NA | 101 | NA |
| 2-sigma error | | | | 29 | |

DRAFT

See footnotes at end of table.

## ATTACHMENT P.III
(continued)

| | |
|---|---|
| Well No. | 4016 |
| Sample ID | 10460 |
| Sample Depth (ft) | 145.0-146.5 |

| | |
|---|---|
| Leached Metals[a] | |
| Fe (mg/g) | 0.38 |
| Mn (mg/g) | 0.15 |
| U-total (ug/g) | 0.033 |
| 2-sigma error | 0.008 |
| TOC[b] (mg/g) | 1.7 |
| CEC[c] (meq/g) | 0.023 |
| < 200 mesh[d] (wt %) | 8.50 |

[a]Sample leached with a solution of acetic acid and hydroxylamine hydrochloride

[b]TOC = total organic carbon

[c]CEC = cation exchange capacity

[d]Weight percent of sample less than 0.075 mm (silt + clay)

[e]Analysis not available

[f]Total uranium before differential-leaching analysis

[g]Total uranium after differential-leaching analysis

DRAFT

## ATTACHMENT P.IV

## ANALYTICAL RESULTS FOR MODELED GROUNDWATERS

| Well No. | 1019 | 1019 | 1073 | 1073 | 1082 |
|---|---|---|---|---|---|
| Sample ID | 3748 | 3944 | 3775 | 3951 | 3765 |
| Sample Date | 12/04/88 | 03/08/89 | 12/04/88 | 03/12/89 | 11/20/88 |
| Round No. | 3 | 4 | 3 | 4 | 3 |
| pH | 7 | 7 | 7.6 | 7.1 | 7 |
| Eh (mV) | NR[a] | NR | NR | NR | NR |
| $O_2$ (mg/L) | 10.6 | 2.8 | 6.25 | 8.1 | 8 |
| T (°C) | 11 | 7 | 12.5 | 10.5 | 13 |
| Cl (mg/L) | 1160 | 490 | 1030 | 1170 | 2 |
| F (mg/L) | 0.48 | 0.5 | 6.25 | 7.25 | 1.25 |
| $HCO_3^-$ (mg/L) | 403.8 | 395.8 | 480.6 | 454.9 | 530.8 |
| $NH_4^+$ (mg/L) | 0.139 | 0.5 | 80.2 | 71.6 | < 0.1[b] |
| $NO_3^-$ (mg/L) | 56.7 | 0.9 | 419.7 | 872 | < 0.4 |
| P (mg/L) | 0.061 | 0.12 | 0.493 | NR | 3.79 |
| $SO_4^{-2}$ (mg/L) | 224 | 250 | 612 | 428 | 510 |
| Ag (mg/L) | < 0.02 | 0.01 | < 0.02 | < 0.0005 | < 0.0005 |
| As (mg/L) | 0.004 | < 0.003 | 0.002 | < 0.002 | < 0.002 |
| Ba (mg/L) | 0.195 | 0.1 | 0.138 | 0.126 | 0.044 |
| Ca (mg/L) | 522 | 300 | 413 | 4000 | 129 |
| Cd (mg/L) | 0.002 | 0.006 | 0.002 | 0.0364 | < 0.002 |
| Cr (mg/L) | < 0.02 | 0.04 | < 0.02 | 0.0464 | < 0.02 |
| Cu (mg/L) | < 0.01 | < 0.01 | 0.014 | 0.0836 | < 0.01 |
| Fe (mg/L) | 1.51 | 0.87 | 0.073 | 0.172 | 0.015 |
| Hg (mg/L) | < 0.0002 | < 0.0002 | 0.0007 | 30.2 | < 0.0002 |
| K (mg/L) | 1.47 | 0.86 | 33 | 0.0007 | 2.42 |
| Mg (mg/L) | 159 | 86 | 325 | 364 | 65 |
| Mn (mg/L) | 1.61 | 1.1 | 2.1 | 0.689 | 0.008 |
| Mo (mg/L) | < 0.02 | 0.02 | 0.533 | 0.58 | 0.033 |

See footnotes at end of table.

## ATTACHMENT P.IV
(continued)

| Well No. | 1019 | 1019 | 1073 | 1073 | 1082 |
|---|---|---|---|---|---|
| Sample ID | 3748 | 3944 | 3775 | 3951 | 3765 |
| Sample Date | 12/04/88 | 03/08/89 | 12/04/88 | 03/12/89 | 11/20/88 |
| Round No. | 3 | 4 | 3 | 4 | 3 |
| Na (mg/L) | 437 | 170 | 149 | 178 | 13.3 |
| Ni (mg/L) | < 0.02 | < 0.03 | 0.066 | 0.114 | < 0.02 |
| Pb (mg/L) | 0.003 | < 0.002 | 0.004 | < 0.002 | < 0.002 |
| Se (mg/L) | < 0.002 | < 0.005 | < 0.002 | < 0.002 | 0.002 |
| Th (mg/L) | < 0.004 | < 0.005 | 0.012 | 0.025 | < 0.006 |
| U (mg/L) | 0.818 | 0.739 | 3.297 | 4.38 | 1.079 |

DRAFT

See footnotes at end of table.

## ATTACHMENT P.IV
(continued)

| Well No. | 1082 | 2013 | 2024 | 2044 | 2045 |
|---|---|---|---|---|---|
| Sample ID | 3949 | 3709 | 3656 | 3682 | 3993 |
| Sample Date | 02/05/89 | 11/15/88 | 11/02/88 | 11/03/88 | 01/23/89 |
| Round No. | 4 | 3 | 3 | 3 | 4 |
| pH | 7.35 | 6.85 | 7.30 | 7.47 | 7.3 |
| Eh (mV) | NR[a] | NR | 152 | NR | NR |
| $O_2$ (mg/L) | 8 | 1.3 | 0.4 | 4.39 | 3.6 |
| T ($^oC$) | 10 | 13 | 10 | 10 | 7 |
| Cl (mg/L) | 19 | 26.5 | 19 | 38 | 15 |
| F (mg/L) | 0.72 | 0.185 | < 0.5[b] | 0.17 | 0.17 |
| $HCO_3^-$ (mg/L) | 517.6 | 328.3 | 422.7 | 308.3 | 344.3 |
| $NH_4^+$ (mg/L) | < 0.1 | < 0.1 | 0.44 | < 0.1 | < 0.1 |
| $NO_3^-$ (mg/L) | < 0.4 | < 0.4 | 0.584 | 1.32 | 8.72 |
| P (mg/L) | 0.65 | < 0.02 | 0.342 | 0.024 | NR |
| $SO_4^{-2}$ (mg/L) | 19.6 | 97.2 | 385 | 121 | 54.2 |
| Ag (mg/L) | < 0.0005 | < 0.01 | < 0.01 | < 0.01 | < 0.0005 |
| As (mg/L) | < 0.002 | < 0.002 | < 0.002 | < 0.002 | < 0.002 |
| Ba (mg/L) | 0.077 | 0.072 | 0.090 | 0.05 | 0.044 |
| Ca (mg/L) | 143 | 119 | 196 | 88.6 | 108 |
| Cd (mg/L) | 0.011 | < 0.002 | < 0.002 | < 0.002 | 0.004 |
| Cr (mg/L) | 0.039 | < 0.02 | < 0.02 | < 0.02 | 0.025 |
| Cu (mg/L) | 0.018 | < 0.01 | < 0.01 | < 0.01 | 0.012 |
| Fe (mg/L) | 0.062 | 2.67 | 4.30 | 0.02 | 0.043 |
| Hg (mg/L) | 0.0012 | < 0.0002 | < 0.0002 | < 0.0002 | 0.0006 |
| K (mg/L) | 2.01 | 2.16 | 1.35 | 2.62 | 2.1 |
| Mg (mg/L) | 72.8 | 27.9 | 33.8 | 24.2 | 25.7 |
| Mn (mg/L) | 0.01 | 0.198 | 0.40 | 0.03 | 0.012 |
| Mo (mg/L) | < 0.02 | < 0.033 | < 0.02 | < 0.02 | < 0.02 |

See footnotes at end of table.

DRAFT

## ATTACHMENT P.IV
(continued)

| Well No. | 1082 | 2013 | 2024 | 2044 | 2045 |
|---|---|---|---|---|---|
| Sample ID | 3949 | 3709 | 3656 | 3682 | 3993 |
| Sample Date | 02/05/89 | 11/15/88 | 11/02/88 | 11/03/88 | 01/23/89 |
| Round No. | 4 | 3 | 3 | 3 | 4 |
| Na (mg/L) | 15.4 | 11.6 | 9.5 | 16.8 | 9.12 |
| Ni (mg/L) | 0.034 | < 0.02 | < 0.02 | < 0.02 | < 0.02 |
| Pb (mg/L) | < 0.002 | < 0.002 | 0.032 | 0.003 | < 0.002 |
| Se (mg/L) | < 0.002 | < 0.002 | < 0.002 | < 0.002 | < 0.002 |
| Th (mg/L) | < 0.008 | < 0.002 | < 0.004 | < 0.002 | 0.005 |
| U (mg/L) | 0.81 | 0.008 | 0.005 | 0.033 | 0.283 |

DRAFT

See footnotes at end of table.

5617

## ATTACHMENT P.IV
(continued)

| Well No. | 2046 | 2060 | 2060 | 2061 | 2094 |
|---|---|---|---|---|---|
| Sample ID | 3997 | 3696 | 3889 | 3890 | 3872 |
| Sample Date | 02/02/89 | 10/25/88 | 02/01/89 | 02/07/89 | 02/01/89 |
| Round No. | 4 | 3 | 4 | 4 | 4 |
| pH | 7.1 | 7.5 | 7.4 | 7.6 | 7.1 |
| Eh (mV) | 441 | NR[a] | 477 | 415 | 75 |
| $O_2$ (mg/L) | 4 | 3.2 | 2 | 0.7 | 0.4 |
| T (°C) | 9 | 11 | 8 | 6 | 15 |
| Cl (mg/L) | 3 | 21 | 22 | 19.5 | 185 |
| F (mg/L) | 0.15 | 0.54 | 0.48 | 0.33 | 0.17 |
| $HCO_3^-$ (mg/L) | 355.3 | 265.5 | 276.6 | 262.5 | 716.6 |
| $NH_4^+$ (mg/L) | < 0.1[b] | < 0.1 | < 0.1 | 0.266 | < 0.1 |
| $NO_3^-$ (mg/L) | 5.98 | 32.8 | 1.51 | 1.73 | < 0.4 |
| P (mg/L) | 0.39 | < 0.02 | 0.03 | 0.02 | 1.92 |
| $SO_4^{-2}$ (mg/L) | 73.5 | 36 | 78.3 | 61.8 | 33 |
| Ag (mg/L) | < 0.0005 | < 0.01 | < 0.0005 | < 0.0005 | < 0.0005 |
| As (mg/L) | < 0.002 | < 0.002 | < 0.002 | < 0.002 | 0.21 |
| Ba (mg/L) | 0.067 | 0.039 | 0.054 | 0.044 | 1.25 |
| Ca (mg/L) | 111 | 81.8 | 90.6 | 87 | 74 |
| Cd (mg/L) | 0.006 | < 0.002 | < 0.02 | 0.006 | 0.011 |
| Cr (mg/L) | 0.023 | < 0.02 | 0.03 | 0.026 | 0.03 |
| Cu (mg/L) | 0.021 | < 0.01 | 0.018 | 0.027 | 0.026 |
| Fe (mg/L) | 0.117 | 0.011 | 0.161 | 0.18 | 21.2 |
| Hg (mg/L) | < 0.0002 | < 0.0002 | 0.001 | < 0.0002 | 0.0085 |
| K (mg/L) | 2.86 | 2.27 | 5.58 | 2.77 | 1800 |
| Mg (mg/L) | 31.8 | 20.8 | 24.3 | 22.6 | 49.4 |
| Mn (mg/L) | 0.017 | 0.001 | 0.01 | 0.016 | 0.256 |
| Mo (mg/L) | < 0.02 | < 0.02 | < 0.02 | < 0.02 | < 0.02 |

See footnotes at end of table.

DRAFT

## ATTACHMENT P.IV
(continued)

| Well No. | 2046 | 2060 | 2060 | 2061 | 2094 |
|---|---|---|---|---|---|
| Sample ID | 3997 | 3696 | 3889 | 3890 | 3872 |
| Sample Date | 02/02/89 | 10/25/88 | 02/01/89 | 02/07/89 | 02/01/89 |
| Round No. | 4 | 3 | 4 | 4 | 4 |
| Na (mg/L) | 10.2 | 10.6 | 13.6 | 10.6 | 109 |
| Ni (mg/L) | 0.02 | < 0.02 | < 0.02 | < 0.02 | 0.052 |
| Pb (mg/L) | 0.006 | < 0.002 | < 0.002 | 0.004 | < 0.002 |
| Se (mg/L) | 0.003 | < 0.002 | < 0.002 | < 0.002 | < 0.002 |
| Th (mg/L) | < 0.002 | < 0.007 | < 0.003 | < 0.003 | < 0.004 |
| U (mg/L) | 0.309 | 0.171 | 0.25 | 0.292 | 0.0045 |

DRAFT

See footnotes at end of table.

## ATTACHMENT P.IV
(continued)

| Well No. | 2095 | 3001 | 3001 | 3013 | 3013 |
|---|---|---|---|---|---|
| Sample ID | 3787 | 3783 | 3936 | 3703 | 3899 |
| Sample Date | 12/06/88 | 12/05/88 | 02/28/89 | 11/14/88 | 02/22/89 |
| Round No. | 3 | 3 | 4 | 3 | 4 |
| pH | 7.33 | 8 | 7.1 | 6.3 | 8.4 |
| Eh (mV) | NR[a] | NR | 81 | NR | 139 |
| $O_2$ (mg/L) | 4.1 | 9.5 | 0.7 | 1.9 | NR |
| T ($^oC$) | 11 | 9 | 11 | 13.5 | 7 |
| Cl (mg/L) | 4 | 19.1 | 21 | 60 | 21 |
| F (mg/L) | 0.24 | 0.19 | 0.1 | 0.113 | 0.45 |
| $HCO_3^-$ (mg/L) | 352.2 | 300.7 | 300.9 | 480.5 | 302.2 |
| $NH_4^+$ (mg/L) | < 0.1 | .131 | 0.5 | < 0.1 | 0.1 |
| $NO_3^-$ (mg/L) | 77.5 | < 0.4 | 0.08 | < 0.4 | 0.4 |
| P (mg/L) | 0.063 | < 0.2 | 0.12 | < 0.02 | 0.02 |
| $SO_4^{-2}$ mg/L) | 17.5 | 176 | 67 | 252 | 130 |
| Ag (mg/L) | < 0.02 | < 0.02 | < 0.01 | < 0.01 | 0.01 |
| As (mg/L) | < 0.002 | < 0.002 | < 0.003 | < 0.002 | < 0.003 |
| Ba (mg/L) | 0.05 | 0.085 | 0.053 | 0.089 | 0.071 |
| Ca (mg/L) | 100 | 173 | 100 | 202 | 68 |
| Cd (mg/L) | < 0.002 | < 0.002 | < 0.005 | 0.007 | 0.007 |
| Cr (mg/L) | < 0.02 | < 0.02 | 0.02 | < 0.02 | 0.4 |
| Cu (mg/L) | 0.014 | < 0.01 | < 0.01 | < 0.01 | 0.01 |
| Fe (mg/L) | 0.032 | 4.5 | 2.5 | 7.21 | 0.05 |
| Hg (mg/L) | 0.0004 | < 0.0002 | < 0.0002 | < 0.0002 | < 0.0002 |
| K (mg/L)B | 2.5 | 5.56 | 2.3 | 3.85 | 2 |
| Mg (mg/L) | 23.3 | 37.9 | 25 | 45.2 | 52 |
| Mn (mg/L) | 0.003 | 0.362 | 0.61 | 0.382 | 0.02 |
| Mo (mg/L) | < 0.02 | < 0.02 | 0.01 | 0.041 | 0.02 |

See footnotes at end of table.

DRAFT

## ATTACHMENT P.IV
(continued)

| Well No. | 2095 | 3001 | 3001 | 3013 | 3013 |
|---|---|---|---|---|---|
| Sample ID | 3787 | 3783 | 3936 | 3703 | 3899 |
| Sample Date | 12/06/88 | 12/05/88 | 02/28/89 | 11/14/88 | 02/22/89 |
| Round No. | 3 | 3 | 4 | 3 | 4 |
| Na (mg/L) | 24.6 | 24.4 | 11 | 45.7 | 18 |
| Ni (mg/L) | < 0.02 | < 0.02 | < 0.03 | < 0.02 | < 0.03 |
| Pb (mg/L) | < 0.002 | < 0.002 | < 0.002 | 0.004 | < 0.002 |
| Se (mg/L) | < 0.002 | < 0.002 | < 0.005 | < 0.002 | < 0.005 |
| Th (mg/L) | < 0.004 | < 0.006 | < 0.003 | < 0.006 | < 0.003 |
| U (mg/L) | 0.177 | 0.015 | 0.015 | 0.011 | 0.490 |

DRAFT

See footnotes at end of table.

## ATTACHMENT P.IV
(continued)

| Well No. | 3014 | 3016 | 3062 | 3069 | 3094 |
|---|---|---|---|---|---|
| Sample ID | 3672 | 3686 | 3780 | 3663 | 3874 |
| Sample Date | 11/06/88 | 11/04/88 | 10/25/88 | 11/07/88 | 02/01/89 |
| Round No. | 3 | 3 | 3 | 3 | 4 |
| pH | 7.75 | 7.6 | 7.9 | 7.6 | 7.1 |
| Eh (mV) | NR[a] | NR | NR | NR | 99 |
| $O_2$ (mg/L) | 6.2 | 5.1 | 6.8 | 3.82 | 0.6 |
| T ($^oC$) | 12 | 13.5 | 11 | 9.5 | 15 |
| Cl (mg/L) | 25.8 | 25.6 | 19.9 | 24.5 | 140 |
| F (mg/L) | 0.16 | 0.15 | 0.32 | 0.18 | 0.13 |
| $HCO_3^-$ (mg/L) | 229.4 | 251.4 | 312.8 | 261.0 | 710.6 |
| $NH_4^+$ (mg/L) | < 0.1[b] | < 0.1 | < 0.1 | 0.17 | 2.4 |
| $NO_3^-$ (mg/L) | 7.44 | 13.5 | < 0.4 | 2.97 | < 0.4 |
| P (mg/L) | < 0.02 | < 0.02 | < 0.02 | 0.662 | 0.88 |
| $SO_4^{-2}$ (mg/L) | 51.4 | 174 | 29 | 92.7 | 41.2 |
| Ag (mg/L) | < 0.01 | < 0.01 | < 0.01 | < 0.01 | < 0.0005 |
| As (mg/L) | < 0.002 | < 0.002 | < 0.002 | < 0.002 | 0.003 |
| Ba (mg/L) | 0.03 | 0.040 | 0.063 | 0.050 | 0.382 |
| Ca (mg/L) | 74.1 | 82.9 | 92.3 | 79.6 | 106 |
| Cd (mg/L) | 0.004 | < 0.002 | < 0.002 | < 0.002 | 0.007 |
| Cr (mg/L) | < 0.02 | < 0.02 | < 0.02 | < 0.02 | 0.032 |
| Cu (mg/L) | < 0.01 | < 0.01 | < 0.01 | < 0.01 | 0.02 |
| Fe (mg/L) | 0.03 | 0.10 | 1 | 0.10 | 4.43 |
| Hg (mg/L) | < 0.0002 | < 0.0002 | < 0.0002 | < 0.0002 | 0.0023 |
| K (mg/L) | 1.94 | 2.53 | 2.16 | 2.15 | 1830 |
| Mg (mg/L) | 18.7 | 21.4 | 22.7 | 20.6 | 58.1 |
| Mn (mg/L) | < 0.001 | 0.050 | 0.396 | 0.10 | 0.241 |
| Mo (mg/L) | < 0.02 | < 0.02 | < 0.02 | < 0.02 | < 0.02 |

See footnotes at end of table.

## ATTACHMENT P.IV
(continued)

| Well No. | 3014 | 3016 | 3062 | 3069 | 3094 |
|---|---|---|---|---|---|
| Sample ID | 3672 | 3686 | 3780 | 3663 | 3874 |
| Sample Date | 11/06/88 | 11/04/88 | 10/25/88 | 11/07/88 | 02/01/89 |
| Round No. | 3 | 3 | 3 | 3 | 4 |
| Na (mg/L) | 10.9 | 11.3 | 12.9 | 11.4 | 90.1 |
| Ni (mg/L) | < 0.02 | < 0.02 | < 0.02 | < 0.02 | 0.066 |
| Pb (mg/L) | 0.016 | 0.003 | < 0.002 | 0.010 | < 0.002 |
| Se (mg/L) | 0.002 | 0.002 | < 0.002 | 0.002 | < 0.002 |
| Th (mg/L) | < 0.007 | NR | < 0.002 | NR | < 0.003 |
| U (mg/L) | 0.028 | 0.008 | 0.041 | 0.005 | 0.0006 |

DRAFT

See footnotes at end of table.

## ATTACHMENT P.IV
(continued)

| | |
|---|---|
| Well No. | 4097 |
| Sample ID | 3988 |
| Sample Date | 02/08/89 |
| Round No. | 4 |

| | |
|---|---|
| pH | 7.1 |
| Eh (mV) | 221 |
| $O_2$ (mg/L) | 0.5 |
| T (°C) | 11 |
| Cl (mg/L) | 25 |
| F (mg/L) | 0.16 |
| $HCO_3^-$ (mg/L) | 329.7 |
| $NH_4^+$ (mg/L) | .247 |
| $NO_3$- (mg/L) | .53 |
| P (mg/L) | 0.11 |
| $SO_4^{-2}$ (mg/L) | 66.4 |
| Ag (mg/L) | < 0.0005[a] |
| As (mg/L) | < 0.002 |
| Ba (mg/L) | 0.055 |
| Ca (mg/L) | 94.7 |
| Cd (mg/L) | 0.006 |
| Cr (mg/L) | 0.024 |
| Cu (mg/L) | 0.01 |
| Fe (mg/L) | 0.743 |
| Hg (mg/L) | 0.0006 |
| K (mg/L) | 2.17 |
| Mg (mg/L) | 27.6 |
| Mn (mg/L) | 0.243 |
| Mo (mg/L) | < 0.02 |

DRAFT

See footnotes at end of table.

5617

## ATTACHMENT P.IV
(continued)

| | |
|---|---|
| Well No. | 4097 |
| Sample ID | 3988 |
| Sample Date | 02/08/89 |
| Round No. | 4 |

| | |
|---|---|
| Na (mg/L) | 15.1 |
| Ni (mg/L) | < 0.02 |
| Pb (mg/L) | < 0.0002 |
| Se (mg/L) | 0.003 |
| Th (mg/L) | < 0.002 |
| U (mg/L) | 0.019 |

[a]NR - Analysis not reported.

[b]Less than sign indicates below detection limit value.

DRAFT

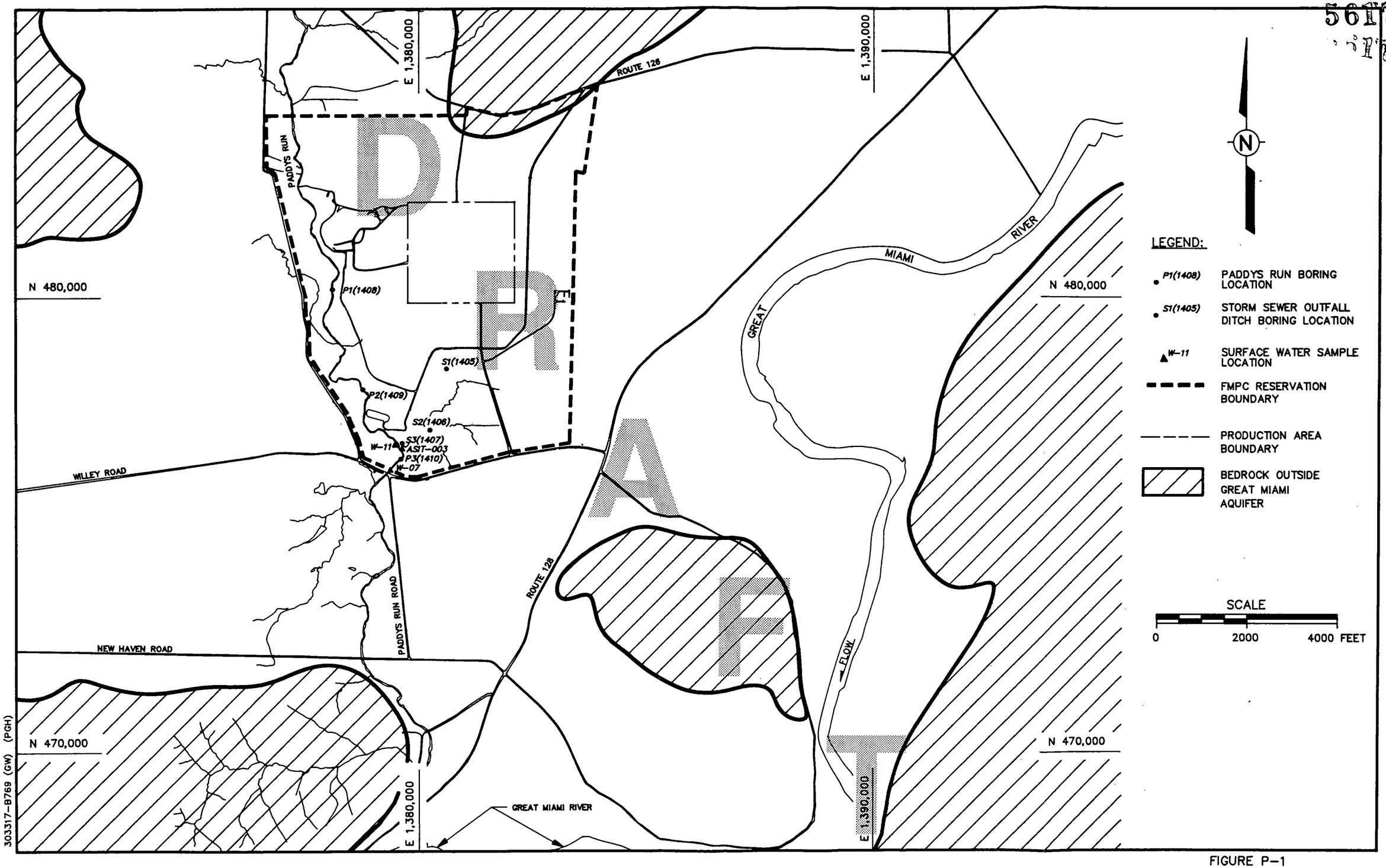


303317-B769 (GW) (PGH)

FIGURE P-1
GEOCHEMICAL PROGRAM ISSUE - 3
SURFACE WATER AND SUBSURFACE
SOIL SAMPLING LOCATIONS

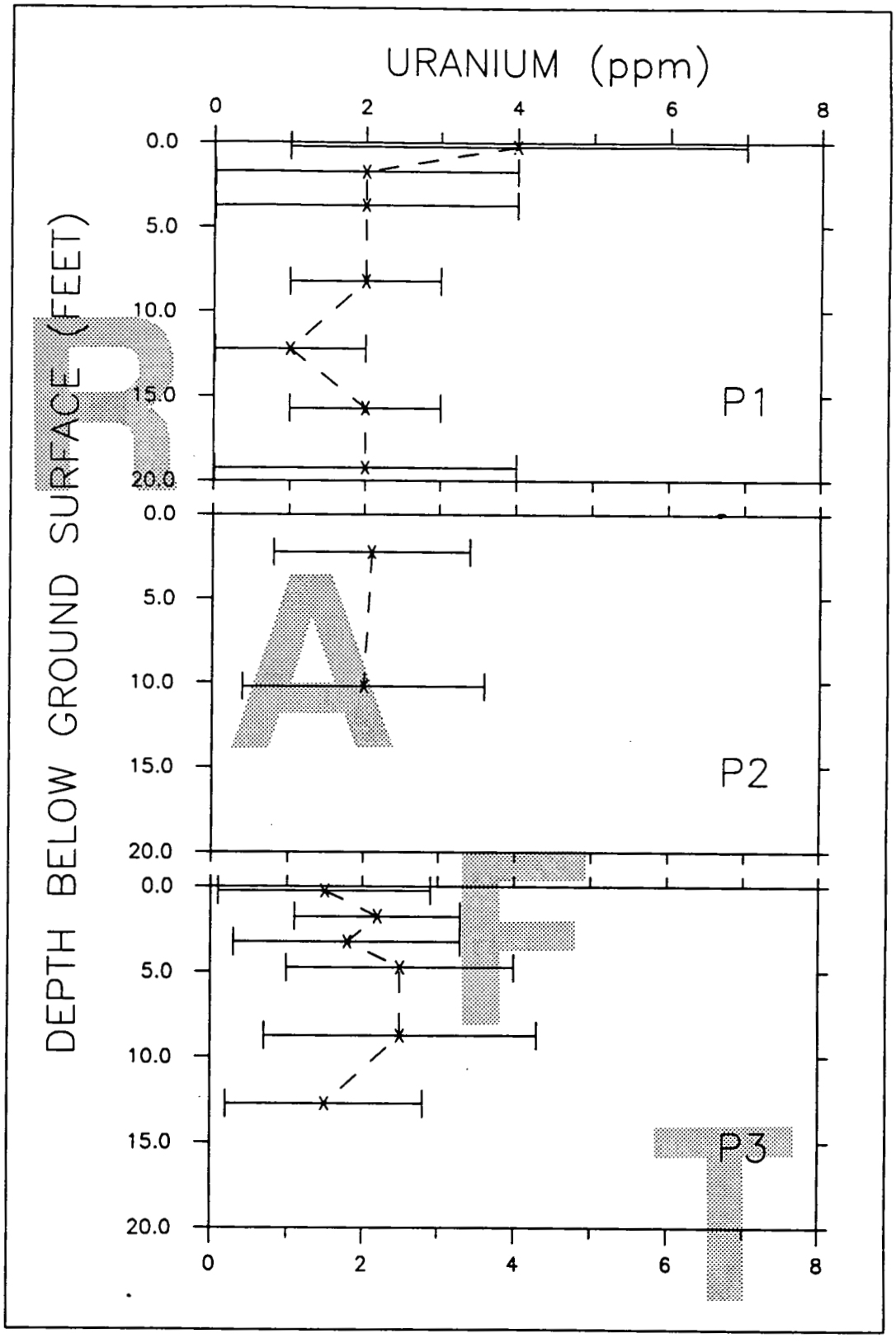


FIGURE P-2. URANIUM CONCENTRATIONS IN SUBSURFACE SOILS OF PADDYS RUN

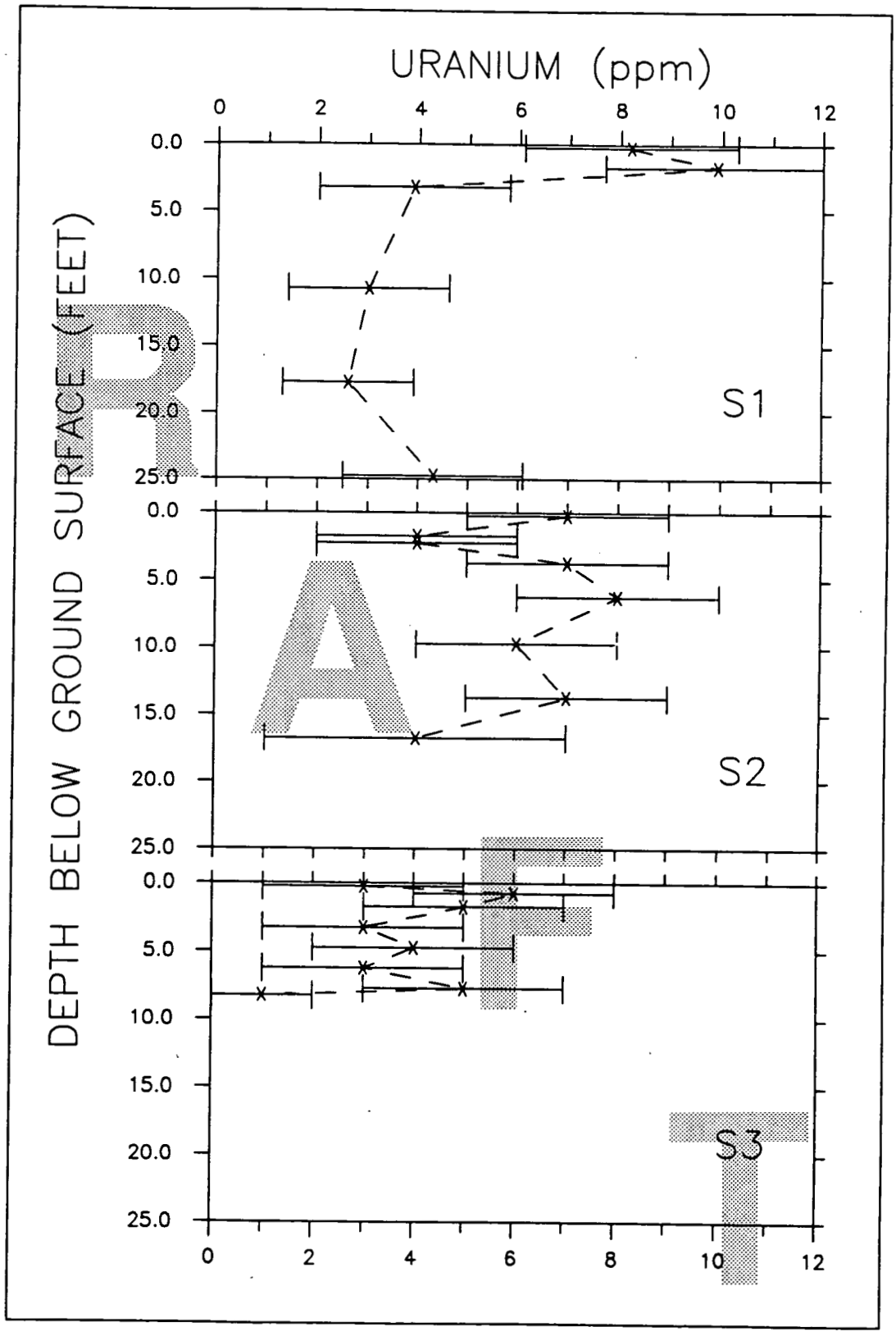


FIGURE P-3. URANIUM CONCENTRATIONS IN SUBSURFACE SOILS OF THE STORM SEWER OUTFALL DITCH

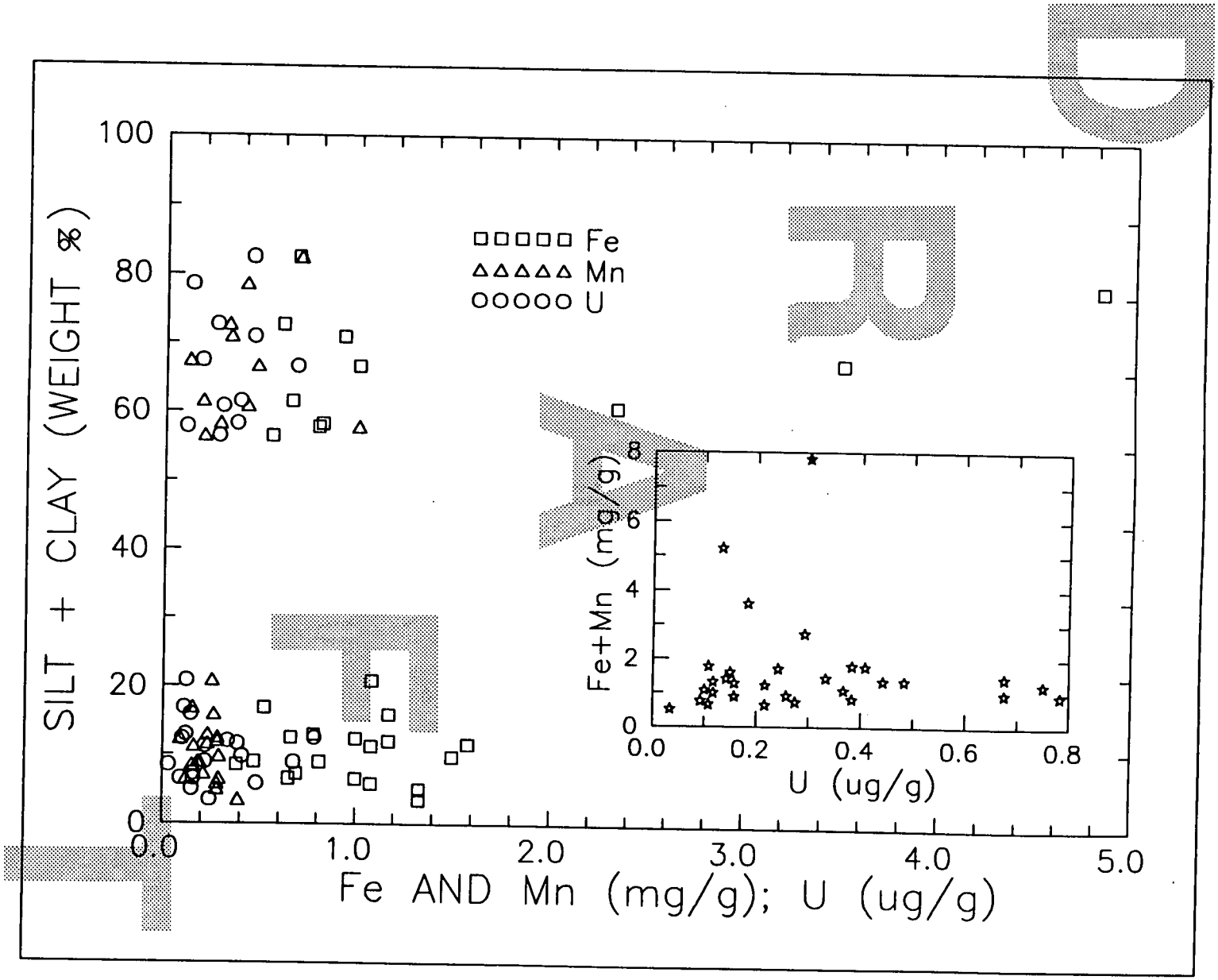


FIGURE P-4. WEIGHT PERCENT OF SILT + CLAY VERSUS LEACHABLE IRON, MANGANESE, AND URANIUM

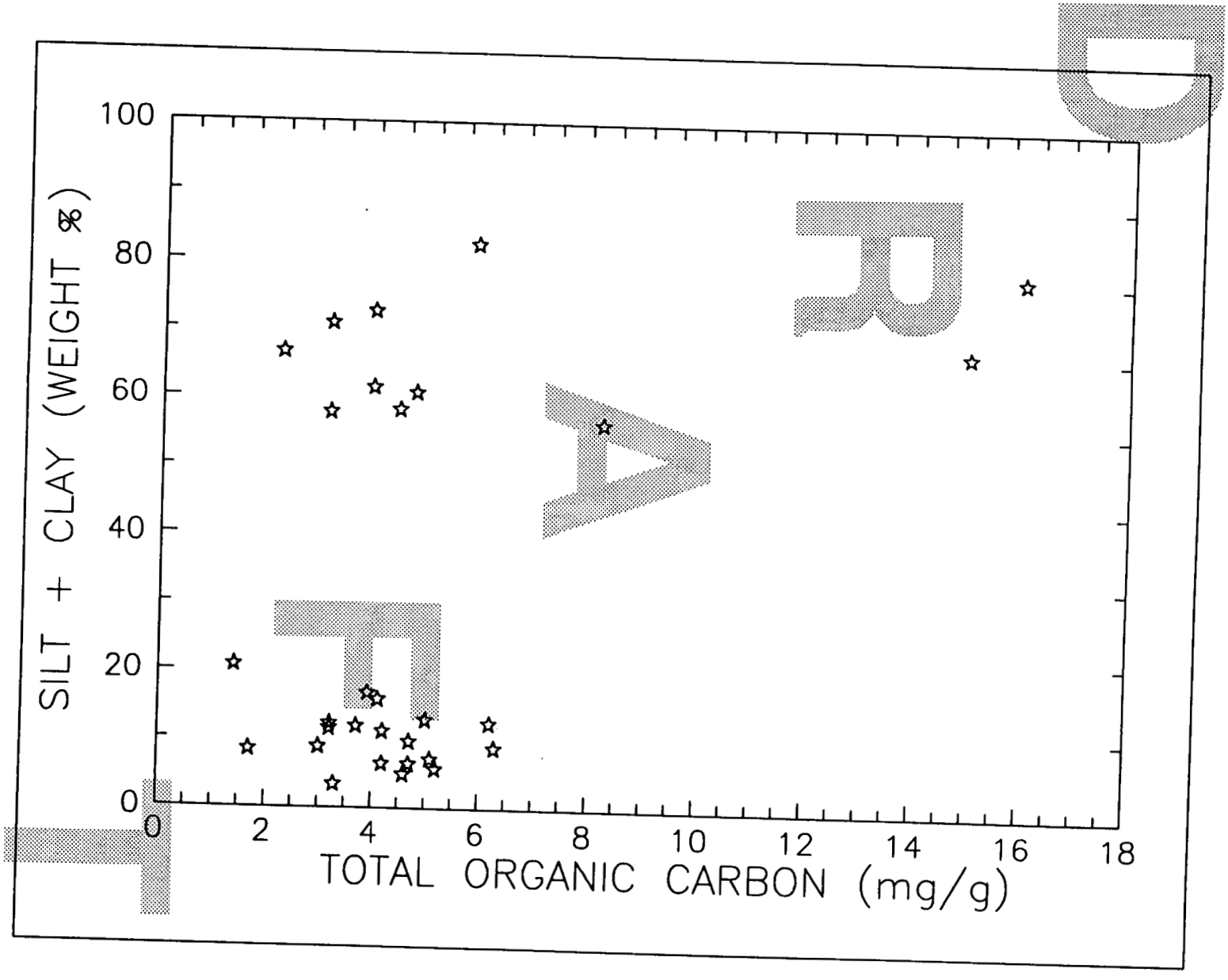


FIGURE P-5. WEIGHT PERCENT OF SILT + CLAY VERSUS TOTAL ORGANIC CARBON

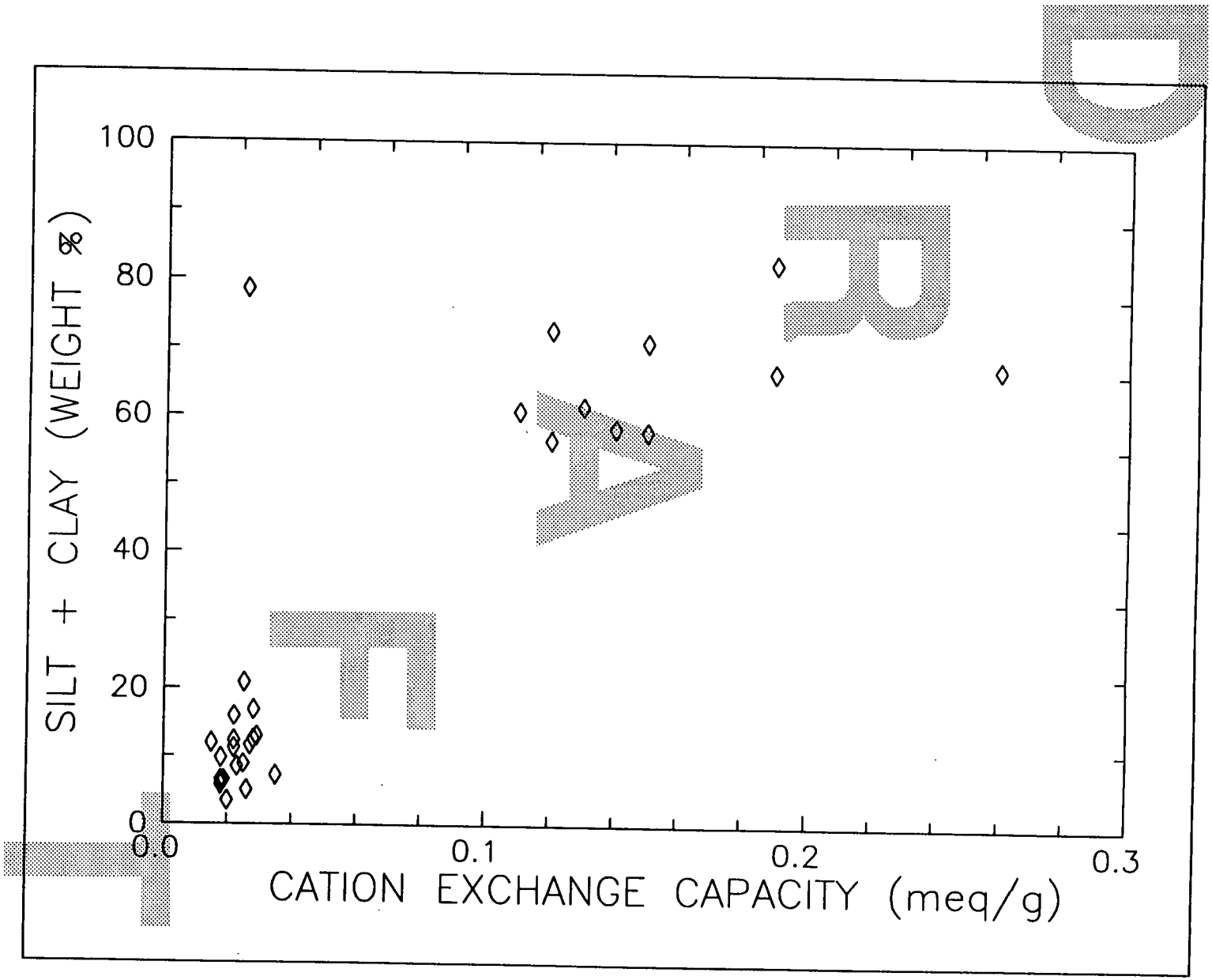


FIGURE P-6. WEIGHT PERCENT OF SILT + CLAY VERSUS CATION EXCHANGE CAPACITY

DRAFT

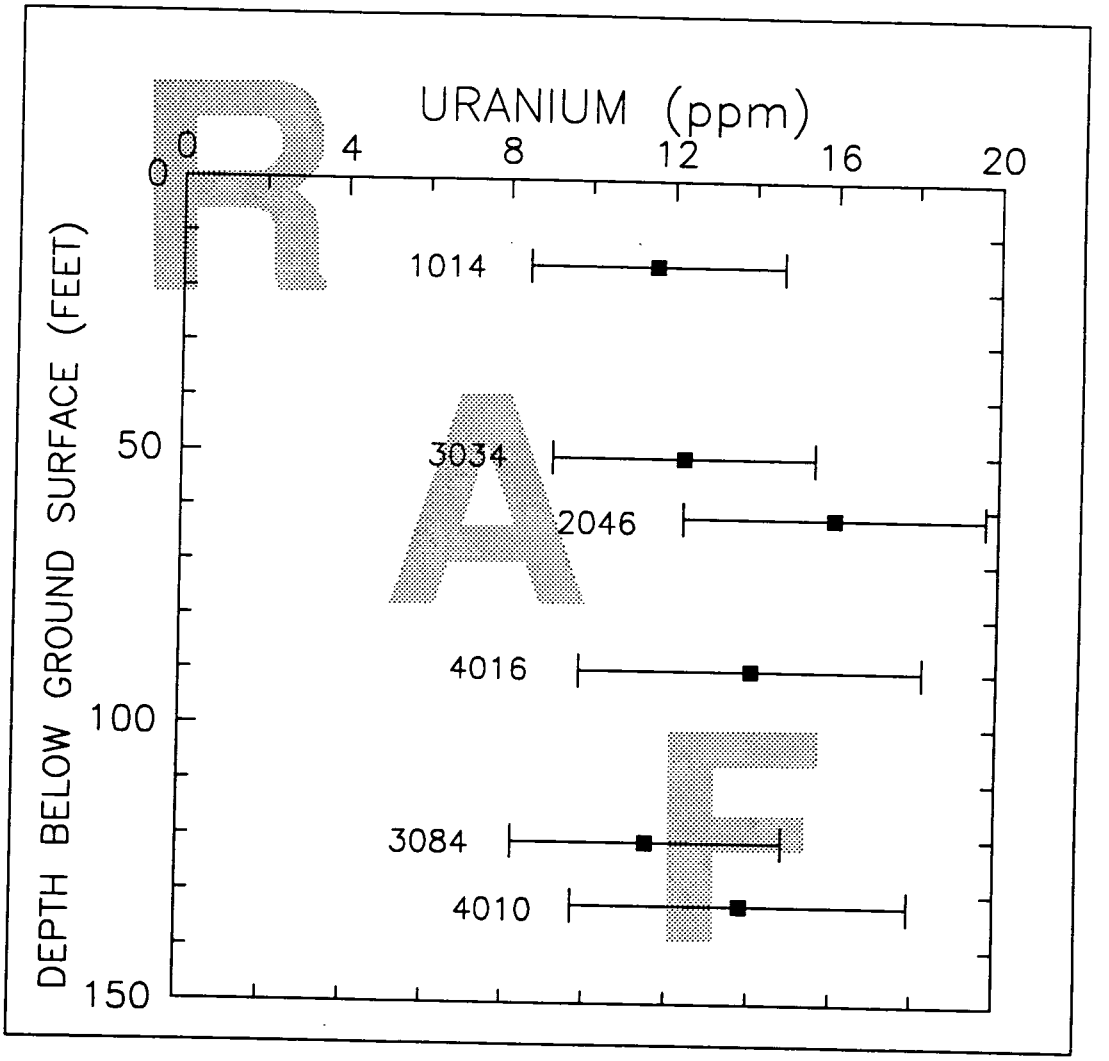


FIGURE P–7. URANIUM CONCENTRATIONS IN AQUIFER SOLIDS

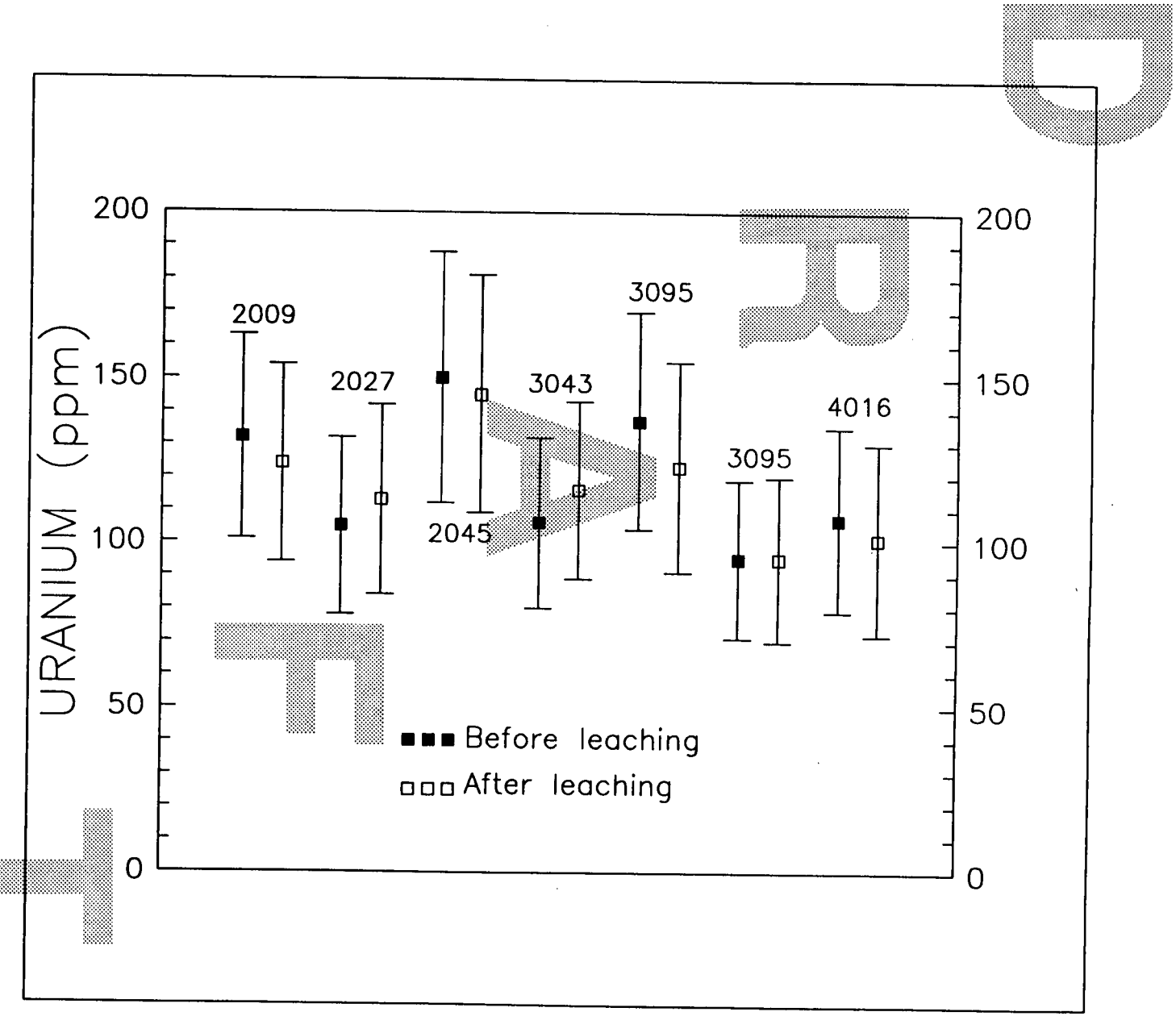


FIGURE P–8. RESULTS OF THE URANIUM DIFFERENTIAL–LEACH TEST

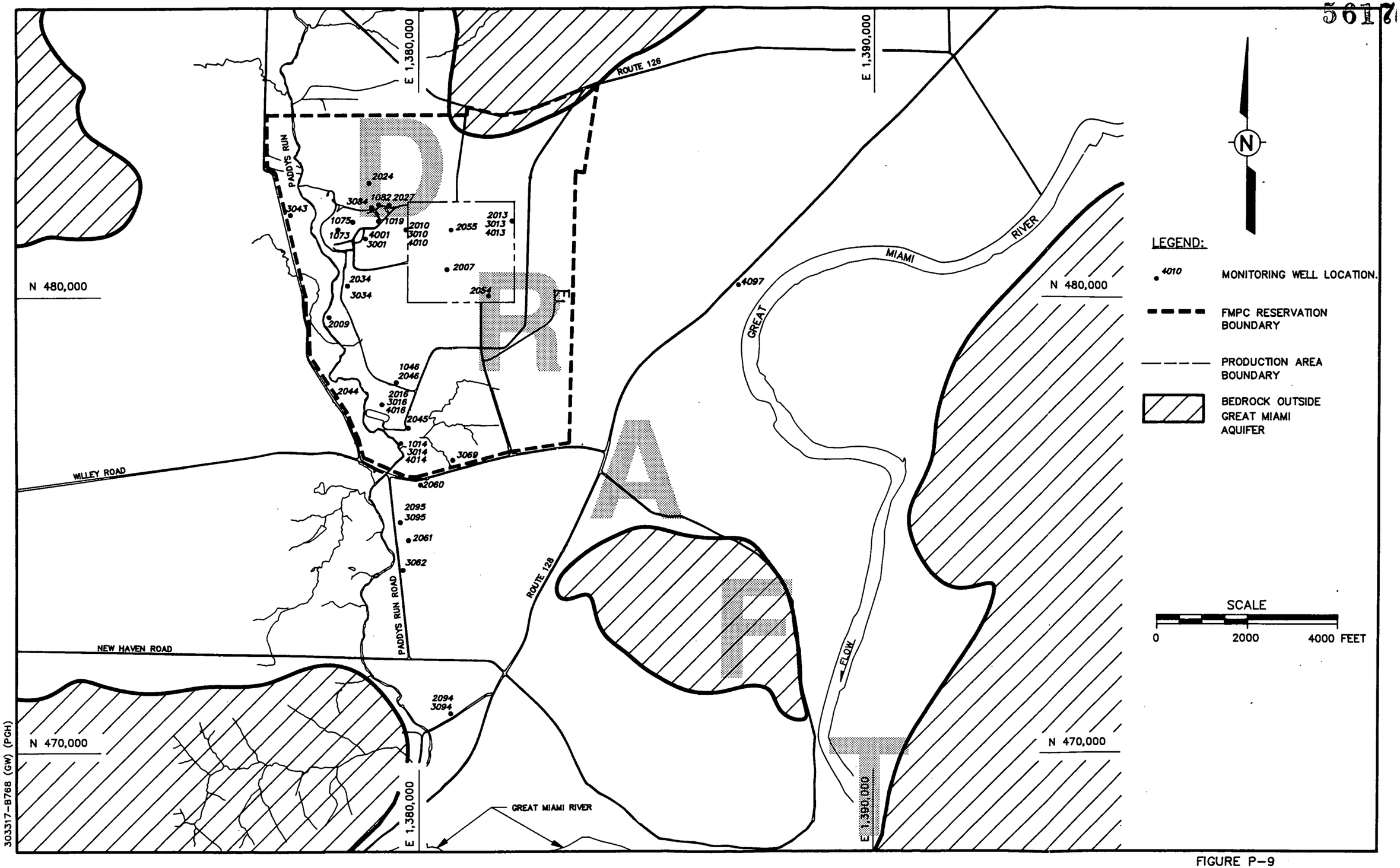


FIGURE P-9
GEOCHEMICAL PROGRAM ISSUE – 5
LOCATION OF GROUNDWATER MONITORING WELLS AND SUBSURFACE BORINGS

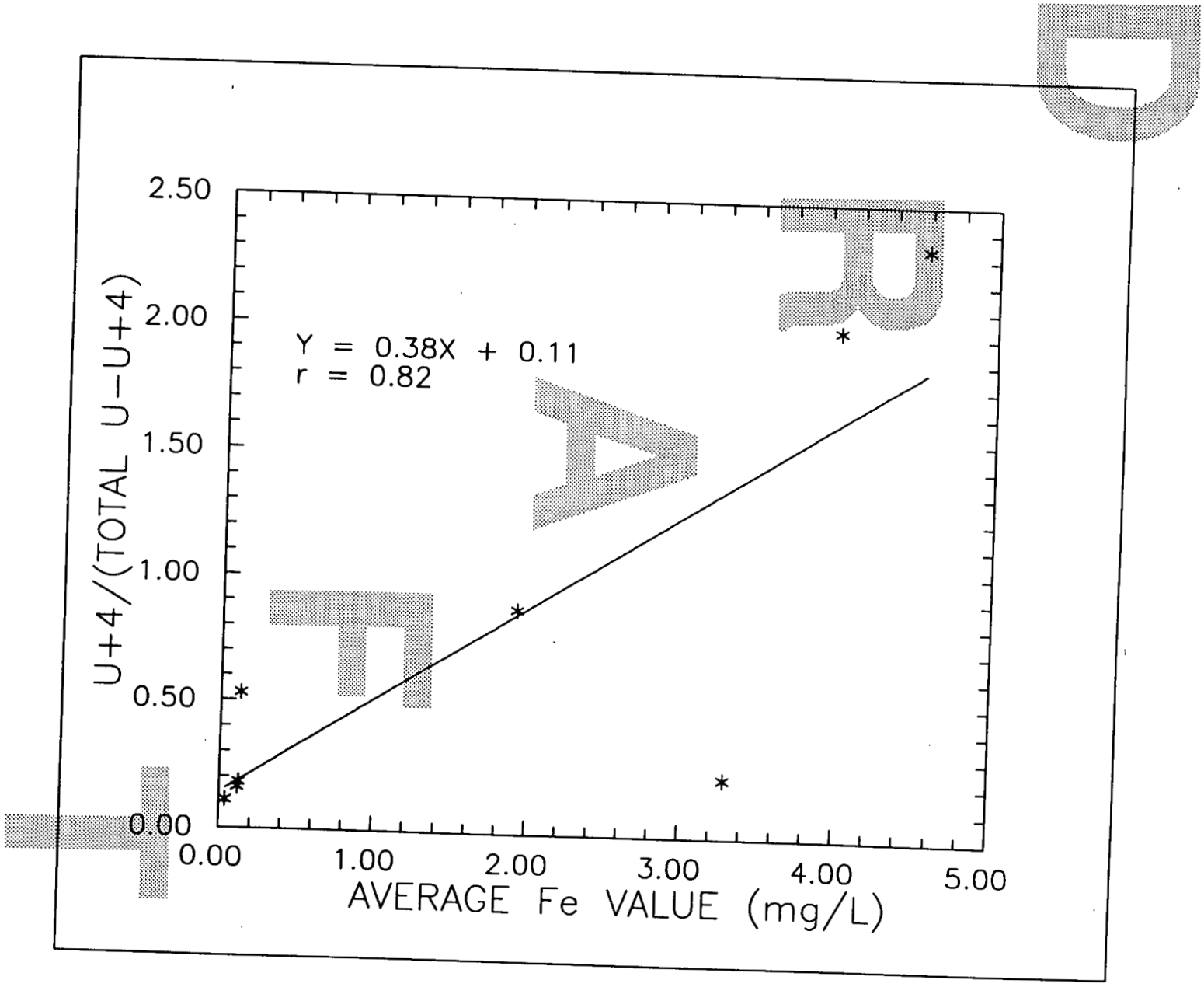


FIGURE P-10. URANIUM REDOX RATIO VERSUS TOTAL IRON

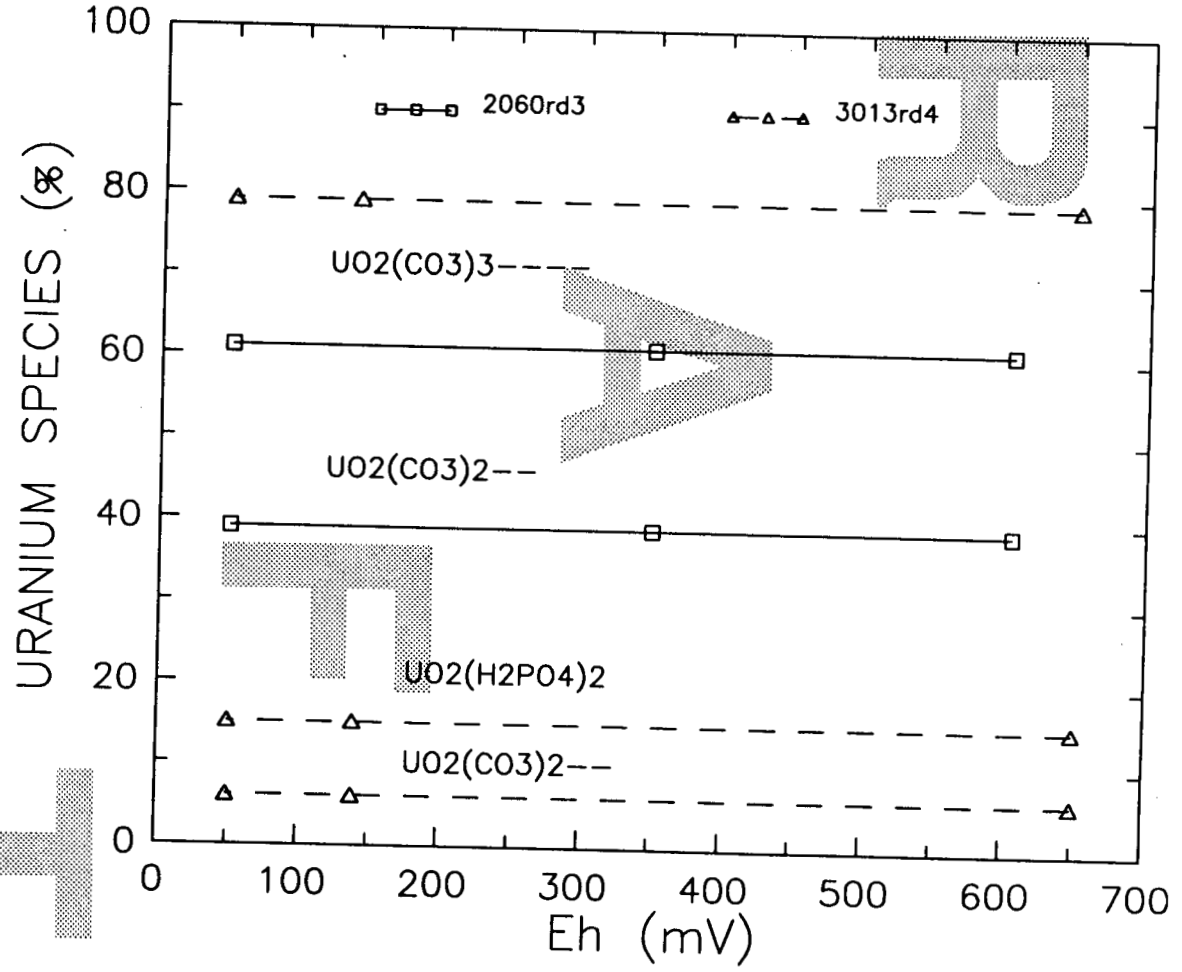


FIGURE P-11. URANIUM SPECIATION AS A FUNCTION OF THE GROUNDWATER Eh

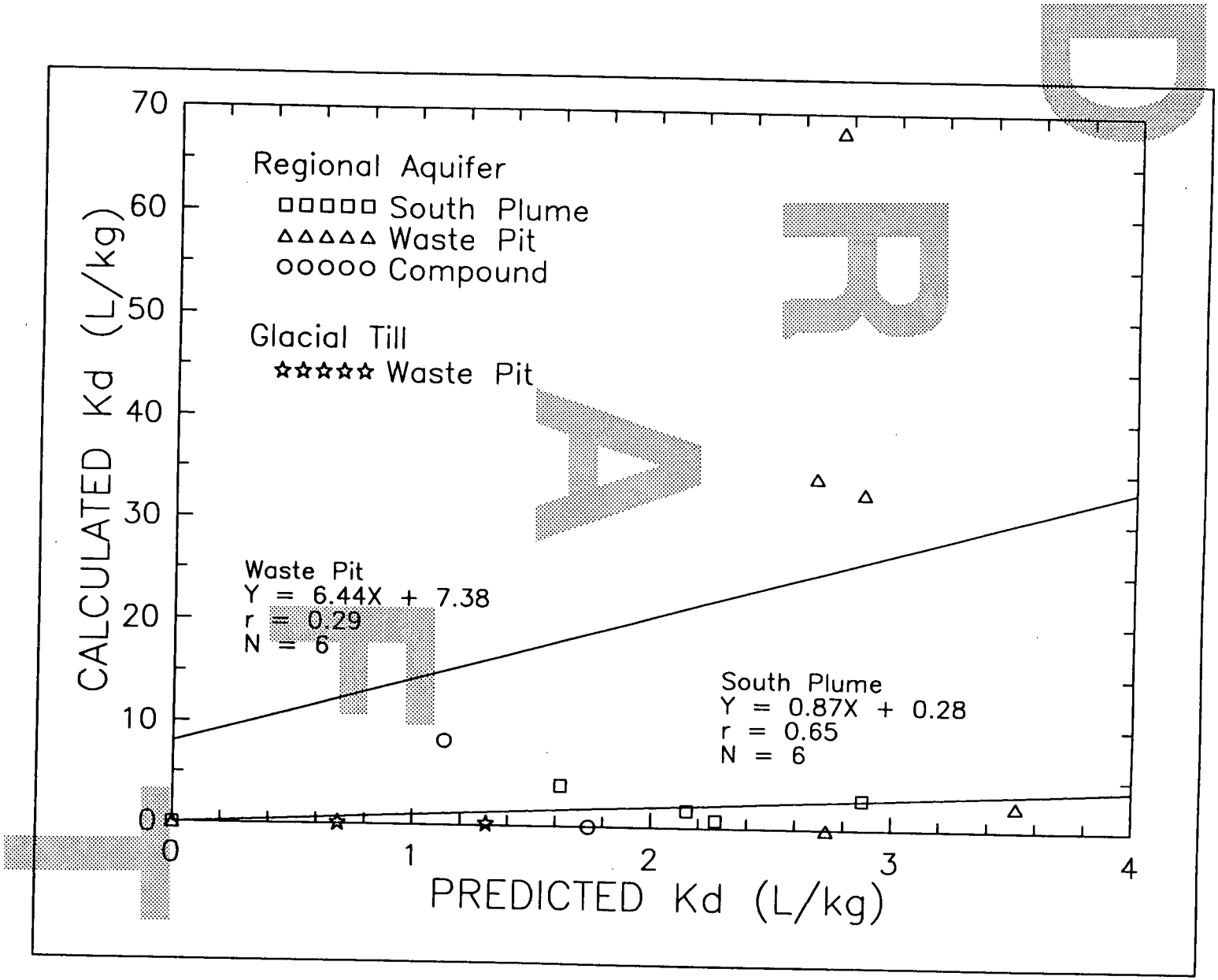


FIGURE P-12. CALCULATED Kd VERSUS PREDICTED Kd

# FENCE DIAGRAMS

Appendix Q contains fence diagrams for Operable Units 1 through 4 based on data from selected 1000 Series borings in each operable unit. The fence diagrams present a three-dimensional projection of the subsurface conditions within the glacial overburden. Appendix A contains the Visual Classification of Soil forms from which the data in the fence diagrams were interpreted.

DRAFT

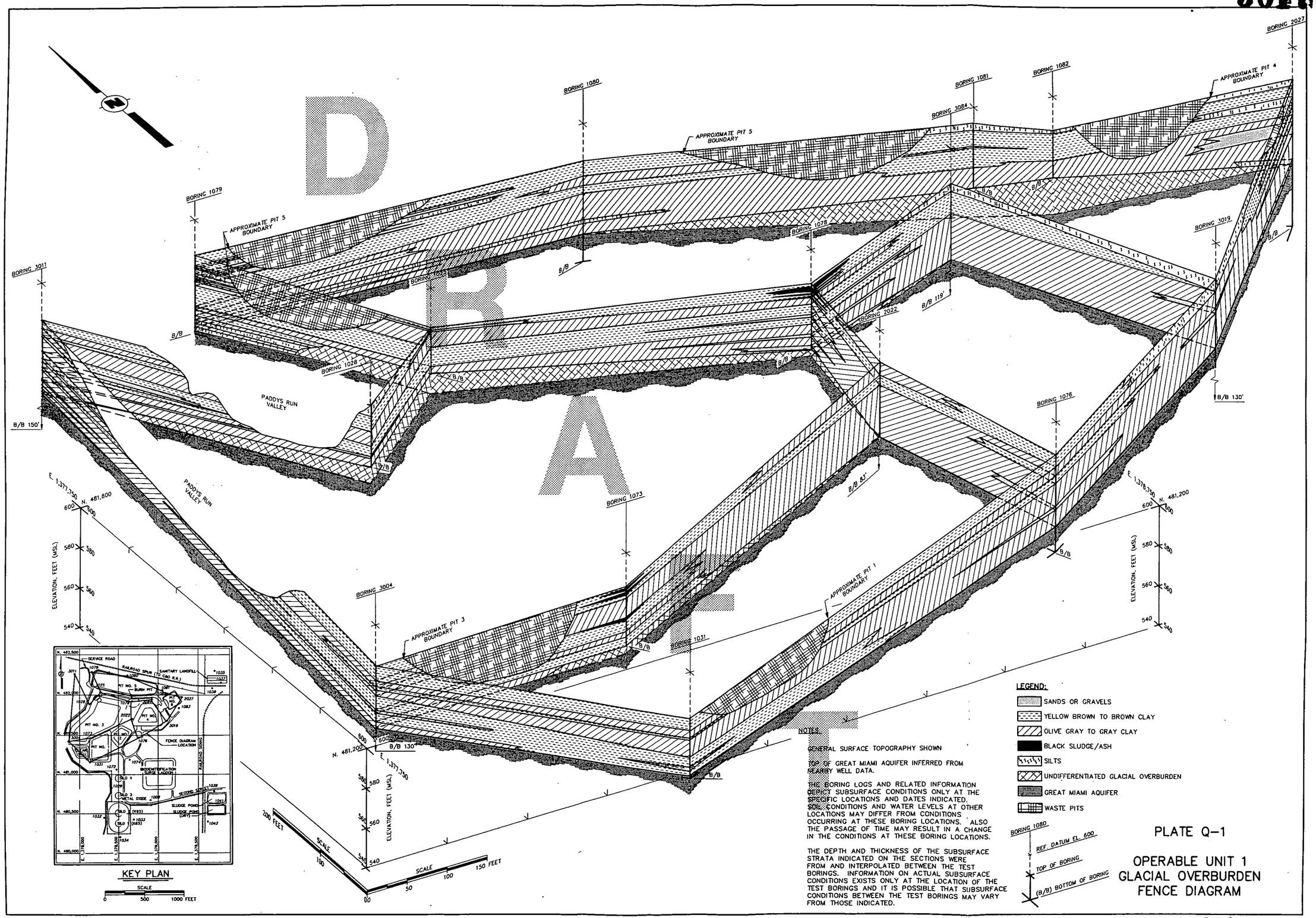


NOTES:

GENERAL SURFACE TOPOGRAPHY SHOWN

TOP OF GREAT MIAMI AQUIFER INFERRED FROM NEARBY WELL DATA.

THE BORING LOGS AND RELATED INFORMATION DEPICT SUBSURFACE CONDITIONS ONLY AT THE SPECIFIC LOCATIONS AND DATES INDICATED. SOIL CONDITIONS AND WATER LEVELS AT OTHER LOCATIONS MAY DIFFER FROM CONDITIONS OCCURRING AT THESE BORING LOCATIONS. ALSO THE PASSAGE OF TIME MAY RESULT IN A CHANGE IN THE CONDITIONS AT THESE BORING LOCATIONS.

THE DEPTH AND THICKNESS OF THE SUBSURFACE STRATA INDICATED ON THE SECTIONS WERE FROM AND INTERPOLATED BETWEEN THE TEST BORINGS. INFORMATION ON ACTUAL SUBSURFACE CONDITIONS EXISTS ONLY AT THE LOCATION OF THE TEST BORINGS AND IT IS POSSIBLE THAT SUBSURFACE CONDITIONS BETWEEN THE TEST BORINGS MAY VARY FROM THOSE INDICATED.

PLATE Q-1

OPERABLE UNIT 1
GLACIAL OVERBURDEN
FENCE DIAGRAM

303317-E79 (GW) (PGH)

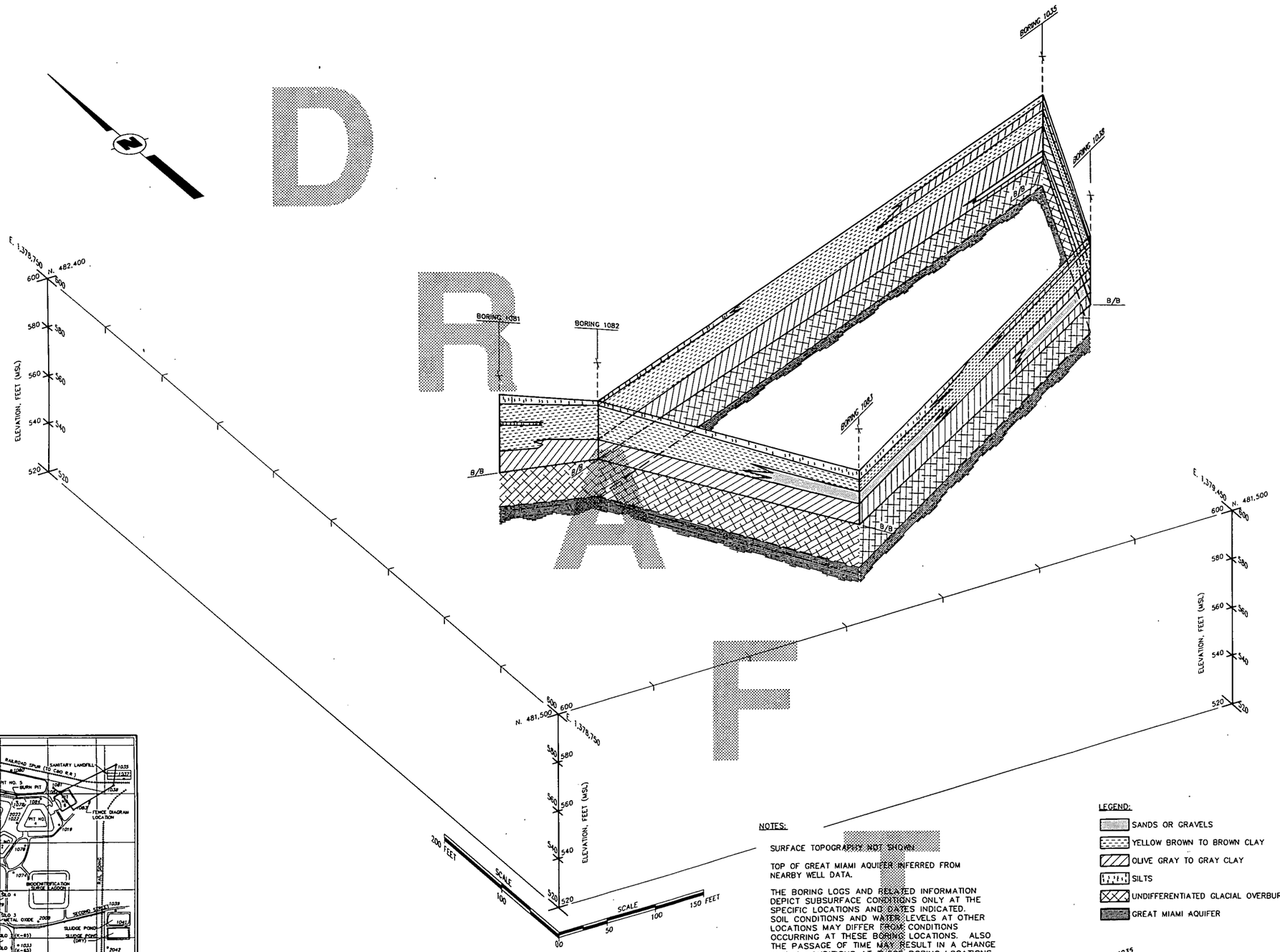


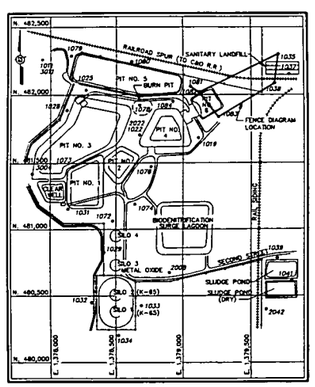


KEY PLAN

SCALE

0 500 1000 FEET

NOTES:

SURFACE TOPOGRAPHY NOT SHOWN.

TOP OF GREAT MIAMI AQUIFER INFERRED FROM NEARBY WELL DATA.

THE BORING LOGS AND RELATED INFORMATION DEPICT SUBSURFACE CONDITIONS ONLY AT THE SPECIFIC LOCATIONS AND DATES INDICATED. SOIL CONDITIONS AND WATER LEVELS AT OTHER LOCATIONS MAY DIFFER FROM CONDITIONS OCCURRING AT THESE BORING LOCATIONS. ALSO THE PASSAGE OF TIME MAY RESULT IN A CHANGE IN THE CONDITIONS AT THESE BORING LOCATIONS.

THE DEPTH AND THICKNESS OF THE SUBSURFACE STRATA INDICATED ON THE SECTIONS WERE FROM AND INTERPOLATED BETWEEN THE TEST BORINGS. INFORMATION ON ACTUAL SUBSURFACE CONDITIONS EXISTS ONLY AT THE LOCATION OF THE TEST BORINGS AND IT IS POSSIBLE THAT SUBSURFACE CONDITIONS BETWEEN THE TEST BORINGS MAY VARY FROM THOSE INDICATED.

LEGEND:

- SANDS OR GRAVELS
- YELLOW BROWN TO BROWN CLAY
- OLIVE GRAY TO GRAY CLAY
- SILTS
- UNDIFFERENTIATED GLACIAL OVERBURDEN
- GREAT MIAMI AQUIFER

BORING 1035
REF. DATUM EL. 600
TOP OF BORING
B/B (BOTTOM OF BORING)

PLATE Q-2

OPERABLE UNIT 2
GLACIAL OVERBURDEN
FENCE DIAGRAM

303317-E80 (GW) (PGH)

5617

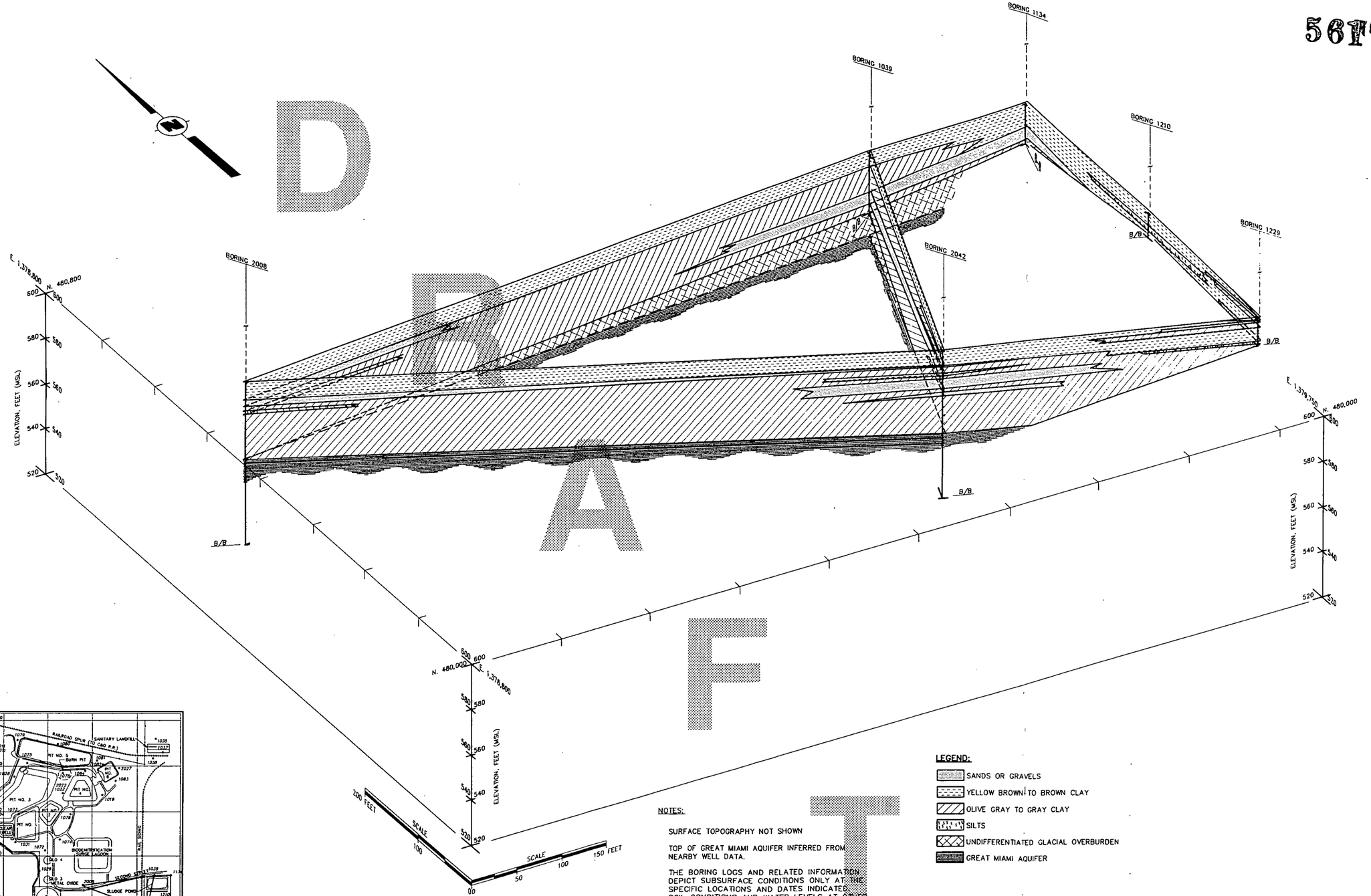


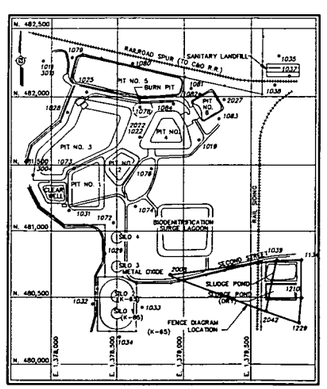


KEY PLAN

SCALE

0 500 1000 FEET

NOTES:

SURFACE TOPOGRAPHY NOT SHOWN

TOP OF GREAT MIAMI AQUIFER INFERRED FROM NEARBY WELL DATA.

THE BORING LOGS AND RELATED INFORMATION DEPICT SUBSURFACE CONDITIONS ONLY AT THE SPECIFIC LOCATIONS AND DATES INDICATED. SOIL CONDITIONS AND WATER LEVELS AT OTHER LOCATIONS MAY DIFFER FROM CONDITIONS OCCURRING AT THESE BORING LOCATIONS. ALSO THE PASSAGE OF TIME MAY RESULT IN A CHANGE IN THE CONDITIONS AT THESE BORING LOCATIONS.

THE DEPTH AND THICKNESS OF THE SUBSURFACE STRATA INDICATED ON THE SECTIONS WERE FROM AND INTERPOLATED BETWEEN THE TEST BORINGS. INFORMATION ON ACTUAL SUBSURFACE CONDITIONS EXISTS ONLY AT THE LOCATION OF THE TEST BORINGS AND IT IS POSSIBLE THAT SUBSURFACE CONDITIONS BETWEEN THE TEST BORINGS MAY VARY FROM THOSE INDICATED.

LEGEND:

- SANDS OR GRAVELS
- YELLOW BROWN TO BROWN CLAY
- OLIVE GRAY TO GRAY CLAY
- SILTS
- UNDIFFERENTIATED GLACIAL OVERBURDEN
- GREAT MIAMI AQUIFER

BORING 1031
REF. DATUM EL. 600
TOP OF BORING
B/B (BOTTOM OF BORING)

PLATE Q-3

OPERABLE UNIT 2
GLACIAL OVERBURDEN
FENCE DIAGRAM

303317-E81 (GW) (PGH)

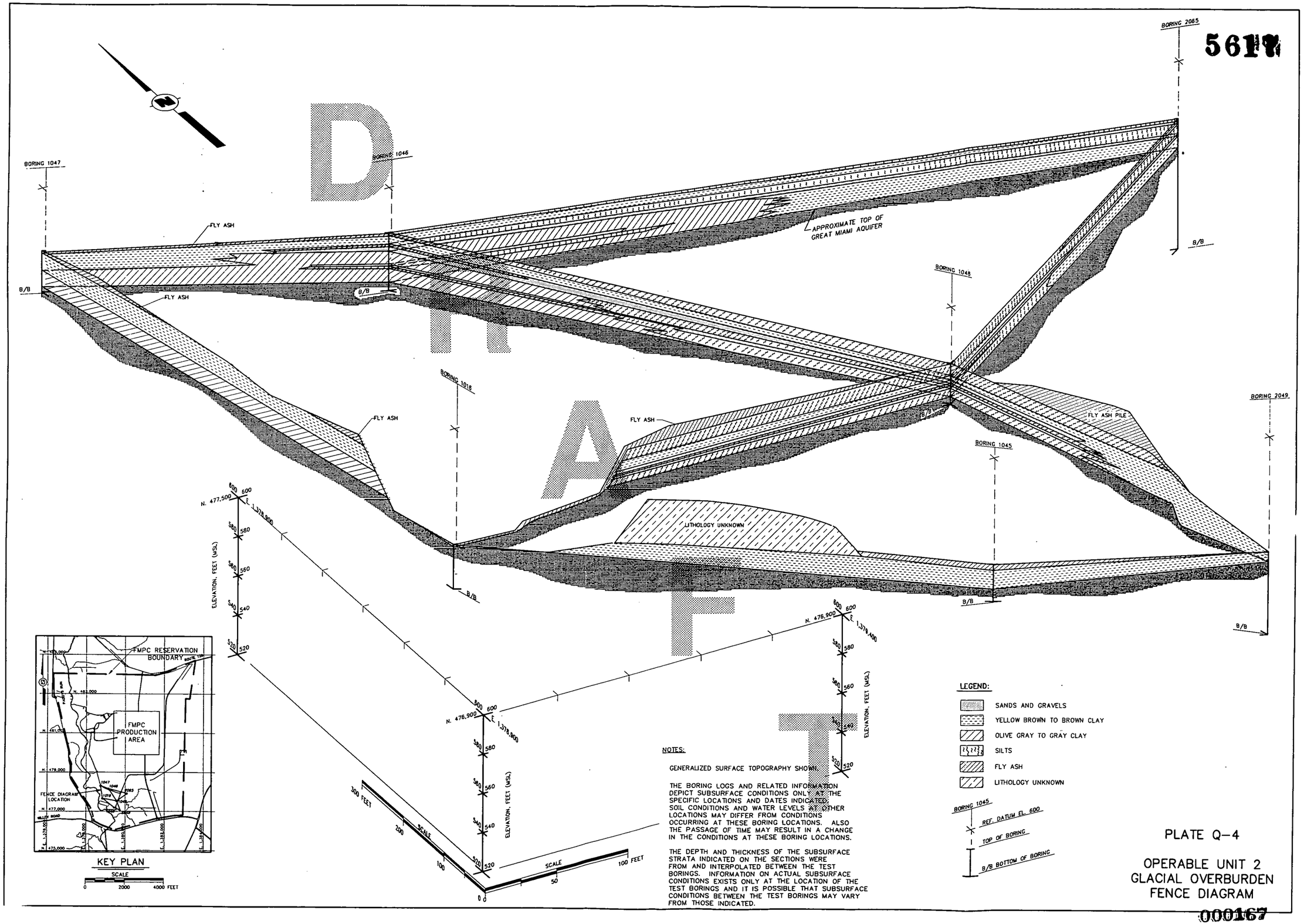


NOTES:

GENERALIZED SURFACE TOPOGRAPHY SHOWN.

THE BORING LOGS AND RELATED INFORMATION DEPICT SUBSURFACE CONDITIONS ONLY AT THE SPECIFIC LOCATIONS AND DATES INDICATED. SOIL CONDITIONS AND WATER LEVELS AT OTHER LOCATIONS MAY DIFFER FROM CONDITIONS OCCURRING AT THESE BORING LOCATIONS. ALSO THE PASSAGE OF TIME MAY RESULT IN A CHANGE IN THE CONDITIONS AT THESE BORING LOCATIONS.

THE DEPTH AND THICKNESS OF THE SUBSURFACE STRATA INDICATED ON THE SECTIONS WERE FROM AND INTERPOLATED BETWEEN THE TEST BORINGS. INFORMATION ON ACTUAL SUBSURFACE CONDITIONS EXISTS ONLY AT THE LOCATION OF THE TEST BORINGS AND IT IS POSSIBLE THAT SUBSURFACE CONDITIONS BETWEEN THE TEST BORINGS MAY VARY FROM THOSE INDICATED.

PLATE Q-4

OPERABLE UNIT 2
GLACIAL OVERBURDEN
FENCE DIAGRAM

303317-E83 (GW) (PGH)

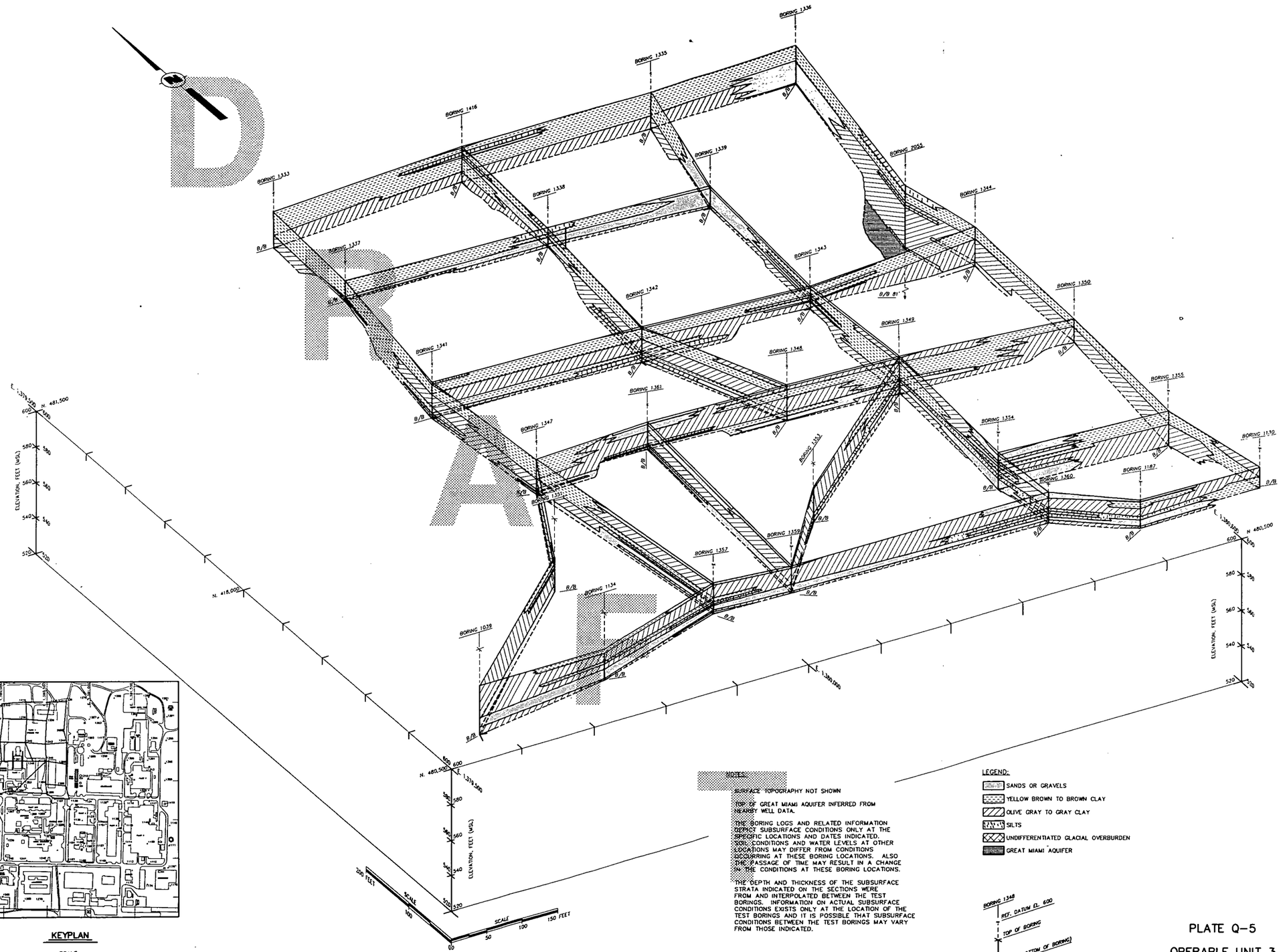


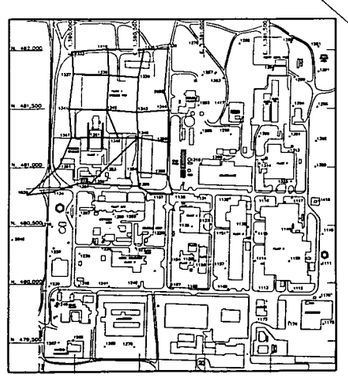

KEYPLAN

SCALE

0 500 1000 FEET

NOTES:

SURFACE TOPOGRAPHY NOT SHOWN

TOP OF GREAT MIAMI AQUIFER INFERRED FROM NEARBY WELL DATA.

THE BORING LOGS AND RELATED INFORMATION REFLECT SUBSURFACE CONDITIONS ONLY AT THE SPECIFIC LOCATIONS AND DATES INDICATED. SOIL CONDITIONS AND WATER LEVELS AT OTHER LOCATIONS MAY DIFFER FROM CONDITIONS OCCURRING AT THESE BORING LOCATIONS. ALSO THE PASSAGE OF TIME MAY RESULT IN A CHANGE IN THE CONDITIONS AT THESE BORING LOCATIONS.

THE DEPTH AND THICKNESS OF THE SUBSURFACE STRATA INDICATED ON THE SECTIONS WERE FROM AND INTERPOLATED BETWEEN THE TEST BORINGS. INFORMATION ON ACTUAL SUBSURFACE CONDITIONS EXISTS ONLY AT THE LOCATION OF THE TEST BORINGS AND IT IS POSSIBLE THAT SUBSURFACE CONDITIONS BETWEEN THE TEST BORINGS MAY VARY FROM THOSE INDICATED.

LEGEND:

- SANDS OR GRAVELS
- YELLOW BROWN TO BROWN CLAY
- OLIVE GRAY TO GRAY CLAY
- SILTS
- UNDIFFERENTIATED GLACIAL OVERBURDEN
- GREAT MIAMI AQUIFER

BORING 1348
REF. DATUM EL. 600
TOP OF BORING
B/B (BOTTOM OF BORING)

PLATE Q-5

OPERABLE UNIT 3
GLACIAL OVERBURDEN
FENCE DIAGRAM

303317-M107 (GW) (PCH)

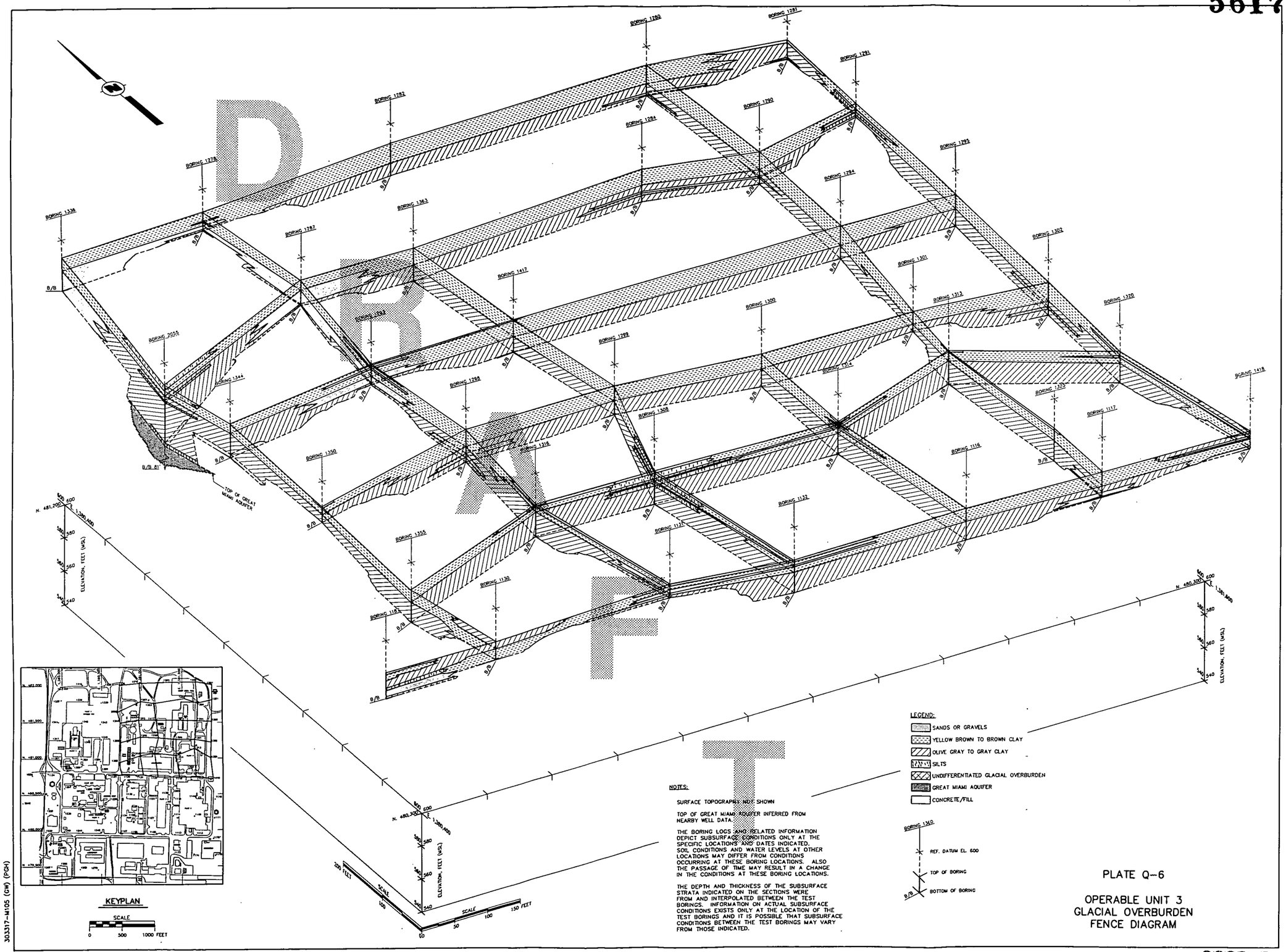


NOTES:

SURFACE TOPOGRAPHY NOT SHOWN

TOP OF GREAT MIAMI AQUIFER INFERRED FROM NEARBY WELL DATA.

THE BORING LOGS AND RELATED INFORMATION DEPICT SUBSURFACE CONDITIONS ONLY AT THE SPECIFIC LOCATIONS AND DATES INDICATED. SOIL CONDITIONS AND WATER LEVELS AT OTHER LOCATIONS MAY DIFFER FROM CONDITIONS OCCURRING AT THESE BORING LOCATIONS. ALSO THE PASSAGE OF TIME MAY RESULT IN A CHANGE IN THE CONDITIONS AT THESE BORING LOCATIONS.

THE DEPTH AND THICKNESS OF THE SUBSURFACE STRATA INDICATED ON THE SECTIONS WERE FROM AND INTERPOLATED BETWEEN THE TEST BORINGS. INFORMATION ON ACTUAL SUBSURFACE CONDITIONS EXISTS ONLY AT THE LOCATION OF THE TEST BORINGS AND IT IS POSSIBLE THAT SUBSURFACE CONDITIONS BETWEEN THE TEST BORINGS MAY VARY FROM THOSE INDICATED.

PLATE Q-6

OPERABLE UNIT 3
GLACIAL OVERBURDEN
FENCE DIAGRAM

303317-M105 (GW) (PGH)

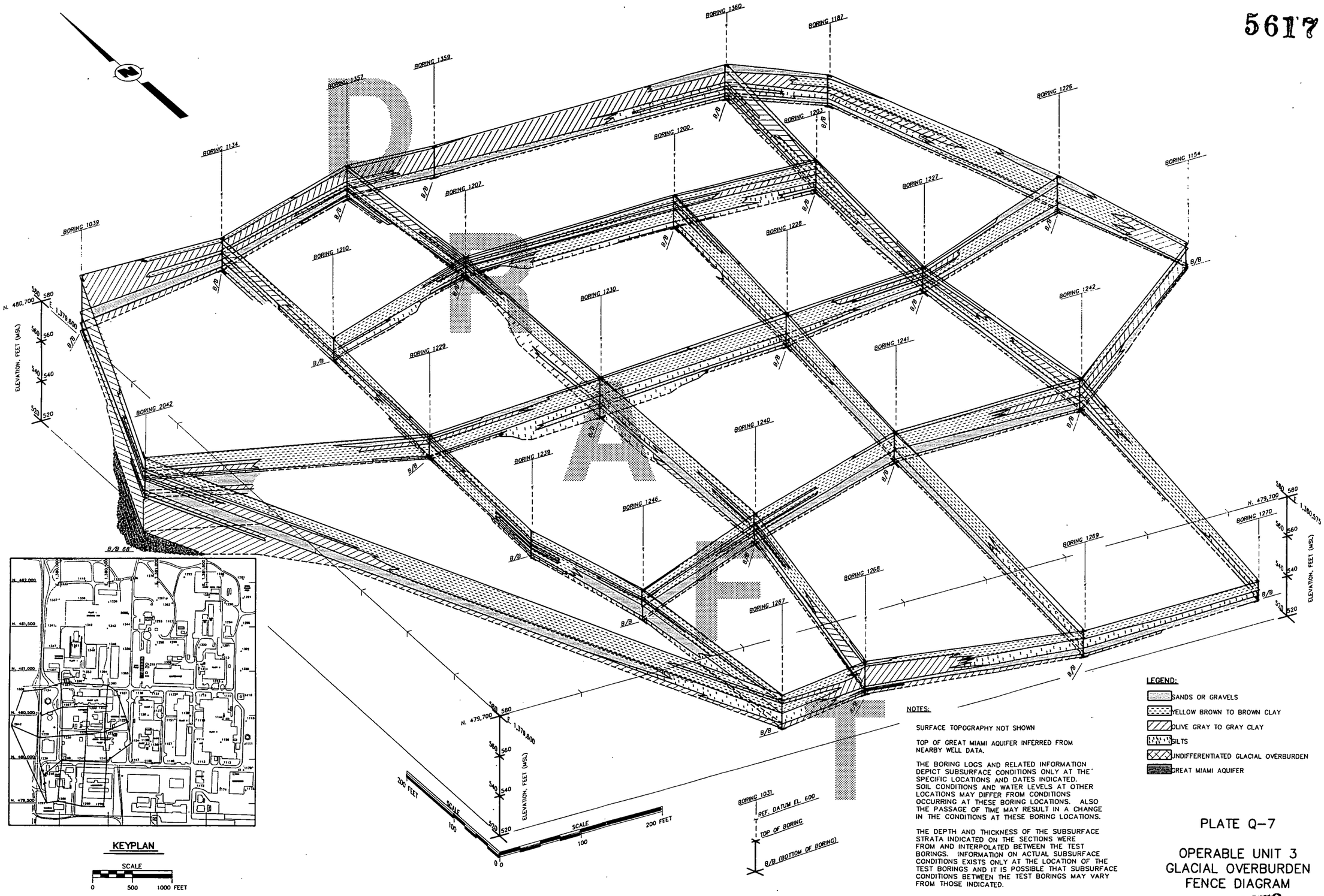


NOTES:

SURFACE TOPOGRAPHY NOT SHOWN

TOP OF GREAT MIAMI AQUIFER INFERRED FROM NEARBY WELL DATA.

THE BORING LOGS AND RELATED INFORMATION DEPICT SUBSURFACE CONDITIONS ONLY AT THE SPECIFIC LOCATIONS AND DATES INDICATED. SOIL CONDITIONS AND WATER LEVELS AT OTHER LOCATIONS MAY DIFFER FROM CONDITIONS OCCURRING AT THESE BORING LOCATIONS. ALSO THE PASSAGE OF TIME MAY RESULT IN A CHANGE IN THE CONDITIONS AT THESE BORING LOCATIONS.

THE DEPTH AND THICKNESS OF THE SUBSURFACE STRATA INDICATED ON THE SECTIONS WERE FROM AND INTERPOLATED BETWEEN THE TEST BORINGS. INFORMATION ON ACTUAL SUBSURFACE CONDITIONS EXISTS ONLY AT THE LOCATION OF THE TEST BORINGS AND IT IS POSSIBLE THAT SUBSURFACE CONDITIONS BETWEEN THE TEST BORINGS MAY VARY FROM THOSE INDICATED.

PLATE Q-7

OPERABLE UNIT 3
GLACIAL OVERBURDEN
FENCE DIAGRAM

303317-EBS (GW) (PGH)

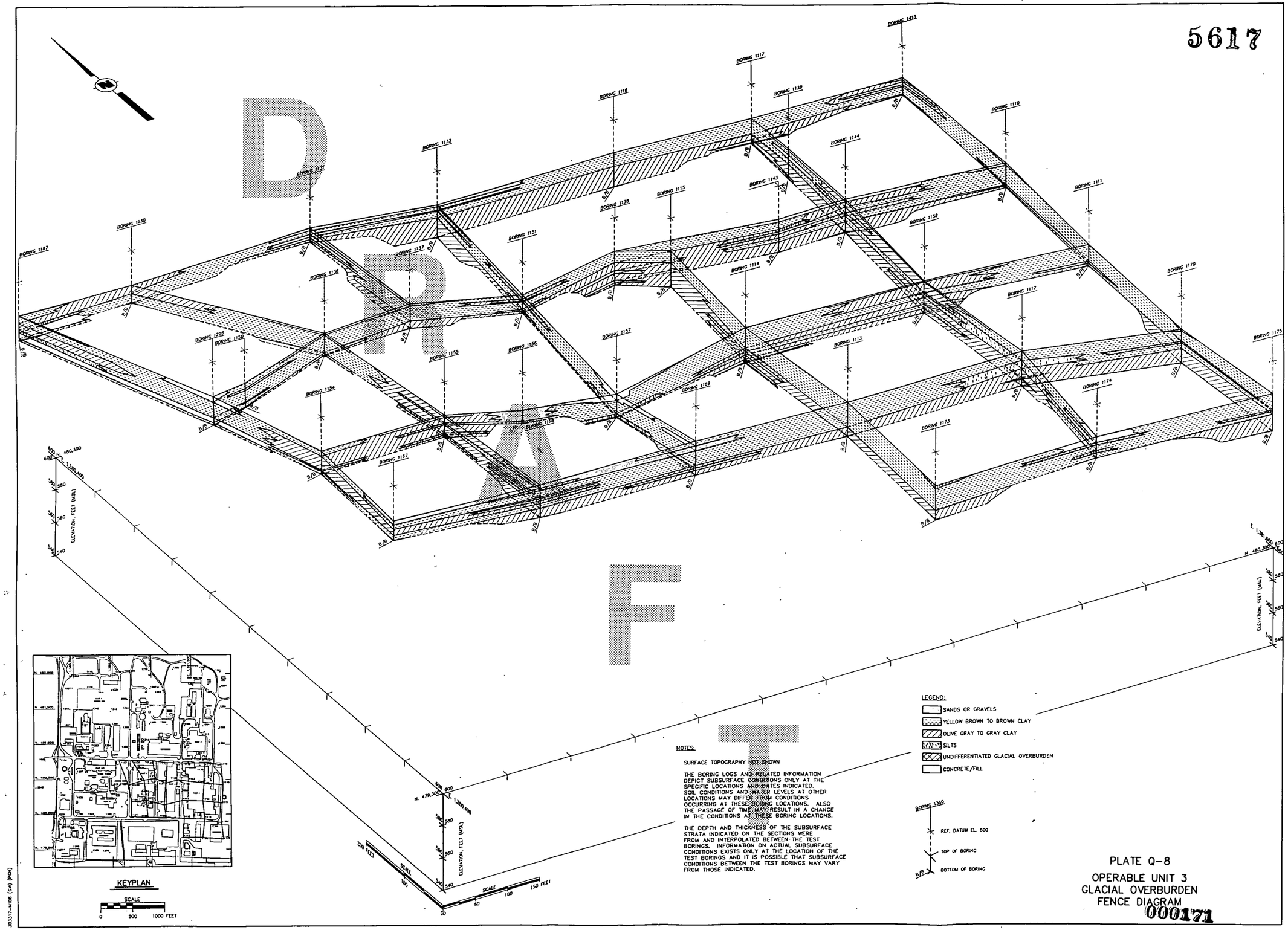


NOTES:

SURFACE TOPOGRAPHY NOT SHOWN

THE BORING LOGS AND RELATED INFORMATION DEPICT SUBSURFACE CONDITIONS ONLY AT THE SPECIFIC LOCATIONS AND DATES INDICATED. SOIL CONDITIONS AND WATER LEVELS AT OTHER LOCATIONS MAY DIFFER FROM CONDITIONS OCCURRING AT THESE BORING LOCATIONS. ALSO THE PASSAGE OF TIME MAY RESULT IN A CHANGE IN THE CONDITIONS AT THESE BORING LOCATIONS.

THE DEPTH AND THICKNESS OF THE SUBSURFACE STRATA INDICATED ON THE SECTIONS WERE FROM AND INTERPOLATED BETWEEN THE TEST BORINGS. INFORMATION ON ACTUAL SUBSURFACE CONDITIONS EXISTS ONLY AT THE LOCATION OF THE TEST BORINGS AND IT IS POSSIBLE THAT SUBSURFACE CONDITIONS BETWEEN THE TEST BORINGS MAY VARY FROM THOSE INDICATED.

PLATE Q-8

OPERABLE UNIT 3
GLACIAL OVERBURDEN
FENCE DIAGRAM



DRAFT

5617

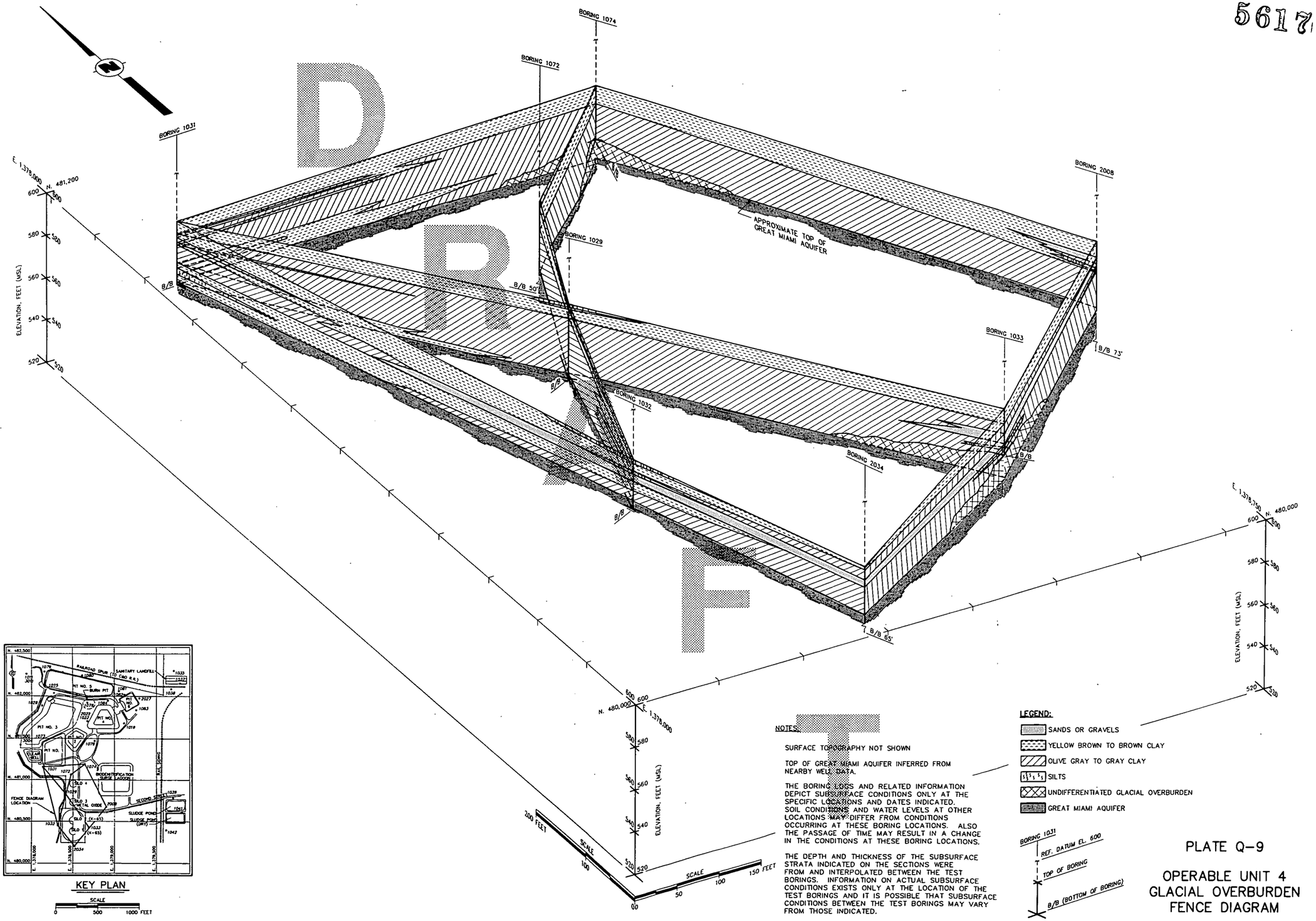


NOTES:

SURFACE TOPOGRAPHY NOT SHOWN

TOP OF GREAT MIAMI AQUIFER INFERRED FROM NEARBY WELL DATA.

THE BORING LOGS AND RELATED INFORMATION DEPICT SUBSURFACE CONDITIONS ONLY AT THE SPECIFIC LOCATIONS AND DATES INDICATED. SOIL CONDITIONS AND WATER LEVELS AT OTHER LOCATIONS MAY DIFFER FROM CONDITIONS OCCURRING AT THESE BORING LOCATIONS. ALSO THE PASSAGE OF TIME MAY RESULT IN A CHANGE IN THE CONDITIONS AT THESE BORING LOCATIONS.

THE DEPTH AND THICKNESS OF THE SUBSURFACE STRATA INDICATED ON THE SECTIONS WERE FROM AND INTERPOLATED BETWEEN THE TEST BORINGS. INFORMATION ON ACTUAL SUBSURFACE CONDITIONS EXISTS ONLY AT THE LOCATION OF THE TEST BORINGS AND IT IS POSSIBLE THAT SUBSURFACE CONDITIONS BETWEEN THE TEST BORINGS MAY VARY FROM THOSE INDICATED.

LEGEND:

- SANDS OR GRAVELS
- YELLOW BROWN TO BROWN CLAY
- OLIVE GRAY TO GRAY CLAY
- SILTS
- UNDIFFERENTIATED GLACIAL OVERBURDEN
- GREAT MIAMI AQUIFER

BORING 1031
REF. DATUM EL. 600
TOP OF BORING
B/B (BOTTOM OF BORING)

PLATE Q-9

OPERABLE UNIT 4
GLACIAL OVERBURDEN
FENCE DIAGRAM

303317-E78 (GW) (PGH)

000172